CLINICAL AND MOLECULAR FEATURES OF INFECTIOUS CARDIOMYOPATHIES: IMPLICATIONS FOR PREVENTION, TREATMENT AND MANAGEMENT

EDITED BY: Maria Nunes, Walderez Ornelas Dutra and Livia Passos

PUBLISHED IN: Frontiers in Cardiovascular Medicine

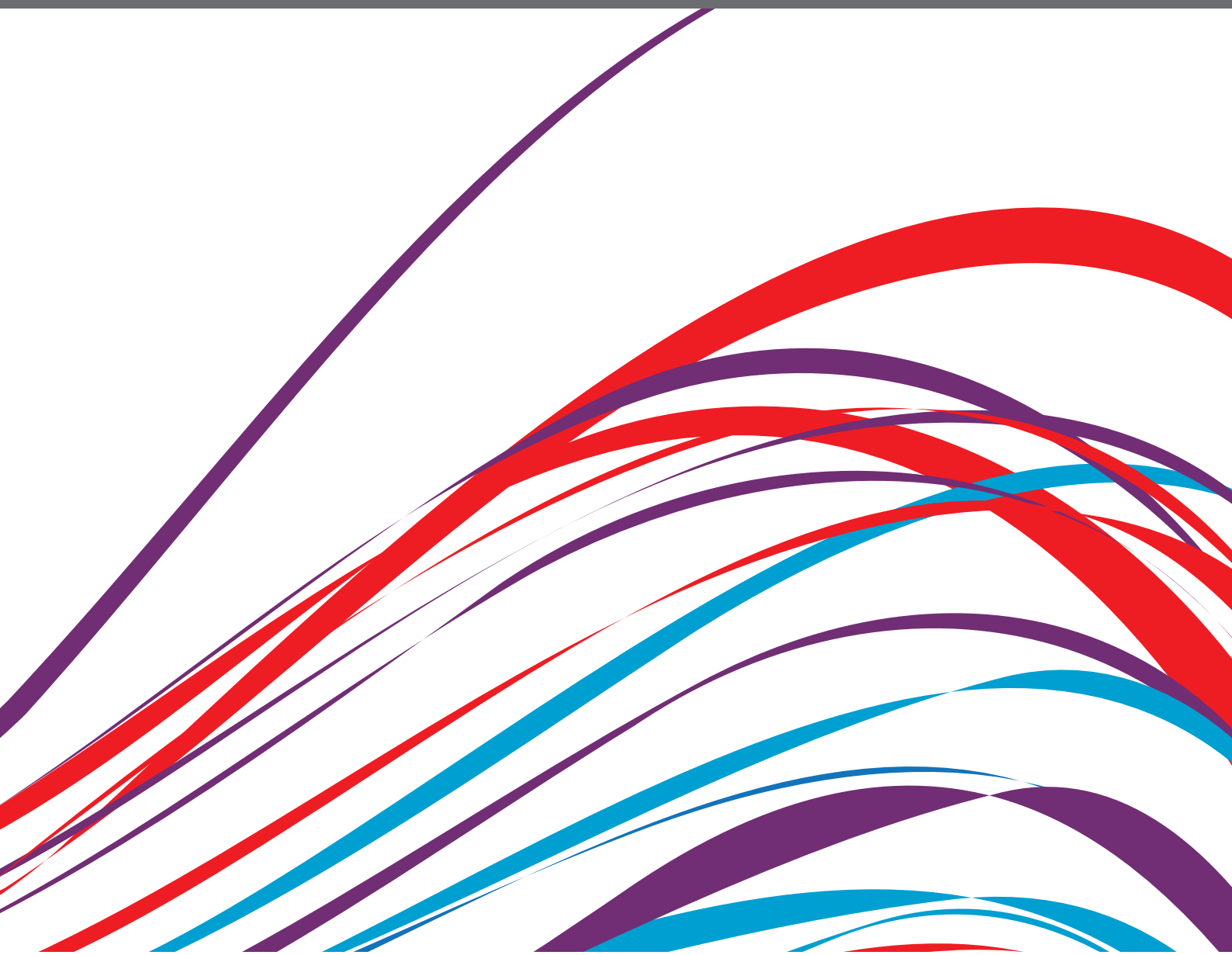

frontiers Research Topics

ISSN 1664-8714
ISBN 978-2-88976-524-9
DOI 10.3389/978-2-88976-524-9

About Frontiers

Frontiers is more than just an open-access publisher of scholarly articles: it is a pioneering approach to the world of academia, radically improving the way scholarly research is managed. The grand vision of Frontiers is a world where all people have an equal opportunity to seek, share and generate knowledge. Frontiers provides immediate and permanent online open access to all its publications, but this alone is not enough to realize our grand goals.

Frontiers Journal Series

The Frontiers Journal Series is a multi-tier and interdisciplinary set of open-access, online journals, promising a paradigm shift from the current review, selection and dissemination processes in academic publishing. All Frontiers journals are driven by researchers for researchers; therefore, they constitute a service to the scholarly community. At the same time, the Frontiers Journal Series operates on a revolutionary invention, the tiered publishing system, initially addressing specific communities of scholars, and gradually climbing up to broader public understanding, thus serving the interests of the lay society, too.

Dedication to Quality

Each Frontiers article is a landmark of the highest quality, thanks to genuinely collaborative interactions between authors and review editors, who include some of the world's best academicians. Research must be certified by peers before entering a stream of knowledge that may eventually reach the public - and shape society; therefore, Frontiers only applies the most rigorous and unbiased reviews.
Frontiers revolutionizes research publishing by freely delivering the most outstanding research, evaluated with no bias from both the academic and social point of view. By applying the most advanced information technologies, Frontiers is catapulting scholarly publishing into a new generation.

What are Frontiers Research Topics?

Frontiers Research Topics are very popular trademarks of the Frontiers Journals Series: they are collections of at least ten articles, all centered on a particular subject. With their unique mix of varied contributions from Original Research to Review Articles, Frontiers Research Topics unify the most influential researchers, the latest key findings and historical advances in a hot research area! Find out more on how to host your own Frontiers Research Topic or contribute to one as an author by contacting the Frontiers Editorial Office: frontiersin.org/about/contact

CLINICAL AND MOLECULAR FEATURES OF INFECTIOUS CARDIOMYOPATHIES: IMPLICATIONS FOR PREVENTION, TREATMENT AND MANAGEMENT

Topic Editors:
Maria Nunes, Federal University of Minas Gerais, Brazil
Walderez Ornelas Dutra, Federal University of Minas Gerais, Brazil
Livia Passos, Brigham and Women's Hospital, Harvard Medical School, United States

Citation: Nunes, M., Dutra, W. O., Passos, L., eds. (2022). Clinical and Molecular Features of Infectious Cardiomyopathies: Implications for Prevention, Treatment and Management. Lausanne: Frontiers Media SA.
doi: 10.3389/978-2-88976-524-9

Table of Contents

frontiers | Frontiers in Cardiovascular Medicine

EDITORIAL
published: 10 June 2022
doi: 10.3389/fcvm.2022.952189

Editorial: Clinical and Molecular Features of Infectious Cardiomyopathies: Implications for Prevention, Treatment and Management

Maria do Carmo Pereira Nunes[1]*, *Lívia Silva Araújo Passos*[2]* and *Walderez Ornelas Dutra*[3,4]*

[1] Graduate Program in Infectology and Tropical Medicine, School of Medicine, Federal University of Minas Gerais, Belo Horizonte, Brazil, [2] Brigham and Women's Hospital, Harvard Medical School, Boston, MA, United States, [3] Cell-Cell Interactions Laboratory, Department of Morphology, Institute of Biological Sciences, Federal University of Minas Gerais, Belo Horizonte, Brazil, [4] Instituto Nacional de Ciência e Tecnologia em Doenças Tropicais (INCT-DT), Salvador, Brazil

Keywords: cardiomyopathy, biomarkers, pathology, Chagas disease—*Trypanosoma cruzi*, infectious diseases

Editorial on the Research Topic

Clinical and Molecular Features of Infectious Cardiomyopathies: Implications for Prevention, Treatment and Management

Heart diseases are the leading cause of death worldwide. The current Research Topic covers aspects associated with the pathogenesis or progression of different cardiomyopathies, ranging from the role of the pathogen, through the influence of diet and host factors. Parasitic infections, which are often associated with cardiac manifestations, account for significant morbidity and mortality in extensive areas of the world, especially in developing countries. Some of these infections may affect the anatomic structures of the heart, such as the myocardium and pericardium, as well as the pulmonary vasculature, producing a wide variety of cardiac manifestations. As an example, Chagas disease, caused by the protozoan *Trypanosoma cruzi*, is a major cause of cardiomyopathies worldwide.

Although the articles presented in the Research Topic discuss myocardial diseases of different etiologies, they are heavily biased toward Chagas disease cardiomyopathy, which is the main Research Topic of eight out of 10 papers. The study by de Oliveira et al. addressed an important issue in Chagas disease, which is the correlation of parasitemia and disease severity. Studying a cohort of 181 patients, they demonstrated that, although the parasitemia is variable amongst chronic patients, high parasitemia is correlated with a reduction of left ventricular ejection fraction, an important prognostic factor in Chagas cardiomyopathy. Intriguingly, the systematic review presented by Bosch-Nicolau et al. in this same Research Topic failed to demonstrate an association between parasite DNA and Chagas cardiomyopathy. Although apparently antagonistic, these studies consider different aspects: myocardial function in cardiac patients, and cardiomyopathy without considering severity of heart damage. These studies add to our knowledge in an area that is still controversial and need further development.

In another study, de Oliveira et al. demonstrated the occurrence of a moderate to high intra-discrete typing unit (DTU) V variability in patients from Bolivia living in Spain. Importantly, this study showed an association between parasite alleles with the lack of cardiac involvement in patients with Chagas disease, suggesting that parasite genetic intra-DTU variability may be a

Edited and reviewed by:
Junjie Xiao,
Shanghai University, China

***Correspondence:**
Maria do Carmo Pereira Nunes
mcarmo@waymail.com.br
Lívia Silva Araújo Passos
liviasap@gmail.com
Walderez Ornelas Dutra
waldutra@gmail.com

Specialty section:
This article was submitted to General Cardiovascular Medicine, a section of the journal Frontiers in Cardiovascular Medicine

Received: *24 May 2022*
Accepted: *26 May 2022*
Published: *10 June 2022*

Citation:
Nunes MdCP, Passos LSA and Dutra WO (2022) Editorial: Clinical and Molecular Features of Infectious Cardiomyopathies: Implications for Prevention, Treatment and Management. Front. Cardiovasc. Med. 9:952189. doi: 10.3389/fcvm.2022.952189

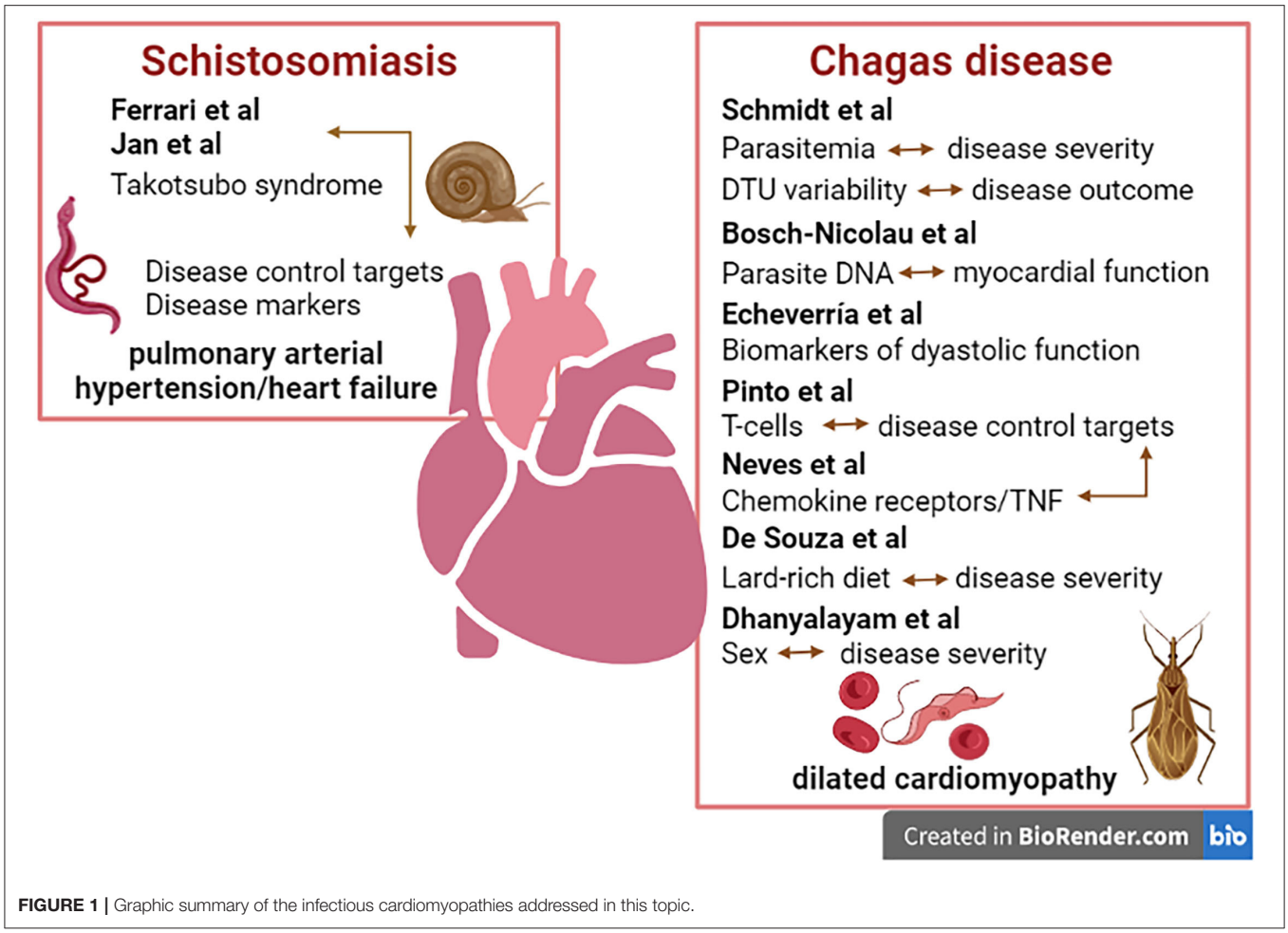

FIGURE 1 | Graphic summary of the infectious cardiomyopathies addressed in this topic.

marker of disease favorable outcome. Echeverría et al. approached the potential use of several molecules as biomarkers of left ventricular diastolic dysfunction. The authors showed that, except for sST2, the levels of all markers analyzed [pro-B type natriuretic peptide (NT-proBNP), galectin-3 (Gal-3), neutrophil gelatinase-associated lipocalin (NGAL), high-sensitivity troponin T (hs-cTnT), soluble (sST2), and cystatin-C (Cys-c)] were associated with high risk of patients having diastolic dysfunction. Amongst these markers, NT-proBNP was the best marker for identifying diastolic dysfunction. These studies, although with relatively low numbers of patients, enlighten the search for much needed markers of disease severity.

The role of the host's immune response was also addressed in this Research Topic. Pinto et al. showed a modulation of activated and regulated T-cell subpopulations by the interactions of CD80/CD86 with CD28/CTLA-4, respectively. This work implicates the network of co-stimulatory signals as potential targets to control Chagas cardiomyopathy. The study by Neves et al. shows an extensive comparison of the expression of cytokines, recruitment and effector molecules between patients with Chagas and idiopathic cardiomyopathies. While the data shows significant immunological differences between the cardiomyopathies, some similarities regarding expression of chemokine receptors and TNF were found, identifying potential common targets of intervention in these diseases. Using experimental models of *T. cruzi* infection, de Souza et al. and Dhanyalayam et al. showed the involvement of a lard-rich diet and of sex in severity of Chagas cardiomyopathy, respectively. These findings contribute to our understanding regarding the role of host and environmental factors in Chagas cardiomyopathy involvement. This, the Research Topic of studies regarding Chagas disease in the current Research Topic, address the influence of parasite, host, and environmental factors in disease development.

Lastly, the studies by Ferrari et al. and Jan et al. discuss pulmonary arterial hypertension, a well-known consequence of infection with the parasite *Schistosoma mansoni*, and acute heart failure associated with Takotsubo syndrome, respectively. These studies highlight potential points of intervention and clinical markers of these diseases.

Overall, the studies presented here add to the current clinical knowledge of these cardiomyopathies, while also providing information regarding their epidemiology, pathogenesis, diagnosis, and treatment. In addition, the studies present

strong suggestions of biomarkers of disease progression and/or cure, to guide patient care. We believe that the content of this Research Topic will aid general practitioners and cardiologists in the identification and treatment of parasitic and infectious cardiomyopathies. **Figure 1** shows the graphic summary of the papers published in this topic.

AUTHOR CONTRIBUTIONS

All authors listed have made a substantial, direct, and intellectual contribution to the work and approved it for publication.

FUNDING

The authors are supported by CNPq, FAPEMIG, INCT-DT, and NIH R01AI138230 grants.

ACKNOWLEDGMENTS

We would like to thank all authors who contributed to this Research Topic for providing relevant information regarding the influence of the pathogen, host and environmental factors in the progression, and severity of the different heart diseases.

Conflict of Interest: The authors declare that the research was conducted in the absence of any commercial or financial relationships that could be construed as a potential conflict of interest.

Publisher's Note: All claims expressed in this article are solely those of the authors and do not necessarily represent those of their affiliated organizations, or those of the publisher, the editors and the reviewers. Any product that may be evaluated in this article, or claim that may be made by its manufacturer, is not guaranteed or endorsed by the publisher.

frontiers in Cardiovascular Medicine

ORIGINAL RESEARCH
published: 20 May 2021
doi: 10.3389/fcvm.2021.665624

Intra-Discrete Typing Unit TcV Genetic Variability of *Trypanosoma cruzi* in Chronic Chagas' Disease Bolivian Immigrant Patients in Barcelona, Spain

Maykon Tavares de Oliveira[1,2], Elena Sulleiro[3], Maria Cláudia da Silva[4], Aroa Silgado[3], Marta de Lana[5], João Santana da Silva[6], Israel Molina[1†] and J. Antônio Marin-Neto[2†]*

[1] Department of Infectious Diseases, Vall d'Hebron University Hospital, Universitat Autònoma de Barcelona, PROSICS Barcelona, Barcelona, Spain, [2] Cardiology Division, Department of Internal Medicine, Medical School of Ribeirão Preto, University of São Paulo, São Paulo, Brazil, [3] Department of Microbiology, Vall d'Hebron University Hospital, Universitat Autònoma de Barcelona, PROSICS Barcelona, Barcelona, Spain, [4] Department of Biochemistry and Immunology, Ribeirão Preto Medical School, University of São Paulo, São Paulo, Brazil, [5] Pharmacy School and Center of Research in Biological Sciences, Federal University of Ouro Preto, Ouro Preto, Brazil, [6] Fiocruz-Bi-Institutional Translational Medicine Plataform, Ribeirão Preto, Brazil

OPEN ACCESS

Edited by:
Walderez Ornelas Dutra, Federal University of Minas Gerais, Brazil

Reviewed by:
Luisa Magalhaes, Universidade Federal de Minas Gerais, Brazil
Lúcia Maria Da Cunha Galvão, Federal University of Rio Grande do Norte, Brazil

***Correspondence:**
Maykon Tavares de Oliveira
maykontavares@yahoo.com.br

†These authors share last authorship

Specialty section:
This article was submitted to General Cardiovascular Medicine, a section of the journal Frontiers in Cardiovascular Medicine

Received: *08 February 2021*
Accepted: *20 April 2021*
Published: *20 May 2021*

Citation:
Oliveira MT, Sulleiro E, Silva MCd, Silgado A, de Lana M, da Silva JS, Molina I and Marin-Neto JA (2021) Intra-Discrete Typing Unit TcV Genetic Variability of Trypanosoma cruzi in Chronic Chagas' Disease Bolivian Immigrant Patients in Barcelona, Spain. Front. Cardiovasc. Med. 8:665624. doi: 10.3389/fcvm.2021.665624

Background: *Trypanosoma cruzi* has a high rate of biological and genetic variability, and its population structure is divided into seven distinct genetic groups (TcI-TcVI and Tcbat). Due to immigration, Chagas disease (ChD), caused by *T. cruzi*, has become a serious global health problem including in Europe. Therefore, the aim of this study was to evaluate the existence of genetic variability within discrete typing unit (DTU) TcV of *T. cruzi* in Bolivian patients with chronic ChD residing in Barcelona, Spain.

Methods: The DNA was extracted from the peripheral blood of 27 patients infected with *T. cruzi* DTU TcV and the fragments of the genetic material were amplificated through the low stringency single primer-polymerase chain reaction (LSSP-PCR). The data generated after amplification were submitted to bioinformatics analysis.

Results: Of the 27 patients evaluated in the study, 8/27 (29.6%) were male and 19/27 (70.4%) female, 17/27 (62.9%) were previously classified with the indeterminate clinical form of Chagas disease and 10/27 (37.1%) with Chagas cardiomyopathy. The LSSP-PCR detected 432 band fragments from 80 to 1,500 bp. The unweighted pair-group method analysis and principal coordinated analysis data demonstrated the existence of three distinct genetic groups with moderate-high rates of intraspecific genetic variability/diversity that had shared parasite's alleles in patients with the indeterminate and cardiomyopathy forms of ChD.

Conclusions: This study demonstrated the existence of a moderate to high rate of intra-DTU TcV variability in *T. cruzi*. Certain alleles of the parasite were associated with

the absence of clinical manifestations in patients harboring the indeterminate form of ChD. These results support the need to search for increasingly specific targets in the genome of *T. cruzi* to be correlated with its main biological properties and clinical features in patients with chronic ChD.

Keywords: Chagas disease, *Trypanosoma cruzi*, DTU TcV, genetic variability, cardiac form

INTRODUCTION

Chagas disease (ChD) is caused by the hemoflagellate protozoan *Trypanosoma cruzi* and chronic Chagas cardiomyopathy is the most severe manifestation (1). According to recent data from the World Health Organization (WHO), ∼6 to 7 million people are chronically infected with *T. cruzi* worldwide, and more than 75 million individuals are at risk of infection (2).

The genetic structure of *T. cruzi* is currently divided into seven distinct genetic groups, also known as discrete typing units (DTUs), TcI–TcVI, and TcBat (3, 4). *T. cruzi* presents a high rate of biological and genetic variability (5) and these differences may be linked to the main biological parameters of the different strains of *T. cruzi*, such as geographical distribution and human clinical manifestations of ChD. However, no previous studies have presented sufficient data to confirm effectively such potential correlations (6).

The area of spread of ChD is wide across the American continent. One of the most notable changes in the epidemiology of parasitic diseases in recent decades is the emergence of ChD in European countries, and the associated risk of *T. cruzi* transmission outside endemic areas (7). Europe is currently hosting large immigrant populations, with recent data estimating that immigrant populations represented 8.7% of the total European population in 2010 (8). The prevalence of ChD infection in Latin American immigrants living in Europe is estimated in 4.2%, with the highest prevalence among migrants from Bolivia (18.1%) and Paraguay (5.5%) (9). Population movement over recent years has led to an increased prevalence of ChD in these countries, primarily due to high numbers of Latin American immigrants chronically infected with *T. cruzi* (10).

Although direct vector transmission cannot occur in Europe, ChD can be transmitted in non-endemic countries *via* blood transfusion and organs transplantation, or even vertical transmission (9). Measures to control vertical transmission have been designed and implemented in some countries to avoid spreading ChD in Europe, although these measures have not been shown to be entirely viable (11).

Assessing the real burden and implications for public health of ChD in European countries is crucial. Therefore, this study aimed to evaluate the intraspecific genetic variability of DTU TcV from *T. cruzi* in immigrant patients with chronic ChD residing in Barcelona, Spain, and to correlate the genetic differences intra-DTU with the correspondent clinical forms of ChD.

MATERIALS AND METHODS

Patients and Blood Samples

Were evaluated twenty-seven patients with ChD infected by DTU TcV previously genotyped by our group (12). Diagnosis of ChD was confirmed for all 27 patients *via* two positive serological tests and real-time PCR, according to the WHO recommendations. All patients were clinically evaluated at Vall d'Hebron University Hospital, Barcelona, Spain, between 2015 and 2019. From all patients, 5 mL of peripheral blood were collected and mixed with an equal volume of guanidine 6 M/EDTA 0.2 M pH 8 (13). The Guanidine-EDTA Blood lysates (GEB) were boiled for 15 min, incubated at room temperature for 24 h, and stored at 4°C until use (14).

Extraction of DNA From Blood/Guanidine and EDTA Samples

DNA was extracted from 200 μL of guanidine/EDTA blood (GEB) samples and eluted in 55 μL using the NucliSens easyMAG® system (Biomerieux, France), according to the manufacturer's instructions.

Clinical Evaluation of Patients

The 27 patients with positive serology and real-time PCR for ChD, were clinically evaluated at the Infectious Diseases Division, Vall d'Hebron University Hospital, Barcelona, Spain, through anamnesis, 12-lead electrocardiogram, chest, esophageal, and colon X-rays, and rest transthoracic echocardiography. The patients were classified as having different clinical forms of chronic ChD (15, 16).

Intra-DTU TcV Genetic Variability

To assess the intraspecific genetic variability of the previously genotyped *T. cruzi* DTU TcV (11) present in the peripheral blood of patients with chronic ChD, low stringency single primer (LSSP-PCR) methodology (17) was performed. To obtain the genetic signature of *T. cruzi* kDNA, the following steps were performed: (A) amplification of the 330 bp fragment specific to *T. cruzi* kDNA (18). The amplified products were run on a 1.5% agarose gel (Sigma®), stained with Syber (Midori Green Advanced DNA Strain, Nippon Genetics Europe Gmbh) and viewed on the Biorad photo documentation platform (Molecular Imager, Gel DOC XR, Imaging System). The 330 bp fragments were removed from the agarose gel, heated to 100°C, and diluted in ultrapure water at a 1:10 dilution. (B) DNA of the diluted 330 bp band fragments was subjected to a new amplification cycle using the LSSP-PCR technique with the S35G* primer (5′-AAA TAA TGT ACG GGG GAG AT-3′). A volume of 1 μL of diluted DNA was added to the 10 μL of the reaction mixture containing 6.38 μL of sterile milli-Q water, 2.0 μL of sample buffer, 0.2 μL of each deoxynucleotide (dATP, dCTP, dGTP, and dTTP–Sigma, St. Louis, MO, USA), 0.1 μL of the S35G * primer (450 μM), and 0.32 μL of Taq DNA polymerase (Go Taq-Promega) (18). Amplification occurred under the following conditions: an initial DNA denaturation stage at 95°C for 5 min, annealing at 30°C

for 1 min, and extension at 72°C for 1 min, followed by 40 amplification cycles consisting of a denaturation step at 94°C for 1 min, one cycle of annealing at 30°C for 1 min, followed by a final extension step at 72°C for 10 min. The LSSP-PCR products were separated in 6% polyacrylamide gel electrophoresis and revealed with NaOH and formaldehyde after silver staining (19). After photo documentation the differences in the patterns of band profiles were analyzed *via* bioinformatics tests.

Bioinformatics Analysis

The LSSP-PCR profiles were used to build a presence/absence matrix of each visualized band, allowing a similarity analysis to be built using NTSYSpc software. The relationships between *T. cruzi* strains were estimated using a dendrogram representative of the LSSP-PCR data. These were constructed based on the coefficient of association (20) and the analysis of unweighted peer groups [unweighted pair-group method analysis (UPGMA)] using Mega 6.04 Beta software. To estimate Shannon's diversity, the cophenetic correlation coefficient, heterozygosity by locus (He), and principal coordinated analysis (PCoA) were performed using the GenAlEx 6.5 software. In this case, a genetic distance matrix was built. This calculation of genetic distances took place in pairs for binaries. Data followed the methods of Huff and collaborators (21), wherein any comparison with the same state generates a value of 0 (for both 0 vs. 0 comparisons and comparisons 1 vs. 1), while any comparison of different states (0 vs. 1 or 1 vs. 0) generates a value of 1.

Ethical Approval

This study was approved by the Human Research Ethics Committee of the Vall d'Hebron University Hospital. All patients who agreed to participate in the study signed an informed consent form.

RESULTS

Patient Characteristics

This study included 27 patients with chronic ChD, identified *via* positive serology (IgG anti-*T. cruzi*) and real-time PCR for ChD, who were clinically managed at the Infectious Disease Clinic of the Vall d'Hebron University Hospital, Barcelona, Spain between 2015 and 2019. All patients reside in Barcelona, Spain, and are immigrants from Bolivia, 8/27 (29.6%) being male and 19/27 (70.4%) female (**Table 1**). The mean age of the patients was 47.1 ± 12.44 years (**Table 1**). Taking into account clinical features, echocardiography (ECG) and radiological exams, 17/27 (62.9%) of the patients, presented the indeterminate form of ChD and 10/27 (37.1%) the cardiomyopathy form. All patients with Chagas cardiomyopathy' were categorized in stage B1 of clinical evolution according to the European Society of Cardiology (13). No patient had the digestive, nervous, or mixed clinical forms of ChD.

TABLE 1 | General information of patients with Chagas disease involved in the study.

Sample code	Age (years)	Gender	Clinical form	DTU
1	32	F	Cardiac	TcV
2	27	F	Indeterminate	TcV
3	43	M	Cardiac	TcV
4	65	F	Cardiac	TcV
5	68	F	Cardiac	TcV
6	39	M	Indeterminate	TcV
7	60	F	Indeterminate	TcV
8	41	M	Indeterminate	TcV
9	46	M	Indeterminate	TcV
10	38	F	Cardiac	TcV
11	56	F	Indeterminate	TcV
12	67	F	Indeterminate	TcV
13	35	M	Indeterminate	TcV
14	44	F	Indeterminate	TcV
15	56	F	Indeterminate	TcV
16	28	M	Indeterminate	TcV
17	27	F	Indeterminate	TcV
18	39	F	Indeterminate	TcV
19	37	F	Indeterminate	TcV
20	56	F	Indeterminate	TcV
21	60	F	Cardiac	TcV
22	53	F	Cardiac	TcV
23	56	F	Indeterminate	TcV
24	44	M	Cardiac	TcV
25	62	M	Cardiac	TcV
26	43	F	Cardiac	TcV
27	50	F	Indeterminate	TcV

F, Female; M, Male; TcV, T. cruzi DTU; DTU, Discrete Typing Unit.

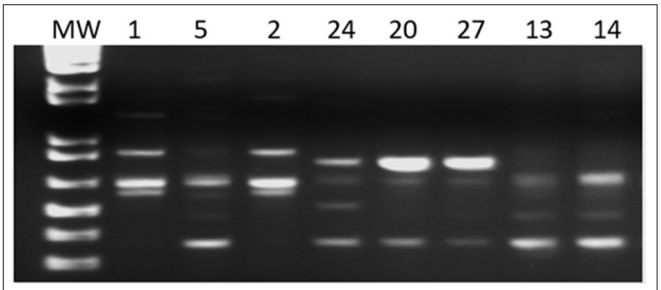

FIGURE 1 | Gel representative of the amplified products of the LSSP-PCR. MW–Molecular Weight: 1 kb; 1, 5, 2, 24, 20, 27, 13, and 14 patient samples.

Intra DTU TcV Genetic Variability of *Trypanosoma cruzi*

The LSSP-PCR analysis showed that the reaction amplified the 330 pb fragment of the *T. cruzi* kDNA in all 27 DNA samples from patients infected with TcV DTU. After the second amplification cycle, a total of 432 fragments were detected, and the products amplified were evaluated. The sizes of the bands varied between 80 and 1,500 bp (**Figure 1**). Sixteen profiles of the amplified products of the LSSP-PCR were obtained and only one (6.25%) was shared among all samples. The percentage of polymorphic loci was 93.84%, demonstrating the

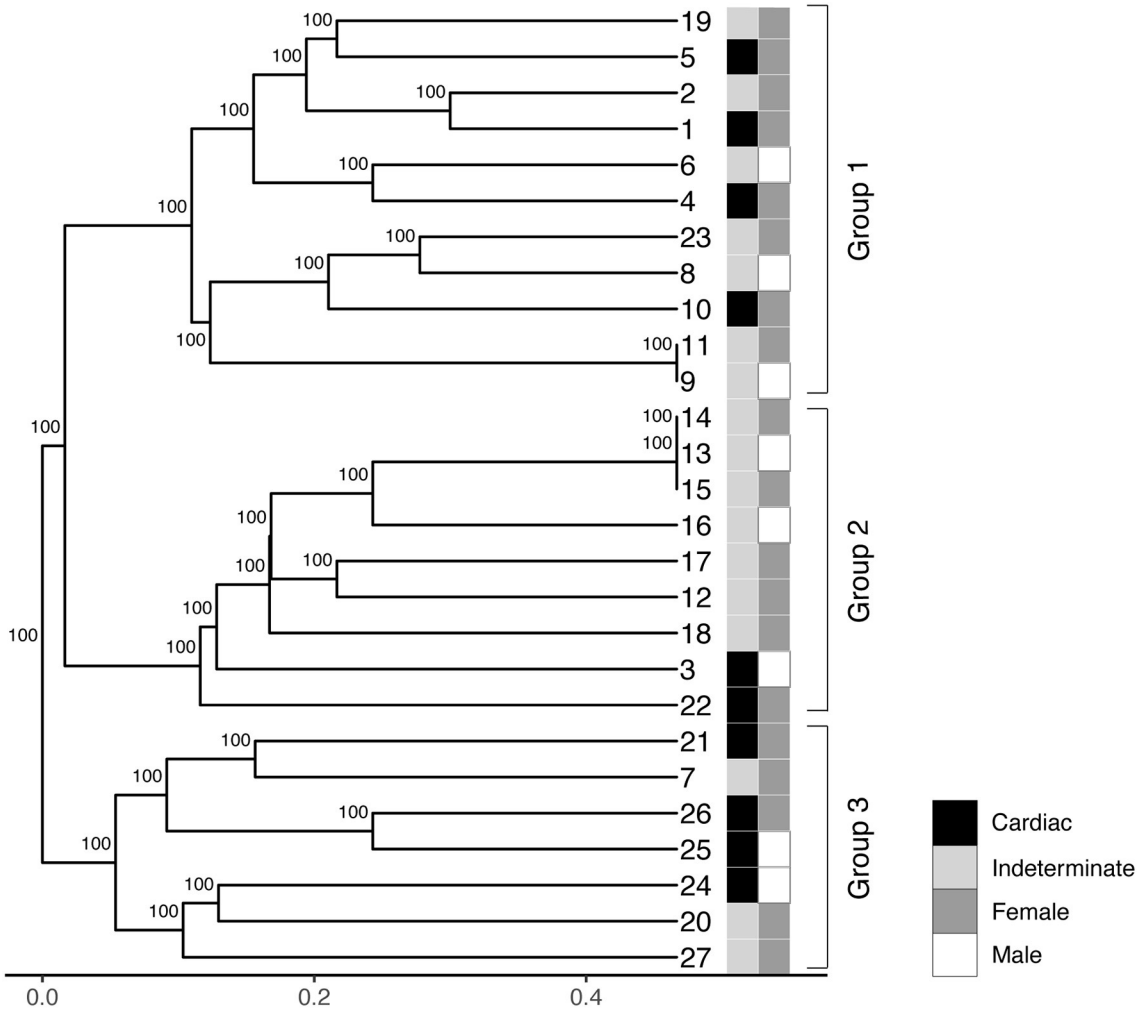

FIGURE 2 | Phenogram containing UPGMA (unweighted pair-group method analysis) of the 27 samples of *T. cruzi* belonging to DTU TcV. The numbers on the horizontal scale were obtained from the similarity coefficient of data. Different colors represent the clinical forms (indeterminate and cardiac) and gender of each patient (male or female).

existence of a high rate of genetic variability among the samples. The cophenetic correlation coefficient, which verifies that the dendrogram preserved the distances in pairs between the original unmodeled data points, obtained a value of 0.851, confirming the high representation of the similarity matrices in the dendrogram. The UPGMA dendrogram distinguished *T. cruzi* DTU TcV samples into three distinct groups (**Figure 2**). Patients with the indeterminate form of ChD were clearly grouped in two groups (group 1 and 2) of the dendrogram, what showed that the genomes of these protozoa share certain alleles that may indicate common genetic characteristics and less intraspecific variability. For patients with the cardiac form of ChD, no sharing of distinct alleles was observed, indicating a higher rate of intraspecific genetic variability and complexity (**Figure 2**).

The DICE similarity coefficient corroborated the data contained in the dendrogram and UPGMA. This analysis was used to assess the variability of alleles in each sample in the range 0 to ± 1 (**Figure 3**). When comparing DNA samples from patients with the Indeterminate clinical form of Chagas disease, it was observed that the color intensity in **Figure 3** tends to become darker, approaching the number 1 staining score. This may indicate a high degree of similarity between these samples.

The analysis of the principal coordinated analysis (PCoA) in the two axes demonstrated 80.30% (35.1 + 45.2%) of the variability between the components (**Figure 4**) and, in total, three distinct groups were formed, as shown in the UPGMA dendrogram. The average expected He was 0.296, indicative of moderate-high genetic diversity among the 27 samples. In addition, Shannon Weaver's diversity index (H′ = 3,159), a quantitative measure that defines the genetic diversity of species taking into account their variability, was also considered moderate to high. This assessment was used to describe the richness of the intra-DTU TcV variability of *T. cruzi*.

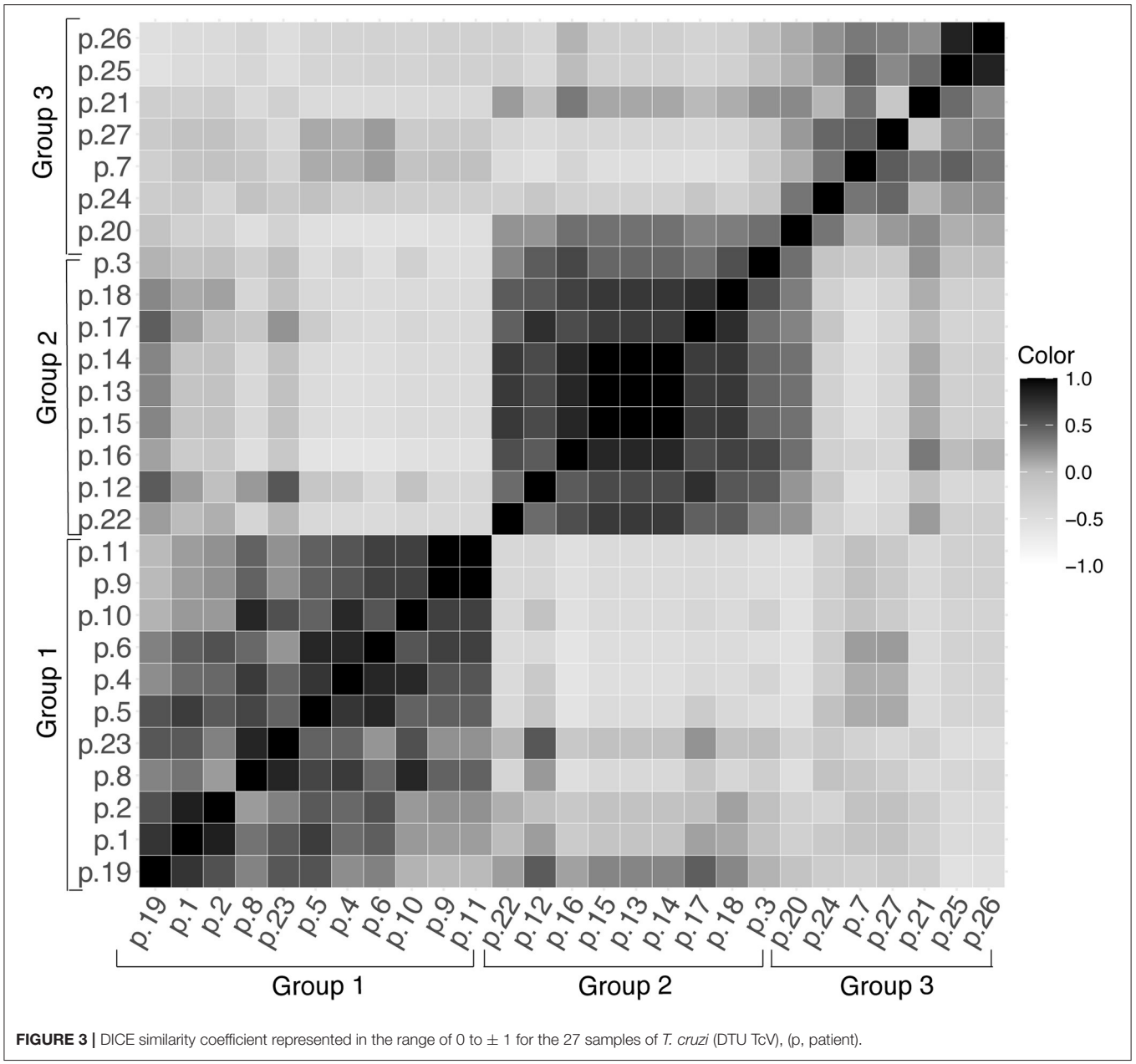

FIGURE 3 | DICE similarity coefficient represented in the range of 0 to ± 1 for the 27 samples of *T. cruzi* (DTU TcV), (p, patient).

DISCUSSION

Trypanosoma Cruzi specie includes heterogeneous subpopulations that circulate in both domestic and wild cycles (22), and this diversity can be observed at the morphological (23), biological, antigenic (24), and genetic (5, 25) levels. Moreover, *T. cruzi* is currently subdivided into seven distinct genetic groups (DTUs TcI-TcVI and Tcbat) (4), and each DTU has its own characteristics (3). In order to better understand the disease in each geographical region it is necessary to study the molecular epidemiology of this parasite, inherently related to the main biological characteristics, which consequently have clinical implications on Chagas disease clinical features and evolution.

ChD is endemic in Latin America; however, the epidemiology of this infection has changed, mainly due to recent population migration for countries of distinct continents. At present, ChD is an important public health problem in other non-endemic regions, such as Europe (8). Immigration to Europe from Latin American countries has increased steadily over the last 2 years, especially to southern European countries, such as Spain and Italy. More recently, there is evidence for Latin American immigration to northern countries in Europe as well (10, 26). These population movements have increased the occurrence of ChD in these countries (9), since a considerable proportion of Latin American immigrants are chronically infected with *T. cruzi*, added to the occurrence of autochthone

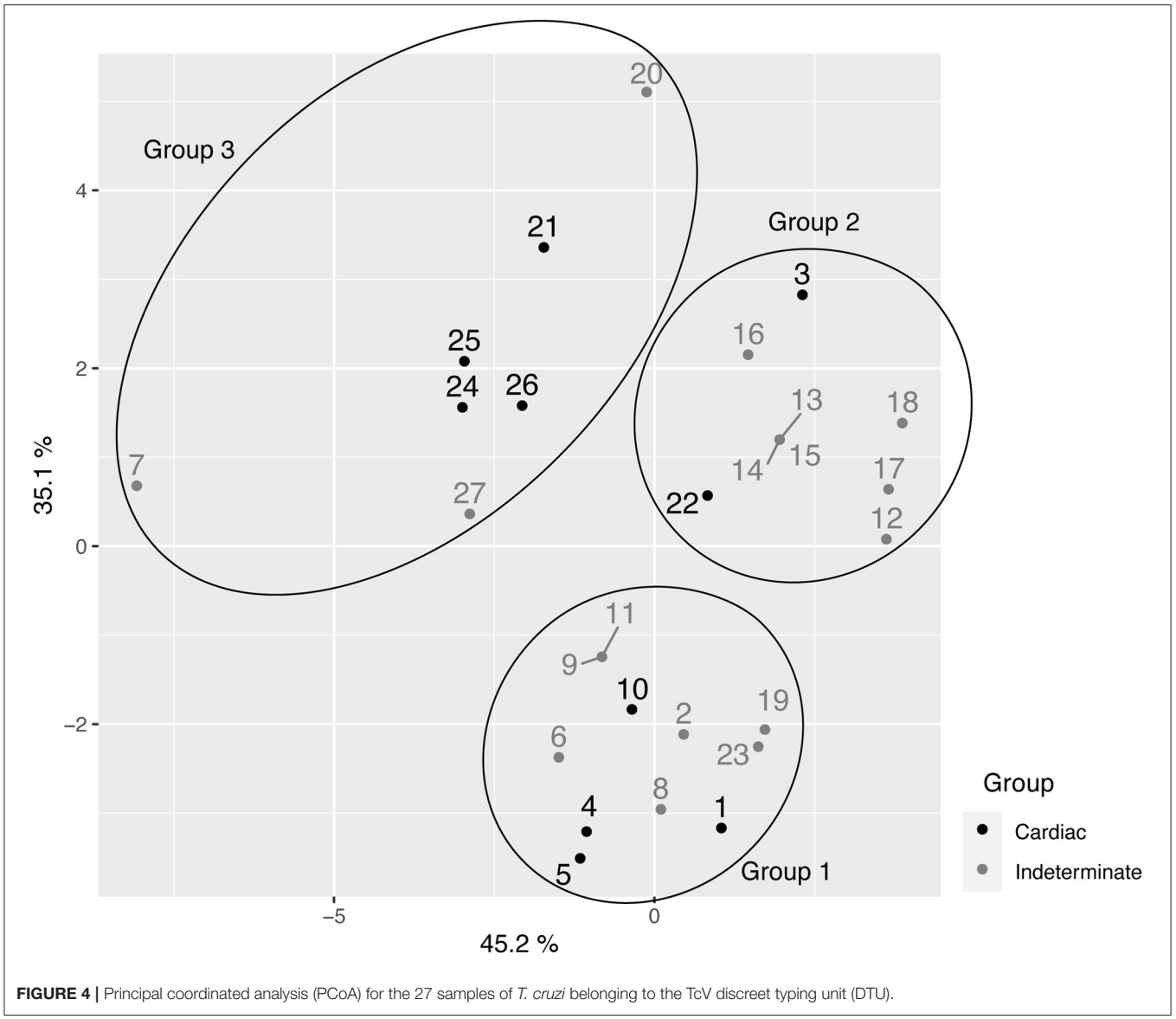

FIGURE 4 | Principal coordinated analysis (PCoA) for the 27 samples of *T. cruzi* belonging to the TcV discreet typing unit (DTU).

cases transmitted by mechanisms independent to triatomine vectors. Consequently, the number of reported cases of ChD with or without cardiac involvement has increased dramatically in recent years, especially in European countries, such as Spain, Italy, and Switzerland, where most Latino immigrants have settled (27, 28). Thus, studies aiming to evaluate the possible association between the intraspecific genetic variability of *T. cruzi* with the specific clinical forms of ChD are necessary.

It is known that DTU TcV is closely related to the domestic cycle of ChD associated with human disease in countries such as Argentina, Bolivia, Chile and Paraguay (6). This genotype is related to the presentation of clinical cardiac and digestive symptoms in patients from countries in the southern cone and little is known about their natural mammalian reservoirs (3). Previous studies have demonstrating the existence of genetic variability within TcI (29) and TcII (30) isolates. In the present study, a pioneering moderate-high rate of genetic variability within DTU TcV of *T. cruzi in a* specific population of Bolivian immigrants in Spain was assessed by LSSP-PCR. Furthermore, an association was detected between the indeterminate form of ChD and sharing certain alleles present in the parasite's genome.

It is relevant to emphasize that the LSSP-PCR methodology had been described and widely used to identify *T. cruzi* underlines before the first genotyping criteria emerged in 2009 (31–33). Burgos and collaborators used this methodology to evaluate the decrease of certain subclasses of the parasite kDNA minicircles in the peripheral blood and brain tissue of a patient infected with human immunodeficiency virus and with *T. cruzi* (TcII) during treatment for Chagas disease (34). Similarly, Costales and collaborators employed LSSP-PCR to investigate the presence of polyclonal infection of the parasite belonging to the TcI genotype in a cardiomyopathic

patient with reactivation of the infection after heart transplantation (35).

Lages-Silva et al. (30) also tried to establish the association of intra-DTU genetic variability with the different clinical manifestations of patients infected with *T. cruzi*. It is worth mentioning that the authors used the same molecular technique (LSSP-PCR) employing different genes, and as in the present study, they were unable to detect an effective correlation, what demonstrated the need to search for genetic targets that are increasingly intrinsic in the parasite's genome. In the work involving DTU TcI (29), the study group sought to assess the association between the TcI genotype and the home and wild distribution of the genetic lineage in its hosts and biological aspects of the strains. It is worth mentioning that the TcV DTU is a hybrid strain, originating from several hybridization processes between TcI and TcII, with loss of heterozygosity between the progeny to produce TcIII and TcIV, followed by a second more recent hybridization event between TcII and TcIII to produce both, TcV and TcVI (36).

Lima and collaborators evaluated a family with two generations of patients with chronic ChD infected with DTU TcII, and attempted to establish the DTU/clinical forms correlation. However, no satisfactory results were obtained, possibly due to the low number of clinical samples. Despite of similarly to the present study, in addition, they reported low genetic variability/diversity in samples of the parasite belonging to the TcII genotype (37).

In our study the UPGMA analysis of the samples demonstrated the existence of three large groups within the *T. cruzi* TcV genotype, including a high rate of intraspecific genetic variability/diversity of this DTU. Similar data were obtained by some of us using *T. cruzi* DTU TcII and TcVI genotypes (38). We demonstrated, through UPGMA and PCoA of random amplification of polymorphic DNA, the existence of a high rate of genetic variability within DTU TcII and TcVI of *T. cruzi* in samples from patients with chronic ChD residing in an important endemic region of Minas Gerais state, Brazil.

Additionally, in accordance with the UPGMA results of our study, Macchiaverna and collaborators showed that the sequencing data of the *T. cruzi* TcMK (mevalonate kinase) gene in clinical samples from chronic patients in Argentina, revealed a low rate of genetic variability within the DTU TcV, and showing apparently two robust subgroups of isolates (39).

Few studies have undertaken a more detailed intra-DTU approach in an attempt to detect the appropriate correlations with the clinical forms of ChD presented by the patients. A more common approach has been to search correlation between *T. cruzi* DTUs and the clinical forms of ChD. However, it is reasonable to speculate that small genetic modifications or alterations in parasite genomes at intra-DTU level may be more related to the induction of distinct clinical manifestations of this disease, and even responses to a specific treatment against the *T. cruzi,* favoring a better understanding of the clinical and epidemiological aspects of this disease in endemic and non-endemic regions.

Therefore, knowing the genetic variability of *T. cruzi* intra-DTU TcV in immigrant patients with chronic ChD residing in Barcelona, Spain, is crucial to understanding the public health implications of ChD in European countries. Improving this understanding could contribute for the adequate design and planning of more effective public health interventions to improve the health of the immigrants and control the vertical transmission of ChD, which is a serious problem in Europe nowadays.

CONCLUSIONS

This study demonstrated the existence of a moderate to high rate of intra-DTU TcV variability in *T. cruzi*, in a specific population of Bolivian immigrants in Spain. Being demonstrated association of sharing of certain alleles of the parasite with the absence of clinical manifestations in patients harboring the indeterminate clinical form of ChD, a trend to be assessed in a larger population. The information provided in this study could affect the planning of more effective public health interventions to improve the health of immigrants, vertical transmission control, and improvement of ChD treatment in countries with predominance of infection by TcV genotype. The results of this study support the need to search for increasingly intrinsic and specific targets in the genome of *T. cruzi* to be correlated with its main biological properties and clinical features in patients with chronic ChD.

DATA AVAILABILITY STATEMENT

The original contributions presented in the study are included in the article/supplementary material, further inquiries can be directed to the corresponding author/s.

ETHICS STATEMENT

The studies involving human participants were reviewed and approved by Human Research Ethics Committee of the Vall d'Hebron University Hospital. The patients/participants provided their written informed consent to participate in this study.

AUTHOR CONTRIBUTIONS

MO, ES, AS, and IM: conceptualization. MO, ES, and IM: data curation. MO: formal analysis, validation, and writing—original draft. MO and JM-N: funding acquisition. MO, ML, and JS: investigation. MO, ES, and AS: methodology. JM-N and IM: project administration and supervision. MO, ES, ML, and IM: resources. MO, ES, AS, ML, JM-N, and IM: visualization. MO, MS, ML, JS, JM-N, and IM: writing—review and editing. All authors contributed to the article and approved the submitted version.

FUNDING

This work was supported by São Paulo Research Foundation (FAPESP)- fapesp.br/en (Grant No. 2018/22093-4), São Paulo Research Foundation (FAPESP)- fapesp.br/en (Grant No.

2019/11943-0), São Paulo Research Foundation (FAPESP)-fapesp.br/en (Grant No. 2016/25403-9), and Universitat Autònoma de Barcelona, Vall d'Hebron University Hospital, PROSICS Barcelona, Spain.

ACKNOWLEDGMENTS

We thank Pilar Alcubilla for her technical support and Mercedes Guerrero Murillo for bioinformatics analysis.

REFERENCES

1. Rassi A, Rassi A, Marcondes de Rezende J. American trypanosomiasis (Chagas disease). *Infect Dis Clin North Am.* (2012) 26:275–91. doi: 10.1016/j.idc.2012.03.002
2. WHO. *Chagas Disease* (*American trypanosomiasis*). Fact sheet No. 340. WHO (2018).
3. Zingales B. *Trypanosoma cruzi* genetic diversity: something new for something known about Chagas disease manifestations, serodiagnosis and drug sensitivity. *Acta Trop.* (2018) 184:38–52. doi: 10.1016/j.actatropica.2017.09.017
4. Zingales B, Andrade SG, Briones MRS, Campbell DA, Chiari E, Fernandes O, et al. A new consensus for *Trypanosoma cruzi* intraspecific nomenclature: second revision meeting recommends TcI to TcVI. *Mem Inst Oswaldo Cruz.* (2009) 104:1051–4. doi: 10.1590/S0074-02762009000700021
5. Tibayrenc M. Genetic subdivisions within *Trypanosoma cruzi* (discrete typing units) and their relevance for molecular epidemiology and experimental evolution. *Kinetoplastid Biol Dis.* (2003) 2:12. doi: 10.1186/1475-9292-2-12
6. Zingales B, Miles MA, Campbell DA, Tibayrenc M, Macedo AM, Teixeira MMG, et al. The revised *Trypanosoma cruzi* subspecific nomenclature: rationale, epidemiological relevance and research applications. *Infect Genet Evol.* (2012) 12:240–53. doi: 10.1016/j.meegid.2011.12.009
7. Requena-Méndez A, Aldasoro E, de Lazzari E, Sicuri E, Brown M, Moore DAJ, et al. Prevalence of chagas disease in Latin-American migrants living in Europe: a systematic review and meta-analysis. *PLoS Negl Trop Dis.* (2015) 9:e0003540. doi: 10.1371/journal.pntd.0003540
8. Rechel B, Mladovsky P, Ingleby D, Mackenbach JP, McKee M. Migration and health in an increasingly diverse Europe. *Lancet.* (2013) 381:1235–45. doi: 10.1016/S0140-6736(12)62086-8
9. Pérez-Molina JA, Molina I. Chagas disease. *Lancet.* (2018) 391:82–94. doi: 10.1016/S0140-6736(17)31612-4
10. Basile L, Jansà JM, Carlier Y, Salamanca DD, Angheben A, Bartoloni A, et al. Chagas disease in european countries: the challenge of a surveillance system. *Eurosurveillance.* (2011) 16:3. doi: 10.2807/ese.16.37.19968-en
11. Muñoz J, Coll O, Juncosa T, Vergés M, Pino M Del, Fumado V, et al. Prevalence and vertical transmission of *Trypanosoma cruzi* infection among pregnant latin american women attending 2 maternity clinics in barcelona, spain. *Clin Infect Dis.* (2009) 48:1736–40. doi: 10.1086/599223
12. de Oliveira MT, Sulleiro E, Gimenez AS, de Lana M, Zingales B, da Silva JS, et al. Quantification of parasite burden of *Trypanosoma cruzi* and identification of discrete typing units (Dtus) in blood samples of latin american immigrants residing in Barcelona, Spain. *PLoS Negl Trop Dis.* (2020) 14:e0008311. doi: 10.1371/journal.pntd.0008311
13. Avila HA, Sigman DS, Cohen LM, Millikan RC, Simpson L. Polymerase chain reaction amplification of *Trypanosoma cruzi* kinetoplast minicircle DNA isolated from whole blood lysates: diagnosis of chronic Chagas' disease. *Mol Biochem Parasitol.* (1991) 48:11–21. doi: 10.1016/0166-6851(91)90116-n
14. Britto C, Cardoso MA, Wincker P, Morel CM. A simple protocol for the physical cleavage of *Trypanosoma cruzi* kinetoplast DNA present in blood samples and its use in polymerase chain reaction (PCR)-based diagnosis of chronic Chagas disease. *Mem Inst Oswaldo Cruz.* (1993) 88:171–2. doi: 10.1590/s0074-02761993000100030
15. Dias JCP, Ramos AN, Gontijo ED, Luquetti A, Shikanai-Yasuda MA, Coura JR, et al. Aspectos Gerais da epidemiologia da doença de chagas com especial atenção ao Brasil. *Epidemiol Serv Saude Rev Sist Unico Saude Bras.* (2016) 25:7–86. doi: 10.5123/S1679-49742016000500002
16. Mora G. Chagas cardiomyopathy. *E J Cardiol Pract?* (2016) 14:31–28. https://www.escardio.org/Journals/E-Journal-of-Cardiology-Practice/Volume-14/Chagas-cardiomyopathy
17. Vago AR, Macedo AM, Oliveira RP, Andrade LO, Chiari E, Galvão LMC, et al. Kinetoplast DNA signatures of *Trypanosoma cruzi* strains obtained directly from infected tissues. *Am J Pathol.* (1996) 149:2153–59.
18. Gomes ML, Macedo AM, Vago AR, Pena SDJ, Galvão LMC, Chiari E. *Trypanosoma cruzi*: optimization of polymerase chain reaction for detection in human blood. *Exp Parasitol.* (1998) 88:28–33. doi: 10.1006/expr.1998.4191
19. Santos FR, Pena SDJ, Epplen JT. Genetic and population study of a Y-linked tetranucleotide repeat DNA polymorphism with a simple non-isotopic technique. *Hum Genet.* (1993) 90:655–6. doi: 10.1007/BF00202486
20. Dice LR. Measures of the amount of ecologic association between species. *Ecology.* (1945) 26:297–302. doi: 10.2307/1932409
21. Huff DR, Peakall R, Smouse PE. RAPD variation within and among natural populations of outcrossing buffalograss [Buchloë dactyloides (Nutt.) Engelm.]. *Theor Appl Genet.* (1993) 86:927–34. doi: 10.1007/BF00211043
22. Tibayrenc M, Ward P, Moya A, Ayala FJ. Natural populations of *Trypanosoma cruzi*, the agent of Chagas disease, have a complex multiclonal structure. *Proc Natl Acad Sci USA.* (1986) 83:115–9. doi: 10.1073/pnas.83.1.115
23. Brener Z, Chiari E. Varia C Oes morfol'ogicas observadas em diferentes amostras DE. *Rev Inst Med Trop São Paulo.* (1963) 19:220–224.
24. Maguire JH, Hoff R, Sleigh AC, Mott KE, Ramos NB, Sherlock IA. An outbreak of Chagas' disease in southwestern Bahia, Brazil. *Am J Trop Med Hyg.* (1986) 35:931–6. doi: 10.4269/ajtmh.1986.35.931
25. Tibayrenc M, Ayala FJ. The population genetics of *Trypanosoma cruzi* revisited in the light of the predominant clonal evolution model. *Acta Trop.* (2015) 151:156–65. doi: 10.1016/j.actatropica.2015.05.006
26. Gascon J, Bern C, Pinazo MJ. Chagas disease in Spain, the United States and other non-endemic countries. *Acta Trop.* (2010) 115:22–7. doi: 10.1016/j.actatropica.2009.07.019
27. Jackson Y, Gétaz L, Wolff H, Holst M, Mauris A, Tardin A, et al. Prevalence, clinical staging and risk for blood-borne transmission of chagas disease among Latin American migrants in Geneva, Switzerland. *PLoS Negl Trop Dis.* (2010) 4:e592. doi: 10.1371/journal.pntd.0000592
28. Coura JR, Vias PA. Chagas disease: a new worldwide challenge. *Nature.* (2010) 465:S6–7. doi: 10.1038/nature09221
29. León CM, Hernández C, Montilla M, Ramírez JD. Retrospective distribution of *Trypanosoma cruzi* I genotypes in Colombia. *Mem Inst Oswaldo Cruz.* (2015) 110:387–93. doi: 10.1590/0074-02760140402
30. Lages-Silva E, Ramírez LE, Pedrosa AL, Crema E, Da Cunha Galvão LM, Pena SDJ, et al. Variability of kinetoplast DNA gene signatures of *Trypanosoma cruzi* II strains from patients with different clinical forms of Chagas' disease in Brazil. *J Clin Microbiol.* (2006) 44:2167–71. doi: 10.1128/JCM.02124-05
31. Vago AR, Andrade LO, Leite AA, d'Ávila Reis D, Macedo AM, Adad SJ, et al., Filho GB, Pena SDJ. Genetic characterization of *Trypanosoma cruzi* directly from tissues of patients with chronic chagas disease: differential distribution of genetic types into diverse organs. *Am J Pathol.* (2000) 156:1805–9. doi: 10.1016/S0002-9440(10)65052-3
32. Franco DJ, Vago AR, Chiari E, Meira FCA, Galvão LMC, Machado CRS. *Trypanosoma cruzi*: mixture of two populations can modify virulence and tissue tropism in rat. *Exp Parasitol.* (2003) 104:54–61. doi: 10.1016/S0014-4894(03)00119-X
33. Segatto M, Rodrigues CM, Machado CR, Franco GR, Pena SDJ, Macedo AM. LSSP-PCR of *Trypanosoma cruzi*: how the single primer sequence affects the kDNA signature. *BMC Res Notes.* (2013) 6:174. doi: 10.1186/1756-0500-6-174
34. Burgos JM, Begher SB, Freitas JM, Bisio M, Duffy T, Altcheh J, et al. Molecular diagnosis and typing of *Trypanosoma cruzi* populations and lineages in cerebral chagas disease in a patient with AIDS. *Am J Trop Med Hyg.* (2005) 73:1016–8. doi: 10.4269/ajtmh.2005.73.1016
35. Costales JA, Kotton CN, Zurita-Leal AC, Garcia-Perez J, Llewellyn MS, Messenger LA, et al. Chagas disease reactivation in a heart transplant patient

infected by domestic *Trypanosoma cruzi* discrete typing unit i (TcIDOM). *Parasit Vect.* (2015) 8:435. doi: 10.1186/s13071-015-1039-3
36. Freitas JM, Augusto-Pinto L, Pimenta JR, Bastos-Rodrigues L, Gonçalves VF, Teixeira SMR, et al. Ancestral genomes, sex, and the population structure of *Trypanosoma cruzi*. *Plos Pathog.* (2006) 2:e24. doi: 10.1371/journal.ppat.0020024
37. Lima APB, de Oliveira MT, Silva RR, Torres RM, Veloso VM, de Lana M, et al. Evaluation of parasite and host genetics in two generations of a family with Chagas disease. *Parasitol Res.* (2018) 117:3009–13. doi: 10.1007/s00436-018-5969-5
38. De Oliveira MT, MacHado De Assis GF, Oliveira E Silva JCV, MacHado EMM, Da Silva GN, Veloso VM, et al. *Trypanosoma cruzi* Discret Typing Units (TcII and TcVI) in samples of patients from two municipalities of the Jequitinhonha Valley, MG, Brazil, using two molecular typing strategies. *Parasites and Vectors.* (2015) 8: doi: 10.1186/s13071-015-1161-2
39. Macchiaverna NP, Enriquez GF, Buscaglia CA, Balouz V, Gürtler RE, Cardinal MV. New human isolates of *Trypanosoma cruzi* confirm the predominance of hybrid lineages in domestic transmission cycle of the Argentinean Chaco. *Infect Genet Evol.* (2018) 66:229–35. doi: 10.1016/j.meegid.2018.10.001

Conflict of Interest: The authors declare that the research was conducted in the absence of any commercial or financial relationships that could be construed as a potential conflict of interest.

frontiers in Cardiovascular Medicine

ORIGINAL RESEARCH
published: 25 May 2021
doi: 10.3389/fcvm.2021.667580

Diet Rich in Lard Promotes a Metabolic Environment Favorable to *Trypanosoma cruzi* Growth

Débora Maria Soares de Souza[1,2,3†], Maria Cláudia Silva[4†], Silvia Elvira Barros Farias[1], Ana Paula de J. Menezes[1], Cristiane Maria Milanezi[4], Karine de P. Lúcio[5], Nívia Carolina N. Paiva[6], Paula Melo de Abreu[2], Daniela Caldeira Costa[3,5], Kelerson Mauro de Castro Pinto[1,7], Guilherme de Paula Costa[1,3], João Santana Silva[4,8] and André Talvani[1,3,9]*

[1] Laboratory of Immunobiology of Inflammation, Department of Biological Sciences, Federal University of Ouro Preto, Ouro Preto, Brazil, [2] Biological Science Post-graduate Program, Federal University of Ouro Preto, Ouro Preto, Brazil, [3] Health and Nutrition Post-graduate Program, Federal University of Ouro Preto, Ouro Preto, Brazil, [4] Department of Biochemistry and Immunology, Ribeirão Preto Medical School, University of São Paulo, São Paulo, Brazil, [5] Laboratory of Metabolic Biochemistry, Department of Biological Sciences, Federal University of Ouro Preto, Ouro Preto, Brazil, [6] Center of Research in Biological Sciences, Federal University of Ouro Preto, Ouro Preto, Brazil, [7] School of Physical Education, Federal University of Ouro Preto, Ouro Preto, Brazil, [8] Fiocruz-Bi-Institutional Translational Medicine Plataform, Ribeirão Preto Medical School, University of São Paulo, São Paulo, Brazil, [9] Health Science, Infectology and Tropical Medicine Post-graduate Program, Federal University of Minas Gerais, Belo Horizonte, Brazil

OPEN ACCESS

Edited by:
Livia Passos, Brigham and Women's Hospital and Harvard Medical School, United States

Reviewed by:
Ana Carolina Leao, Baylor College of Medicine, United States
Amelie Vromman, Brigham and Women's Hospital and Harvard Medical School, United States

***Correspondence:**
André Talvani
talvani@ufop.edu.br

[†] These authors have contributed equally to this work

Specialty section:
This article was submitted to General Cardiovascular Medicine, a section of the journal Frontiers in Cardiovascular Medicine

Received: *13 February 2021*
Accepted: *15 April 2021*
Published: *25 May 2021*

Citation:
Souza DMS, Silva MC, Farias SEB, Menezes APJ, Milanezi CM, Lúcio KP, Paiva NCN, Abreu PM, Costa DC, Pinto KMC, Costa GP, Silva JS and Talvani A (2021) Diet Rich in Lard Promotes a Metabolic Environment Favorable to Trypanosoma cruzi Growth. Front. Cardiovasc. Med. 8:667580. doi: 10.3389/fcvm.2021.667580

Background: *Trypanosoma cruzi* is a protozoan parasite that causes Chagas disease and affects 6–7 million people mainly in Latin America and worldwide. Here, we investigated the effects of hyperlipidic diets, mainly composed of olive oil or lard on experimental *T. cruzi* infection. C57BL/6 mice were fed two different dietary types in which the main sources of fatty acids were either monounsaturated (olive oil diet) or saturated (lard diet).

Methods: After 60 days on the diet, mice were infected with 50 trypomastigote forms of *T. cruzi* Colombian strain. We evaluated the systemic and tissue parasitism, tissue inflammation, and the redox status of mice after 30 days of infection.

Results: Lipid levels in the liver of mice fed with the lard diet increased compared with that of the mice fed with olive oil or normolipidic diets. The lard diet group presented with an increased parasitic load in the heart and adipose tissues following infection as well as an increased expression of *Tlr2* and *Tlr9* in the heart. However, no changes were seen in the survival rates across the dietary groups. Infected mice receiving all diets presented comparable levels of recruited inflammatory cells at 30 days post-infection but, at this time, we observed lard diet inducing an overproduction of CCL2 in the cardiac tissue and its inhibition in the adipose tissue. *T. cruzi* infection altered liver antioxidant levels in mice, with the lard diet group demonstrating decreased catalase (CAT) activity compared with that of other dietary groups.

Conclusions: Our data demonstrated that *T. cruzi* growth is more favorable on tissue of mice subjected to the lard diet. Our findings supported our hypothesis of a relationship between the source of dietary lipids and parasite-induced immunopathology.

Keywords: inflammation, *Trypanosoma cruzi*, saturated fatty acids, monounsaturated fatty acids, adipose tissue, cardiac tissue

INTRODUCTION

The protozoan *Trypanosoma cruzi*, the etiological agent of Chagas' disease, affects 6–7 million people worldwide (1). The parasite triggers an intense tissue inflammatory response in the mammalian host (2, 3), which culminates in damage to cardiac cells. The progressive myocarditis is associated with high mortality and morbidity rates (4, 5).

In the absence of an effective pharmacological treatment against the *T. cruzi*, there has been a growing demand for methods that control the parasite replication and regulate the parasite induced immune response to minimize tissue damage in infected hosts (6). In this sense, it has been argued that the nutritional status and dietary quality might be of importance for the regulation of the host immune responses and in the progression of infection (7–9). Diets rich in saturated fatty acids have been linked to increasing adiposity and comorbidities such as diabetes, hypertension, atherosclerosis, as well as interfering in the immune response that favor the growth of *T. cruzi* (10, 11). Diets rich in monounsaturated and polyunsaturated fatty acids are beneficial to the body as they improve cardiac function and modulate the immune system (12, 13).

Considering that *T. cruzi* infection causes a chronic systemic and cardiac pattern of inflammatory response, and different lipids are present in the intra- and extracellular environmental of the parasites, the present study we aimed to investigate the interference of monounsaturated and saturated fatty acid diets in the course of *T. cruzi* infection related inflammation.

MATERIALS AND METHODS

Ethical Approval

All the methodologies performed are in accordance with the standards of the National Council for Control of Animal Experimentation (CONCEA), and were previously approved by the Animal Research Ethics Committee of the Federal University of Ouro Preto (CEUA-UFOP), under the protocol number 36/2015. The experiments comply with the standards of animal research explicit in Law 11.749, of 2008, regulated by Decree No. 6.899, of July 15, 2009.

Animals, Study Design, and Diets

C57BL/6 male mice aged 21-days were used. The animals were divided into groups according to the composition of diet they received: normolipidic diet, monounsaturated fatty acid diet with olive oil (olive oil diet) and saturated fatty acid diet with lard (lard diet) (**Table 1**). The diets administration was initiated after weaning and, after 60 days of diet, mice were infected with *T. cruzi*. The analyses were performed at the day 30 post infection (30 dpi), except in three independent experiments in which the survival rate and the blood parasitemia were followed by 60 days, the period when the number of parasites in the blood decreased.

Food Intake and Lee's Index

The food intake was calculated by weighting the food provided every other day divided by the number of mice in the cage. The food intake (g) multiplied by the calorie provided, according to the offered diet) indicates the calorie intake. The Lee's index, indicator of obesity in rodents, proposed by Lee (14) and described by Bernardis and Petterson (15), was calculated by dividing the cubic root of body weight (g) by the naso-anal length (cm) and multiplied the result by 10.

TABLE 1 | Diet composition (1,000 g).

Ingredients (g)	Control diet	Hyperlipidic diet–Olive oil (DOO)	Hyperlipidic diet–Lard (DL)
Corn starch	465.7	287.7	287.7
Casein	140.0	140.0	140.0
Dextrinized starch	155.0	155.0	155.0
Sucrose	100.0	100.0	100.0
Soy oil	40.0	40.0	40.0
Microcrystalline cellulose	50.0	50.0	50.0
Mineral mix AIN93M[a]	35.0	35.0	35.0
Vitamin mix AIN93M[b]	10.0	10.0	10.0
L-cysteine	1.8	1.8	1.8
Choline Bitartrate	2.5	2.5	2.5
Lard[c]	–	–	168.0
Cholesterol	–	–	10.0
Extra virgin olive oil[d]	–	178.0	–
Total caloric value/1,000 g	4020.0	4910.0	4910.0

[a] *Minerals (g/kg): $CaCO_3$ 357.0/$C_6H_5K_3O7.H_2O$ 28.0/KH_2PO_4 250.0/NaCl 74.0/K_2SO_4 46.6/MgO 24.0/C_6H_5 + 4.FexNyO_7 6.06/CO_3Zn 1.65/$MnCO_3$ 0.63/$CuCO_3$ 0.3/KI 0.01/Na_2Se 0.01025/(NH_4) $6Mo_7O_24.4H_2O$ 0.00795/$Na_2SiO_3.9H_2O$ 1.45/KCr (SO_4) 2.12 H_2O 0.275/LiCl 0.0174/H_3BO_3 0.0815/NaF 0.0635/NiCO3 0.0318/NH_4VO_3 0.0066/$C_{12}H_2O_{11}$ 209.806.*

[b] *Vitamins (mg/kg): Niacin 3.0/Calcium pantothenate 1.6/Pyridoxine 0.7/Thiamine 0.6/Riboflavin 0.6/Folic acid 0.2/Biotin 0.02/Vitamin E (500 IU/g) 15.0/Vitamin B12 (0.1%) 2.5/Vitamin A (500,000 IU/g) 0.8/Vitamin D3 (400,000 IU/g) 0.25/Vitamin K1/Dextrose Mix (10 mg/g) 7.50/Sucrose 967.23. Conversion factors: proteins 4 kcal/g, lipids 9 kcal/g, sugars 4 kcal/g.*

[c] *Fatty acid composition of lard (commercial name: Estrela–values referring to 100 g of the product): saturated 40.0/monounsaturated 44.76/polyunsaturated 15.42.*

[d] *Fatty acid composition of extra virgin olive oil (commercial name: Olivenza–values referring to 100 g of product): saturated 14.9/monounsaturated 75.6/polyunsaturated 9.5.*

Biochemical Testing

Total cholesterol and triglycerides were determined using commercial kits from Bioclin® (Belo Horizonte, MG, Brazil) according to protocols available by the manufacturer.

Liver Total Lipids Quantification

The total lipids in the liver were quantified according to Folch method. Briefly, 100 mg liver tissue was macerated in 400 mL of chloroform/methanol (2:1) and centrifuged at 3,000 g, for 10 min at 22°C. Following this, 800 mL of chloroform and 640 mL of NaCl (0.73%) were added to the supernatant, and samples were centrifuged at 3,000 rpm, for 10 min at 22°C. The lower phase was washed three times with 600 mL of Folch solution (a solution of distilled water containing 48% methanol, 3% chloroform, and 2% NaCl at 0.29%) and the extracted lipids were dried overnight at 50°C. The amount of lipid of each sample was calculated by the difference between the weight of samples before and after they were dried.

Mice Infection, Parasitemia, Survival Rate, and Body Weight

Mice were inoculated intraperitoneally with 50 blood trypomastigote forms of the Colombian strain of *T. cruzi*, obtained after two consecutive passages of the strain in swiss mice. After the infection, the blood parasitemia levels were evaluated daily by counting the number of parasites in 5 ml tail-vein blood samples using an optical microscope. Mortality rate among the groups of animals was updated daily. In addition, the body weight was assessed daily by weighing the animals on a digital scale.

DNA Extraction and Parasitism Analysis

The genomic DNA was extracted from 10 mg of heart or adipose tissue using the Wizard® SV Genomic DNA Purification System kit (Promega) according to the manufacturer's instructions. Real-time polymerase chain reaction (PCR) was performed to quantify the heart parasitism as previously described (16).

Histology

To determine the number of cells infiltrated in the heart and epididymal adipose tissue, small pieces of the tissues were fixed in dimethyl sulfoxide (DMSO)-Methanol (1:5) for 30 days, dehydrated through successive incubations in crescent concentrations of ethanol, cleared in xylol and fixed in plastic paraffin (Paraplast®). The paraffin-fixed tissues were cut into sections with a size of 4 μm, stained with hematoxylin and eosin (HE) and the cell nuclei present in the fragments were quantified in 20 images (random fields). The images visualized by the 40X objective were scanned through the Leica DM 5000 B (Leica Application Suite, version 2.4.0R1) and processed through the Leica Qwin V3 image analyzer program.

Quantitative Real-Time PCR

Total RNA from the heart and epididymal adipose tissue was extracted using the TRIzol reagent (Invitrogen) and the SV Total RNA Isolation System kit (Promega) according to the manufacturer's instructions. Complementary DNA was synthesized from 500 ng of RNA through a High Capacity cDNA Reverse Transcription kit (Applied Biosystems). Real-time PCR assays were performed in a StepOnePlus Real-Time PCR System (Applied Biosystems) using SYBR Green Mix reagents (Invitrogen). The mean cycle threshold (Ct) values from duplicate measurements were used to calculate the expression of the two target genes, which were normalized to the housekeeping genes *GAPDH* or *18S*. The sequences of all primers used are described in **Table 2**.

TABLE 2 | Sequences of the primers used.

Targets	Sequences
Tlr2	Forward: *AAGTCTCCGGAATTATCAGTCC* Reverse: *TGATGGATGTCGCGGAT*
Tlr9	Forward: *GGACCTACAGCAGAATAGCTCA* Reverse: *AACTCGGGAACCAGACATG*
T. cruzi	Forward: *AAATAATGTACGGG(T/G)GAGATGCATGA* Reverse: *GGGTTCGATTGGGGTTGGTGT*
18S	Forward: *CCGCAGCTAGGAATAATGGAATA* Reverse: *GCCTCAGTTCCGAAAACCAA*
Gapdh	Forward: *GTGGAGTCATACTGGAACATGTAG* Reverse: *AATGGATGAAGGTCGGTGTG*

Immunoassay

Levels of CCL2 were detected in the supernatant of the homogenized cardiac and adipose tissues. For sample preparation, 20 mg of heart and 40 mg of epididymal adipose tissues were macerated in 200 mL of phosphate buffered saline (PBS) and, after centrifugation at 1,500 g, for 10 min at 4°C, the supernatant was collected. Inflammatory mediators were measured by enzyme-linked immunosorbent assay (ELISA) using a specific kit (Peprotech®) and were performed according to the manufacturer's information. The absorbance values were measured using the eMax ELISA reader (Molecular Devices) at 450 nm.

Catalase Activity Assay

Catalase activity was determined as described by Aebi (17) based on its ability to convert hydrogen peroxide (H_2O_2) into water and molecular oxygen. Briefly, 100 mg liver tissue was macerated in 1 mL of 0.1 M phosphate buffer, pH 7.2, centrifuged at 10,000 g, 10 min at 4°C. For the assay, 10 μL of the supernatant was added in 50 μL of K_2HPO_4, 40 μL of milli-Q water (Millipore, Bedford, MA) and 900 μL of 2.5 mmol/L H_2O_2. The enzyme activity was measured at 240 nm at 30 s, 2 and 3 min by decaying the absorbances. One-unit (U) of catalase is equivalent to the hydrolysis of 1 mmol of H_2O_2 per minute.

Superoxide Dismutase Activity

Pyrogallol undergoes autoxidation producing the superoxide anion (O^-). The SOD enzyme competes for the O^- by decreasing the 3-(4,5-Dimethylthiazol-2-yl) (MTT) reduction. For the assay, the supernatant of 100 mg of liver tissue was mixed with MTT and pyrogallol and incubated at 37°C for 5 min. The reaction was stopped with DMSO and the plate was read at 570 nm. The results were expressed as U of SOD per mg of protein in the supernatant of the liver tissue. One unit of SOD is defined as the amount of enzyme required for 50% inhibition of MTT reduction.

Oxidized and Total Glutathione Quantification Assay

For the dosage of oxidized glutathione (GSSG), we used a standard solution of 10 mM oxidized glutathione for the samples and a standard solution of 50 mM oxidized glutathione in 5% sulfosalicylic acid (SSA) for the curve. The samples were obtained from the supernatant of 100 mg of liver homogenized in 1 mL of 5% sulfosalicylic acid buffer - SSA. Following this, 100 μL of the samples were pipetted in 50 mL tubes and pipetted between 0.5 and 2.0 μL of vinylpyridine and 1–5 μL of triethanolamine (TEA) was added to maintain the pH between 6.0 and 7.0. The tubes were filled with distilled water to a volume of 15 mL, homogenized and kept at room temperature for 1 h. After the incubation, 10 μL of samples were measured at 412 nm. The samples were incubated for additional 5 min at room temperature

and, afterwards, 50 μL of nicotinamide adenine dinucleotide phosphate (NADPH) was added. The plate was read each 1 min during the 5 min incubation. Oxidized glutathione in the samples was calculated based on pre-defined concentrations for the calibration curve (p1: 0.25, p2: 0.125, p3: 0.062, p4: 0.0312, p5: 0.0156). For the measurement of total glutathione, 10 μL of samples were pipetted in a 96-well plate and immediately after the addition of 50 μL of NADPH, the absorbances were read each 1 min during the 5 min incubation. The values for reduced glutathione (GSH) were obtained from the difference between total and oxidized glutathiones.

Statistical Analysis

Data were expressed as means ± SEM. Multiple groups were compared using one-way analysis of variance (ANOVA) followed by Tukey-Kramer *post-test*. The survival rate was compared by log-rank test (Mentel-Cox) and the student's *t*-test was used to compare differences among two experimental groups. All analyzes were performed using the Prism 8 software (GraphPad Software). Groups were considered statistically different when p-values < 0.05.

RESULTS

Hyperlipidic Diet Alters Body and Biochemical Parameters in Mice

Firstly, we evaluated if the intake of normal and hyperlipidic diets, and the calories provided by diets were similar among the groups. To address this point, newly weaned mice were fed with either a normolipidic diet, monounsaturated fatty acid diet (olive oil) or with a saturated fatty acid diet (lard) for 90 days. None of them modified mice's body weight (**Figure 1A**). Although mice fed with normolipidic diet consumed a higher quantity of food than groups fed with olive oil or lard diets (**Figure 1B**), the calorie intake was similar among all animals (**Figure 1C**). The effect of hyperlipidic diets on the biochemical and body parameters of mice were also evaluated. The liver/body weight ratio was not different among animals receiving distinct diets (**Figure 1D**) and mice fed a lard diet presented higher amount of liver lipids when compared to those fed with normolipidic and olive oil diets (**Figure 1E**). We observed a decreased plasma levels of total cholesterol in mice fed with olive oil and lard diets (**Figure 1F**) while triglycerides level was similar among all animals (**Figure 1G**). The Lee's index, an indicative degree of obesity in mice (18), was similar among all animals (**Figure 1H**), but the weight of the epididymal and subcutaneous adipose tissues was higher in association with the lard diet (**Figure 1I**).

Diet Composition Interferes With the Heart and Adipose Tissue Parasitism After *T. cruzi* Infection

To evaluate if the olive oil diet or lard diet would affect the response against the Colombian strain of *T. cruzi*, mice were infected after 60 days of diet. The number of parasites circulating in the mice blood was similar between the infected animals in all days evaluated (**Figure 2A**); the difference was not evident even during the peak of the parasitemia, at day 27 post infection (**Figure 2B**). Interestingly, at the day 30 post infection, mice fed with the lard diet presented higher parasitism in the heart (**Figure 2C**) and adipose tissue (**Figure 2D**) compared to the mice fed with normolipidic diet or olive oil diet. Despite the high number of parasites among the group fed with lard diet, the percentage of survival was not different between the groups that received the different types of diet (**Figure 2E**).

Increased Amount of Olive Oil or Lard in the Diet Did Not Alter the Tissue Inflammation After *T. cruzi* Infection

Since mice fed with lard diets presented with high tissue parasitism, we investigated whether the diets interfere with the migration of inflammatory cells to the heart and adipose tissue following infection. For this purpose, after 60 days of either normolipidic, olive oil or lard diets followed by 30 dpi with *T. cruzi* Colombian strain, the production of the chemokine CCL2 and the tissue inflammation were evaluated. The infection increased the CCL2 production in the heart tissue (**Figure 3A**) and the number of inflammatory cells infiltrating the tissue (**Figures 3B,C**) independently of the diet administered. Although the lard diet increases the heart CCL2 production after infection compared with infected normolipidic group, the number of inflammatory cells in the tissue is similar among the infected groups independent of the dietary type (**Figures 3B,C**). Mice fed with the normolipidic diet presented with an increased production of CCL2 in adipose tissue after infection compared to all other dietary group (**Figure 4A**) despite this, the tissue inflammation increased similarly for all groups (**Figures 4A–C**).

Hyperlipidic Diet Rich in Olive Oil Increases Toll-Like Receptors Expression in the Cardiac Tissue After *T. cruzi* Infection

Since TLRs are particularly important for parasite recognition by immune cells, we investigated whether the hyperlipidic diets could interfere with the TLR expression in the cardiac and adipose tissue cells after *T. cruzi* infection. After receiving either normolipidic, olive oil or lard diets for 60 days, mice were infected by Colombian strain of *T. cruzi* and the mRNA expression levels of *Tlr2* and *Tlr9* were evaluated in the cardiac and adipose tissues of infected and non-infected mice. Infected mice fed with olive oil diet presented higher *Tlr2* and *Tlr9* expression in the heart (**Figures 5A,B**) while those fed with lard diet presented higher *Tlr2* and *Tlr9* expression in the adipose tissue (**Figures 5C,D**).

Hyperlipidic Diet Alters the Redox Status After *T. cruzi* Infection

The *T. cruzi* infection-caused oxidative stress, resulting in the accumulation of free radicals, which altered the expression and/or activity of antioxidant enzymes such as oxidized glutathione (GSSG), catalase (CAT), and superoxide dismutase (SOD). Activities of GSSG, CAT and SOD were evaluated in the liver of mice fed with either a control, olive oil, or lard diet for 60 days, followed by 30 dpi with *T. cruzi*. The infection

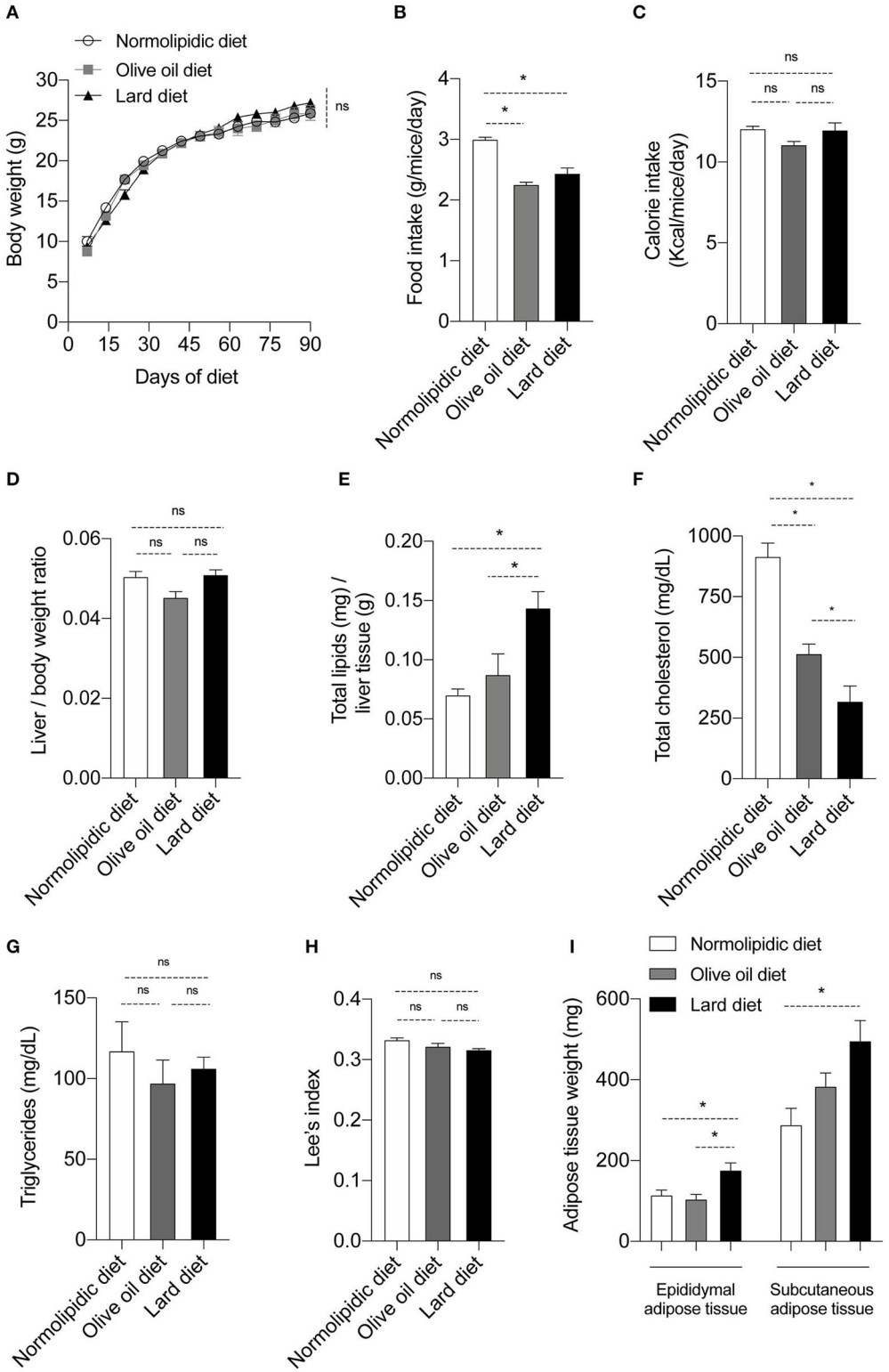

FIGURE 1 | Body and biochemical parameters from mice fed with different types of hyperlipidic diets. Newly weaned C57BL/6 mice were fed with either a normolipidic diet ($n = 8$), monounsaturated fatty acid diet with olive oil ($n = 8$) or saturated fatty acid diet with lard ($n = 8$) and **(A)** the body weight was monitored weekly in a digital scale. The **(B)** food intake and the **(C)** calorie intake were calculated every other day. At the day 90th of diet, mice were euthanized and **(D)** the liver/body weight ratio, **(E)** liver total lipids levels, **(F)** plasma total cholesterol, **(G)** plasma triglycerides, **(H)** Lee's index and **(I)** weight of adipose tissue were evaluated. ns, not statistically different, $^*p < 0.05$ by one-way ANOVA followed by Tukey *post-hoc* test.

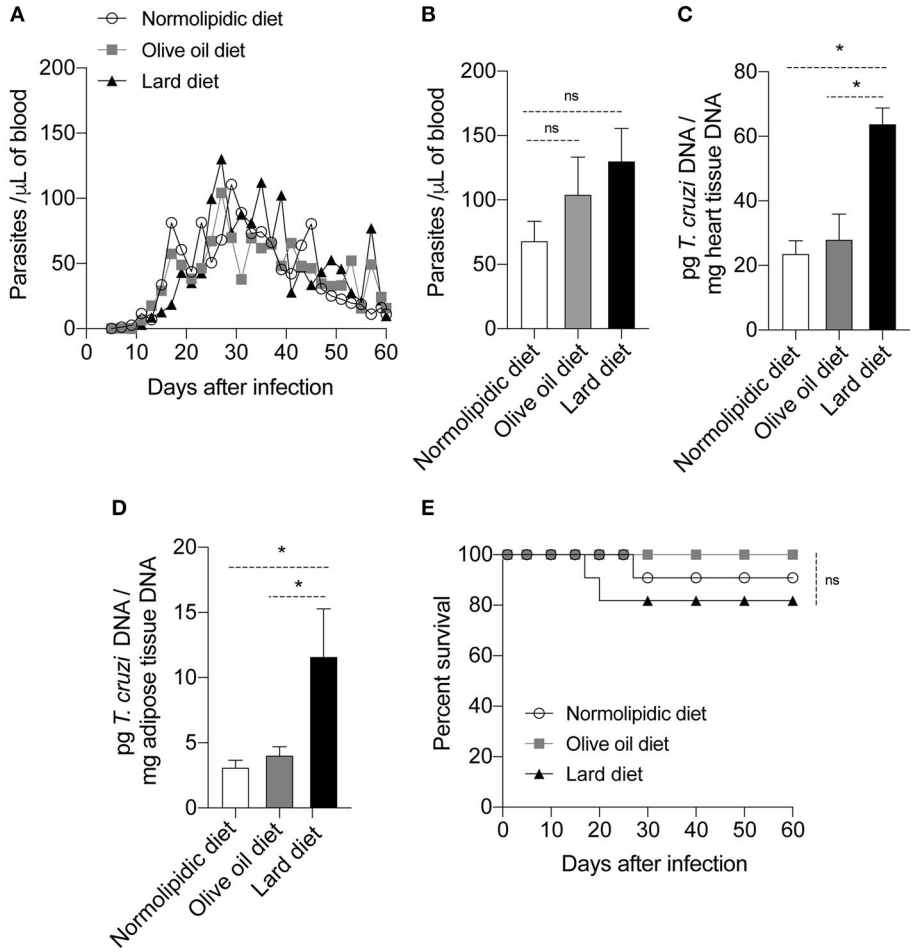

FIGURE 2 | Parasitism and survival rate of mice fed with different types of hyperlipidic diets. Newly weaned C57BL/6 mice were fed with either a normolipidic diet ($n = 8$), monounsaturated fatty acid diet with olive oil ($n = 8$) or saturated fatty acid diet with lard ($n = 8$). At the day 60 of diet, mice were intraperitoneally infected with 50 blood trypomastigote forms of *T. cruzi* Colombian strain and **(A)** the blood parasite levels were monitored daily. **(B)** Number of parasites circulating in the mice blood at the day 27 after infection. At the day 30 post infection the DNA was extracted from **(C)** the heart and **(D)** adipose tissue and the amount of DNA from parasites were quantified in the tissues by real time PCR assay. **(E)** The survival rate of mice fed with normolipidic diet, olive oil diet or lard diet was monitored daily for 35 days. ns, not statistically different; *$p < 0.05$ by one-way ANOVA followed by Tukey *post-hoc* test.

significantly downregulated the GSH/GSSG ratio in a diet-independent manner (**Figure 6A**). In response to the parasite-induced oxidative stress, we observed a slight decreased in the CAT activity in mice under normolipidic or olive oil diets, while infected mice under lard diet presented with intense reduction of catalase activity (**Figure 6B**). In addition, SOD is important for the protection of cells from oxidative insults, and we observed increases in SOD activity after 30 dpi. This increase was independent of the dietary type (**Figure 6C**).

DISCUSSION

The ingested lipids in foods are essential elements that impacts the inflammatory profile or alter the redox status caused by the inflammation (19). Diet exerts an important role during the inflammatory processes, with some nutritional studies demonstrating that ample and restricted consumption of monounsaturated and saturated lipids, respectively, decreases the expression of low-grade inflammatory markers (20, 21). The effects of a high fat diet in inflammation caused by *T. cruzi* are partially known (22, 23), but the effects of different types of lipids remain poorly studied.

Although high consumption of saturated fatty acids is frequently associated with weight gain and obesity in humans and experimental models (24, 25), we did not observe alterations in the body or liver weights in our lard group compared with olive oil and normolipidic dietary groups. Our results were consistent with other studies that have shown that few weeks under high fat diet rich in saturated lipids do not increase the body weight in experimental models (26, 27). Interestingly, Marques and collaborators showed that the diet-induced weight gain depends on the strain of rats and some

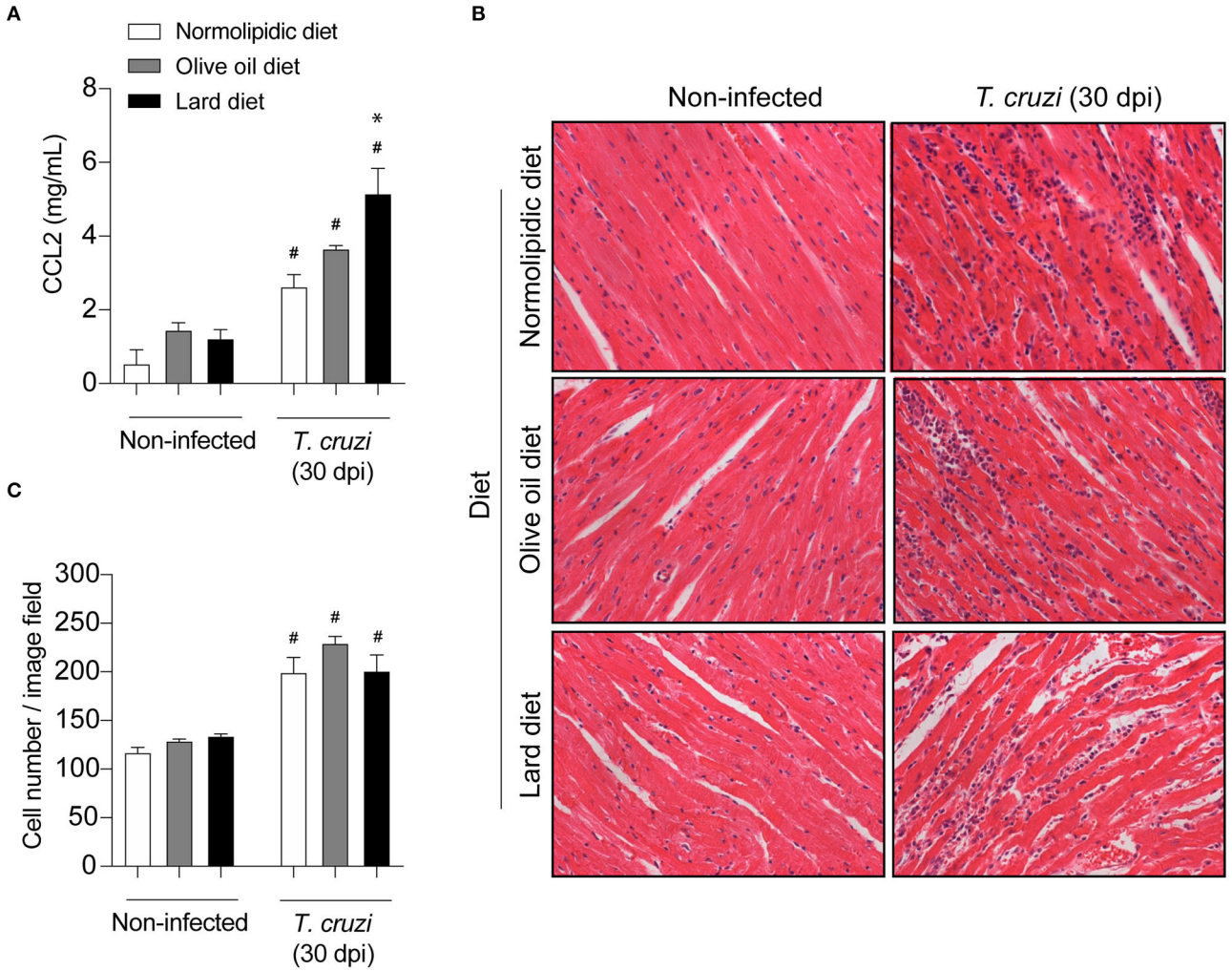

FIGURE 3 | Cardiac inflammatory parameters of *T. cruzi* infected mice fed with different types of hyperlipidic diets. Newly weaned C57BL/6 mice were fed with either a normolipidic diet ($n = 8$), monounsaturated fatty acid diet with olive oil ($n = 8$) or saturated fatty acid diet with lard ($n = 8$). At the day 60 of diet, mice were intraperitoneally infected with 50 blood trypomastigote forms of *T. cruzi* Colombian strain. After 30 dpi **(A)** the concentration of CCL2 was assessed in the heart tissue by ELISA assay. **(B)** The heart tissue was fixed, processed, blocked in paraffin, cut, and stained with hematoxylin and eosin and **(C)** the number of cells in the tissue was quantified. $^{\#}p < 0.05$ compared with the non-infected group and $^{*}p < 0.05$ compared with infected normolipidic diet group by one-way ANOVA followed by Tukey *post-hoc* test.

strains require longer exposure to the diets to gain weight (28). Although the weight was comparable across dietary groups, the lard diet increased the liver lipid deposition. This could indicate hepatic steatosis commonly observed after hyperlipidic diets (11). In addition, there are unclear points that limit the interpretation of rodent lipid metabolism with the same optical prism used to humans (29). Of note, the majority of human plasma cholesterol is transported as low-density lipoproteins (LDL), but mice do not have cholesteryl ester transfer protein, and for this reason, significant amounts of cholesterol are identified as high-density lipoproteins (HDL) in these animals. Another point, when animals have a high consumption of carbohydrates (e.g., normolipidic diet - AIN-93M), they can modify cholesterol metabolism increasing it in the blood (30), even under a low-lipid diet, as we have shown in this current study.

Hyperlipidic diets discussed here present equal energy density, however, the lard diet is the more efficient in transforming calories into adipose tissue assuming the normolipidic diet as reference. No change was observed in the body composition of animals under the effect of the different diets, according to Lee's index, however, the increased epididymal adipose tissue related to a lard diet may be favoring parasite interaction with host cells due to the presence of saturated fatty acids and the increased cell internalization of cholesterol, as previously demonstrated (7, 31–34). Then, considering the cholesterol analogs for the parasite invasion and replication and, considering both olive oil and lard diets have similar total lipid

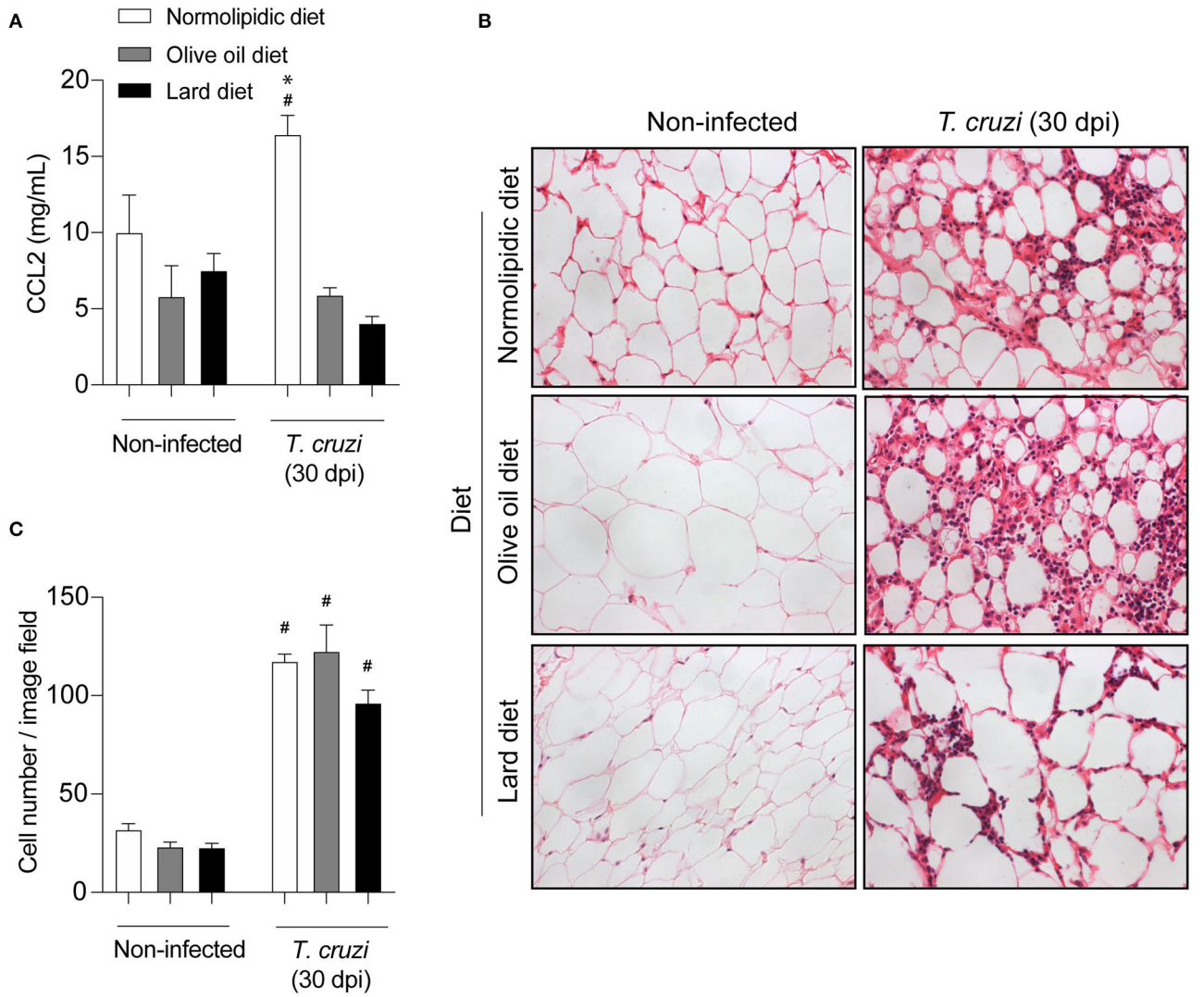

FIGURE 4 | Adipose tissue inflammatory parameters of *T. cruzi* infected mice fed with different types of hyperlipidic diets. Newly weaned C57BL/6 mice were fed with either a normolipidic diet ($n = 8$), monounsaturated fatty acid diet with olive oil ($n = 8$) or saturated fatty acid diet with lard ($n = 8$). At the day 60 of diet, mice were intraperitoneally infected with 50 blood trypomastigote forms of *T. cruzi* Colombian strain. After 30 dpi **(A)** the concentration of CCL2 was assessed in the adipose tissue by ELISA assay. **(B)** The adipose tissue was fixed, processed, blocked in paraffin, cut, and stained with hematoxylin and eosin and **(C)** the number of cells in the tissue was quantified. $^{\#}p < 0.05$ compared with the non-infected group and $^{*}p < 0.05$ compared with infected olive oil and lard diets by one-way ANOVA followed by Tukey *post-hoc* test.

percentage, we supplemented the lard diet with 1% cholesterol attempting to understand how it could be favorable or not to the *T. cruzi*.

Previously published results have showed that the *T. cruzi* infects and proliferates within brown and white adipose tissue (32, 35). In accordance with this, we showed that, although the blood parasitemia was the same in mice from the hyperlipidic and normolipidic dietary groups, mice under lard diet showed increased parasitism in both the adipose and cardiac tissues. Despite high tissue parasitism, the survival rate was the same among all dietary groups. In contrast, using the Brazil strain of *T. cruzi*, Nagajyothi et al. demonstrated that a high fat diet increases survival rate in infected mice (7). Of note, studies involving *T. cruzi* must pay attention to the strain used. A limitation of our study was that, given that mice fed a normolipidic diet survived the infection with the Colombian strain, we were not able to observe higher survival rates in infected animals from the other dietary groups.

Chemokine production and tissue recruitment of inflammatory cells in *T. cruzi* infected animals are essential for proper parasite control (36). In fact, our findings demonstrated an increase in heart CCL2 expression and the number of inflammatory cells in the heart and adipose tissues following infection in all dietary groups. Although

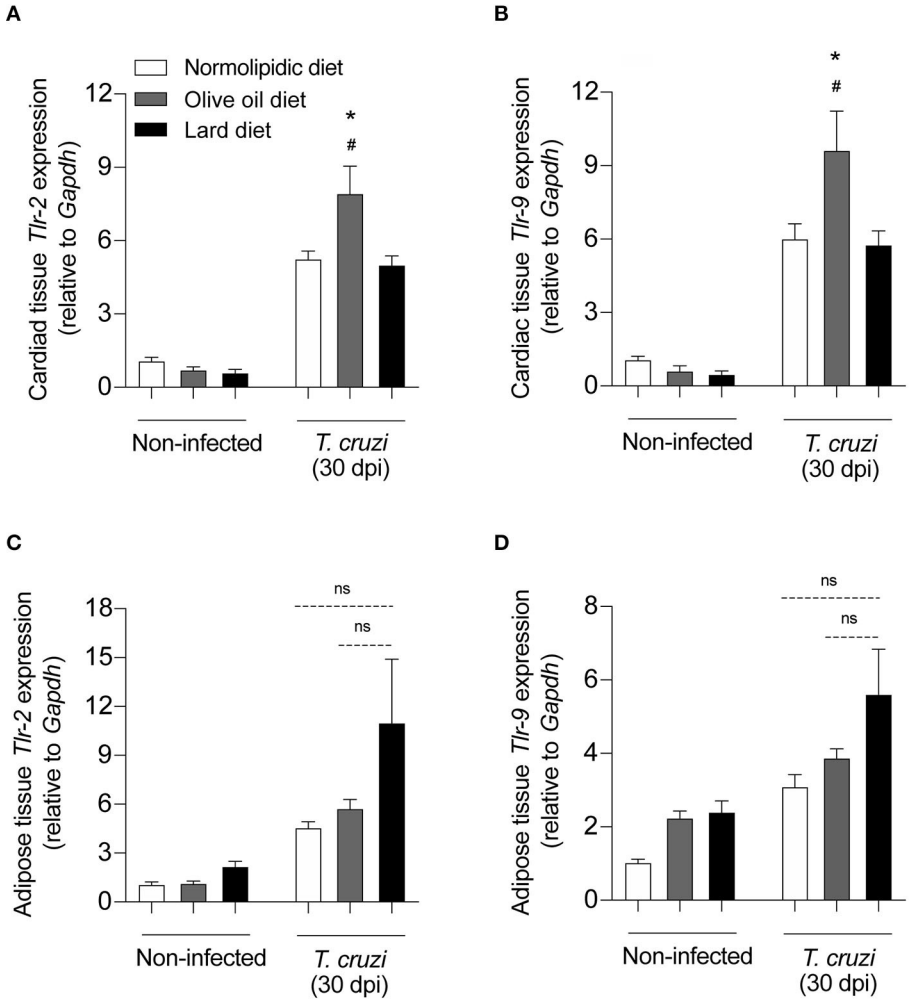

FIGURE 5 | TLRs expression on the heart and adipose tissue from *T. cruzi* infected mice fed with different types of hyperlipidic diets. Newly weaned C57BL/6 mice were fed with either a normolipidic diet ($n = 5$), monounsaturated fatty acid diet with olive oil ($n = 5$) or saturated fatty acid diet with lard ($n = 5$). At the day 60 of diet, mice were intraperitoneally infected with 50 blood trypomastigote forms of *T. cruzi* Colombian strain. After 30 dpi the mRNA expression levels of *Tlr2* and *Tlr9* were measured in the heart **(A,B)** and adipose tissue **(C,D)** by real time quantitative PCR. *Gapdh* and *18S* were used as housekeeping genes for the heart and adipose tissues, respectively. ns, not statistically different. $^{\#}p < 0.05$ compared with the non-infected group and $^{*}p < 0.05$ compared with infected group by one-way ANOVA followed by Tukey *post-hoc* test.

an increase in CCL2-producing macrophages is expected in the adipose tissues of infected mice (37), mice from lard dietary group presented with adipose tissue inflammation, independent of CCL2 production. Worth highlighting that caloric restriction has been shown to reduces migration of peripheral inflammatory monocytes from the bone marrow to the circulation and tissues by interference on the CCL2 production in a mechanism dependent on the peroxisome proliferator-activator receptor alpha and the activated protein kinase (38). In our study, animals fed with normolipidic performed higher ingestion of food in relation to those feed with olive oil or lard diets, however without differences in the calorie intake. In addition, the lard diet promoted a higher parasites load in both evaluated sites evaluated with the distinct pattern of CCL2 expression, after 48 h of the peak of parasitemia concerning Colombian strain of *T. cruzi*. At this representative moment of the experimental *T. cruzi* infection, no difference in inflammatory infiltration was detected through histological sections, but based on our previous experience, higher expression of CCL2 represents a higher release of this chemokine, an increasing of leukocyte recruitment, higher cardiac tissue damage and mortality in those infected animals (39).

Also essential to parasite control by immune cells is the recognition of *T. cruzi* structures by cellular receptors. The importance of TLR-2 and TLR-9 during the *T. cruzi* infection was previously reported (40). Our results demonstrated an overexpression of *Tlr2* and *Tlr9* mRNA in adipose tissue

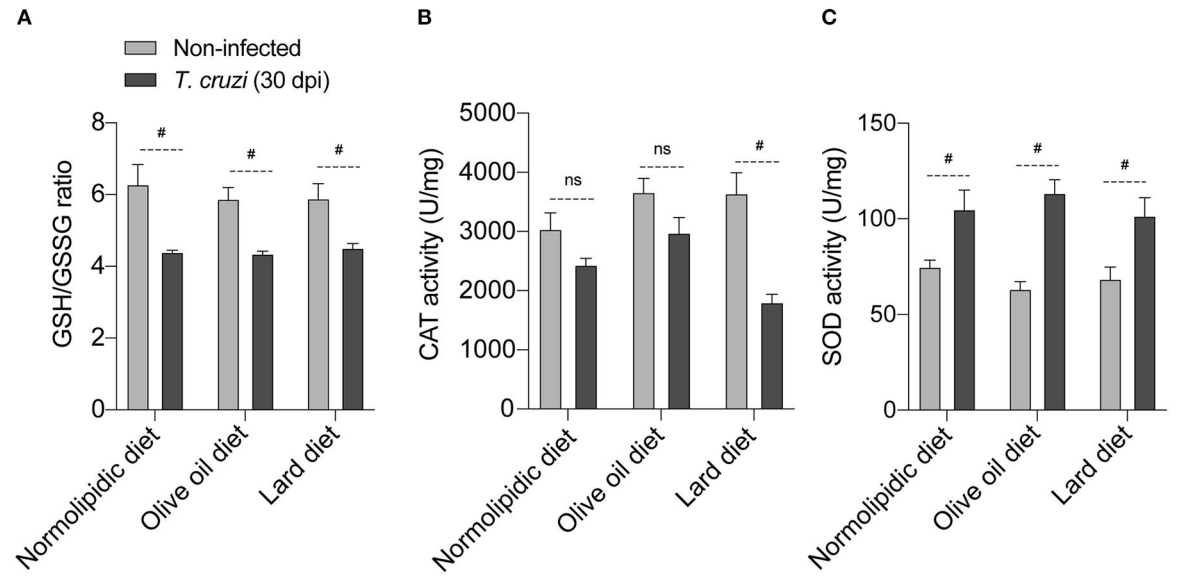

FIGURE 6 | Redox status of *T. cruzi* infected mice fed with different types of hyperlipidic diets. Newly weaned C57BL/6 mice were fed with either a normolipidic diet ($n = 5$), monounsaturated fatty acid diet with olive oil ($n = 5$) or saturated fatty acid diet with lard ($n = 5$). At the day 60 of diet, mice were intraperitoneally infected with 50 blood trypomastigote forms of *T. cruzi* Colombian strain. After 30 dpi **(A)** the GSH/GSSG ratio, **(B)** CAT activity and **(C)** SOD activity were measured in the supernatant of a macerated piece of liver. GSH, reduced glutathione; GSSH, oxidized glutathione; CAT, catalase; SOD, superoxide dismutase; ns, not statistically different; $^{\#}p < 0.05$ by student *t*-test.

and in cardiac tissue driven by lard and olive oil diets, respectively. Recent evidence suggest that saturated fatty acids can promote TLR-2 and TLR-4 activation while polyunsaturated fatty acids can inhibit these receptors (41). In parallel, *T. cruzi*-glycosylphosphatidylinositol membrane anchor is recognized by both, TLR-2 and TLR-9, and exert a role in the prognosis of asymptomatic and cardiac clinical forms of Chagas disease (42). In note, *T. cruzi* infection increases *Tlr2* and *Tlr9* expression in brown and white adipose tissues, respectively, as well as in other immune cells (43), and, together, they act in the balance between modulatory and inflammatory responses. This duality observed in the expression of *Tlr2* and *Tlr9* under high-fat diets effects might interfere in the parasite-host interaction and the immunopathogenesis since the deficiency of these receptors or of the Myd88 promotes susceptibility in infected mice (40) or the activation of *TLR2* and NF-Kb triggers cardiomyocyte hypertrophy (44, 45). Remarkably, the toll-like receptors act as a bridge between diet-induced endocrine and immune response, but further investigations are necessary to better understand this network.

Finally, both lipid-rich diets and *T. cruzi* infection cause oxidative stress (46, 47), and consequently, require the regulation of the antioxidant levels to reduce the high free radicals levels. The parasite decreases the GSH/GSSG ratio and CAT activity and increases SOD activity increasing the oxidative stress (48, 49). Interestingly, and in accordance with previous published data (23), our mice fed with saturated lipid-rich diet showed decreased CAT activity compared with mice from the normolipidic and unsaturated lipid-rich dietary groups. The antioxidant CAT rescues the cardiac dysfunction induced by high fat diets in mice (50). This suggests that the reduced CAT levels during infection may contribute to parasite-caused cardiac pathogenesis.

In summary, our findings provided evidence that diets rich in saturated lipids (e.g., lard diet) promote growth of *T. cruzi* in tissues following infection, and decrease the liver antioxidant production, contributing to the tissue damage.

DATA AVAILABILITY STATEMENT

The raw data supporting the conclusions of this article will be made available by the authors, without undue reservation.

ETHICS STATEMENT

The animal study was reviewed and approved by Animal Research Ethics Committee of the Federal University of Ouro Preto (CEUA-UFOP), under protocol number 36/2015.

AUTHOR CONTRIBUTIONS

DMSS, MCS, and AT: design, writing, and final content. DMSS, SEBF, APJM, CMM, KPL, NCNP, PMA, DCC, and GPC: performed the experiments. DMSS, MCS, and KMCP: data analysis. JSS and AT: funding acquisition. All authors have read and approved the final version of this manuscript.

FUNDING

This research was supported by CNPq, CAPES, and FAPEMIG funding agencies in Brazil as well as the Universidade Federal de Ouro Preto (UFOP, Brazil). JSS was grateful to FAPESP (Grant Agreement Number 2013/08216-2–Center for Research in Inflammatory Disease–CRID). AT (Process # 305634/2017-8) and JSS (Process # 308490/2014-5) were greateful to CNPq.

REFERENCES

1. Pérez-Molina JA, Molina I. Chagas disease. *Lancet.* (2018) 391:82–94. doi: 10.1016/S0140-6736(17)31612-4
2. Coura JR, Borges-Pereira J. Chagas disease: 100 years after its discovery. A systemic review. *Acta Trop.* (2010) 115:5–13. doi: 10.1016/j.actatropica.2010.03.008
3. Brener Z, Gazzinelli RT. Immnunological control of *Trypanosoma cruzi* infection and pathogenesis of Chagas' disease. *Int Arch Allergy Immunol.* (1997) 114:103–10. doi: 10.1159/000237653
4. Rassi A, Rassi A, Little WC. Chagas' heart disease. *Clin Cardiol.* (2000) 23:883–9. doi: 10.1002/clc.4960231205
5. Duque TLA, Cascabulho CM, Oliveira GM, Henriques-Pons A, Menna-Barreto RFS. Rapamycin treatment reduces acute myocarditis induced by *Trypanosoma cruzi* infection. *J Innate Immun.* (2020) 12:321–32. doi: 10.1159/000504322
6. Molina I, Salvador F, Sánchez-Montalvá A, Treviño B, Serre N, Avilés AS, et al. Toxic profile of benznidazole in patients with chronic chagas disease: risk factors and comparison of the product from two different manufacturers. *Antimicrob Agents Chemother.* (2015) 59:6125–31. doi: 10.1128/AAC.04660-14
7. Nagajyothi F, Weiss LM, Zhao D, Koba W, Jelicks LA, Cui MH, et al. High fat diet modulates *Trypanosoma cruzi* infection associated myocarditis. *PLoS Negl Trop Dis.* (2014) 8:e3118. doi: 10.1371/journal.pntd.0003118
8. Carvalho LSC, Camargos ERS, Almeida CT, Peluzio M do CG, Alvarez-Leite JI, Chiari E, et al. Á. Vitamin E deficiency enhances pathology in acute *Trypanosoma cruzi*-infected rats. *Trans R Soc Trop Med Hyg.* (2006) 100:1025–31. doi: 10.1016/j.trstmh.2005.12.009
9. De Castilhos MP, Huguenin GVB, Rodrigues PRM, Do Nascimento EM, Pereira B de B, Pedrosa RC. Diet quality of patients with chronic chagas disease in a tertiary hospital: a case-control study. *Rev Soc Bras Med Trop.* (2017) 50:795–804. doi: 10.1590/0037-8682-0237-2017
10. Milanski M, Degasperi G, Coope A, Morari J, Denis R, Cintra DE, et al. Saturated fatty acids produce an inflammatory response predominantly through the activation of TLR4 signaling in hypothalamus: implications for the pathogenesis of obesity. *J Neurosci.* (2009) 29:359–70. doi: 10.1523/JNEUROSCI.2760-08.2009
11. Figueiredo VP, Junior ESL, Lopes LR, Simões NF, Penitente AR, Bearzoti E, et al. High fat diet modulates inflammatory parameters in the heart and liver during acute *Trypanosoma cruzi* infection. *Int Immunopharmacol.* (2018) 64:192–200. doi: 10.1016/j.intimp.2018.08.036
12. Lovo-Martins MI, Malvezi AD, da Silva RV., Zanluqui NG, Tatakihara VLH, Câmara NOS, et al. Fish oil supplementation benefits the murine host during the acute phase of a parasitic infection from *Trypanosoma cruzi*. *Nutr Res.* (2017) 41:73–85. doi: 10.1016/j.nutres.2017.04.007
13. Medeiros-De-Moraes IM, Gonçalves-De-Albuquerque CF, Kurz ARM, De Jesus Oliveira FM, Pereira de Abreu VH, Torres RC, et al. Omega-9 oleic acid, the main compound of olive oil, mitigates inflammation during experimental sepsis. *Oxid Med Cell Longev.* (2018) 2018:6053492. doi: 10.1155/2018/6053492
14. Lee MO. Determination of the surface area of the white rat with its application to the expression of metabolic results. *Am J Physiol Content.* (1929) 89:24–33. doi: 10.1152/ajplegacy.1929.89.1.24
15. Bernardis LL, Patterson BD. Correlation between "Lee index" and carcass fat content in weanling and adult female rats with hypothalamic lesions. *J Endocrinol.* (1968) 40:527–8. doi: 10.1677/joe.0.0400527
16. Cummings KL, Tarleton RL. Rapid quantitation of *Trypanosoma cruzi* in host tissue by real-time PCR. *Mol Biochem Parasitol.* (2003) 129:53–9. doi: 10.1016/S0166-6851(03)00093-8
17. Aebi H. Catalase *in vitro*. *Methods Enzymol.* (1984) 105:121–6. doi: 10.1016/S0076-6879(84)05016-3
18. Rogers P, Webb GP. Estimation of body fat in normal and obese mice. *Br J Nutr.* (1980) 43:83–6. doi: 10.1079/BJN19800066
19. López-Muñoz RA, Molina-Berríos A, Campos-Estrada C, Abarca-Sanhueza P, Urrutia-Llancaqueo L, Peña-Espinoza M, et al. Inflammatory and pro-resolving lipids in trypanosomatid infections: a key to understanding parasite control. *Front Microbiol.* (2018) 9:1961. doi: 10.3389/fmicb.2018.01961
20. Kolehmainen M, Ulven SM, Paananen J, De Mello V, Schwab U, Carlberg C, et al. Healthy Nordic diet downregulates the expression of genes involved in inflammation in subcutaneous adipose tissue in individuals with features of the metabolic syndrome. *Am J Clin Nutr.* (2015) 101:228–39. doi: 10.3945/ajcn.114.092783
21. Uusitupa M, Hermansen K, Savolainen MJ, Schwab U, Kolehmainen M, Brader L, et al. Effects of an isocaloric healthy Nordic diet on insulin sensitivity, lipid profile and inflammation markers in metabolic syndrome - a randomized study (SYSDIET). *J Intern Med.* (2013) 274:52–66. doi: 10.1111/joim.12044
22. Tanowitz HB, Machado FS, Spray DC, Friedman JM, Weiss OS, Lora JN, et al. Developments in the management of Chagas cardiomyopathy. *Expert Rev Cardiovasc Ther.* (2015) 13:1393–409. doi: 10.1586/14779072.2015.1103648
23. Ayyappan JP, Nagajyothi JF. Diet modulates adipose tissue oxidative stress in a murine acute chagas model. *JSM Atheroscler.* (2017) 2:1030.
24. Corella D, Arnett DK, Tucker KL, Kabagambe EK, Tsai M, Parnell LD, et al. A high intake of saturated fatty acids strengthens the association between the fat mass and obesity-associated gene and BMI. *J Nutr.* (2011) 141:2219–25. doi: 10.3945/jn.111.143826
25. Viggiano E, Mollica M, Lionetti L, Cavaliere G, Trinchese G, Filippo C, et al. Effects of an high-fat diet enriched in lard or in fish oil on the hypothalamic amp-activated protein kinase and inflammatory mediators. *Front Cell Neurosci.* (2016) 10:150. doi: 10.3389/fncel.2016.00150
26. Wang Y, Dellatore P, Douard V, Qin L, Watford M, Ferraris RP, et al. High fat diet enriched with saturated, but not monounsaturated fatty acids adversely affects femur, and both diets increase calcium absorption in older female mice. *Nutr Res.* (2016) 36:742–50. doi: 10.1016/j.nutres.2016.03.002
27. Song Z, Xie W, Chen S, Strong JA, Print MS, Wang JI, et al. High-fat diet increases pain behaviors in rats with or without obesity. *Sci Rep.* (2017) 7:10350. doi: 10.1038/s41598-017-10458-z
28. Marques C, Meireles M, Norberto S, Leite J, Freitas J, Pestana D, et al. High-fat diet-induced obesity rat model: a comparison between Wistar and Sprague-Dawley rat. *Adipocyte.* (2016) 5:11–21. doi: 10.1080/21623945.2015.1061723
29. Bergen WG, Mersmann HJ. Comparative aspects of lipid metabolism: impact on contemporary research and use of animal models. *J Nutr.* (2005) 135:2499–502. doi: 10.1093/jn/135.11.2499
30. Parhofer KG. Interaction between glucose and lipid metabolism: more than diabetic dyslipidemia. *Diabetes Metab J.* (2015) 39:353–62. doi: 10.4093/dmj.2015.39.5.353
31. Nagajyothi F, Desruisseaux MS, Machado FS, Upadhya R, Zhao D, Schwartz GJ, et al. Response of adipose tissue to early infection with *Trypanosoma cruzi* (Brazil strain). *J Infect Dis.* (2012) 205:830–40. doi: 10.1093/infdis/jir840
32. Matos Ferreira AV, Segatto M, Menezes Z, Macedo AM, Gelape C, de Oliveira Andrade L, et al. Evidence for *Trypanosoma cruzi* in adipose tissue in human chronic Chagas disease. *Microbes Infect.* (2011) 13:1002–5. doi: 10.1016/j.micinf.2011.06.002
33. Johndrow C, Nelson R, Tanowitz H, Weiss LM, Nagajyothi F. *Trypanosoma cruzi* infection results in an increase in intracellular cholesterol. *Microbes Infect.* (2014) 16:337–44. doi: 10.1016/j.micinf.2014.01.001
34. Tanowitz HB, Jelicks LA, Machado FS, Esper L, Qi X, Desruisseaux MS, et al. Adipose tissue, diabetes and chagas disease. *Adv Parasitol.* (2011) 76:235–50. doi: 10.1016/B978-0-12-385895-5.00010-4
35. Combs TP, Nagajyothi, Mukherjee S, De Almeida CJG, Jelicks LA, Schubert W, et al. The adipocyte as an important target cell for *Trypanosoma*

cruzi infection. *J Biol Chem.* (2005) 280:24085–94. doi: 10.1074/jbc.M412802200
36. Talvani A, Ribeiro CS, Aliberti JCS, Michailowsky V, Santos PVA, Murta SMF, et al. Kinetics of cytokine gene expression in experimental chagasic cardiomyopathy: tissue parasitism and endogenous IFN-γ as important determinants of chemokine mRNA expression during infection with *Trypanosoma cruzi*. *Microbes Infect.* (2000) 2:851–66. doi: 10.1016/S1286-4579(00)00388-9
37. Cabalén ME, Cabral MF, Sanmarco LM, Andrada MC, Onofrio LI, Ponce NE, et al. Chronic *Trypanosoma cruzi* infection potentiates adipose tissue macrophage polarization toward an anti-inflammatory M2 phenotype and contributes to diabetes progression in a diet-induced obesity model. *Oncotarget.* (2016) 7:13400–15. doi: 10.18632/oncotarget.7630
38. Jordan S, Tung N, Casanova-Acebes M, Chang C, Cantoni C, Zhang D, et al. Dietary intake regulates the circulating inflammatory monocyte pool. *Cell.* (2019) 178:1102–14.e17. doi: 10.1016/j.cell.2019.07.050
39. Shrestha D, Bajracharya B, Paula-Costa G, Salles BC, Leite ALJ, Menezes APJ, et al. Expression and production of cardiac angiogenic mediators depend on the *Trypanosoma cruzi*-genetic population in experimental C57BL/6 mice infection. *Microvasc Res.* (2017) 110:56–63. doi: 10.1016/j.mvr.2016.12.002
40. Bafica A, Santiago HC, Goldszmid R, Ropert C, Gazzinelli RT, Sher A. Cutting edge: TLR9 and TLR2 signaling together account for MyD88-dependent control of parasitemia in *Trypanosoma cruzi* infection. *J Immunol.* (2006) 177:3515–9. doi: 10.4049/jimmunol.177.6.3515
41. Huang S, Rutkowsky JM, Snodgrass RG, Ono-Moore KD, Schneider DA, Newman JW, et al. Saturated fatty acids activate TLR-mediated proinflammatory signaling pathways. *J Lipid Res.* (2012) 53:2002–13. doi: 10.1194/jlr.D029546
42. Mendes da Silva LD, Gatto M, Miziara de Abreu Teodoro M, de Assis Golim M, Pelisson Nunes da Costa A, Capel Tavares Carvalho F, et al. Participation of TLR2 and TLR4 in cytokines production by patients with symptomatic and asymptomatic chronic Chagas disease. *Scand J Immunol.* (2017) 85:58–65. doi: 10.1111/sji.12501
43. Gravina HD, Antonelli L, Gazzinelli RT, Ropert C. Differential use of TLR2 and TLR9 in the regulation of immune responses during the infection with *Trypanosoma cruzi*. *PLoS ONE.* (2013) 8:e63100. doi: 10.1371/journal.pone.0063100
44. Higashikuni Y, Tanaka K, Kato M, Nureki O, Hirata Y, Nagai R, et al. Toll-like receptor-2 mediates adaptive cardiac hypertrophy in response to pressure overload through interleukin-1β upregulation via nuclear factor κB activation. *J Am Heart Assoc.* (2013) 2:e000267. doi: 10.1161/JAHA.113.000267
45. Ferenčić A, Cuculić D, Stemberga V, Šešo B, Arbanas S, Jakovac H. Left ventricular hypertrophy is associated with overexpression of HSP60, TLR2, and TLR4 in the myocardium. *Scand J Clin Lab Invest.* (2020) 80:236–46. doi: 10.1080/00365513.2020.1725977
46. Den Hartigh LJ, Han CY, Wang S, Omer M, Chait A. 10E,12Z-conjugated linoleic acid impairs adipocyte triglyceride storage by enhancing fatty acid oxidation, lipolysis, and mitochondrial reactive oxygen species. *J Lipid Res.* (2013) 54:2964–78. doi: 10.1194/jlr.M035188
47. Wen JJ, Nagajyothi F, Machado FS, Weiss LM, Scherer PE, Tanowitz HB, Garg NJ. Markers of oxidative stress in adipose tissue during *Trypanosoma cruzi* infection. *Parasitol Res.* (2014) 113:3159–65. doi: 10.1007/s00436-014-3977-7
48. Souza ABF, Chírico MTT, Cartelle CT, Costa GP, Talvani A, Cangussú SD, et al. High-fat diet increases HMGB1 expression and promotes lung inflammation in mice subjected to mechanical ventilation. *Oxid Med Cell Longev.* (2018) 2018:7457054. doi: 10.1155/2018/7457054
49. Santos RS, Silva PL, Oliveira GP, Cruz FF, Ornellas DS, Morales MM, et al. Effects of oleanolic acid on pulmonary morphofunctional and biochemical variables in experimental acute lung injury. *Respir Physiol Neurobiol.* (2011) 179:129–36. doi: 10.1016/j.resp.2011.07.008
50. Liang L, Shou XL, Zhao HK, Ren G qun, Wang JB, Wang XH, et al. Antioxidant catalase rescues against high fat diet-induced cardiac dysfunction via an IKKβ-AMPK-dependent regulation of autophagy. *Biochim Biophys Acta Mol Basis Dis.* (2015) 1852:343–52. doi: 10.1016/j.bbadis.2014.06.027

Conflict of Interest: The authors declare that the research was conducted in the absence of any commercial or financial relationships that could be construed as a potential conflict of interest.

frontiers in Cardiovascular Medicine

ORIGINAL RESEARCH
published: 16 September 2021
doi: 10.3389/fcvm.2021.741347

Parasitic Load Correlates With Left Ventricular Dysfunction in Patients With Chronic Chagas Cardiomyopathy

Maykon Tavares de Oliveira[1], André Schmidt[1], Maria Cláudia da Silva[2], Eduardo Antônio Donadi[3], João Santana da Silva[2,4] and José Antônio Marin-Neto[1]*

[1] Cardiology Division, Department of Internal Medicine, Medical School of Ribeirão Preto, University of São Paulo, Ribeirão Preto, Brazil, [2] Department of Biochemistry and Immunology, Ribeirão Preto Medical School, University of São Paulo, Ribeirão Preto, Brazil, [3] Division of Clinical Immunology, Department of Internal Medicine, Ribeirão Preto Medical School, University of São Paulo, Ribeirão Preto, Brazil, [4] Fiocruz-Bi-Institutional Translational Medicine Plataform, Ribeirão Preto, Brazil

OPEN ACCESS

Edited by:
Walderez Ornelas Dutra, Federal University of Minas Gerais, Brazil

Reviewed by:
Juliana A. S. Gomes, Federal University of Minas Gerais, Brazil
Chen Gao, UCLA Department of Anesthesiology and Perioperative Medicine, United States

***Correspondence:**
Maykon Tavares de Oliveira
maykontavares@yahoo.com.br

Specialty section:
This article was submitted to General Cardiovascular Medicine, a section of the journal Frontiers in Cardiovascular Medicine

Received: *14 July 2021*
Accepted: *24 August 2021*
Published: *16 September 2021*

Citation:
de Oliveira MT, Schmidt A, da Silva MC, Donadi EA, da Silva JS and Marin-Neto JA (2021) Parasitic Load Correlates With Left Ventricular Dysfunction in Patients With Chronic Chagas Cardiomyopathy. Front. Cardiovasc. Med. 8:741347. doi: 10.3389/fcvm.2021.741347

Background: Chronic Chagas disease (CChD), one of the infectious parasitic diseases with the greatest social and economic impact upon a large part of the American continent, has distinct clinical manifestations in humans (cardiac, digestive, or mixed clinical forms). The mechanisms underlying the development of the most common and ominous clinical form, the chronic Chagas cardiomyopathy (CCC) have not been completely elucidated, despite the fact that a high intensity of parasite persistence in the myocardium is deemed responsible for an untoward evolution of the disease. The present study aimed to assess the parasite load CCC and its relation to left ventricular ejection fraction (LVEF), a definite prognostic marker in patients with CCC.

Methods: Patients with CCC were clinically evaluated using 12-lead-electrocardiogram, echocardiogram, chest X-ray. Peripheral blood sampling (5 ml of venous blood in guanidine/EDTA) was collected from each patient for subsequent DNA extraction and the quantification of the parasite load using real-time PCR.

Results: One-hundred and eighty-one patients with CCC were evaluated. A total of 140 (77.3%) had preserved left ventricular ejection fraction (of $\geq$40%), and 41 individuals had LV dysfunction (LVEF of $<$ 40%). A wide variation in parasite load was observed with a, mean of 1.3460 $\pm$ 2.0593 (0.01 to 12.3830) par. Eq./mL. The mean $\pm$ SD of the parasite load was 0.6768 $\pm$ 0.9874 par. Eq./mL and 3.6312 $\pm$ 2.9414 par. Eq./mL in the patients with LVEF $\geq$ 40% and $<$40%, respectively.

Conclusion: The blood parasite load is highly variable and seems to be directly related to the reduction of LVEF, an important prognostic factor in CCC patients.

Keywords: *Trypanosoma cruzi*, Chagas disease, chronic Chagas cardiomyopathy, left ventricular ejection fraction, parasite burden

INTRODUCTION

Chagas disease (ChD) is caused by the hemoflagellate protozoan *Trypanosoma cruzi* (1). According to the World Health Organization (2), ∼6–7 million people are infected with *T. cruzi* globally, and more than 75 million individuals are at risk of infection. The endemic area of ChD is relatively wide, extending from the southern United States to Argentina (3). This disease is still one of the infectious and parasitic diseases with the greatest social and economic impact upon much of the American continent, due to its high transmission rates mainly in the Andean countries (4) and to the large bulk of infected individuals in most Latin American countries where disease control is not properly carried out (5, 6).

Its most severe clinical manifestations are attributed to the cardiac involvement leading to heart failure, thromboembolic events, arrhythmias and especially sudden death, with digestive tract manifestations occurring in isolation or in association with the cardiac manifestations (6–9). The pathological changes causing megaesophagus and/or megacolon are deemed to be mainly associated with the extensive destruction of the intramural autonomic system, especially of the Auerbach and Meisner myenteric plexuses of patients chronically infected with the *T. cruzi* (10, 11).

In contrast, although cardiac autonomic derangements also have been demonstrated, the main pathogenic mechanisms leading to the appearance of CCC are now thought to depend on inflammation directly related to tissue parasite multiplication and the superimposed immunological reaction thus triggered (12).

Also, it is recognized that development and aggravation of CCC in a specific individual is dependent on other relevant pathogenic aspects that generate myocardial inflammation, related to both host and parasite genetics, as well as the tropism inherent to the strain of the parasite infection (13–15).

Since the intensity of tissue inflammation and the evolution of CCC are thought to be dependent upon the parasite persistence and multiplication in the myocardium that may be reflected by the parasite burden as assessed with blood real-time qPCR, in the present study we evaluated the relation between the parasite load in the peripheral blood of patients with CCC and its relation to one of the most important prognostic factors for such patients, the left ventricular systolic function.

MATERIALS AND METHODS

Patients With Chronic Chagas Cardiomyopathy

This study evaluated 181 patients who were managed at the Chagas Disease Outpatient Clinic, Division of Cardiology, Ribeirão Preto Medical School, University of São Paulo (FMRP-USP) between 2012 and 2018. All fulfilled the basic inclusion criteria of having undergone at least two distinct serological tests with positive results for Chagas disease, possess more than 18 years of age, presenting only cardiac abnormalities compatible with Chagas disease and signing the free and informed consent to participate in the study.

All patients included had a thorough clinical evaluation that comprised the assessment of left ventricular ejection fraction (LVEF) through a transthoracic echocardiogram obtained at rest, using standard methods (16, 17).

Peripheral blood (5 ml) was collected before treatment with Benznidazole, from each patient and added to the same volume of 6 M guanidine Hydrochloride 0.2 M ethylenediaminetetraacetic acid buffer (EDTA) solution (pH 8.0) (18), for further DNA extraction. Guanidine-EDTA blood lysates (GEB) were boiled for 15 min, incubated at room temperature for 24 h, and stored at 4°C until use (19).

For Ethical Clearance

The study was approved by the Human Research Ethics Committee of the Clinical Hospital, Ribeirão Preto Medical School, University of São Paulo (FMRP/USP—CAAE: 09948419.3.0000.5440). Written informed consent was obtained from all the patients.

DNA Extraction

DNA was extracted from 200 μL of GEB samples and eluted with 55 μL of NucliSens easyMAG system (Biomerieux, France), according to the manufacturer's instructions.

Parasitic Load Quantification by qPCR

Quantitative real-time PCR (qPCR) was performed according to a previously proposed methodology (20), using the multiplex *TaqMan* system targeting the 195 bp region of *T. cruzi* satellite DNA (**Table 1**). The qPCR reactions were carried out at a final volume of 25 μL containing 5 μL DNA from each sample (20 ng/μL), 400 nM of the two primers, and 100 nM of the TaqMan probe. The Quantitec Multiplex PCR kit (Qiagen, Manchester, United Kingdom) was used, and the CFX Real-Time PCR detection system (Bio-Rad, Hercules, CA) was used for amplification. The standard curve of the qPCR results was obtained by extracting DNA from serial dilutions of 10^6 epimastigote forms of the Y strain (DTU TcII), with a detection limit of 0.01 parasite. Equivalents/mL, as proposed by Cummings et al. (20). Positive, negative, and reagent internal controls were used for all qPCR reactions.

Statistical Analysis

All experiments were performed using at least two technical replicates. The categorical data were expressed as percentages, and continuous data were expressed as mean ± standard deviation (SD) or median and intervals according to the normality or nonparametric characteristics of the variable

TABLE 1 | Specific primers for *Trypanosoma cruzi*.

Primers name	Sequence
TCZ-F	5′-GCTCTTGCCCACAMGGGTGC-3′
TCZ-R	5′-CCAAGCAGCGGATAGTTCAGG-3′

TCZ-F, Trypanosoma cruzi—Forward primer; TCZ-R, Trypanosoma cruzi—Reverse primer.

TABLE 2 | Clinical and laboratory parameters of 181 chronic Chagas cardiomyopathy patients.

		N (%)
Female		86 (47.5)
Male		95 (52.5)
Age (mean)		53.2
Cardiac pacemaker		31 (17.0)
Implantable cardiac defibrillator		5 (2.8)
NYHA CLASS	I	129 (71.3)
	II	41 (22.6)
	III	11 (6.1)
	IV	0 (0)
LVEF	>70%	18 (9.9)
	50–70%	86 (47.5)
	40–49%	31 (17.1)
	30–39%	23 (12.7)
	<30%	18 (9.9)
		Five patients had subjective LVEF above 50%

LVEF, left ventricular ejection fraction; NYHA, New York Heart Association.

distribution. Student's *t*-test was used to analyze the significance of the statistical differences. For analysis of the correlation, Pearson's test was carried out. The results were deemed statistically significant when the *p*-values were <0.05. The analysis was conducted using GraphPad Prism (version 7.00) for Windows, GraphPad Software, La Jolla California USA, www.graphpad.com.

RESULTS

Clinical Characteristics of the Patients Included in This Study

The 181 patients included in the study came from several Brazilian states: São Paulo (∼36.4%), Minas Gerais (∼53.6%), Bahia (∼6.6%), Paraíba (∼0.5%), Alagoas (∼1.6%), and Goiás (∼1.1%). Eighty-six (47.5%) were male and 95 (52.5%) were female. The mean age was 53.2 years (range, 24–79 years).

Clinical Evaluation

Clinical data is summarized in **Table 2**. Most of them (129 individuals −71%) were in New York Heart Association (NYHA) class I and none in NYHA class IV.

The cardiac evaluation based on the echocardiogram showed that 140 patients had a left ventricular ejection fraction (LVEF) of ≥40% with a mean ± SD of 58.96 ± 10.60%, while 41 individuals had an LVEF of <40% and mean ± SD of 29.68 ± 6.27% (**Figure 1A**). The difference for the LVEF in the two groups was statistically significant with a *p*-value of 0.0003.

Parasitic Load

A wide variation in the parasite load was observed in the peripheral blood of the 181 patients with chronic Chagas cardiomyopathy (CCC) included in the study from 0.01 to 12.3830 par. Eq./mL, with a mean ± SD of 1.3460 ± 2.0593 par. Eq./mL. There was no difference in the parasite load in relation to gender ($p = 0.44$; **Table 3**).

The mean ± SD of the parasite load was 0.6768 ± 0.9874 par. Eq./mL in the group of patients with LVEF of ≥40% and 3.6312 ± 2.9414 par. Eq./mL in those with LVEF of <40%, *p*-value of 0.0001 (**Figure 1B**). A significant correlation between par. Eq./mL and LVEF was noted ($r = 0.49$; $p < 0.0001$; **Figure 1C**).

DISCUSSION

The use of real-time quantitative PCR (qPCR) for monitoring Chagas disease (ChD) was an important milestone in the development of sensitive and reliable tools for molecular diagnosis and post-therapeutic evaluation of patients infected with the *T. cruzi* (21). Thus, qPCR has been increasingly applied for quantification of the parasitic load of *T. cruzi* in the peripheral blood, serum, cardiac tissue, umbilical cord blood, and skin tissue samples from patients with acute and chronic phases of Chagas disease. The method was also used to identify the DTUs of the parasites (22–25) and has become very useful for clinical and research purposes, especially during the chronic phase of the disease, where direct parasitological diagnostic methods are generally ineffective due to inherently low-grade parasitemia (26, 27).

In our study a wide variation in the value of qPCR was observed among patients with CCC. In addition, the individual pPCR values were significantly and inversely correlated with the correspondent individual values of the LVEF. These two main results of our investigation may be coherent with the notion that the biological aspects of the parasite and the host are both likely to play a fundamental role in defining the installation and clinical course of human Chagas disease (28).

Although widely variable, the low parasite burden in our sample of patients with CCC corroborates the results in several previous studies that reported on a low parasite load in patients with chronic ChD, especially those studies that assessed therapeutic failures (26, 29, 30). One of these pioneer studies evaluated the parasite load in patients with chronic ChD from different Latin American countries and described the ability to identify a low parasite load in most samples (detection limit of 0.70 par. Eq./mL) (31).

Cancino-Faure et al. (32) in studying a group of immigrant Latino patients living on the island of Mallorca in Spain, also observed a low parasite load similar to the findings of our study, with an average amount of *T. cruzi* DNA in the blood samples of <1 par. Eq./mL.

Another study evaluated a sample population of patients with the indeterminate or cardiomyopathy forms of chronic Chagas Disease from the state of Minas Gerais in Brazil and found results which were comparable to our findings, with a mean parasite load of 1.18 [0.39–4.23] par. Eq./mL, ranging between 0.01 and 116.10 par. Eq./mL (30).

The wide individual variation of parasite load was also reported in a similar study that evaluated the genetic variability of *T. cruzi* in chronic patients with ChD from different regions

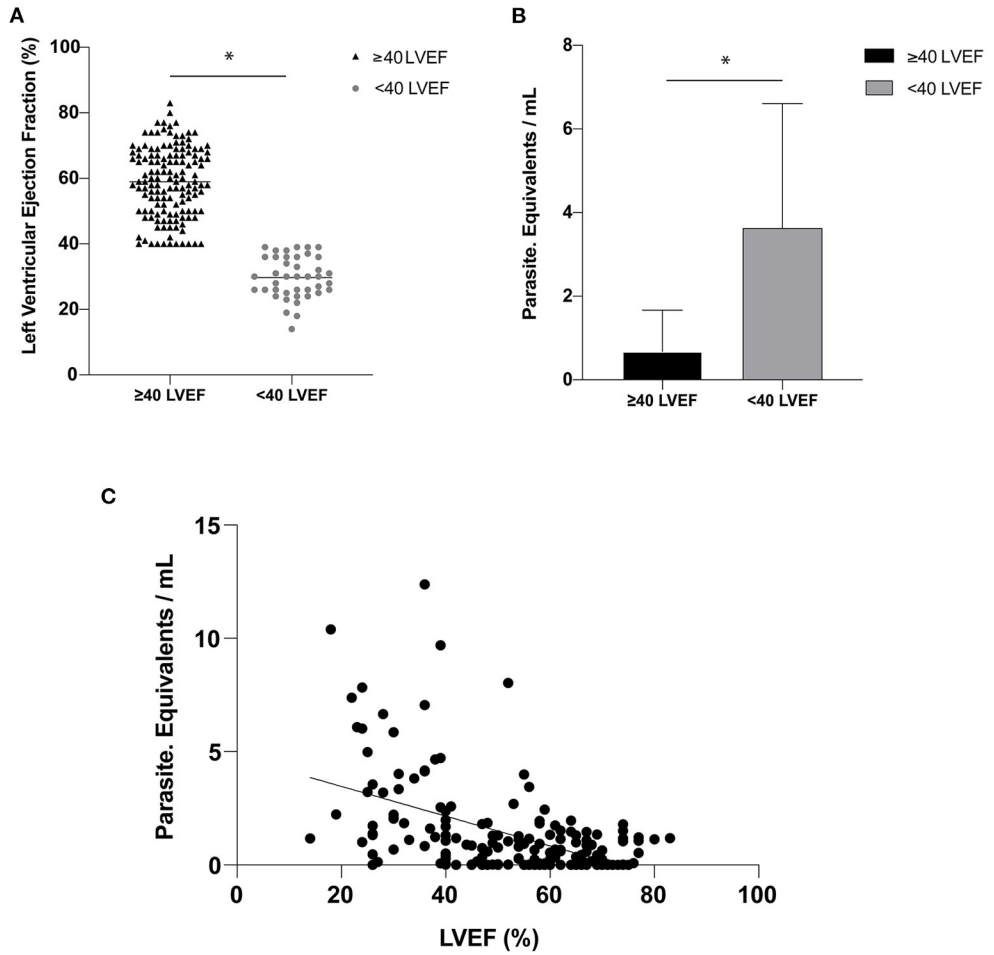

FIGURE 1 | (A) Left ventricular ejection fraction (LVEF) expressed as a percentage (%)—(horizontal line represented the mean of the LVEF values for each group). **(B)** Parasitic load expressed in parasite equivalents per milliliter of blood for Left ventricular categories below and equal or above 40%. **(C)** Correlation between parasitic load and LVEF ($r = 0.49$; $p < 0.0001$). The symbol (*) indicates a significant difference between the groups with $p < 0.05$.

TABLE 3 | Correlation between parasite load and gender.

	Gender	*N*	Mean	SD
Parasites Eq/mL (gender)	M	86	1.265	2.064
	F	95	1.506	2.178

N, number; SD, Standard deviation.

of Brazil (33). However, they reported a mean parasite load higher than that found in the present study (mean parasite load of all positive patients was 2.54 [1.43–11.14] par. Eq./mL, with the load ranging from 0.12 to 153.66 par. Eq./ml). The authors obtained the blood samples from patients residing in highly endemic regions with active vectorial transmission of ChD, which predisposes patients to reinfection. This may have influenced the findings of higher parasite burden.

Geographical factors other than reinfection may possibly explain the finding of moderate to high parasite loads in immigrant patients residing in a European country, again with great variation of the parasitemia load [0.001–22.2 *T. cruzi* DNA (fg)/blood DNA (ng)] (34).

Only one previous study evaluating the serum parasite load with qPCR correlated the results with the clinical prognosis of Colombian patients with CCC during 2 years of follow-up. The authors reported findings that are somewhat similar to those of our study, in which detectable parasitemia (considered to be low parasitemia) was associated with markers of myocardial injury severity and higher risk (35). It is plausible to interpret their results, as well as our own findings of an association between more severe cardiac damage (as expressed by a lower LVEF) and higher blood parasite burden, could be attributed to the less vigorous immune response in patients evolving to more marked forms organic involvement (35–38).

Hence a high parasite load may reflect a weaker immune response against the parasite, and the consequent more serious damage to the cardiac tissue due to parasitic replication, myocardial cell disruption, and the establishment of autoimmunity in Chagas disease patients. However, a robust immune response might paradoxically lead to a worsening of the inflammatory cascade and produce more myocardial damage (14). This possibility is opposite to the predominant view that an effective immunological response to the parasite is definitely necessary to efficiently reduce the parasite load and minimize the organic damage (39, 40).

Therefore, additional studies similar to our investigation are warranted to assess the parasitic burden and its relation to markers of severity of the cardiomyopathy and of clinical prognosis. If confirmed, our present findings will have important implications for the control and monitoring of public health, the implementation of medical care, through the introduction of additional controls for blood banks, and training of personnel to diagnose and treat Chagas disease. Also, it would be relevant to overcome a limitation of the present study, if a cohort study could demonstrate that a high blood parasite burden is associated with future deterioration of left ventricular function.

CONCLUSIONS

The data from this study corroborate previous reports that indicate the prevalence of low blood parasite load in chronic patients with Chagas cardiomyopathy in Brazil. The study additional finding of a significant correlation between the individual parasite burden and the degree of left ventricular dysfunction is coherent with the concept that a high level of parasite persistence and load may bear relevant prognostic and therapeutic implications for the management of CCC.

DATA AVAILABILITY STATEMENT

The original contributions presented in the study are included in the article/supplementary material, further inquiries can be directed to the corresponding author/s.

ETHICS STATEMENT

The studies involving human participants were reviewed and approved by Human Research Ethics Committee of the Clinical Hospital, Ribeirão Preto Medical School, University of São Paulo (FMRP/USP—CAAE: 09948419.3.0000.5440). The patients/participants provided their written informed consent to participate in this study.

AUTHOR CONTRIBUTIONS

MO, AS, and JM-N: conceptualization. MO, AS, ED, JS, and JM-N: data curation. MO: formal analysis, validation, and writing—original draft. MO and JM-N: funding acquisition and resources. MO, MS, and JS: investigation. MO and MS: methodology. JM-N: project administration and supervision. MO, AS, MS, ED, JS, and JM-N: visualization and writing—review and editing. All authors contributed to the article and approved the submitted version.

FUNDING

This study was supported by Grant 2018/22093-4 - São Paulo Research Foundation (FAPESP)- fapesp.br/en – and, 256 Grant 2016/25403-9 - São Paulo Research Foundation (FAPESP)- fapesp.br/en.

ACKNOWLEDGMENTS

We thank Diego Franca da Cunha and Patrícia Cristina de Oliveira Campos for her technical support.

REFERENCES

1. Chagas C. Nova tripanozomiase humana. Estudos sobre a morfolojia e o ciclo evolutivo do *Schizotrypanum cruzi* n. gen., n. sp., ajente etilógico *de nova* entidade morbida do homem. *Mem Inst Oswaldo Cruz*. (1909) 1:159–218. doi: 10.1590/S0074-02761909000200008
2. WHO Chagas Disease (American trypanosomiasis). Fact Sheet N°340 (2018).
3. Miles MA. The discovery of Chagas disease: progress and prejudice. *Infect Dis Clin North Am*. (2004) 18:247–60. doi: 10.1016/j.idc.2004.01.005
4. Solari A, Wallace A, Ortiz S, Venegas J, Sanchez G. Biological characterization of *Trypanosoma cruzi* stocks from Chilean insect vectors. *Exp Parasitol*. (1998) 89:312–22. doi: 10.1006/expr.1998.4289
5. Dias JC. [Chagas' disease and its control in Latin America: an analysis of possibilities]. *Cad Saude Publ*. (1993) 9:201–9. doi: 10.1590/S0102-311X1993000200012
6. Coura JR, Junqueira AC. Chagas disease. What is known and what should be improved: a systemic review. *Rev Soc Bras Med Trop*. (2012) 45:286–96. doi: 10.1590/S0037-86822012000300002
7. Rezende JM, Moreira H. Megacolon chagásico. In: Porto JAF, editors. *Clínica das Doenças Intestinais*. Atheneu (1997). p. 481–74.
8. Rassi A Jr, Rassi A, Marin-Neto JA. Chagas disease. *Lancet*. (2010) 375:1388–402. doi: 10.1016/S0140-6736(10)60061-X
9. Rassi A Jr, Rassi A. Another disappointing result with implantable cardioverter-defibrillator therapy in patients with Chagas disease. *Europace*. (2013) 15:1383. doi: 10.1093/europace/eut092
10. de Oliveira RB, Ballart C, Abràs A, Gállego M, Marin-Neto JA. Chagas disease: an unknown and neglected disease. In: Pinazo Delgado MJ, Gascón J, editors. *Chagas Disease*. Cham: Springer (2020). p. 1–26.
11. Delgado MJP, Gascón J. *Chagas Disease: A Neglected Tropical Disease*. Springer. (2020).
12. Dutra WO, Menezes CA, Magalhães LM, Gollob KJ. Immunoregulatory networks in human Chagas disease. *Parasite Immunol*. (2014) 36:377–87. doi: 10.1111/pim.12107
13. Dias JCP. Epidemiological surveillance of Chagas disease. *Cad Saúde Publ*. (2000) 16(Suppl. 2):43–59. doi: 10.1590/S0102-311X2000000800005
14. Marin-Neto JA, Cunha-Neto E, Maciel BC, Simões MV. Pathogenesis of chronic Chagas heart disease. *Circulation*. (2007) 115:1109–23. doi: 10.1161/CIRCULATIONAHA.106.624296
15. Rassi A Jr, Marin-Neto JA, Rassi A. Chronic Chagas cardiomyopathy: a review of the main pathogenic mechanisms and the efficacy of aetiological treatment following the BENznidazole Evaluation for Interrupting

Trypanosomiasis (BENEFIT) trial. *Mem Inst Oswaldo Cruz*. (2017) 112:224–35. doi: 10.1590/0074-02760160334
16. Lang RM, Badano LP, Mor-Avi V, Afilalo J, Armstrong A, Ernande L, et al. Recommendations for cardiac chamber quantification by echocardiography in adults: an update from the American Society of Echocardiography and the European Association of Cardiovascular Imaging. *J Am Soc Echocardiogr*. (2015) 28:1–39.e14. doi: 10.1016/j.echo.2014.10.003
17. Schmidt A, Dias Romano MM, Marin-Neto JA, Rao-Melacini P, Rassi A Jr, Mattos A, et al. Effects of trypanocidal treatment on echocardiographic parameters in Chagas cardiomyopathy and prognostic value of wall motion score index: a BENEFIT trial echocardiographic substudy. *J Am Soc Echocardiogr*. (2019) 32:286–95.e3. doi: 10.1016/j.echo.2018.09.006
18. Avila HA, Sigman DS, Cohen LM, Millikan RC, Simpson L. Polymerase chain reaction amplification of *Trypanosoma cruzi* kinetoplast minicircle DNA isolated from whole blood lysates: diagnosis of chronic Chagas' disease. *Mol Biochem Parasitol*. (1991) 48:11–21. doi: 10.1016/0166-6851(91)90116-N
19. Britto C, Cardoso MA, Wincker P, Morel CM. A simple protocol for the physical cleavage of *Trypanosoma cruzi* kinetoplast DNA present in blood samples and its use in polymerase chain reaction (PCR)-based diagnosis of chronic Chagas disease. *Mem Inst Oswaldo Cruz*. (1993) 88:171–2. doi: 10.1590/S0074-02761993000100030
20. Cummings KL, Tarleton RL. Rapid quantitation of *Trypanosoma cruzi* in host tissue by real-time PCR. *Mol Biochem Parasitol*. (2003) 129:53–9. doi: 10.1016/S0166-6851(03)00093-8
21. Schijman AG, Bisio M, Orellana L, Sued M, Duffy T, Mejia Jaramillo AM, et al. International study to evaluate PCR methods for detection of *Trypanosoma cruzi* DNA in blood samples from Chagas disease patients. *PLoS Negl Trop Dis*. (2011) 5:e931. doi: 10.1371/journal.pntd.0000931
22. Piron M, Fisa R, Casamitjana N, López-Chejade P, Puig L, Vergés M, et al. Development of a real-time PCR assay for *Trypanosoma cruzi* detection in blood samples. *Acta Trop*. (2007) 103:195–200. doi: 10.1016/j.actatropica.2007.05.019
23. Britto CC. Usefulness of PCR-based assays to assess drug efficacy in Chagas disease chemotherapy: value and limitations. *Mem Inst Oswaldo Cruz*. (2009) 104(Suppl. 1):122–35. doi: 10.1590/S0074-02762009000900018
24. Cura CI, Duffy T, Lucero RH, Bisio M, Péneau J, Jimenez-Coello M, et al. Multiplex real-time PCR assay using TaqMan probes for the identification of *Trypanosoma cruzi* DTUs in biological and clinical samples. *PLoS Negl Trop Dis*. (2015) 9:e0003765. doi: 10.1371/journal.pntd.0003765
25. Zingales B, Miles AM, Campbell AD, Tibayrenc M, Macedo AM, Teixeira MMG, et al. The revised *Trypanosoma cruzi* subspecific nomenclature: rationale, epidemiological relevance and research applications. *Infect Genet Evol*. (2012) 12:240–53. doi: 10.1016/j.meegid.2011.12.009
26. Moreira OC, Ramirez JD, Velazquez E et al. Towards the establishment of a consensus real-time qPCR to monitor *Trypanosoma cruzi* parasitemia in patients with chronic Chagas disease cardiomyopathy: a substudy from the BENEFIT trial. *Acta Trop*. (2013) 125:23–31. doi: 10.1016/j.actatropica.2012.08.020
27. Moreira OC, Ramírez JD, Velázquez E, Melo MF, Lima-Ferreira C, Guhl F, et al. Randomized trial of posaconazole and benznidazole for chronic Chagas' disease. *N Engl J Med*. (2014) 370:1899–908. doi: 10.1056/NEJMoa1313122
28. Yoshida N, Cortez M. *Trypanosoma cruzi*: parasite and host cell signaling during the invasion process. *Subcell Biochem*. (2008) 47:82–91. doi: 10.1007/978-0-387-78267-6_6
29. Hernández C, Salazar C, Brochero H, Teherán A, Buitrago LS, Vera M, et al. Untangling the transmission dynamics of primary and secondary vectors of *Trypanosoma cruzi* in Colombia: parasite infection, feeding sources and discrete typing units. *Parasit Vectors*. (2016) 9:620. doi: 10.1186/s13071-016-1907-5
30. D'Ávila DA, Galvão LMC, Sousa GR, Britto C, Moreira OC, Chiari E. Monitoring the parasite load in chronic Chagas disease patients: comparison between blood culture and quantitative real time PCR. *PLoS One*. (2018) 13:e0208133. doi: 10.1371/journal.pone.0208133
31. Duffy T, Cura CI, Ramirez JC, Abate T, Cayo NM, Parrado R, et al. Analytical performance of a multiplex Real-Time PCR assay using TaqMan probes for quantification of Trypanosoma cruzi satellite DNA in blood samples. *PLoS Negl Trop Dis*. (2013) 7:e2000. doi: 10.1371/journal.pntd.0002000
32. Cancino-Faure B, Fisa R, Riera C, Bula I, Girona-Llobera E, Jimenez-Marco T. Evidence of meaningful levels of *Trypanosoma cruzi* in platelet concentrates from seropositive blood donors. *Transfusion*. (2015) 55:1249–55. doi: 10.1111/trf.12989
33. Rodrigues-Dos-Santos Í, Melo MF, de Castro L, Hasslocher-Moreno AM, do Brasil PEAA, Silvestre de Sousa A, et al. Exploring the parasite load and molecular diversity of *Trypanosoma cruzi* in patients with chronic Chagas disease from different regions of Brazil. *PLoS Negl Trop Dis*. (2018) 12:e0006939. doi: 10.1371/journal.pntd.0006939
34. Tavares de Oliveira M, Sulleiro E, Silgado Gimenez A, de Lana M, Zingales B, Santana da Silva J, et al. Quantification of parasite burden of *Trypanosoma cruzi* and identification of Discrete Typing Units (DTUs) in blood samples of Latin American immigrants residing in Barcelona, Spain. *PLoS Negl Trop Dis*. (2020) 14:e0008311. doi: 10.1371/journal.pntd.0008311
35. Echeverría LE, Rojas LZ, Rueda-Ochoa OL, Gómez-Ochoa SA, González Rugeles CI, Díaz ML, et al. Circulating *Trypanosoma cruzi* load and major cardiovascular outcomes in patients with chronic Chagas cardiomyopathy: a prospective cohort study. *Trop Med Int Health*. (2020) 25:1534–41. doi: 10.1111/tmi.13487
36. Cunha-Neto E, Kalil J. Autoimmunity in Chagas' heart disease. *São Paulo Med J*. (1995) 113:757–66. doi: 10.1590/S1516-31801995000200005
37. Leon JS, Engman DM. Autoimmunity in Chagas heart disease. *Int J Parasitol*. (2001) 31:555–61. doi: 10.1016/S0020-7519(01)00163-1
38. Kaplinski M, Jois M, Galdos-Cardenas G, Rendell VR, Shah V, Do RQ, et al. Sustained domestic vector exposure is associated with increased chagas cardiomyopathy risk but decreased Parasitemia and congenital transmission risk among young women in Bolivia. *Clin Infect Dis*. (2015) 61:918–26. doi: 10.1093/cid/civ446
39. Dutra WO, Gollob KJ. Current concepts in immunoregulation and pathology of human Chagas disease. *Curr Opin Infect Dis*. (2008) 21:287–92. doi: 10.1097/QCO.0b013e3282f88b80
40. Bacal F, Silva CP, Pires PV, Mangini S, Fiorelli AI, Stolf NG, et al. Transplantation for Chagas' disease: an overview of immunosuppression and reactivation in the last two decades. *Clin Transplant*. (2010) 24:E29–E34. doi: 10.1111/j.1399-0012.2009.01202.x

Conflict of Interest: The authors declare that the research was conducted in the absence of any commercial or financial relationships that could be construed as a potential conflict of interest.

Publisher's Note: All claims expressed in this article are solely those of the authors and do not necessarily represent those of their affiliated organizations, or those of the publisher, the editors and the reviewers. Any product that may be evaluated in this article, or claim that may be made by its manufacturer, is not guaranteed or endorsed by the publisher.

frontiers in Cardiovascular Medicine

ORIGINAL RESEARCH
published: 23 September 2021
doi: 10.3389/fcvm.2021.752232

Catecholamine-Induced Secondary Takotsubo Syndrome in Children With Severe Enterovirus 71 Infection and Acute Heart Failure: A 20-year Experience of a Single Institute

Sheng-Ling Jan[1,2,3], Yun-Ching Fu[1,2], Ching-Shiang Chi[4], Hsiu-Fen Lee[1], Fang-Liang Huang[1], Chung-Chi Wang[5], Hao-Ji Wei[5], Ming-Chih Lin[1,2], Po-Yen Chen[1] and Betau Hwang[4]*

[1] Department of Pediatrics, Children's Medical Center, Taichung Veterans General Hospital, Taichung, Taiwan, [2] Department of Pediatrics, School of Medicine, National Yang-Ming University, Taipei, Taiwan, [3] Department of Pediatrics, School of Medicine, Kaohsiung Medical University, Kaohsiung, Taiwan, [4] Department of Pediatrics, Tungs' Taichung Metroharbor Hospital, Taichung, Taiwan, [5] Department of Cardiovascular Surgery, Cardiovascular Medical Center, Taichung Veterans General Hospital, Taichung, Taiwan

OPEN ACCESS

Edited by:
Walderez Ornelas Dutra, Federal University of Minas Gerais, Brazil

Reviewed by:
John David Horowitz, University of Adelaide, Australia
Andre Rodrigues Duraes, Federal University of Bahia, Brazil

***Correspondence:**
Sheng-Ling Jan
sljan@vghtc.gov.tw

Specialty section:
This article was submitted to General Cardiovascular Medicine, a section of the journal Frontiers in Cardiovascular Medicine

Received: *03 August 2021*
Accepted: *30 August 2021*
Published: *23 September 2021*

Citation:
Jan S-L, Fu Y-C, Chi C-S, Lee H-F, Huang F-L, Wang C-C, Wei H-J, Lin M-C, Chen P-Y and Hwang B (2021) Catecholamine-Induced Secondary Takotsubo Syndrome in Children With Severe Enterovirus 71 Infection and Acute Heart Failure: A 20-year Experience of a Single Institute. Front. Cardiovasc. Med. 8:752232. doi: 10.3389/fcvm.2021.752232

Background: Acute heart failure (AHF) is the major cause of death in children with severe enterovirus 71 (EV71) infection. This study aimed to report our clinical experience with EV71-related AHF, as well as to discuss its pathogenesis and relationship to Takotsubo syndrome (TTS).

Methods: A total 27 children with EV71-related AHF between 1998 and 2018 were studied. The TTS diagnosis was based on the International Takotsubo Diagnostic Criteria.

Results: Acute heart failure-related early death occurred in 10 (37%) of the patients. Sinus tachycardia, systemic hypertension, and pulmonary edema in 100, 85, and 81% of the patients, respectively, preceded AHF. Cardiac biomarkers were significantly increased in most patients. The main echocardiographic findings included transient and reversible left ventricular (LV) regional wall motion abnormality (RWMA) with apical ballooning. High concentrations of catecholamines either preceded or coexisted with AHF. Myocardial pathology revealed no evidence of myocarditis, which was consistent with catecholamine-induced cardiotoxic damage. Patients with EV71-related AHF who had received close monitoring of their cardiac function, along with early intervention involving extracorporeal life support (ECLS), had a higher survival rate (82 vs. 30%, $p = 0.013$) and better neurological outcomes (59 vs. 0%, $p = 0.003$).

Conclusion: EV 71-related AHF was preceded by brain stem encephalitis-related hypercatecholaminemia, which resulted in a high mortality rate. Careful monitoring is merited so that any life-threatening cardiogenic shock may be appropriately treated. In view of the similarities in their clinical manifestations, natural course direction, pathological findings, and possible mechanisms, TTS and EV71-related AHF may represent the same syndrome. Therefore, we suggest that EV71-related AHF could constitute a direct causal link to catecholamine-induced secondary TTS.

Keywords: catecholamine, enterovirus 71, heart failure, dilated cardiomyopathy, Takotsubo syndrome

INTRODUCTION

Most children infected by enterovirus 71 (EV71) develop either hand-foot-mouth disease (HFMD) or herpetic angina. Less than 0.01% of the patients are complicated by central nervous system (CNS) involvement, pulmonary edema, acute heart failure (AHF), shock, or early death (1–5). Our previous study found that EV71-related early deaths are usually accompanied by acute left ventricular (LV) dysfunction and LV regional wall motion abnormality (RWMA) (4–11). Therefore, AHF has been proposed as the major cause of early death in these patients (4–12), with EV-71 brainstem encephalitis-related hypercatecholaminemia believed as having a direct impact on the cardiotoxicity leading to AHF (7, 11, 13). Jan and Fu et al. found that patients with severe EV71 infection and AHF have clinical manifestations of sympathetic hyperactivity and significantly increased catecholamine concentrations. This result supports the hypothesis that hypercatecholaminemia is the cause of EV-71 related AHF (7, 11).

Takotsubo syndrome (TTS) was first reported in Japan in 1990 (14). The condition is characterized by reversible LV systolic dysfunction, which has a unique pattern similar to RWMA occurring in acute coronary syndrome (ACS), but without occluded coronary arteries, thus explaining the pattern of transient LV dysfunction. The syndrome is usually preceded by an emotional or a physical stress factor (15, 16). Although TTS is generally presented as a benign disease, serious complications, including AHF and cardiogenic shock, can lead to increased mortality. The reported incidence of cardiogenic shock in TTS patients ranges from 6 to 20% (15). Takotsubo syndrome most commonly occurs in postmenopausal women (15, 16), but is an uncommon condition in children (17, 18). The pathogenesis of TTS remains largely uncertain. Catecholamine-mediated cardiac stunning may be the main cause (15, 16, 19–21). The pathophysiology of TTS appears to be similar to the hypothesis of hypercatecholaminemia-related AHF in severe EV71 infection. In the present study, we describe the first study performed on children with severe EV71 infection and AHF, while presenting a clinical picture resembling TTS. A review of our previous studies is presented, with those findings shedding light on the pathophysiological concepts involved in this novel cardiac syndrome affecting children with severe EV71 infection.

METHODS

Study Population

Data from a total of 27 children, each with a laboratory-confirmed clinical diagnosis of severe EV71 infection and AHF from the years 1998 to 2018, were collected. Viral identification was also confirmed by the Taiwan Centers for Disease Control. The clinical features of EV71 infection have been divided into four stages and modified from the previous study (22). Stage 1, HFMD or herpangina without complication; Stage 2, CNS involvement with encephalomyelitis; Stage 3, Autonomic dysregulation; and Stage 4, Acute heart failure, including acute LV systolic dysfunction and shock. Severe EV71 infection was defined as EV71 infection beyond Stage 2. Patients suffering from neuromuscular diseases, craniofacial anomalies, genetic diseases, or previous cardiovascular diseases, as well as those who could not participate due to other reasons were excluded. Amongst the 27 children with severe EV71 infection and AHF (Stage 4), 10 received only conventional medical treatment between 1998 and 2000, and were defined as the pre-ECLS era cohort. Seventeen of the 27 patients experienced a poor response to conventional medical treatments and were rescued through extracorporeal life support (ECLS) between 2000 and 2018. These 17 were defined as the post-ECLS era cohort.

Diagnostic Imaging Study

Chest X-ray and a complete transthoracic echocardiography, using the Philips Sonos 5500, 7500 or iE33 ultrasound system (Philips, Andover, Massachusetts, USA), were performed on all patients within half an hour of entering the pediatric intensive care unit (PICU), and repeated as needed. Key echocardiographic features in this study consisted of LV systolic dysfunction and circumferential RWMA involving the mid-ventricular segments. If RWMA existed, the ejection fraction (EF) was measured using the biplane Simpson's rule. Possible causes of ventricular dysfunction, such as congenital coronary artery anomalies and severe ventricular outflow obstruction, were excluded. All echocardiographic studies were performed by experienced pediatric cardiologists (S-LJ, Y-CF, M-CL) (4–11).

Myocardial Histology Study

Myocardial histology using the elastic tissue-Masson technique, hematoxylin and eosin stain, and *in situ* terminal deoxyribonucleotidyl transferase-mediated dUTP nick end labeling assay were all studied. All myocardial specimens were sent for an enterovirus culture and analyzed by real-time polymerase chain reaction (7).

Cardiac Biomarkers Study

Laboratory data including complete blood count, blood glucose, biochemical tests, C-reactive protein, and cardiac biomarkers such as creatinine kinase (CK), muscle-brain fraction of creatine kinase (CK-MB), cardiac troponin I, B-type natriuretic peptide (BNP), or N-terminal prohormone of BNP (NT-proBNP) were studied (4–11). Hyperglycemia was defined as being a blood glucose concentration over 150 mg/dL on admission to the PICU. The upper limits of normal were 150 units/L for CPK, 5% for CK-MB, 1 ng/ml for cardiac troponin I, 100 pg/ml for BNP, and 125 pg/ml for NT-proBNP.

Catecholamine Study

Blood samples were collected upon admission to the PICU, and with the plasma stored at −70°C until analysis. After collection, urine samples were protected from light and stored at 4°C. They were then acidified with concentrated hydrochloric acid and stored at −20°C until analysis. Measured epinephrine (Epi), norepinephrine (NE), and vanillylmandelic acid (VMA) samples were taken using commercially available high-performance liquid chromatography, combined with the electrochemical detection method (7, 11). We corrected the relative concentration of urine catecholamine and VMA based on urine creatinine

TABLE 1 | Comparison of cohort data from before and after the era of using ECLS to rescue severe EV71-related acute heart failure.

Variables	Total years (1998–2018) ($n = 27$)	Pre-ECLS era (1998-2000) ($n = 10$)	Post-ECLS era (2000-2018) ($n = 17$)	*P* value
Clinical Data				
Age (months)	21 ± 16 (17)	18 ± 14 (13)	23 ± 17 (20)	0.505
Gender	17 M/10 F	5 M/5 F	12 M/5 F	0.415
BW (kg)	11 ± 4 (11)	10 ± 3 (10)	12 ± 5 (11)	0.334
Onset to admission (days)	4 ± 1 (3)	4 ± 1 (4)	3 ± 1 (3)	0.243
MaxHR (bpm)	206 ± 28 (205)	204 ± 37 (209)	207 ± 22 (200)	0.980
MaxSBP (mmHg)	119 ± 27 (123)	117 ± 15 (118)	120 ± 32 (131)	0.141
Diagnostic Imaging				
CTR in CxR	0.50 ± 0.04 (0.52)	0.50 ± 0.06 (0.53)	0.50 ± 0.04 (0.52)	0.824
Pulmonary edema	22 (81%)	9 (90%)	13 (76%)	0.621
LVEDD, Z-score	1.2 ± 2.1 (0.8)	0.9 ± 1.9 (1.0)	1.3 ± 2.2 (0.8)	0.639
Initial EF%	36 ± 11 (36)	38 ± 14 (36)	35 ± 9 (36)	0.570
RWMA	23 (85%)	8 (80%)	15 (88%)	0.613
Laboratory Data				
CK (IU/L)	330 ± 297 (344)	344 ± 445 (183)	323 ± 168 (369)	0.201
CK-MB (IU/L)	65 ± 237 (20)	135 ± 383 (11)	23 ± 10 (22)	0.182
Glucose (mg/dl)	268 ± 228 (199)	251 ± 137 (232)	276 ± 267 (140)	0.525
Intervention and Outcomes				
Rescued by ECLS	15 (56%)	0 (0%)	15 (88%)	0.000
Good neurological outcome	10 (37%)	0 (0%)	10 (59%)	0.003
Survival rate (>7 days)	17 (63%)	3 (30%)	14 (82%)	0.013
	10 early deaths	7 early deaths	3 early deaths	
	4 late deaths	3 late deaths	1 late death	

Data are presented as mean ± standard deviation (median) or case numbers (%). BW, body weight; CK, creatine kinase; CK-MB, muscle-brain fraction of creatine kinase; CTR, cardiothoracic ratio; CXR, chest radiography; ECLS, extracorporeal life support; EF, ejection fraction of the left ventricle; EV71, enterovirus 71; MaxHR, maximum heart rate; LVEDD, left ventricular end-diastolic dimension; MaxSBP, maximum systolic blood pressure; RWMA, regional wall motion abnormalities. Good neurological outcome is defined as survival to discharge with a Pediatric Cerebral Performance Category Scale of 1, 2, or 3 upon hospital discharge. Comparison of data between pre-ECLS era and post-ECLS era cohorts were analyzed by the Mann-Whitney U-test, Pearson's Chi-square test, or Fisher's exact test.

concentration and then expressed it as a ratio to the creatinine concentration (7, 11).

Diagnosis of TTS

The TTS diagnosis in this study was mainly based on the international Takotsubo diagnostic criteria (19), including (1) acute onset of symptoms; (2) transient RWMA with acute LV dysfunction by transthoracic echocardiography; (3) elevation in levels of cardiac biomarkers, CK-MB, cardiac troponin I, BNP, or NT-proBNP; (4) no evidence of infectious myocarditis; and (5) complete normalization of wall motion abnormality and LVEF, except in patients who died prior to evidence of recovery being captured.

Statistical Analysis

The data was displayed as the numbers of the case, percentage, median, or mean ± standard deviation. *SPSS, Version 22.0 for Windows* (SPSS, Chicago, IL, USA) was used for statistical analysis. The Mann-Whitney *U*-test, Pearson's Chi-square test, or Fisher's exact test were used to compare clinical manifestations, laboratory features, and outcomes between the pre-ECLS era and post-ECLS era cohorts. The Kaplan-Meier method was used to analyze the survival rate of EV71-related AHF patients. A two-tailed test result of $P < 0.05$ was considered statistically significant.

RESULTS

Patient Profiles

The demographic data, clinical manifestations, and outcomes of the patients are shown in **Table 1**. The median age of the patients was 17 months (4–69 months), with the male/female ratio being 1.7. Enterovirus 71-related AHF occurred in patients 2–4 days (median of 3 days) after EV71 infection symptoms were noted. All 27 patients experienced brainstem encephalitis (**Figure 1A**) and sinus tachycardia, with their maximum heart rate ranging from 185 to 260 bpm. Twenty-three (85%) patients on arrival to the PICU had preexisting systemic hypertension, while hypotension was diagnosed in 4 (15%), if cardiogenic shock occurred. Comparing the cohorts between the pre-ECLS era and post-ECLS era, there were 7 (70%) and 3 (18%) patients who experienced early death due to AHF, while three (30%) and 1 (6%) experienced late death due to encephalopathy, respectively. Compared with the pre-ECLS era cohort, patients

in the post-ECLS cohort had better neurological outcomes (good neurological outcomes of 59 vs. 0%, $p = 0.003$), as well as higher survival rates (82 vs. 30%, $p = 0.013$) (5, 7, 8).

Diagnostic Imaging Study

The cardiothoracic ratios measured on chest radiographs ranged from 0.39 to 0.55 (median 0.52). In the chest X-rays of all patients, heart size was normal for age. Twenty-two (81%) patients developed pulmonary edema (**Figure 1B**). The M-mode z-score values of LV end-diastolic diameter ranged from −2.1 to 4.6 (median of 0.84), which was consistent with the normal heart sizes shown on chest radiography. Initial abnormal LVEF ranged from 17 to 46% (median of 36%) by echocardiography. There were 23 (85%) patients who had typical RWMA and 4 (15%) with late stage AHF who had diffuse LV akinesia (**Figures 2A–D**; **Supplementary Videos 1**, **2**).

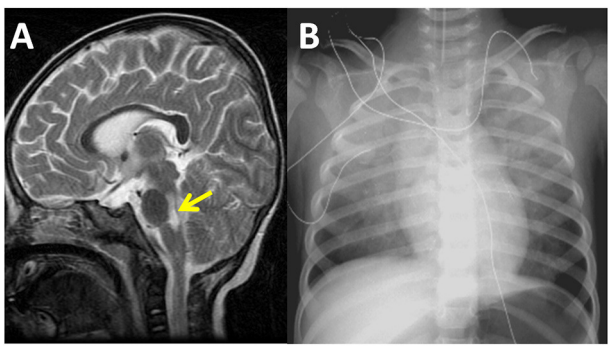

FIGURE 1 | Sagittal magnetic resonance imaging of the brain reveals high signal intensity over the dorsal regions of the brain stem and cervical spinal cord in a 16-month-old patient with severe enterovirus 71 infection and acute heart failure in the year 2001 **(A)**. Chest radiography demonstrates bilateral pulmonary edema and a normal heart size. The ejection fraction of the left ventricle was 27% as measured by echocardiography at this time **(B)**.

Myocardial Histology Study

Histological examination of the myocardium of seven patients revealed that all myocardial specimens demonstrated obvious myofibrillar degeneration with coagulative myocytolysis, with most of the nuclei showing significant pyknosis and irregular shape. Myofibrillar waving, dissolution, and different degrees of cardiomyocyte apoptosis could be observed. The LV was more remarkably involved than the right ventricle. Through either viral culture, real-time polymerase chain reaction for virus detection or inflammatory cell infiltration, all heart specimens showed no evidence of viral myocarditis (7).

Cardiac Biomarkers and Catecholamine Study

Laboratory findings revealed hyperglycemia, elevated CK, CK-MB, cardiac troponin I, BNP, and NT-proBNP in 15 (56%), 16/26 (62%), 24/26 (92%), 7/8 (88%), 4/4 (100%), and 4/4 (100%) patients, respectively. The cardiac biomarkers CK-MB, cardiac troponin I, BNP, and NT-proBNP were 65 ± 237 IU/L (median of 20), 3.94 ± 2.77 ng/ml (median of 1.48), 296 ± 162 pg/ml (median of 238), and 3,956 ± 2,908 pg/ml (median of 3,095), respectively. Catecholamines were measured in SIX patients, including plasma catecholamines which were measured in three patients who showed high concentrations, with their Epi levels being 3,461, 7,505, and 6,137 pg/ml (normal range <70 pg/ml), and NE levels at 4,723, 54,418, and 579 pg/ml (normal range 100–400 pg/ml). Urine catecholamines were measured in three

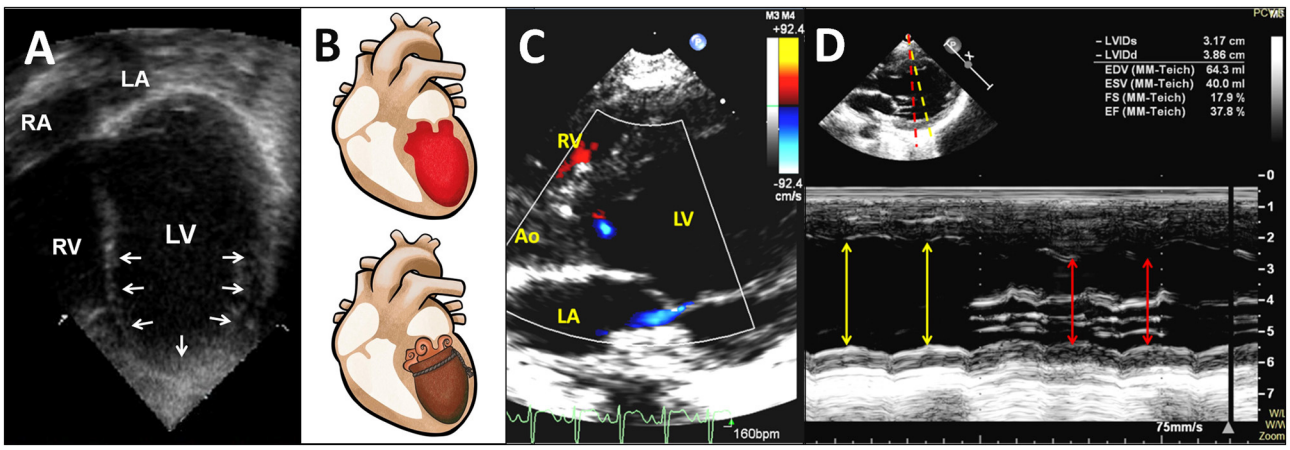

FIGURE 2 | Transthoracic two-dimensional echocardiogram in the apical four-chamber view shows a mid-ventricular pattern of a circumferential regional wall motion abnormality with conspicuous apical ballooning of the LV in a 20-month-old patient in the year 2000 **(A)** (also see **Supplementary Video 1**). Diagram demonstrates the apical ballooning shape of the LV with an appearance resembling an octopus pot (called Tako-tsubo) **(B)**. Transthoracic color Doppler echocardiogram in the parasternal long-axis view shows LV dysfunction with a circumferential regional wall motion abnormality resulting in apical ballooning of the LV during systole, and mild mitral regurgitation in a 3-year-old patient in the year 2018 **(C)** (also see **Supplementary Video 2**). An M-mode echocardiographic recording from the level of the mitral valve chordae to the level of the mitral valve reveals a circumferential LV regional wall motion abnormality along yellow and red lines **(D)**. Ao, aorta; LA, left atrium; LV, left ventricle; RA, right atrium; RV, right ventricle.

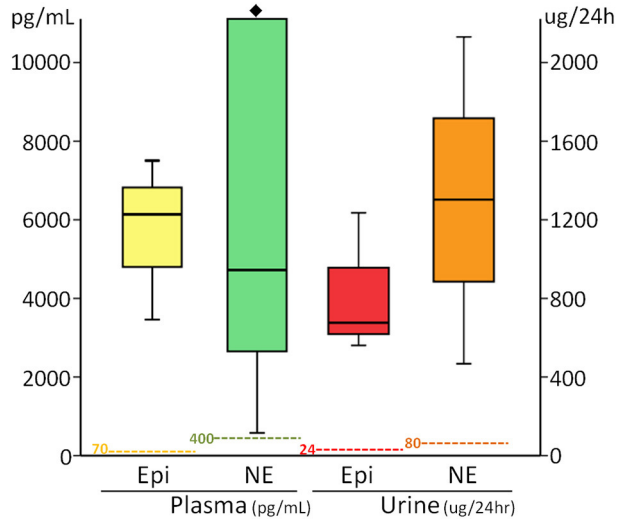

FIGURE 3 | Box-plots show significant elevation of plasma and urine catecholamine concentrations in patients with enterovirus 71-related heart failure. Dash lines indicate individual upper limits of normal. ♦, Outliers: the patient's values that are between 1.5 and 3 box lengths from either end of the box. Epi, epinephrine; NE, norepinephrine.

patients who displayed high Epi concentrations levels of 561, 677, and 1,236 μg/24 h (normal range 0–24 μg/24 h), NE levels of 1,303, 467, and 2,131 μg/24 h (normal range 10–80 μg/24 h), and VMA levels of 37.6, 14.2 and 28.4 mg/24 h (normal range 1–7 mg/24 h), respectively (**Figure 3**). Patients with EV71-related AHF had significantly higher troponin I, CK-MB, BNP, NT-proBNP, and catecholamine levels than those of patients without AHF. Using the cut-off values of BNP >100 pg/ml, urine Epi >134 μg/gCr, and urine NE >176 μg/gCr to identify EV71-infected patients with AHF, their sensitivity and specificity were both 100% for all when compared with those patients without AHF (7, 10, 11).

Diagnosis of TTS

An acute onset of symptoms and acute LV dysfunction occurred in all patients. Echocardiographic findings with typical RWMA met the diagnosis criteria in 23 (85%) patients, whereas four patients with diffuse LV akinesia, possibly due to a late stage of AHF upon arrival, did not meet the diagnostic criteria. There was insufficient laboratory data seen in both cardiac biomarkers and histological examination of the myocardial to allow for a full analysis, but the available parameters were elevated in most of the patients. There was no evidence of infectious myocarditis in 7 of 7 (100%) patients, while BNP and NT-proBNP both significantly increased in 4 of 4 (100%) patients. In 17 of the 27 patients, there was complete normalization of wall motion abnormality and LVEF, although early death occurred in the other 10 patients prior to complete normalization of LVEF. Most of the recovery time of LV systolic function was about 3–5 days.

DISCUSSION

Children with enterovirus infection are more likely to experience no complications, except when the pathogen is EV71. Enterovirus 71 was first discovered in California patients in 1974, where they were presented with serious neurologic complications. The virus is related to sporadic cases and outbreaks, and is distributed globally. Countries including Bulgaria in 1975 (44 deaths), Hungary in 1978 (47 deaths), Malaysia in 1997 (more than 31 deaths), and Taiwan in 1998 (78 deaths) have all been noted (1–3, 7). Brain stem encephalitis was the main neurological complication and was present in all of the fatal EV71 infection cases (1–3). However, AHF was the main cause of early mortality (4–9). All patients ran a similar fulminant course resulting in death. After experiencing several days of HFMD symptoms, herpangina, or febrile illness (Stage 1), patients developed brain stem encephalitis (Stage 2), with some developing sympathetic hyperactivity (Stage 3), and a few progressing to AHF with or without pulmonary edema (Stage 4), shock, and even rapid death, despite intensive management attempts (1–5).

EV71 Encephalitis, Hypersympathetic Activity, and Hypercatecholaminemia

Although hypersympathetic activity is preceded by CNS involvement, its pathophysiology remains unclear. The main pathological finding in EV71 encephalomyelitis is CNS inflammation, predominantly involving the whole brain stem and gray matter of the spinal cord. The lesions in these regions can increase hypersympathetic activity, and may result in peripheral vascular constriction, diaphoresis, tachycardia, and systemic hypertension, with surges of hypercatecholaminemia (13). In previous studies, we proved that there were significantly high concentrations of catecholamines in patients with EV71-related AHF which was preceded by hypersympathetic symptoms (7, 10, 11).

EV71-Related AHF

Based upon our prior knowledge and observations of the clinical manifestations, the characteristic presentations of patients with EV71-related AHF seem to include several issues. First, typical echocardiographic findings involved a mid-ventricular pattern of circumferential LV RWMA with apical ballooning, known as "panic or shivering heart", as well as acute LV dysfunction. Second, pulmonary edema and a normal heart size were noted in most patients experiencing heart failure, which has been termed, "heart function-chest radiograph dissociation." If only chest radiographs are used for assessment, this phenomenon may lead to unrecognized cardiac dysfunction in these patients. Third, there was no evidence of infectious myocarditis through patients' histology. Fourth, sympathetic hyperactivity and high concentrations of catecholamines were either followed by or coexisted with LV dysfunction. Fifth, most patients had a significant increase in cardiac biomarkers, indicating a certain degree of cardiac damage. Sixth, myocardial pathology results possibly indicated catecholamine-induced cardiac damage. Seventh, LV dysfunction was both acute and transient, but also usually fatal. Eighth, shock patients with

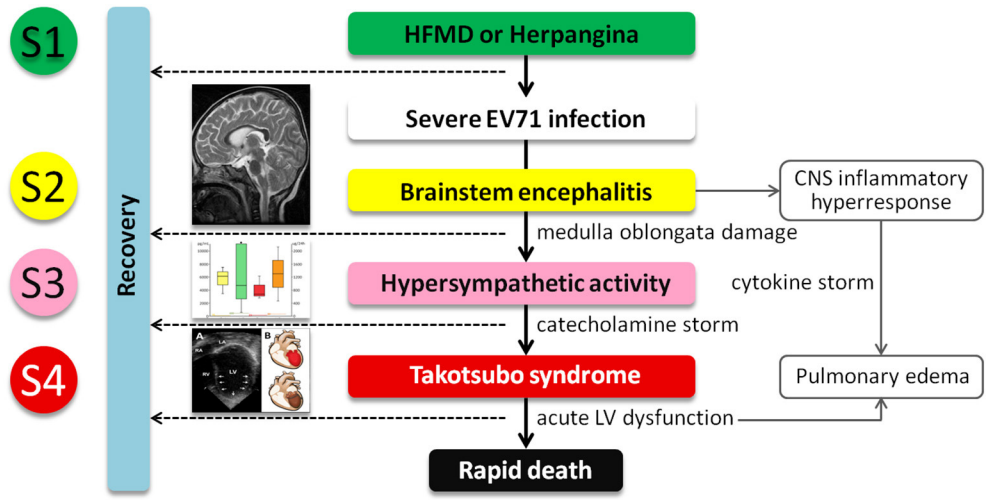

FIGURE 4 | The postulated pathogenesis of severe EV71 infection associated with catecholamine-induced secondary Takotsubo syndrome (TTS). Central nervous system indicates central nervous system; EV71, enterovirus 71; HFMD, hand-foot-and-mouth disease; LV, left ventricular; and S1–4, Stage 1–4.

hypotension more often experienced rapid clinical deterioration and adverse neurological outcomes. Ninth, short-term ECLS support treatment for transient cardiac dysfunction caused by catecholamine storm had a lower mortality rate and fewer neurological sequelae.

EV71-Related AHF and TTS

Catecholamines seem to play an important role in the pathogenesis of TTS, reflecting the comprehensive response of the cardiovascular system to either a sudden increase in the concentration of endogenous catecholamines, which is usually related to acute severe stress, or exogenous catecholamines (15, 16, 19–21). Cases can be classified as primary or secondary TTS (23). Biopsy samples obtained from patients in the acute phase of TTS are similar to those resulting from the direct effects observed after catecholamine-induced cardiotoxicity (16). Evidence from clinical studies supports the hypothesis that excess catecholamine serves as triggers for TTS (15, 16, 19–21). Paur et al. (24) reported an animal study concerning TTS that revealed a high epinephrine concentration can induce LV apical ballooning by injecting an exogenously high-dose of epinephrine. Fu et al. (25) developed a feline model of NE cardiotoxicity and compared it to children with EV71-related AHF. His study concluded that AHF in patients with EV71 encephalitis was similar to that in cats experiencing NE cardiotoxicity. In view of the similarities in clinical manifestations, natural course direction, pathological findings and possible pathogenesis, TTS and EV71-related AHF may represent the same syndrome. Therefore, we suggest that there is a direct causal link between EV71-related AHF and catecholamine-induced secondary TTS.

Pathogenesis of EV71-Related TTS

Our postulated pathogenesis of EV71-related TTS is presented in **Figure 4**. The pathophysiology of severe EV71 infection-related AHF and TTS can be generally divided into two phases. The first starts with an increased release of catecholamines, such as Epi and NE, initiated by EV71-related encephalitis, thus causing damage to the brain stem. The serum catecholamine concentration of severe EV71 patients is significantly higher at the time of AHF when compared with those in their non-AHF counterparts. These differences indicate that susceptible individuals may release excessive catecholamines. However, the thresholds for EV71-related encephalitis and excessive catecholamine release are incompletely understood. In recent years, several published reports have revealed the role of this brain-heart axis in the pathogenesis of TTS. Templin et al. (26) reported less functional connectivity in the limbic system of patients with TTS compared with healthy individuals. That region is important in emotional management and autonomic system regulation. Based on this reasoning, we consider that children with severe EV71 infection who develop TTS may have different autonomic regulation and the limbic system functions. The second phase is the cardiovascular reactions to the surge in circulating catecholamines. At this stage, catecholamine-induced TTS can be characterized by peripheral arterial vasoconstriction leading to an increase in afterload and transient high LV end-systolic pressure, acute coronary artery vasospasm resulting in both myocardial ischemia and a subsequent reduction in cardiac output with systemic hypotension, and finally catecholamine-mediated myocardial stunning which occurs directly at the apex where the β-adrenergic receptor gradient is highest. This area is highly sensitive to circulating catecholamines (16, 23). Despite the presence of hypercatecholaminemia, the development of hypotension may be the late stage of cardiogenic shock, or an aberrant response to catecholamine secretion, with the development of biased beta-2-mediated post-receptor signaling, and thus excessive release of the vasodilator nitric oxide (NO). Patients with TTS are hyper-responsive to NO, and in combination with the release (via catecholamines) of superoxide anion, generate peroxynitrite, a major inflammatory

mediator. This "nitrosative stress" is responsible for damage to the glycocalyx lining the vasculature (for example, via plasma concentrations of the glycocalyx component SD-1), facilitating increases in vascular permeability. Thus, despite the high catecholamine levels, patients with TTS develop both hypotension (partially via NO effect, partially via volume depletion) and peripheral edema.

LIMITATIONS

Due to the rarity of the condition, studies of children with severe EV71-related AHF are mostly limited to either case reports or series (3, 12). Although we have 20-years of experience treating children with EV71-related AHF at our institute, the case numbers in this study are limited. However, although similar clinical presentations have been found (3, 12), to the best of our knowledge this study is the largest case series in this field. Second, although there is currently a lack of non-invasive tools for a quick and reliable diagnosis of TTS, coronary angiography and left ventriculography are considered to be the gold standard diagnostic tools for confirming TTS. We lacked any evidence of absence of coronary artery disease (CAD) in this study, and also could not fully exclude any other conditions of secondary TTS, such as acute subarachnoid hemorrhage and pheochromocytoma. However, those conditions are uncommon in young children, and most published reports on TTS do not comply with these exclusion rules (19, 27). We cannot completely rule out the possibility that ACS-induced TTS may be the main event in our cohort, which in turn caused EV71 infection resulting in encephalitis and AHF. Nevertheless, the clinical manifestations (no history of heart disease predisposed to ACS prior to the event, and no myocarditis at autopsy) are more consistent with TTS being the initial precipitating event. Moreover, the prevalence of concomitant CAD in adult patients ranges from 10 to 29% (19). Therefore, the existence of CAD should not be regarded as an exclusion criterion, as acknowledged by International Takotsubo Diagnostic Criteria (19). Third, although cardiac magnetic resonance (CMR) with new parametric techniques has become an important tool for the non-invasive assessment of the TTS at the time of acute presentation and can help distinguish between TTS and other important differential diagnoses, such as myocarditis and myocardial infarction (28), we did not perform CMR for patients in this study due to all of them were hemodynamically unstable at the time of acute presentation. Fourth, we did not check cytokine profiles in this study. Cytokine storm can lead to AHF by IL-6-induced diastolic dysfunction and increased cardiomyocyte stiffness. Moreover, IL-1β and TNF-α produce negative inotropic effects and may induce cardiomyocyte pyroptosis and apoptosis, respectively (29, 30). However, there are limited data on cytokine storm-induced AHF (31, 32), and its clinical presentations and echocardiographic findings are not consistent with EV71-related AHF and TTS. Fifth, we did not perform specific immunohistological staining in this study. Immunohistological studies in patients with TTS and in rat models of TTS show that there is considerable inflammation, both cellular (leukocyte and macrophage infiltration) and humoral (thioredoxin-interacting protein), together with increased tissue 3-nitrotyrosine and poly(ADP-ribose) contents (33). Finally, the recognition of RWMA is subjective and involves substantial interoperative variability, despite all echocardiographic examinations being performed by experienced pediatric cardiologists in this study. Huang et al. (34) reported that automated interpretation of echocardiography by deep neural networks could be used to assist in the recognition of RWMA. Therefore, we consider that using these deep neural networks to automate the recognition of RWMA would be valuable in both supporting clinical reporting and improving efficiency in the future treatment of children with severe EV71 infection and AHF.

CONCLUSION

Severe EV71 infection with AHF preceded by brain stem encephalitis-related hypercatecholaminemia has a high mortality rate. Enterovirus 71-related hypercatecholaminemia may serve as a trigger factor for TTS in the same manner as severe physical stress factors. Additionally, patients with EV71-related AHF can be considered to have secondary TTS, which manifests itself as a form of chemical and toxic cardiomyopathy. Obtaining a detailed medical history, closely monitoring vital signs and clinical symptoms, routine measurement of NT-proBNP and troponin concentrations, follow-up echocardiography, as well as follow-up CMR may all aid in the diagnosis of TTS in EV71 patients with AHF. Speckle tracking echocardiography should be used to monitor cardiac function, not just ejection fraction. They also need to be carefully monitored in order to treat any life-threatening cardiogenic shock which may occur at the appropriate time. Further research is still required in order to help clarify the hypotheses discussed herein and increase our understanding of the thresholds for excess catecholamine release and the cardiovascular responses to EV71-related encephalitis. These additional studies will also help the medical community better understand the pathophysiology underpinning severe EV71 infection-induced secondary TTS in young children.

DATA AVAILABILITY STATEMENT

The raw data supporting the conclusions of this article will be made available by the authors, without undue reservation.

ETHICS STATEMENT

The studies involving human participants were reviewed and approved by The study complied with the Declaration of Helsinki, and all published studies were approved by the Institutional Ethics Committee of Taichung Veterans General Hospital. Written informed consent to participate in this study was provided by the participants' legal guardian/next of kin.

AUTHOR CONTRIBUTIONS

S-LJ and Y-CF contributed to the concept and design of this study, drafting of the manuscript, and statistical analysis. S-LJ, H-FL, F-LH, C-CW, and H-JW contributed to acquisition, analysis, and interpretation of the data. C-SC, M-CL, P-YC, and BH contributed to revision and finalize the manuscript. All authors contributed to the article and approved the submitted version.

ACKNOWLEDGMENTS

We would like to thank Dr. Christine Lee for her work on the drawings seen in **Figure 2B**. We would also like to thank Mr. Peter Wilds and Mr. Dean Spencer Dowers for their assistance with the English language editing of the manuscript. Finally, we remain grateful to all of our colleagues at the Children's Medical Center, Taichung Veterans General Hospital for their help.

SUPPLEMENTARY MATERIAL

The Supplementary Material for this article can be found online at: https://www.frontiersin.org/articles/10.3389/fcvm.2021.752232/full#supplementary-material

Supplementary Video 1 | RWMA with apical ballooning of the LV in the four-chamber view.

Supplementary Video 2 | RWMA with apical ballooning of the LV in the long-axis view.

REFERENCES

1. Ho M, Chen ER, Hsu KH, Twu SJ, Chen KT, Tsai SF, et al. An epidemic of enterovirus 71 infection in Taiwan. Taiwan Enterovirus Epidemic Working Group *N Engl J Med.* (1999) 341:929–35. doi: 10.1056/NEJM199909233411301
2. Huang CC, Liu CC, Chang YC, Chen CY, Wang ST, Yeh TF. Neurologic complications in children with enterovirus 71 infection. *N Engl J Med.* (1999) 341:936–42. doi: 10.1056/NEJM199909233411302
3. Chan LG, Parashar UD, Lye MS, Ong FG, Zaki SR, Alexander JP, et al. Deaths of children during an outbreak of hand, foot, and mouth disease in Sarawak, Malaysia: clinical and pathological characteristics of the disease. For the Outbreak Study Group. *Clin Infect Dis.* (2000) 31:678–83. doi: 10.1086/314032
4. Jan SL, Chi CS, Hwang B, Fu YC, Chen PY, Mak SC. Cardiac manifestations of fatal enterovirus infection during the 1998 outbreak in Taiwan. *Zhonghua Yi Xue Za Zhi (Taipei)*. (2000) 63:612–8.
5. Huang FL, Jan SL, Chen PY, Chi CS, Wang TM, Fu YC, et al. Left ventricular dysfunction in children with fulminant enterovirus 71 infection: an evaluation of the clinical course. *Clin Infect Dis.* (2002) 34:1020–4. doi: 10.1086/339445
6. Fu YC, Chi CS, Jan SL, Wang TM, Chen PY, Chang Y, et al. Pulmonary edema of enterovirus 71 encephalomyelitis is associated with left ventricular failure: implications for treatment. *Pediatr Pulmonol.* (2003) 35:263–8. doi: 10.1002/ppul.10258
7. Fu YC, Chi CS, Chiu YT, Hsu SL, Hwang B, Jan SL, et al. Cardiac complications of enterovirus rhombencephalitis. *Arch Dis Child.* (2004) 89:368–73. doi: 10.1136/adc.2003.029645
8. Jan SL, Lin SJ, Fu YC, Chi CS, Wang CC, Wei HJ, et al. Extracorporeal life support for treatment of children with enterovirus 71 infection-related cardiopulmonary failure. *Intensive Care Med.* (2010) 36:520–7. doi: 10.1007/s00134-009-1739-2
9. Lee HF, Chi CS, Jan SL, Fu YC, Huang FL, Chen PY, et al. Extracorporeal life support for critical enterovirus 71 rhombencephalomyelitis: long-term neurologic follow-up. *Pediatr Neurol.* (2012) 46:225–30. doi: 10.1016/j.pediatrneurol.2012.02.008
10. Jan SL, Lin SJ, Fu YC, Lin MC, Chan SC, Hwang B. Plasma B-type natriuretic peptide study in children with severe enterovirus 71 infection: a pilot study. *Int J Infect Dis.* (2013) 17:e1166–1171. doi: 10.1016/j.ijid.2013.06.012
11. Jan SL, Lin MC, Chan SC, Lee HF, Chen PY, Huang FL. Urine catecholamines in children with severe Enterovirus A71 infection: comparison with paediatric septic shock. *Biomarkers.* (2019) 24:277–85. doi: 10.1080/1354750X.2018.1556339
12. Huang YF, Chiu PC, Chen CC, Chen YY, Hsieh KS, Liu YC, et al. Cardiac troponin I: a reliable marker and early myocardial involvement with meningoencephalitis after fatal enterovirus-71 infection. *J Infect.* (2003) 46:238–43. doi: 10.1053/jinf.2002.1117
13. Solomon T, Lewthwaite P, Perera D, Cardosa MJ, McMinn P, Ooi MH. Virology, epidemiology, pathogenesis, and control of enterovirus 71. *Lancet Infect Dis.* (2010) 10:778–90. doi: 10.1016/S1473-3099(10)70194-8
14. Sato H, Tateishi H, Uchida T. Takotsubo-type cardiomyopathy due to multivessel spasm. In: Kodama K, Haze K, Hon M, editors. *Clinical Aspect of Myocardial Injury: From Ischemia to Heart Failure*. Tokyo: Kagakuhyouronsha (1990). p. 56–64.
15. Almendro-Delia M, Núñez-Gil IJ, Lobo M, Andrés M, Vedia O, Sionis A, et al. Short- and long-term prognostic relevance of cardiogenic shock in Takotsubo syndrome: results from the RETAKO registry. *JACC Heart Fail.* (2018) 6:928–36. doi: 10.1016/j.jchf.2018.05.015
16. Akashi YJ, Nef HM, Lyon AR. Epidemiology and pathophysiology of Takotsubo syndrome. *Nat Rev Cardiol.* (2015) 12:387–97. doi: 10.1038/nrcardio.2015.39
17. Sendi P, Martinez P, Chegondi M, Totapally BR. Takotsubo cardiomyopathy in children. *Cardiol Young.* (2020) 30:1711–5. doi: 10.1017/S1047951120002632
18. Topal Y, Topal H, Dogan C, Tiryaki SB, Biteker M. Takotsubo (stress) cardiomyopathy in childhood. *Eur J Pediatr.* (2020) 179:619–25. doi: 10.1007/s00431-019-03536-z
19. Ghadri JR, Wittstein IS, Prasad A, Sharkey S, Dote K, Akashi YJ, et al. International expert consensus document on Takotsubo syndrome (part I): clinical characteristics, diagnostic criteria, and pathophysiology. *Eur Heart J.* (2018) 39:2032–46. doi: 10.1093/eurheartj/ehy076
20. Wang X, Pei J, Hu X. The brain-heart connection in Takotsubo syndrome: the central nervous system, sympathetic nervous system, and catecholamine overload. *Cardiol Res Pract.* (2020) 2020:4150291. doi: 10.1155/2020/4150291
21. Prokudina ES, Kurbatov BK, Zavadovsky KV, Vrublevsky AV, Naryzhnaya NV, Lishmanov YB, et al. Takotsubo syndrome: clinical manifestations, etiology and pathogenesis. *Curr Cardiol Rev.* (2021) 17:188–203. doi: 10.2174/1573403X16666200129114330
22. Lin TY, Chang LY, Hsia SH, Huang YC, Chiu CH, Hsueh C, et al. The 1998 enterovirus 71 outbreak in Taiwan: pathogenesis and management. *Clin Infect Dis.* (2002) 34(Suppl 2):S52–7. doi: 10.1086/338819
23. Lyon AR, Bossone E, Schneider B, Sechtem U, Citro R, Underwood SR, et al. Current state of knowledge on Takotsubo syndrome: a position statement from the taskforce on Takotsubo syndrome of the Heart Failure Association of the European Society of Cardiology. *Eur J Heart Fail.* (2016) 18:8–27. doi: 10.1002/ejhf.424
24. Paur H, Wright PT, Sikkel MB, Tranter MH, Mansfield C, O'Gara P, et al. High levels of circulating epinephrine trigger apical cardiodepression in a β2-adrenergic receptor/Gi-dependent manner: a new model of Takotsubo cardiomyopathy. *Circulation.* (2012) 126:697–706. doi: 10.1161/CIRCULATIONAHA.112.111591
25. Fu YC, Chi CS, Lin NN, Cheng CC, Jan SL, Hwang B, et al. Comparison of heart failure in children with enterovirus 71 rhombencephalitis and cats with norepinephrine cardiotoxicity. *Pediatr Cardiol.* (2006) 27:577–84. doi: 10.1007/s00246-005-0915-6
26. Templin C, Hänggi J, Klein C, Topka MS, Hiestand T, Levinson RA, et al. Altered limbic and autonomic processing supports brain-heart axis in Takotsubo syndrome. *Eur Heart J.* (2019) 40:1183–7. doi: 10.1093/eurheartj/ehz068

27. Madias JE. Why the current diagnostic criteria of Takotsubo syndrome are outmoded: a proposal for new criteria. *Int J Cardiol.* (2014) 174:468–70. doi: 10.1016/j.ijcard.2014.04.241
28. Klein C, Hiestand T, Ghadri JR, Templin C, Jäncke L, Hänggi J. Takotsubo syndrome - predictable from brain imaging data. *Sci Rep.* (2017) 7:5434. doi: 10.1038/s41598-017-05592-7
29. Shirazi LF, Bissett J, Romeo F, Mehta JL. Role of inflammation in heart failure. *Atheroscler Rep.* (2017) 19:27. doi: 10.1007/s11883-017-0660-3
30. Murphy SP, Kakkar R, McCarthy CP, Januzzi JL Jr. Inflammation in heart failure: JACC state-of-the-art review. *J Am Coll Cardiol.* (2020) 75:1324–40. doi: 10.1016/j.jacc.2020.01.014
31. Chitturi KR, Thacker S, Al-Saadi MA, Kassi M. Successful treatment of acute heart failure in COVID-19-induced cytokine storm with tocilizumab: a case report. *Eur Heart J Case Rep.* (2020) 4:1–6. doi: 10.1093/ehjcr/ytaa188
32. Peng X, Wang Y, Xi X, Jia Y, Tian J, Yu B, et al. Promising Therapy for heart failure in patients with severe COVID-19: calming the cytokine storm. *Cardiovasc Drugs Ther.* (2021) 35:231–47. doi: 10.1007/s10557-020-07120-8
33. Surikow SY, Nguyen TH, Stafford I, Chapman M, Chacko S, Singh K, et al. Nitrosative Stress as a modulator of inflammatory change in a model of Takotsubo syndrome. *JACC Basic Transl Sci.* (2018) 3:213–26. doi: 10.1016/j.jacbts.2017.10.002
34. Huang MS, Wang CS, Chiang JH, Liu PY, Tsai WC. Automated recognition of regional wall motion abnormalities through deep neural network interpretation of transthoracic echocardiography. *Circulation.* (2020) 142:1510–20. doi: 10.1161/CIRCULATIONAHA.120.047530

Conflict of Interest: The authors declare that the research was conducted in the absence of any commercial or financial relationships that could be construed as a potential conflict of interest.

Publisher's Note: All claims expressed in this article are solely those of the authors and do not necessarily represent those of their affiliated organizations, or those of the publisher, the editors and the reviewers. Any product that may be evaluated in this article, or claim that may be made by its manufacturer, is not guaranteed or endorsed by the publisher.

frontiers in Cardiovascular Medicine

MINI REVIEW
published: 05 October 2021
doi: 10.3389/fcvm.2021.724254

Schistosome-Associated Pulmonary Arterial Hypertension: A Review Emphasizing Pathogenesis

Teresa Cristina Abreu Ferrari[1,2]*, *Ana Cristina Lopes Albricker*[3], *Ina Morais Gonçalves*[4] *and Cláudia Maria Vilas Freire*[2]

[1] Departamento de Clínica Médica, Faculdade de Medicina, Universidade Federal de Minas Gerais, Belo Horizonte, Brazil, [2] Hospital das Clínicas, Universidade Federal de Minas Gerais, Belo Horizonte, Brazil, [3] Programa de Pós-Graduação em Ciências Aplicadas à Saúde do Adulto, Universidade Federal de Minas Gerais, Belo Horizonte, Brazil, [4] Graduação em Medicina, Centro Universitário de Belo Horizonte, Belo Horizonte, Brazil

Schistosomiasis, especially due to *Schistosoma mansoni*, is a well-recognized cause of pulmonary arterial hypertension (PAH). The high prevalence of this helminthiasis makes schistosome-related PAH (Sch-PAH) one of the most common causes of this disorder worldwide. The pathogenic mechanisms underlying Sch-PAH remain largely unknown. Available evidence suggests that schistosome eggs reach the lung via portocaval shunts formed as a consequence of portal hypertension due to hepatosplenic schistosomiasis. Once deposited into the lungs, the eggs elicit an immune response resulting in periovular granuloma formation. Immune mediators drive transforming growth factor-β (TGF-β) release, which gives rise to pulmonary vascular inflammation with subsequent remodeling and development of angiomatoid and plexiform lesions. These mechanisms elicited by the eggs seem to become autonomous and the vascular lesions progress independently of the antigen. Portopulmonary hypertension, which pathogenesis is still uncertain, may also play a role in the genesis of Sch-PAH. Recently, there have been substantial advances in the diagnosis and treatment of PAH, but it remains a difficult condition to recognize and manage, and patients still die prematurely from right-heart failure. Echocardiography is used for screening, and the formal diagnosis requires right-heart catheterization. The experience in treating Sch-PAH is largely limited to the phosphodiesterase type 5 inhibitors, with evidence suggesting that these vasodilators improve symptoms and may also improve survival. Considering the great deal of uncertainty about Sch-PAH pathogenesis, course, and treatment, the aim of this review is to summarize current knowledge on this condition emphasizing its pathogenesis.

Keywords: pulmonary hypertension, pulmonary arterial hypertension, schistosomiasis, hepatosplenic schistosomiasis, TGF-β

OPEN ACCESS

Edited by:
Livia Passos, Brigham and Women's Hospital and Harvard Medical School, United States

Reviewed by:
Susana Hoette, University of São Paulo, Brazil
Martin Nelwan, Nelwan Institution for Human Resource Development, Indonesia

***Correspondence:**
Teresa Cristina Abreu Ferrari
tferrari@medicina.ufmg.br

Specialty section:
This article was submitted to General Cardiovascular Medicine, a section of the journal Frontiers in Cardiovascular Medicine

Received: *12 June 2021*
Accepted: *13 September 2021*
Published: *05 October 2021*

Citation:
Ferrari TCA, Albricker ACL, Gonçalves IM and Freire CMV (2021) Schistosome-Associated Pulmonary Arterial Hypertension: A Review Emphasizing Pathogenesis. Front. Cardiovasc. Med. 8:724254. doi: 10.3389/fcvm.2021.724254

INTRODUCTION

Pulmonary hypertension (PH) is a hemodynamic and pathophysiologic condition that comprises heterogeneous disorders, leads to right-heart failure if untreated, and carries substantial morbidity and mortality (1–4). It is defined as a mean pulmonary arterial pressure exceeding 20 mmHg at rest as assessed by right-heart catheterization (5). According to the recent World Health Organization (WHO) classification,

it is grouped into five categories: pulmonary arterial hypertension (PAH) (Group 1), left-heart-related (Group 2), lung-related (Group 3), chronic thromboembolic (Group 4), and miscellaneous (Group 5) PH (5). Schistosome-associated PH is classified as Group 1.

Pulmonary arterial hypertension is a chronically progressive condition that results from elevation in precapillary pulmonary artery pressure due to inflammation, vascular tone imbalance, and progressive remodeling of the pulmonary vasculature (4). Schistosomiasis is a well-recognized cause of PAH, which is estimated to occur in about 5–15% of patients with the severe hepatosplenic form of schistosomiasis, particularly due to *Schistosoma mansoni* (6, 7). Although PAH is an uncommon complication of schistosome infection, the high prevalence of this helminthiasis makes schistosome-associated PAH (Sch-PAH) one of the most common causes of this disorder worldwide (7).

Patients with Sch-PAH present clinical, laboratory, and hemodynamic profiles similar to those observed in PAH due to other etiologies (8). However, the pathogenic mechanisms underlying Sch-PAH remain largely unknown (9, 10), though available evidence suggests that egg deposition into the lung and consequent inflammatory response are key events in the genesis of these disorder. Over the last two decades, there have been substantial advances in the diagnosis and treatment of Sch-PAH, but it remains a difficult condition to recognize and manage, and patients still die prematurely from right-heart failure (11). In synthesis, there is a great deal of uncertainty about Sch-PAH pathogenesis, course, and treatment. Therefore, the aim of this mini-review is to summarize the current knowledge regarding Sch-PAH emphasizing its pathogenesis.

ETIOPATHOGENESIS AND COURSE OF SCHISTOSOME INFECTION

Schistosomiasis is a neglected tropical parasitic disease caused by trematode flukes of the genus *Schistosoma*. These blood flukes use man and other mammals as definitive hosts, and aquatic and amphibian snails as intermediate hosts. *Schistosoma mansoni*, *S. haematobium*, and *S. japonicum* are the most common disease-causing species and the most widely distributed, whereas *S. guineensis*, *S. intercalatum*, and *S. mekongi* occur in a few geographical areas and are only of local importance (12–15). According to available estimates, schistosomiasis affects more than 230 million people in parts of the Middle East, South America, Southeast Asia and, particularly, in sub-Saharan Africa (14, 15). The infection is more common in rural areas, but it also occurs in the periphery of urban centers associated with poor sanitation.

The schistosome species differ from each other in several characteristics and these differences are important determinants of the clinical presentations of the infection. *Schistosoma haematobium* inhabits the pelvic plexuses and damages the urinary tract. The other species reside in the portal and mesenteric veins, and cause intestinal and liver disease (12–15).

Schistosome eggs are shed into the environment through feces or urine. The eggs that reach freshwater release the ciliated miracidium larva that infects the intermediate host. After multiplying asexually into sporocysts and later into cercarial larvae, they are shed by the snail. On finding a definitive host, the cercariae penetrate the skin, lose their bifurcated tail transforming into schistosomula, which migrate in blood to the lungs and, then, to the liver, where they grow into adult worms, mate and follow the path to the mesenteric venules of the colon (*S. mansoni*), small intestine (*S. japonicum*), or pelvic plexus (*S. haematobium*), where eggs are laid (**Figure 1A**). About a third of the eggs are eliminated through feces or urine. Those not eliminated remain trapped in the intestinal or bladder wall, or are transported by blood to the liver or other organs (12–15). Eggs trapped into tissues elicit a cell-mediated periovular granulomatous reaction. As the infection progresses, a down modulation of the immune response originate progressive smaller granulomas (16), which are gradually replaced by fibrotic deposits (12, 15). Thus, in late infection, organ-specific clinical manifestations usually positively correlate with infection intensity, and are chiefly mediated by egg induced inflammation and granulomatous reaction (15, 16).

The course of schistosome infection is classified into acute and chronic phases and different clinical forms (17). Acute schistosomiasis is mostly seen in travelers after primary infection. Commonly, it presents as sudden onset of fever, malaise, myalgia, headache, eosinophilia, fatigue, diarrhea (with or without blood), abdominal pain, hepatomegaly, non-productive cough with pulmonary infiltrates on chest X-ray and, in case of *S. haematobium* infection, hematuria. These symptoms often subside spontaneously over a few weeks (15–17).

The chronic phase is usually asymptomatic, but individuals who live in endemic areas may present clinical manifestations that progress insidiously without specific treatment. The intensity and duration of the infection determine the severity of the chronic fibro-obstructive disease (12–17). In the intestinal form, eggs tapered into the gut wall provoke mucosal granulomatous inflammation that may cause chronic or intermittent abdominal pain and discomfort with or without diarrhea that may contain blood. Granulomatous inflammation around eggs embolized to presinusoidal periportal spaces of the liver that occur in the early stages of the chronic phase may cause hepatomegaly, which characterizes the hepatointestinal form. In long-standing intense infections, periportal collagen deposition leads to fibrosis and progressive occlusion of terminal branches of the portal veins causing portal hypertension. This clinical form is called hepatosplenic and presents with splenomegaly, collateral venous circulation, portocaval shunting, and esophagogastric varices [(12–14, 16, 17); **Figures 1B–D**]. The mild urinary form results from granulomatous inflammation around *S. haematobium* eggs tapered in the bladder and ureteral walls. Its defining symptom is hematuria, often associated with urinary frequency, burning micturition, dysuria and suprapubic discomfort. In high-intensity late chronic infections, obstruction of the urinary tract may develop due to accumulation of dead calcified eggs and fibrosis formation in vesical and ureteral walls (12–14, 16, 17).

Portosystemic shunts resulting from portal hypertension in hepatosplenic schistosomiasis enables egg embolization from the portal venous system to the systemic venous circulation,

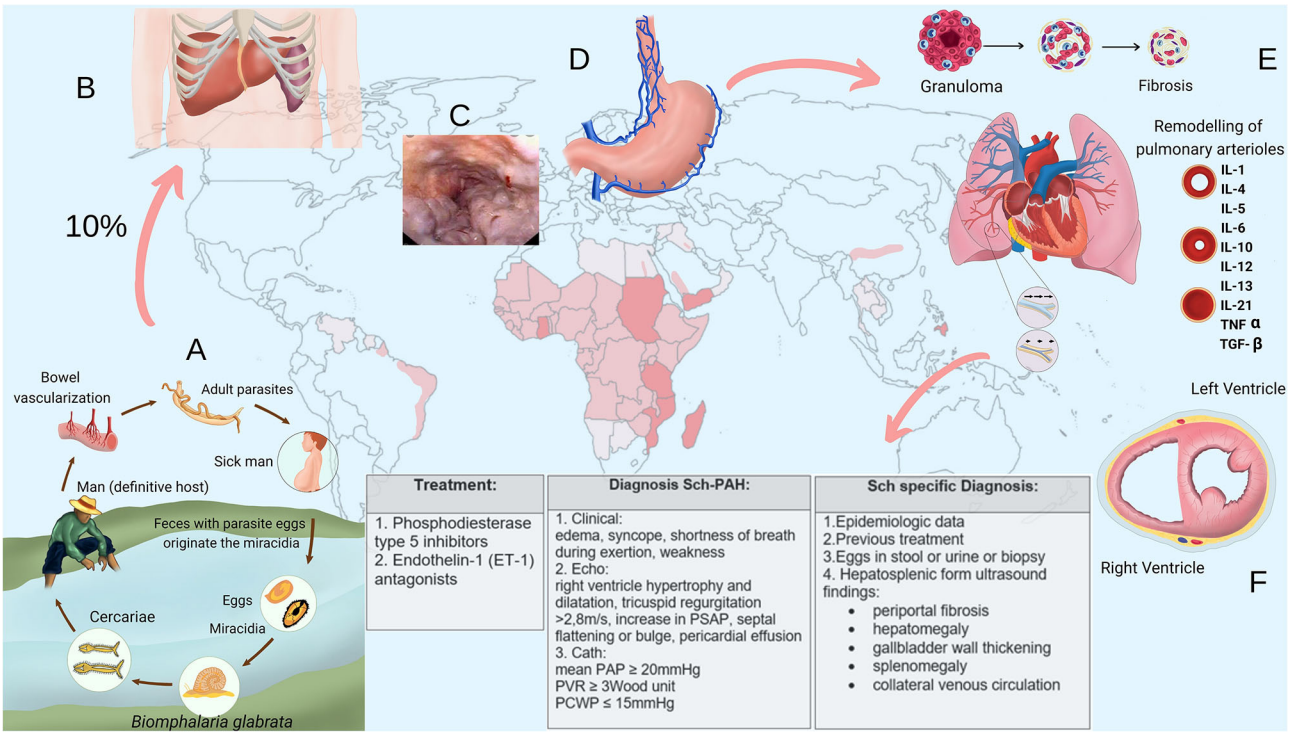

FIGURE 1 | (A) Schistosome life cycle. **(B)** Enlarged liver and spleen in hepatosplenic schistosomiasis. **(C)** Endoscopic aspect of esophageal varices. **(D)** Collateral venous circulation. **(E)** Pulmonary vascular remodeling in schistosome-associated pulmonary arterial hypertension. **(F)** Right-heart strain (cross section of the heart). IL, interleukin; TNF, tumor necrosis factor; TGF, transforming growth factor; Echo, echocardiography; Cath, right-heart catheterization.

and then to the lungs, which may cause PH in about 5–10% of patients with this severe form of schistosomiasis, particularly when the etiologic agent is *S. mansoni* (7). Although preexisting hepatosplenic disease is considered essential for the development of Sch-PAH, in rare reported cases, it was described the occurrence of this condition in chronic schistosomiasis without evidence of portal hypertension (18). However, in these situations, it is not possible to rule out the possibility that the patients actually presented schistosome infection associated with PH of another etiology. This may also be the explanation for the rare reported cases of PH associated with *S. haematobium* infection (19).

SCHISTOSOME-RELATED PULMONARY ARTERIAL HYPERTENSION

Schistosomiasis is the most common parasitic disease associated with PH (20, 21); and Sch-PAH might represent one of the most prevalent causes of this condition worldwide (22). Interest in this disorder has increased in recent years due to the current availability of PAH treatment. However, Sch-PAH is still underdiagnosed and undertreated.

Currently, Sch-PAH is defined by the combination of the following criteria: (1) mean pulmonary arterial pressure >20 mmHg, pulmonary arterial wedge pressure ≤15 mmHg (current criteria of precapillary PH) associated with a pulmonary vascular resistance >3 Wood Units, assessed at rest by right-heart catheterization; (2) history of schistosome infection, as evidenced by current or prior presence of schistosome eggs in stool examination or rectal biopsy, prior schistosome specific treatment, or prior exposure to the infection in a schistosome endemic area; and (3) ultrasonographic findings consistent with hepatosplenic schistosomiasis, which include periportal fibrosis, enlargement of the left lobe of the liver, and thickening of the gallbladder wall (23) associated with signs of portal hypertension such as splenomegaly and collateral venous circulation [(7); **Figures 1B–D**].

Pathogenesis

The exact pathogenesis of Sch-PAH remains unclear; however, mechanical obstruction of lung vasculature by embolized eggs, pulmonary vascular inflammation and remodeling, and portopulmonary hypertension-like pathophysiology have been suggested as the most probably pathogenic mechanisms for this condition (6, 18). The immunopathogenesis of the disease is also unclear, although there are similarities with the immunologic features of idiopathic PAH (18).

After being embolized to lungs via portosystemic shunts, the eggs elicit a predominantly T helper type-2 (Th2) cells immune response resulting in periovular granuloma formation. These granulomas affect both lung parenchyma and pulmonary vasculature causing parenchyma damage and fibrosis, and a certain extend of distal pulmonary vascular bed loss with consequent elevation in pulmonary vascular resistance. This mechanism is similar to what occurs in liver after egg deposition in the portal branches of portal vein, which results in some grade of fibrosis, tissue destruction, and obstruction of the portal flow (7, 18). Although this mechanism was originally considered the principal explanation for Sch-PAH, currently, it has been suggested that mechanical obstruction of the pulmonary arteries by the eggs may not cause significant increase in pulmonary vascular resistance and that Sch-PAH is especially due to a proliferative vasculopathy [(18, 24); **Figure 1E**].

A diffuse and heterogeneously distributed pulmonary vasculopathy is an important pathogenic mechanism underlying Sch-PAH (7, 18, 24–26). Alterations in the structure and function of the endothelial cells develop in association with growth of neointimal, medial, and adventitial layers, resulting in an occlusive arteriopathy, which increases the resistance to the blood flow. Angiomatoid and plexiform lesions also develop (6, 7, 22, 26). The exact pathogenesis of this vasculopathy is still unclear, though inflammatory mechanisms are strongly suspected (27). Some evidence indicates that transforming growth factor (TGF)-β plays a key role in the vascular remodeling (7, 9, 28–30); and, in Sch-PAH, the release of this cytokine is probably a consequence of the Th2 inflammation elicited by eggs deposited into lungs through a series of cellular and signaling events (7, 9, 29). However, Sch-PAH shares TGF-β-dependent vascular remodeling with idiopathic, heritable and autoimmune-associated etiologies of PAH (30). An interesting aspect is the fact that TGF-β activation, seems to become autonomous and independent of schistosome antigen resulting in a persistent vascular disease despite parasite eradication (7, 31). Some evidence suggests that TGF-β can induce a shift from glucose oxidation toward uncoupled aerobic glycolysis in pulmonary artery smooth muscle cells (PASMCs), which, then, undergo increased glycolysis, similar to the anaerobic glycolysis or "Warburg" effect observed in cancer cells. This effect may contribute to the proliferative, apoptosis resistant, cancer-like phenotype observed in PASMCs, pulmonary artery endothelial cells, and adventitial fibroblasts in established PAH. Increased cytosolic calcium, probably due to changes in ion channels, also seems to contribute to the contractile, hyperproliferative, and anti-apoptotic phenotype of PAH PASMCs (24). It has also been suggested that an infection (e.g., viruses) from propagating a number of inflammatory pathways that lead to vascular cell proliferation, migration, and extracellular matrix deposition may contribute to the structural remodeling characteristic of PAH (32, 33). In this context, Kim et al. demonstrated that patients with PAH exhibit a unique gut microbiome profile that produces bacterial metabolites and molecules, which may play a role in the pathogenesis of PAH (34). The obstructive vascular remodeling increases right-ventricle (RV) afterload leading to its hypertrophy. Over time, changes in the RV such as fibrosis and ischemia may develop causing RV dysfunction [(24); **Figure 1F**].

It has also been suggested that portopulmonary hypertension (PoPH), which is a serious complication of chronic liver diseases that course with portal hypertension, may contribute to the pathogenesis of Sch-PAH (6, 18, 26). Portopulmonary hypertension pathogenesis is unknown, but several hypotheses have been proposed: (1) imbalance of vasoconstrictive and vasodilatory mediators is the most widely accepted explanation. According to it, mediators that are normally metabolized by the liver, reach the pulmonary circulation via portosystemic shunts causing PoPH; (2) hyperdynamic pulmonary circulation with increased RV output and blood flow through the pulmonary vascular bed causing increased sheer stress on the vascular wall and then PoPH; (3) genetic predisposition; (4) pulmonary thromboembolism from the portal venous system. Emboli from the portal circulation may reach pulmonary vessels through portosystemic shunts causing PH; and (5) inflammation (6, 35).

Clinical Profile and Diagnosis

The clinical manifestations of Sch-PAH are indistinguishable from those of PAH of the other etiologies and result from progressive right-heart failure, including shortness of breath on exertion, peripheral edema, and syncope. However, pulmonary artery enlargement is more pronounced in Sch-PAH, independently of mean pulmonary artery pressure level, suggesting that this is more likely a feature of Sch-PAH (36). Furthermore, the clinical course of Sch-PAH seems to be more benign than that of idiopathic and connective tissue disease-associated PAH (37, 38).

As Sch-PAH is an important cause of PAH worldwide, particularly in developing countries, it is worth investigating this helminthiasis in people with PAH. The diagnosis of schistosomiasis is based on the history of environmental exposure to the infection, prior treatment of the parasitosis, or detection of eggs in stool, urine or rectal biopsy. Serologic testing is more helpful in the evaluation of patients from non-endemic areas because of the high rate of false positive results in persons who live in schistosome endemic areas (14, 17). Techniques to detect parasite antigens have been used and are commercially available in a point-of-care format (39). Polymerase chain reaction (PCR) and loop-mediated isothermal amplification (LAMP) on stool, urine or serum are sensitive but still of limited use. Hepatosplenic schistosomiasis diagnosis is based on ultrasonographic findings as previously described (23). Abdominal computed tomography (CT) scan and magnetic resonance imaging (MRI) may also demonstrate the findings of this form of schistosomiasis.

Echocardiography is usually the first exam performed in patients with suspicion of PH. Signs of RV overload such as RV hypertrophy and dilation, increase in pulmonary artery systolic pressure (PASP), and septal flattening or bulge are usually present. As measurement of pulmonary pressure by echocardiography is subject to limitations and its correlation with invasive measurements depends on optimal technical conditions, echocardiography is recommended for screening purposes. Studies have consistently shown that in nearly 50% of

cases, PASP Doppler estimates differ by more than 10 mmHg from the values obtained by right-heart catheterization (40–42). However, echocardiogram can give important additional and prognostic information, such as right and left heart function, and right atrial area and presence of pericardial effusion, which are associated with prognosis (42, 43).

If PH probability is intermediate or high on echocardiography, it should be considered to perform a ventilation/perfusion (V/Q) scan, comprehensive heart evaluation, and pulmonary tests to rule out the WHO 2, 3, and 4 PH groups. Right-heart catheterization is mandatory to confirm the presence of PH and to distinguish pre-capillary and post-capillary predominance (22, 44).

Clinical Management

Patients with Sch-PAH require close monitoring. Although reducing pulmonary pressure is the principal focus of the therapeutic approach, symptomatic, and supportive treatment remains an important component of patients' care. Diuretics are indicated to prevent or treat edema and the effects of volume overload on RV function and remodeling. Supplemental oxygen to maintain saturations above 90% helps to avoid hypoxia-induced pulmonary vascular constriction and consequent additional increase in pulmonary vascular resistance (4). Patients with portal hypertension have elevated bleeding risk from esophagogastric varices thus anticoagulation is usually not recommended (45).

Sch-PAH patients present improvements in functional class, 6-min walk distance, and hemodynamic parameters in response to PAH specific treatment (7, 46). Additionally, treated patients seem to have better survival rates than those untreated, at 5 years (47). Currently, PAH therapies target one or more of three major pathways implicated in disease progression: the nitric oxide (NO) pathway, which includes phosphodiesterase type 5 inhibitors (sildenafil and tadalafil) and soluble guanylyl cyclase stimulators (riociguat); the endothelin-1 (ET-1) pathway, which includes receptor antagonists (bosentan, ambrisentan, and macitentan); and the prostacyclin (PGI2) pathway, which includes prostacyclin analogs (epoprostenol, treprostinil, and iloprost) and the non-prostanoid IP-receptor agonist selexipag (7, 48). Considering resource limitations, only a few of these agents are available for clinical use in schistosomiasis endemic areas. Thus, the major drug used in those areas is sildenafil. However, as Sch-PAH shares pathophysiologic characteristics with the other WHO Group 1 PAH etiologies, creates the opportunity of treating Sch-PAH patients with the other agents (7). As a consequence of the better understanding of PAH pathophysiology, combination therapy, targeting the NO, ET-1, and PGI2 pathways, has emerged as the contemporary standard in the treatment of PAH patients (49). This approach requires investigation in Sch-PAH.

Sotatercept is an investigational ligand trap for TGF-β that was recently studied in patients with other forms of PAH. In these patients treated with standard therapy, the addition of sotatercept improved pulmonary vascular resistance, exercise tolerance, and serum levels of brain natriuretic peptide in comparison to placebo. As TGF-β activation may be a final common pathway in PAH pathogenesis, which is driven by different routes such as Th2 immune response in schistosomiasis, sotatercept may also be useful in the treatment of Sch-PAH patients (50).

The effect of anti-schistosome therapy in the lung parenchyma and vasculature has not been established. However, some authors suggest treating all Sch-PAH patients with praziquantel due to the severity of the disease and low risk of harm (51).

SUMMARY AND CONCLUSIONS

Schistosome pulmonary arterial hypertension is one of the most common causes of WHO Group 1 PAH worldwide. Thus, even in non-endemic areas, epidemiologic information about schistosomiasis exposure is important to be elicited. This form of PH develops in patients with the severe hepatosplenic form of schistosomiasis, especially due to *S. mansoni* infection, following egg embolization to the lungs via collaterals that form as a consequence of portal hypertension. Although Sch-PAH pathogenesis is largely unknown, progressive remodeling of pulmonary vasculature is considered a key mechanism in the genesis of this disease. It has been suggested that TGF-β signaling as a consequence of the Th2 immune response elicited by eggs deposited into the lungs triggers the vascular remodeling. The clinical, laboratory, and hemodynamic profiles of Sch-PAH are similar to those of the other forms of PAH. Screening for the disease is performed using echocardiography, and definite diagnosis requires right-heart catheterization. Although patients with Sch-PAH show a more favorable hemodynamic profile and better survival compared to those with other forms PAH, its outcome remains poor, carrying a significant morbidity and mortality. Data on treatment of Sch-PAH patients with pulmonary vasodilators are limited, but recent evidence suggests that such therapies improve symptoms and may also improve survival.

AUTHOR CONTRIBUTIONS

TF, AA, and CF: conception and design of the article, literature review, drafted the article, revised it critically, and approved the submitted version. IG: drafted and prepared the final version of the figure, and approved the submitted version. All authors contributed to the article and approved the submitted version.

ACKNOWLEDGMENTS

TF participates in the Conselho Nacional de Desenvolvimento Científico e Tecnológico (CNPq) Research Fellowship Program (PQ), process 303933/2019-4.

REFERENCES

1. Hsu CH, Ho WJ, Huang WC, Chiu YW, Hsu TS, Kuo PH, et al. 2014 Guidelines of Taiwan Society of Cardiology (TSOC) for the management of pulmonary arterial hypertension. *Acta Cardiol Sin*. (2014) 30:401–44.
2. Lan NSH, Massam BD, Kulkarni SS, Lang CC. Pulmonary arterial hypertension: pathophysiology and treatment. *Diseases*. (2018) 6:38. doi: 10.3390/diseases6020038
3. Parikh V, Bhardwaj A, Nair A. Pharmacotherapy for pulmonary arterial hypertension. *J Thorac Dis*. (2019) 11:S1767–81. doi: 10.21037/jtd.2019.09.14
4. Ishak Gabra NB, Mahmoud O, Ishikawa O, Shah V, Altshul E, Oron M, et al. Pulmonary arterial hypertension and therapeutic interventions. *Int J Angiol*. (2019) 28:80–92. doi: 10.1055/s-0039-1692452
5. Simonneau G, Montani D, Celermajer DS, Denton CP, Gatzoulis MA, Krowka M, et al. Haemodynamic definitions and updated clinical classification of pulmonary hypertension. *Eur Respir J*. (2019) 53:1801913. doi: 10.1183/13993003.01913-2018
6. Nunes MC, Guimarães Júnior MH, Diamantino AC, Gelape CL, Ferrari TC. Cardiac manifestations of parasitic diseases. *Heart*. (2017) 103:651–8. doi: 10.1136/heartjnl-2016-309870
7. Sibomana JP, Campeche A, Carvalho-Filho RJ, Correa RA, Duani H, Pacheco Guimaraes V, et al. Schistosomiasis pulmonary arterial hypertension. *Front Immunol*. (2020) 11:608883. doi: 10.3389/fimmu.2020.608883
8. Mendes AA, Roncal CGP, Oliveira FRA, Albuquerque ES, Góes GHB, Piscoya ICV, et al. Demographic and clinical characteristics of pulmonary arterial hypertension caused by schistosomiasis are indistinguishable from other etiologies. *Rev Soc Bras Med Trop*. (2020) 53:e20190418. doi: 10.1590/0037-8682-0418-2019
9. Graham BB, Chabon J, Gebreab L, Poole J, Debella E, Davis L, et al. TGF-β signaling promotes pulmonary hypertension caused by *Schistosoma mansoni*. *Circulation*. (2013) 128:1354–64. doi: 10.1161/CIRCULATIONAHA.113.003072
10. Chester AH, Yacoub MH, Moncada S. Nitric oxide and pulmonary arterial hypertension. *Glob Cardiol Sci Pract*. (2017) 2017:14. doi: 10.21542/gcsp.2017.14
11. Wilkins MR, Aman J, Harbaum L, Ulrich A, Wharton J, Rhodes CJ. Recent advances in pulmonary arterial hypertension. *F1000Res*. (2018) 7:1128–38. doi: 10.12688/f1000research.14984.1
12. Gryseels B, Polman K, Clerinx J, Kestens L. Human schistosomiasis. *Lancet*. (2006) 368:1106–18. doi: 10.1016/S0140-6736(06)69440-3
13. Gryseels B. Schistosomiasis. *Infect Dis Clin North Am*. (2012) 26:383–97. doi: 10.1016/j.idc.2012.03.004
14. Colley DG, Bustinduy AL, Secor WE, King CH. Human schistosomiasis. *Lancet*. (2014) 383:2253–64. doi: 10.1016/S0140-6736(13)61949-2
15. McManus DP, Dunne DW, Sacko M, Utzinger J, Vennervald BJ, Zhou XN. Schistosomiasis. *Nat Rev Dis Primers*. (2018) 4:13. doi: 10.1038/s41572-018-0013-8
16. Ferrari TCA. Neuroschistosomiasis. In: Bentivoglio M, Cavalheiro EA, Kristensson K, Patel N, editors. *Neglected Tropical Diseases and Conditions of the Nervous System*. New York, NY: Springer (2014). p. 111–26.
17. Ferrari TCA, Moreira PRR. Neuroschistosomiasis: clinical symptoms and pathogenesis. *Lancet Neurol*. (2011) 10:853–64. doi: 10.1016/S1474-4422(11)70170-3
18. Papamatheakis DG, Mocumbi AOH, Kim NH, Mandel J. Schistosomiasis associated pulmonary hypertension. *Pulm Circ*. (2014) 4:596–611. doi: 10.1086/678507
19. Bourée P, Piveteau J, Gerbal JL, Halpen G. Pulmonary arterial hypertension due to bilharziasis. Apropos of a case due to *Schistosoma haematobium* having been cured by praziquantel. *Bull Soc Pathol Exot*. (1990) 83:66–71.
20. Kolosionek E, Graham BB, Tuder RM, Butrous G. Pulmonary vascular disease associated with parasitic infection – the role of schistosomiasis. *Clin Microbiol Infect*. (2011) 17:15–24. doi: 10.1111/j.1469-0691.2010.03308.x
21. Butrous G. Schistosome infection and its effect on pulmonary circulation. *Glob Cardiol Sci Pract*. (2019) 2019:5. doi: 10.21542/gcsp.2019.5
22. Gavilanes F, Fernandes CJ, Souza R. Pulmonary arterial hypertension in schistosomiasis. *Curr Opin Pulm Med*. (2016) 22:408–14. doi: 10.1097/MCP.0000000000000300
23. Richter J, Hatz C, Campagne G, Bergquist N, Jenkins R, Jennifer M, et al. *Ultrasound in Schistosomiasis: A Practical Guide to the Standardized Use of Ultrasonography for the Assessment of Schistosomiasis-Related Morbidity*. Geneva: World Health Organization (2000).
24. Thenappan T, Ormiston ML, Ryan JJ, Archer SL. Pulmonary arterial hypertension: pathogenesis and clinical management. *BMJ*. (2018) 360:j5492. doi: 10.1136/bmj.j5492
25. Rabinovitch M, Guignabert C, Humbert M, Nicolls MR. Inflammation and immunity in the pathogenesis of pulmonary arterial hypertension. *Circ Res*. (2014) 115:165–75. doi: 10.1161/CIRCRESAHA.113.301141
26. Graham BB, Bandeira AP, Morrell NW, Butrous G, Tuder RM. Schistosomiasis-associated pulmonary hypertension pulmonary vascular disease: the global perspective. *Chest*. (2010) 137:20–9S. doi: 10.1378/chest.10-0048
27. Kolosionek E, King J, Rollinson D, Schermuly RT, Grimminger F, Graham BB, et al. Schistosomiasis causes remodeling of pulmonary vessels in the lung in a heterogeneous localized manner: detailed study. *Pulm Circ*. (2013) 3:356–62. doi: 10.4103/2045-8932.114764
28. Graham BB, Kumar R. Schistosomiasis and the pulmonary vasculature (2013 Grover Conference series). *Pulm Circ*. (2014) 4:353–62. doi: 10.1086/675983
29. Kumar R, Mickael C, Chabon J, Gebreab L, Rutebemberwa A, Garcia AR, et al. The causal role of IL-4 and IL-13 in *Schistosoma mansoni* pulmonary hypertension. *Am J Respir Crit Care Med*. (2015) 192:998–1008. doi: 10.1164/rccm.201410-1820OC
30. Kumar R, Mickael C, Kassa B, Gebreab L, Robinson JC, Koyanagi DE, et al. TGF-β activation by bone marrow-derived thrombospondin-1 causes schistosoma- and hypoxia-induced pulmonary hypertension. *Nat Commun*. (2017) 8:15494. doi: 10.1038/ncomms15494
31. Spiekerkoetter E, Goncharova EA, Guignabert C, Stenmark K, Kwapiszewska G, Rabinovitch M, et al. Hot topics in the mechanisms of pulmonary arterial hypertension disease: cancer-like pathobiology, the role of the adventitia, systemic involvement, and right ventricular failure. *Pulm Circ*. (2019) 9:2045894019889775. doi: 10.1177/2045894019889775
32. Cool CD, Voelkel NF, Bull T. Viral infection and pulmonary hypertension: is there an association? *Expert Rev Respir Med*. (2011) 5:207–16. doi: 10.1586/ers.11.17
33. Pullamsetti SS, Savai R, Janssen W, Dahal BK, Seeger W, Grimminger F. Inflammation, immunological reaction and role of infection in pulmonary hypertension. *Clin Microbiol Infect*. (2011) 17:7–14. doi: 10.1111/j.1469-0691.2010.03285.x
34. Kim S, Rigatto K, Gazzana MB, Knorst MM, Richards EM, Pepine CJ, et al. Altered gut microbiome profile in patients with pulmonary arterial hypertension. *Hypertension*. (2020) 75:1063–71. doi: 10.1161/HYPERTENSIONAHA.119.14294
35. Safdar Z, Bartolome S, Sussman N. Portopulmonary hypertension: an update. *Liver Transpl*. (2012) 18:881–91. doi: 10.1002/lt.23485
36. Hoette S, Figueiredo C, Dias B, Alves JL Jr., Gavilanes F, Prada LF, et al. Pulmonary artery enlargement in schistosomiasis associated pulmonary arterial hypertension. *BMC Pulm Med*. (2015) 15:118. doi: 10.1186/s12890-015-0115-y
37. Alves JL, Gavilanes F, Jardim C, Fernandes CJCDS, Morinaga LTK, Dias B, et al. Pulmonary arterial hypertension in the southern hemisphere: results from a registry of incident Brazilian cases. *Chest*. (2015) 147:495–501. doi: 10.1378/chest.14-1036
38. dos Santos Fernandes CJ, Jardim CV, Hovnanian A, Hoette S, Dias BA, Souza S, et al. Survival in schistosomiasis-associated pulmonary arterial hypertension. *J Am Coll Cardiol*. (2010) 56:715–20. doi: 10.1016/j.jacc.2010.03.065
39. Ruberanziza E, Wittmann U, Mbituyumuremyi A, Mutabazi A, Campbell CH, Colley DG, et al. Nationwide remapping of *Schistosoma mansoni* infection in Rwanda using circulating cathodic antigen rapid test: taking steps toward elimination. *Am J Trop Med Hyg*. (2020) 103:315–24. doi: 10.4269/ajtmh.19-0866
40. Mazurek JA, Forfia PR. Enhancing the accuracy of echocardiography in the diagnosis of pulmonary arterial hypertension: looking at the heart to learn about the lungs. *Curr Opin Pulm Med*. (2013) 19:437–45. doi: 10.1097/MCP.0b013e3283645966

41. Montani D, Günther S, Dorfmüller P, Perros F, Girerd B, Garcia G, et al. Pulmonary arterial hypertension. *Orphanet J Rare Dis.* (2013) 8:97. doi: 10.1186/1750-1172-8-97
42. Augustine DX, Coates-Bradshaw LD, Willis J, Harkness A, Ring L, Grapsa J, et al. Echocardiographic assessment of pulmonary hypertension: a guideline protocol from the British Society of Echocardiography. *Echo Res Pract.* (2018) 5:G11–24. doi: 10.1530/ERP-17-0071
43. Leuchte HH, Ten Freyhaus H, Gall H, Halank M, Hoeper MM, Kaemmerer H, et al. Risk stratification strategy and assessment of disease progression in patients with pulmonary arterial hypertension: updated recommendations from the cologne consensus conference 2018. *Int J Cardiol.* (2018) 272S:20–9. doi: 10.1016/j.ijcard.2018.08.084
44. Frost A, Badesch D, Gibbs JSR, Gopalan D, Khanna D, Manes A, et al. Diagnosis of pulmonary hypertension. *Eur Respir J.* (2019) 53:1801904. doi: 10.1183/13993003.01904-2018
45. Galiè N, Humbert M, Vachiery JL, Gibbs S, Lang I, Torbicki A, et al. 2015 ESC/ERS Guidelines for the diagnosis and treatment of pulmonary hypertension: The Joint Task Force for the Diagnosis and Treatment of Pulmonary Hypertension of the European Society of Cardiology (ESC) and the European Respiratory Society (ERS): Endorsed by: Association for European Paediatric and Congenital Cardiology (AEPC), International Society for Heart and Lung Transplantation (ISHLT). *Eur Heart J.* (2016) 37:67–119. doi: 10.1093/eurheartj/ehv317
46. Japyassú FAA, Mendes AA, Bandeira ÂP, Oliveira FRA, Sobral Filho D. Hemodynamic profile of severity at pulmonary vasoreactivity test in schistosomiasis patients. *Arq Bras Cardiol.* (2012) 99:789–96. doi: 10.1590/s0066-782x2012005000071
47. Fernandes CJC, Piloto B, Castro M, Gavilanes Oleas F, Alves JL, Lopes Prada LF, et al. Survival of patients with schistosomiasis-associated pulmonary arterial hypertension in the modern management era. *Eur Respir J.* (2018) 51:1800307. doi: 10.1183/13993003.00307-2018
48. Tyagi S, Batra V. Novel therapeutic approaches of pulmonary arterial hypertension. *Int J Angiol.* (2019) 28:112–7. doi: 10.1055/s-0039-1692140
49. Mayeux JD, Pan IZ, Dechand J, Jacobs JA, Jones TL, McKellar SH, et al. Management of pulmonary arterial hypertension. *Curr Cardiovasc Risk Rep.* (2021) 15:2. doi: 10.1007/s12170-020-00663-3
50. Humbert M, McLaughlin V, Gibbs JSR, Gomberg-Maitland M, Hoeper MM, Preston IR, et al. Sotatercept for the treatment of pulmonary arterial hypertension. *N Engl J Med.* (2021) 384:1204–15. doi: 10.1056/NEJMoa2024277
51. Fernandes CJCDS, Jardim CVP, Hovnanian A, Hoette S, Morinaga LK, Souza R. Schistosomiasis and pulmonary hypertension. *Expert Rev Respir Med.* (2011) 5:675–81. doi: 10.1586/ers.11.58

Conflict of Interest: The authors declare that the research was conducted in the absence of any commercial or financial relationships that could be construed as a potential conflict of interest.

Publisher's Note: All claims expressed in this article are solely those of the authors and do not necessarily represent those of their affiliated organizations, or those of the publisher, the editors and the reviewers. Any product that may be evaluated in this article, or claim that may be made by its manufacturer, is not guaranteed or endorsed by the publisher.

frontiers in Cardiovascular Medicine

ORIGINAL RESEARCH
published: 29 November 2021
doi: 10.3389/fcvm.2021.751415

Cardiovascular Biomarkers and Diastolic Dysfunction in Patients With Chronic Chagas Cardiomyopathy

Luis E. Echeverría[1], Sergio Alejandro Gómez-Ochoa[2], Lyda Z. Rojas[3], Karen Andrea García-Rueda[4], Pedro López-Aldana[1], Taulant Muka[5] and Carlos A. Morillo[6]*

[1] Heart Failure and Heart Transplant Clinic, Fundación Cardiovascular de Colombia, Floridablanca, Colombia, [2] Public Health and Epidemiological Studies Group, Cardiovascular Foundation of Colombia, Floridablanca, Colombia, [3] Research Group and Development of Nursing Knowledge (GIDCEN-FCV), Research Center, Cardiovascular Foundation of Colombia, Floridablanca, Colombia, [4] Department of Internal Medicine, Universidad de Antioquia, Medellín, Antioquia, Colombia, [5] Institute of Social and Preventive Medicine (ISPM), University of Bern, Bern, Switzerland, [6] Department of Cardiac Sciences, Libin Cardiovascular Institute of Alberta, Cumming School of Medicine, University of Calgary, Calgary, AB, Canada

OPEN ACCESS

Edited by:
Walderez Ornelas Dutra, Federal University of Minas Gerais, Brazil

Reviewed by:
Israel Molina, Vall d'Hebron University Hospital, Spain
Cristiane Menezes, Federal University of Minas Gerais, Brazil
Luciano Fonseca Lemos de Oliveira, Federal University of Minas Gerais, Brazil
Søren Møller, University of Copenhagen, Denmark

***Correspondence:**
Luis E. Echeverría
luisecheverria@fcv.org; luisedo10@gmail.com

Specialty section:
This article was submitted to General Cardiovascular Medicine, a section of the journal Frontiers in Cardiovascular Medicine

Received: *01 August 2021*
Accepted: *19 October 2021*
Published: *29 November 2021*

Citation:
Echeverría LE, Gómez-Ochoa SA, Rojas LZ, García-Rueda KA, López-Aldana P, Muka T and Morillo CA (2021) Cardiovascular Biomarkers and Diastolic Dysfunction in Patients With Chronic Chagas Cardiomyopathy. Front. Cardiovasc. Med. 8:751415. doi: 10.3389/fcvm.2021.751415

Background: Chronic Chagas Cardiomyopathy is a unique form of cardiomyopathy, with a significantly higher mortality risk than other heart failure etiologies. Diastolic dysfunction (DD) plays an important role in the prognosis of CCM; however, the value of serum biomarkers in identifying and stratifying DD has been poorly studied in this context. We aimed to analyze the correlation of six biochemical markers with diastolic function echocardiographic markers and DD diagnosis in patients with CCM.

Methods: Cross-sectional study of 100 adults with different stages of CCM. Serum concentrations of amino-terminal pro-B type natriuretic peptide (NT-proBNP), galectin-3 (Gal-3), neutrophil gelatinase-associated lipocalin (NGAL), high-sensitivity troponin T (hs-cTnT), soluble (sST2), and cystatin-C (Cys-c) were measured. Tissue Doppler imaging was used to measure echocardiographic parameters indicating DD. Multivariate logistic regression models adjusted by age, sex, BMI, and NYHA classification were used to evaluate the association between the biomarkers and DD.

Results: From the total patients included (55% male with a median age of 62 years), 38% had a preserved LVEF, but only 14% had a normal global longitudinal strain. Moreover, 64% had a diagnosis of diastolic dysfunction, with most of the patients showing a restrictive pattern ($n = 28$). The median levels of all biomarkers (except for sST2) were significantly higher in the group of patients with DD. Higher levels of natural log-transformed NTproBNP (per 1-unit increase, OR = 3.41, $p < 0.001$), Hs-cTnT (per 1-unit increase, OR = 3.24, $p = 0.001$), NGAL (per 1-unit increase, OR = 5.24, $p = 0.003$), and Cys-C (per 1-unit increase, OR = 22.26, $p = 0.008$) were associated with increased odds of having diastolic dysfunction in the multivariate analyses. Finally, NT-proBNP had the highest AUC value (88.54) for discriminating DD presence.

Conclusion: Cardiovascular biomarkers represent valuable tools for diastolic dysfunction assessment in the context of CCM. Additional studies focusing mainly on patients with HFpEF are required to validate the performance of these cardiovascular biomarkers in CCM, allowing for an optimal assessment of this unique population.

Keywords: Chagas disease, Chagas cardiomyopathy, biomarkers, diastolic dysfunction (DD), echocardiograph

INTRODUCTION

Chagas disease, or American trypanosomiasis, is an infectious disease endemic in Latin America caused by hemoparasite *Trypanosomacruzi (T. cruzi)* (1). According to the World Health Organization (WHO) estimates published in 2015, 5,742,167 individuals with Chagas disease were living in Latin American countries (2). Moreover, estimated 300,000 infected individuals live in the U.S.A, and almost 100,000 live in the European Union with this disease, while the pooled prevalence of infection in Latin American migrants is estimated to be 4.2% (3, 4). The main transmission route of *T. cruzi* is vectorial (including parts or stool of ingestion triatomine insects); nevertheless, other important forms of the transmission include vertical (5), blood transfusions (6), and solid organ transplant (7). Although the acute infection is generally oligosymptomatic, almost 30% of the infected patients develop the chronic form of the disease after a few decades (8).

In its chronic phase, Chagas disease can involve the nervous system, the gastrointestinal tract (essentially the esophagus and the colon), and the heart (9). Chronic Chagas cardiomyopathy (CCM) represents one of the most severe forms of organ involvement, highlighting a high incidence of arrhythmias, leading to systemic embolisms and sudden cardiac death (10). Furthermore, it is associated with a severe myocardial involvement resulting in functional valvular regurgitation and dilated cardiomyopathy (11). Classically, heart failure in the context of Chagas disease has been related to a predominant systolic dysfunction profile (11, 12); however, diastolic dysfunction (DD) in the setting of CCM has also been associated with a worse clinical status and a higher incidence of adverse cardiovascular outcomes (13–16). This highlights the importance of making a prompt diagnosis of DD, which is usually achieved by echocardiography (17, 18).

Nevertheless, echocardiographic diagnosis of DD may suffer from the characteristic interobserver variability of this method (19). Moreover, patients with CD usually live in rural, secluded areas, significantly limiting the possibility of performing echocardiographic studies due to its restricted availability outside hospitals and associated costs (11). In this context, cardiovascular (CV) biomarkers could overcome these limitations, as samples can be collected and stored for a sufficient time to allow transportation to a nearby laboratory, the measurements do not depend on the availability of a trained cardiac sonographer, and the cost of the tests are significantly lower compared with echocardiography (20, 21). Moreover, CV biomarkers may also represent a viable option for identifying DD in this special population, as it has been observed that biomarkers such as NT-proBNP are significantly associated with DD diagnosis in heart failure of other etiologies (22–25). We aimed to analyze the correlation of six biochemical markers with diastolic function echocardiographic markers and DD diagnosis in patients with CCM. We hypothesize that NT-proBNP will have a significantly higher discriminative capacity to detect DD compared with the other CV biomarkers.

MATERIALS AND METHODS

Study Population

This cross-sectional study was conducted between July and December 2015 at the Heart Failure and Heart Transplant Clinic of Fundación Cardiovascular in Floridablanca, Colombia. Adult outpatients (>18 years old) with a positive serological diagnosis of *T. cruzi* infection (positive IgG antibodies) and echocardiographic (echo) or electrocardiographic (ECG) abnormalities consistent with chronic Chagas cardiomyopathy (a left anterior fascicular block, a right bundle branch block, atrioventricular blocks, ventricular premature beats, atrial fibrillation or flutter, bradycardia ≤50 h/min or echocardiographic finding suggesting myocardial alterations as evaluated by a cardiologist) were included. We enrolled patients across all the severity stages, including individuals with implantable devices and refractory heart failure. The study sample was obtained from the patients with CCM, attending their follow-up evaluations; the first 100 individuals who fulfilled the inclusion criteria were enrolled. We excluded individuals with diabetes mellitus, coronary heart disease history, mitral stenosis, or uncontrolled hypertension. The Institutional Committee on Research Ethics approved the research protocol of the study. All the patients provided written informed consent for their participation in the study.

Data Collection

Information on socioeconomic status, lifestyle factors, and medication use was recorded. Body-mass index, left ventricular ejection fraction (LVEF) calculated by Simpson's rule from the four-chamber view, and global longitudinal strain by speckle tracking (GLS) were also measured. Finally, fasting serum samples were collected from each individual for the assessment of the six biomarkers. High-sensitivity troponin T (hs-cTnT) was quantified with a fifth generation assay on an automated platform (ECLIA Elecsys 2010 analyzer, Roche Diagnostics, Germany). Galectin-3 (Gal-3) was assessed by using a quantitative method, specifically an ELFA (enzyme-linked fluorescent assay) technique (VIDAS, Biomerieux, Marcy l'Étoile, France). Amino-terminal pro-B-type natriuretic peptide (NT-proBNP) levels were measured using the electrochemiluminescence method (Roche Diagnostics GmbH, Mannheim, Germany). The Alere Triage® NGAL test was used to assess Neutrophil Gelatinase-Associated Lipocalin (NGAL). Soluble ST2 (sST2) was measured from banked serum by a Critical Diagnostics Presage™ sST2 assay kit via enzyme-linked immunosorbent assay (ELISA). Finally, Cystatin c (Cys-c) was quantified by an immunologic turbid metric assay (Tina-quant Cystatin C cobas®).

Echocardiography

Transthoracic echocardiography was performed using a GE Vivid S6 ultrasound system with an M4S matrix-array transducer of 1.6–4.3 MHz. Acquisitions were performed by a single certified and experienced cardiac sonographer blinded to the patient data (MCV). All echocardiograms were read and measured by a single cardiologist certified in echocardiography (LEE). Cardiac dimensions and Doppler measurements were obtained

in accordance with American Society of Echocardiography and European Association of Echocardiography recommendations. M-mode echocardiography was used to measure the left atrial (LA) diameter and LV end-diastolic and end-systolic diameters (as recommended by the 2010 Guidelines of the American Society of Echocardiography at the time the study was initiated).

Two-dimensional LA and LV volumes were determined using modified Simpson's rule, with images obtained from the apical four-chamber and two-chamber views. Pulsed-wave Doppler was performed in the apical four-chamber view. From transmitral recordings, early peak (E) and late (A) diastolic filling velocities, E/A ratio, E wave deceleration time, velocity-time integral (VTI) of the E-wave (VTIE), A-wave VTI (VTIA), and LA filling fraction [VTIA/(VTIE + VTIA)] were obtained. The e' lateral velocity (tissue Doppler) and the E/e' ratio were calculated. Isovolumic relaxation time was measured from continuous-wave Doppler obtained in the apical five-chamber view. RV systolic pressure was derived from continuous-wave Doppler interrogation of tricuspid regurgitation. RV systolic function was evaluated by measuring the peak systolic myocardial velocity (RV S0) of the lateral tricuspid annulus, and tricuspid annular plane systolic excursion (TAPSE).

Regarding diastolic dysfunction, the patients were classified into four groups according to the echocardiographic characteristics observed. The patients without alterations compatible with DD were classified as having a normal filling pattern; moreover, individuals with DD were divided into three groups: abnormal relaxation pattern, pseudonormal pattern, and restrictive pattern (including both reversible and fixed defects) according to the recommendations for the evaluation of left ventricular diastolic function by echocardiography of the American Society of Echocardiography and the European Association of Cardiovascular Imaging.

Statistical Analysis

Categorical variables were presented as numbers and proportions, while continuous variables were reported as medians and interquartile ranges. The Chi-square and Fischer exact tests were used to assess for differences in categorical variables by the DD group, while the Mann—Whitney *U*-test and the Kruskal—Wallis test were used for continuous variables. The Pearson's correlation test was used to assess whether the biomarkers were correlated with relevant continuous echocardiographic parameters of diastolic dysfunction. Furthermore, we used natural log-transformed values of biomarkers concentrations to approximate a normal distribution. ANOVA tests and the Bonferroni *post hoc* pairwise comparisons test were used to explore whether levels of natural log-transformed biomarkers were different across DD groups. Afterward, all biomarkers were analyzed using univariate logistic regression analyses in relation to DD diagnosis, and then adjusting for age, sex, body mass index, and NYHA classification. We quantified the discriminatory ability of the biomarkers with the area under the receiver-operating characteristic curve (AUC-ROC). The Youden index was used to identify the best biomarkers cut-off level to distinguish patients with and without DD. Also, we compared the AUC of NT-proBNP vs. all biomarkers. All statistical tests were two-sided. A p-value < 0.05 was considered statistically significant for all tests. All analyses were performed using Statistical Package STATA version 15 (Station College, Texas, USA).

Sensitivity Analyses

To explore whether the associations of the levels of the biomarkers with the outcome of diastolic disfunction would differ by ejection fraction classification, an interaction term of each biomarker and the LVEF was tested. Furthermore, the performance of the biomarker was evaluated only in patients with a preserved ejection fraction to assess for differences that may have clinical implications in this context.

RESULTS

Population Characteristics

One hundred individuals were included, 55% male with a median age of 62 [interquartile range (IQR) 53–70] years at baseline assessment. About 38% of the patients had a preserved LVEF, but only 14% of the included patients had a normal global longitudinal strain (GLS) value. Moreover, 64 patients (64%) had a diagnosis of diastolic dysfunction (DD), with most of the patients showing a restrictive pattern ($n = 28$). Patients with DD had a significantly higher body mass index (BMI) and were more frequently prescribed heart failure drugs, including ACEI/ARB, MRAs, beta-blockers, and diuretics, compared with patients without DD. Moreover, the individuals with DD had a significantly lower LVEF (Median in patients with DD: 17.5 vs. median in patients with non-DD: 42.5. $p < 0.001$) (**Table 1**).

Biomarkers and Diastolic Dysfunction in CCM

Significant differences in the levels of the biomarkers were observed when comparing patients with and without DD and across DD groups (**Tables 1**, **2**). At first, the median levels of NT-proBNP (1,695 vs. 132 pg/ml), Hs-cTnT (15.9 vs. 5.1 ng/L), Cys-C (1.3 vs. 0.9 mg/L), NGAL (110 vs. 73.5 ng/ml), and Galectin-3 (15.3 vs. 12.9 ng/ml) were significantly higher in the group of patients with DD compared with those without this diagnosis. Similarly, the levels of the biomarker also increased with more severe forms of diastolic dysfunction, being significantly different across DD groups (**Supplementary Table 1**, **Figure 1**). Furthermore, most of the evaluated biomarkers were significantly correlated with diastolic function echocardiographic variables, being the NT-proBNP and the Cys-C the biomarkers with the highest correlation values across the assessed variables (**Supplementary Table 2**). Interestingly, Mitral flow E velocity was correlated only with the renal biomarkers (Cys-C and NGAL) (**Supplementary Table 2**).

Furthermore, multivariate logistic regression models adjusted by age, sex, BMI, and NYHA classification revealed that all logarithm-transformed biomarkers (except for Galectin-3 and sST2) were significantly associated with DD diagnosis (**Table 3**). In this context, higher levels of natural log-transformed NTproBNP (per 1-unit increase, OR = 3.41, $p < 0.001$), Hs-cTnT (per 1-unit increase, OR = 3.24, $p = 0.001$), NGAL (per 1-unit

TABLE 1 | Characteristics of the patients with chronic Chagas cardiomyopathy evaluated according to diastolic dysfunction diagnosis ($n = 100$).

	Patients without DD ($N = 36$)	Patients with DD ($N = 64$)	Total ($N = 100$)	*p* value
Males	18 (50.0%)	37 (57.8%)	55 (55.0%)	0.451
Age	60.5 (52.7, 71.0)	63.0 (56.0, 68.2)	62.0 (54.0, 69.5)	0.217
AHA/ACC Classification				0.066
A	1 (2.8%)	0 (0.0%)	1 (1.0%)	
B	9 (25.0%)	7 (10.9%)	16 (16.0%)	
C	26 (72.2%)	53 (82.8%)	79 (79.0%)	
D	0 (0.0%)	4 (6.2%)	4 (4.0%)	
NYHA				0.853
I	15 (41.7%)	28 (43.8%)	43 (43.0%)	
II	14 (38.9%)	25 (39.1%)	39 (39.0%)	
III	7 (19.4%)	10 (15.6%)	17 (17.0%)	
IV	0 (0.0%)	1 (1.6%)	1 (1.0%)	
BMI	27.3 (24.5, 29.7)	24.4 (21.9, 27.6)	26.2 (22.7, 28.2)	0.008
ACEI/ARB	16 (44.4%)	54 (84.4%)	70 (70%)	<0.001
MRA	9 (25.0%)	47 (73.4%)	56 (56%)	<0.001
Beta-blockers	19 (52.8%)	59 (92.2%)	78 (78%)	<0.001
Diuretics	10 (27.8%)	37 (57.8%)	47 (47.0%)	0.004
LVEF	42.5 (35.2, 46.2)	17.5 (8.7, 30.2)	27.000 (13.0, 40.2)	<0.001
NT-proBNP	132.0 (54.4, 319.6)	1695.0 (665.9, 3892.0)	703.6 (178.9, 2818.7)	<0.001
Hs-cTnT	5.1 (3.5, 11.2)	15.9 (9.5, 29.1)	11.7 (5.6, 22.4)	<0.001
Cys-C	1.0 (0.9, 1.1)	1.2 (1.0, 1.5)	1.1 (0.9, 1.4)	<0.001
NGAL	73.5 (61.2, 98.5)	110.0 (80.0, 160.2)	96.5 (69.0, 145.2)	<0.001
Galectin-3	12.9 (10.8, 15.1)	15.3 (12.2, 20.5)	14.2 (11.5, 18.2)	0.006
sST2	22.9 (19.4, 26.0)	26.7 (20.5, 33.5)	24.7 (20.1, 31.9)	0.091

BMI, body mass index; ACEI/ARB, angiotensin-converting enzyme inhibitor/angiotensin receptor blocker; MRA, mineralocorticoid receptor antagonists; LVEF, left ventricular ejection fraction; NT-proBNP, N-terminal-proB-type natiuretic peptide; Hs-cTnT, high-sensitive cardiac troponin T; Cys-C, cystatin C; NGAL, neutrophil gelatinase- associated lipocalin; sST2, soluble ST2.

TABLE 2 | Characteristics of the patients with chronic Chagas cardiomyopathy evaluated according to diastolic dysfunction classification ($n = 100$).

	0 ($N = 36$)	I ($N = 22$)	II ($N = 14$)	III and IV ($N = 28$)	Total ($N = 100$)	*p* value
Males	18 (50.0%)	12 (54.5%)	7 (50.0%)	18 (64.3%)	55 (55.0%)	0.686
Age	60.5 (52.7, 71.0)	62.0 (56.2, 67.7)	62.500 (55.0, 66.7)	64.500 (55.7, 69.7)	62.0 (54.0, 69.5)	0.660
			AHA/ACC Classification			**0.019**
A	1 (2.8%)	0 (0.0%)	0 (0.0%)	0 (0.0%)	1 (1.0%)	
B	9 (25.0%)	2 (9.1%)	5 (35.7%)	0 (0.0%)	16 (16.0%)	
C	26 (72.2%)	20 (90.9%)	8 (57.1%)	25 (89.3%)	79 (79.0%)	
D	0 (0.0%)	0 (0.0%)	1 (7.1%)	3 (10.7%)	4 (4.0%)	
			NYHA			0.650
I	15 (41.7%)	8 (36.4%)	8 (57.1%)	12 (42.9%)	43 (43.0%)	
II	14 (38.9%)	12 (54.5%)	4 (28.6%)	9 (32.1%)	39 (39.0%)	
III	7 (19.4%)	2 (9.1%)	2 (14.3%)	6 (21.4%)	17 (17.0%)	
IV	0 (0.0%)	0 (0.0%)	0 (0.0%)	1 (3.6%)	1 (1.0%)	
BMI	27.3 (24.5, 29.7)	27.2 (23.2, 28.0)	23.7 (21.4, 27.1)	23.1 (21.6, 27.5)	26.2 (22.7, 28.2)	**0.012**
ACEI/ARB	16 (44.4%)	17 (77.3%)	13 (92.9%)	24 (85.7%)	70 (70%)	**<0.001**
Beta-blockers	19 (52.8%)	21 (95.5%)	13 (92.9%)	25 (89.3%)	78 (78%)	**<0.001**
MRA	9 (25%)	16 (72.7%)	9 (64.3%)	22 (78.6%)	56 (56%)	**<0.001**
Diuretics	10 (27.8%)	11 (50.0%)	5 (35.7%)	21 (75.0%)	47 (47.0%)	**0.002**
LVEF	42.5 (35.2, 46.2)	26.5 (13.7, 32.5)	20.5 (10.0, 30.7)	14.0 (6.0, 21.2)	27.0 (13.0, 40.2)	**<0.001**

BMI, body mass index; ACEI/ARB, angiotensin-converting enzyme inhibitor/angiotensin receptor blocker; MRA, mineralocorticoid receptor antagonists; LVEF, left ventricular ejection fraction. Bold values indicate a statistically significant difference, P-value < 0.05.

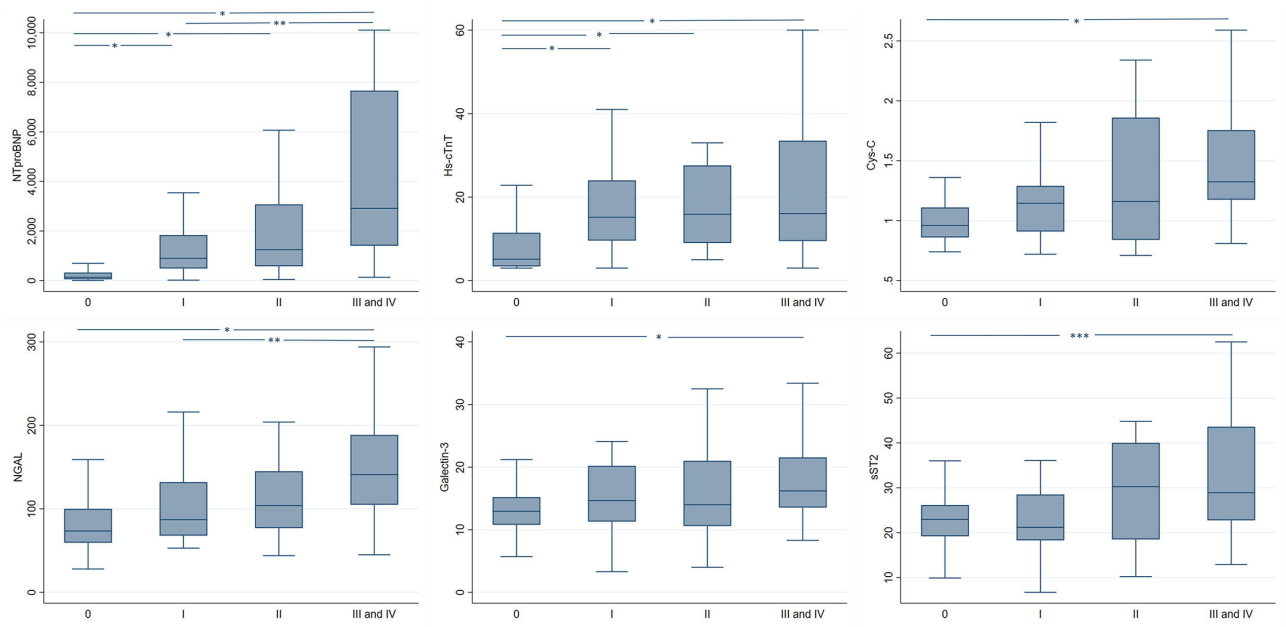

FIGURE 1 | Biomarker levels in patients with chronic Chagas cardiomyopathy with normal and abnormal patterns of diastolic function of the left ventricle. NT-proBNP, N-terminal-proB-type natiuretic peptide; Hs-cTnT, high-sensitive cardiac troponin T; Cys-C, cystatin C; NGAL, neutrophil gelatinase-associated lipocalin; sST2, soluble ST2. *, p-value < 0.001. **, *p*-value < 0.01. ***, *p*-value < 0.05.

increase, OR = 5.24, $p = 0.003$), and Cys-C (per 1-unit increase, OR = 22.26, $p = 0.008$) were associated with increased odds of having diastolic dysfunction.

Diagnostic Evaluation of the Biomarkers

Table 4 shows the best cut-off point for each biomarker and its corresponding AUC-ROC for detecting diastolic dysfunction. NT-proBNP had the highest AUC value (88.54) and was superior in all evaluated parameters (sensitivity, specificity, positive predictive value, negative predictive value, and accuracy) than the other assessed biomarkers. Hs-cTnT and Cystatin-C had the second and third highest AUC values, respectively. Finally, Galectin-3 was the only biomarker that was not significantly associated with DD diagnosis.

When comparing the AUC-ROC, we observed that the value was significantly higher for the NT-proBNP compared with any of the other biomarkers (*p*: 0.015 vs. Hs-cTnT, p: 0.004 vs. sST2, $p < 0.001$ vs. Galectin-3, *p*: 0.004 vs. NGAL, p: 0.010 vs. Cys-C) (**Figure 2**).

Sensitivity Analyses

A significant interaction term by LVEF was observed for NT-proBNP ($p = 0.011$) and Hs-cTnT ($p = 0.021$). Therefore, we assessed the population of patients with preserved ejection fraction apart, as identifying diastolic dysfunction could be more challenging in this subgroup. **Supplementary Table 3** summarizes the characteristics of patients with HF with a preserved ejection fraction according to the diagnosis of DD, evidencing a similar profile to the one observed in the full cohort (**Table 1**). We observed a different performance of the biomarkers in this population, highlighting that NT-proBNP and Hs-cTnT remained as significant predictors of DD. At the same time, NGAL and Cys-C lost statistical significance, and Galectin-3 and sST2 remained not significantly associated with diastolic dysfunction diagnosis (**Supplementary Table 4**).

DISCUSSION

In this study, patients with chronic Chagas cardiomyopathy had high prevalence of DD (64%), with most of the patients showing a restrictive pattern ($n = 28$). Several differences were observed between the patients with and without DD, highlighting a significantly lower LVEF in patients with DD diagnosis. Interestingly, patients with diastolic dysfunction had a significantly lower body mass index compared with those without DD. This finding could reflect the most advanced stage of HF in patients with DD, as these individuals develop a syndrome of cardiac cachexia, which is characterized by significant weight loss in the absence of peripheral edema. Furthermore, significant differences in the levels of NT-proBNP, Hs-cTnT, Cys-C, NGAL, and Galectin-3 were observed when comparing patients with and without DD and across DD groups, which were evidenced. Finally, NT-proBNP had the highest discriminative capacity to identify patients with DD, being its AUC-ROC significantly higher than those of the other assessed biomarkers.

Diastolic dysfunction has been associated with the development of Chagas cardiomyopathy in several studies, highlighting the relevant role of this condition as a potential early marker of myocardial involvement in the context of Chagas disease (13, 14, 17, 26). In the study of García-Alvarez et al., half

TABLE 3 | Association between biomarker levels and diastolic dysfunction diagnosis in patients with chronic Chagas cardiomyopathy.

Biomarkers	Crude estimate			Adjusted estimate[Ω]		
	OR	95% CI	*p*-value	OR	95% CI	*p*-value
NT-proBNP	2.54	1.75–3.67	**<0.001**	3.41	2.02–5.74	**<0.001**
Hs-cTnT	3.41	1.89–6.20	**<0.001**	3.24	1.65–6.37	**0.001**
Cys-C	18.25	3.16–105.38	**0.001**	22.26	2.27–217.7	**0.008**
NGAL	6.42	2.26–18.28	**<0.001**	5.24	1.74–15.78	**0.003**
Galectin-3	3.73	1.20–11.55	**0.023**	2.89	0.87–9.57	0.081
sST2	1.87	0.81–4.32	0.142	1.56	0.63–3.88	0.339

[Ω], *All models were adjusted by age, sex, body mass index, and NYHA classification. NT-proBNP, N-terminal-proB-type natiuretic peptide; Hs-cTnT, high-sensitive cardiac troponin T; Cys-C, cystatin C; NGAL, neutrophil gelatinase-associated lipocalin; sST2, soluble ST2. Bold values indicate a statistically significant difference, P-value < 0.05.*

TABLE 4 | Discriminative characteristics of the evaluated biomarkers for DD in the context of chronic Chagas cardiomyopathy.

Biomarkers[Ω]	Cut-off	AUC (%)	Sensitivity (%)	Specificity (%)	PPV (%)	NPV (%)	Accuracy (%)	*p*-value
NT-proBNP	5.81	88.54	90.63	77.78	87.88	82.35	86	<0.001
Hs-cTnT	2.30	77.30	79.69	66.67	80.95	64.86	75	<0.001
Cystatin-C	0.07	76.22	81.25	50	74.29	60	70	0.002
NGAL	4.48	73.22	79.69	44.44	71.83	55.17	67	0.010
sST2	3.27	72.09	82.81	41.67	71.62	57.69	68	0.066
Galectin-3	2.42	69.57	85.94	33.33	69.62	57.14	67	0.218

[Ω], *The discriminative capacity of the biomarkers was evaluated, considering the models adjusted by age, sex, body mass index, and NYHA classification. NT-proBNP, N-terminal-proB-type natiuretic peptide; Hs-cTnT, high-sensitive cardiac troponin T; Cys-C, cystatin C; NGAL, neutrophil gelatinase-associated lipocalin; sST2, soluble ST2.*

of the patients initially classified as being in the undetermined form of the disease, which showed impaired relaxation patterns. In contrast, half of the individuals with electrocardiographic abnormalities suggestive of CCM had a normal diastolic function (13). Furthermore, DD has also been associated with higher mortality risk among patients with CCM, as Rassi et al. suggested in their study, concluding that left atrial volume predicts adverse cardiovascular outcomes in this context (12). Similarly, Nunes et al. observed a significant association between the E/e' ratio and a composite outcome of mortality and heart transplantation (27). Nevertheless, a significant interaction between the LVEF and the E/e' ratio was observed, as, in patients with a severe LV systolic function (LVEF < 30%), the E/e' ratio had an inverse association with mortality; on the other hand, in patients with LVEF >45%, the E/e' ratio had a direct association with mortality, being a ratio >15 a powerful predictor of the assessed outcome. Interestingly, the septal e' velocity in patients with the composite outcome was >7 cm/sg on average. This observation deserves attention and, probably, an in-depth study of confounding factors that could explain it (27).

On the other hand, serum biomarkers have been gaining relevance as an important tool in the context of CCM. Several studies have highlighted the usefulness of these measurements to detect, classify, and assess the prognosis of patients with Chagas disease and myocardial involvement (28, 29). Among the most relevant ones, NT-proBNP has been the biomarker with the best performance to detect and predict adverse outcomes in patients with CCM, showing an unparalleled discriminative capacity compared with other biomarkers (30–33). Nevertheless, few studies have assessed performance of this biomarker in detecting and classifying DD in CD. Barbosa et al. reported that NT-proBNP levels were significantly associated with diastolic dysfunction in 59 patients with dilated CCM in Brazil. They observed that a marked elevated concentration of this biomarker (>800 pg/ml) had a sensitivity of 90% and specificity of 70.5% for detecting a restrictive filling pattern in this population (14). Similarly, Mady et al. reported that NT-proBNP levels were significantly correlated with DD echocardiographic markers (26). Finally, the study of Nunes MCP et al. concluded that BNP levels were significantly correlated with diastolic function patterns independently of systolic function in a small cohort of patients with CCM. A BNP value of 280.4 pg/ml showed a sensitivity of 96% and a specificity of 75% for predicting a value of E/e' ratio > 15, while the AUC-ROC for BNP to detect an E/e' ratio > 15 was 0.875 (34).

Although several studies have highlighted the potential use of biomarkers as Galectin-3, Cystatin-C, and NGAL to identify DD in patients with different diseases, this represents the first study that assessed these and other relevant cardiovascular biomarkers in the context of CD and CCM (22, 25, 35). Furthermore, NT-proBNP levels are mainly elevated by systolic dysfunction alone, potentially limiting its utility in the context of HF with a preserved ejection fraction (HFpEF) and patients with mild DD (14). Considering this limitation, additional cardiorenal biomarkers could prove useful in this specific context. Our findings of a significant association between Hs-cTnT, Cys-C, NGAL, and Galectin-3 levels with diastolic dysfunction provide valuable evidence regarding the

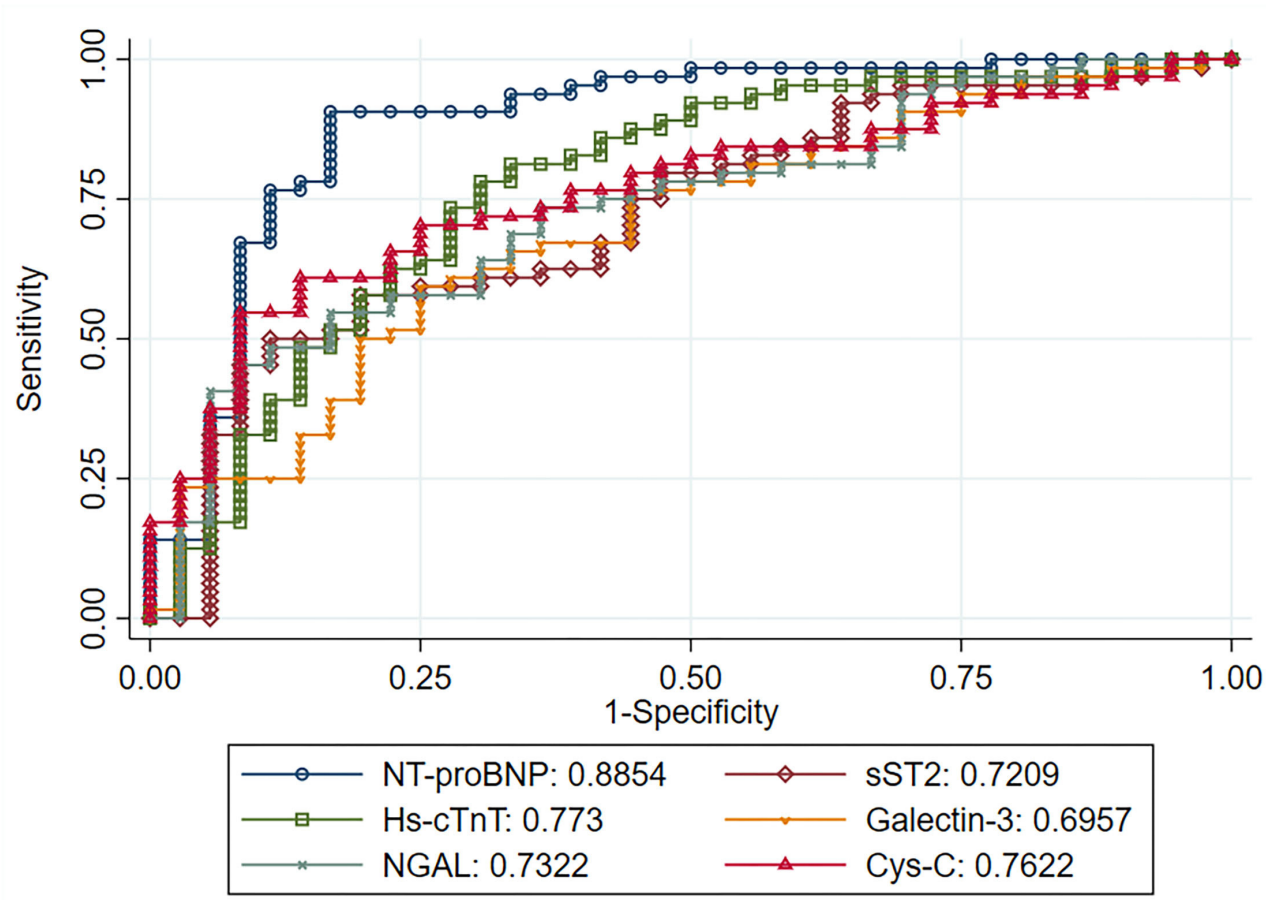

FIGURE 2 | An area under the curve of each natural log-transformed biomarker regarding the ability of discriminating patients with diastolic dysfunction. NT-proBNP, N-terminal-proB-type natiuretic peptide; Hs-cTnT, high-sensitive cardiac troponin T; Cys-C, cystatin C; NGAL, neutrophil gelatinase-associated lipocalin; sST2, soluble ST2.

role of different pathophysiological pathways, reflected in the differential levels of these biomarkers, in the development of diastolic dysfunction in CCM. However, despite showing a statistically significant difference, the difference in the levels of Cys-C in patients with DD compared with those without this condition may not have a relevant clinical significance. Moreover, we also observed that some biomarkers showed a higher correlation with specific echocardiographic markers of DD than NT-proBNP. For example, NGAL had an importantly higher correlation with PSAP (0.53) and the E/A ratio (0.35) compared to NT-proBNP (0.34 and 0.24, respectively). Similarly, Cys-C had a higher correlation with PSAP (0.45) and the E/e' lateral ratio (0.44) compared to NT-proBNP (0.34 and 0.22, respectively). Interestingly, NT-proBNP was not significantly correlated with the mitral flow E velocity, being this measure only correlated with the biomarkers of renal impairment (Cys-C and NGAL).

Finally, it is relevant to highlight that biomarkers are not intended to replace echocardiography regarding DD diagnosis; however, they could be of high utility in settings with limited access to echocardiography by identifying those patients with early CCM with a high risk of functional derangements of the LV, thus optimizing the use of the echocardiographic assessment for only this high-risk group. Nevertheless, the relevance and added value of cardiorenal biomarkers in addition to NT-proBNP in CCM still need to be evaluated in larger cohorts. In addition, the comparative performance of these biomarkers to detect DD in patients with HF of other etiologies is also warranted, as the present results cannot be extrapolated to cardiomyopathies other than CCM due to its unique pathophysiology and patterns of myocardial involvement.

Study Limitations

We must acknowledge the important limitations of our study. At first, diastolic dysfunction diagnosis was not achieved through cardiac catheterization, which is currently considered the gold standard for this purpose. Secondly, the median LVEF was significantly lower in patients in the diastolic dysfunction group than in individuals without DD. It is critical to consider this finding when interpreting the results of our study, as the high prevalence of reduced LVEF in patients with DD from our population can significantly modify the associations

observed. We aimed to overcome this limitation by performing a sensitivity analysis, assessing the performance of the biomarkers separately in patients with preserved LVEF (>40%), observing similar findings for NT-proBNP and Hs-cTnT. However, future studies with larger sample sizes are required to validate these results, as our sample did not include an important number of patients with a preserved ejection fraction; therefore, we could not thoroughly assess the performance of the biomarkers in patients with diastolic dysfunction and preserved LVEF. In addition, a control group of patients with other cardiomyopathies was not included, which precluded the comparison of the discriminative capacity of the biomarkers in non-CCM HF. Finally, we did not measure the intraobserver variability and the coefficient of variation for the assessed biomarkers, limiting the possibility of considering these relevant variables in our analyses.

CONCLUSIONS

Cardiovascular biomarkers represent valuable tools for diastolic dysfunction assessment in the context of CCM. In the present study, NT-proBNP showed the highest discriminative capacity for detecting DD; nevertheless, due to limitations of its use in the setting of reduced LVEF, other biomarkers, such as Hs-cTnT, Cys-C, NGAL, and Galectin-3, could prove useful for detecting and classifying DD when echocardiography or other diagnostic methods are not available. Additional studies focusing mainly on patients with HFpEF are required to validate the performance of cardiovascular biomarkers in CCM, allowing for an optimal assessment of this special population.

DATA AVAILABILITY STATEMENT

The datasets presented in this article are not readily available due to restrictions from the author's host institution. Requests to access the datasets should be directed to Luis Eduardo Echeverría, luisedo10@gmail.com.

ETHICS STATEMENT

The studies involving human participants were reviewed and approved by Comité de Ética en Investigación de la Fundación Cardiovascular de Colombia. The patients/participants provided their written informed consent to participate in this study.

AUTHOR CONTRIBUTIONS

LE, LR, TM, and CM contributed to the conception and design of the study. SG-O, KG-R, and PL-A organized the database. SG-O, LR, and TM performed the statistical analysis. SG-O wrote the first draft of the manuscript. SG-O, LE, LR, KG-R, PL-A, and CM wrote sections of the manuscript. All authors contributed to manuscript revision, read, and approved the submitted version.

FUNDING

LR and TM were supported by St. Gallen University through the Seed Money Grants Call of 2019. LE and LR were also supported by the Colombian government through Departamento Administrativo de Ciencia, Tecnología e Innovación-COLCIENCIAS (project code 501453730398, CT 380–2011); http://www.colciencias.gov.co/. The funder had no role in study design, data collection, analysis, decision to publish, or manuscript preparation.

ACKNOWLEDGMENTS

We thank patients with Chagas disease for their participation in this study.

SUPPLEMENTARY MATERIAL

The Supplementary Material for this article can be found online at: https://www.frontiersin.org/articles/10.3389/fcvm.2021.751415/full#supplementary-material

REFERENCES

1. Rassi A, Rassi A, Marin-Neto JA. Chagas disease. *Lancet Lond Engl.* (2010) 375:1388–402. doi: 10.1016/S0140-6736(10)60061-X
2. World Health Organization. Chagas disease in Latin America: an epidemiological update based on 2010 estimates. *Releve Epidemiol Hebd.* (2015) 90:33–43. Available online at: https://www.who.int/wer/2015/wer9006.pdf?ua=1
3. Manne-Goehler J, U meh CA, Montgomery SP, Wirtz VJ. Estimating the burden of chagas disease in the United States. *PLoS Negl Trop Dis.* (2016) 10:e0005033. doi: 10.1371/journal.pntd.0005033
4. Gascon J, Bern C, Pinazo M-J. Chagas disease in Spain, the United States and other non-endemic countries. *Acta Trop.* (2010) 115:22–7. doi: 10.1016/j.actatropica.2009.07.019
5. Edwards MS, Stimpert KK, Bialek SR, Montgomery SP. Evaluation and Management of Congenital Chagas Disease in the United States. *J Pediatr Infect Dis Soc.* (2019) 8:461–9. doi: 10.1093/jpids/piz018
6. Schmunis GA. Prevention of transfusional Trypanosoma cruzi infection in Latin America. *Mem Inst Oswaldo Cruz.* (1999) 94:93–101. doi: 10.1590/S0074-02761999000700010
7. Fabiani S, Fortunato S, Bruschi F. Solid organ transplant and parasitic diseases: a review of the clinical cases in the last two decades. *Pathog Basel Switz.* (2018) 7:65. doi: 10.3390/pathogens7030065
8. Echeverría LE, Marcus R, Novick G, Sosa-Estani S, Ralston K, Zaidel EJ, et al. WHF IASC roadmap on chagas disease. *Glob Heart.* (2020) 15:26. doi: 10.5334/gh.484
9. Vago AR, Andrade LO, Leite AA, Reis DD, Macedo AM, Adad SJ, et al. Genetic characterization of Trypanosoma cruzi directly from tissues of patients with chronic Chagas disease: differential distribution of genetic types into diverse organs. *Am J Pathol.* (2000) 156:1805–9. doi: 10.1016/S0002-9440(10)65052-3
10. Shen L, Ramires F, Martinez F, Bodanese LC, Echeverría LE, Gómez EA, et al. Contemporary characteristics and outcomes in chagasic heart failure compared with other nonischemic and ischemic cardiomyopathy. *Circ Heart Fail.* (2017) 10:e004361. doi: 10.1161/CIRCHEARTFAILURE.117.004361
11. Echeverria LE, Morillo CA. American trypanosomiasis (Chagas Disease). *Infect Dis Clin North Am.* (2019) 33:119–34. doi: 10.1016/j.idc.2018.10.015

12. Rassi DD, Vieira ML, Arruda AL, Hotta VT, Furtado RG, Rassi DT, et al. Echocardiographic parameters and survival in Chagas heart disease with severe systolic dysfunction. *Arq Bras Cardiol.* (2014) 102:245–52. doi: 10.5935/abc.20140003
13. Garcia-Alvarez A, Sitges M, Pinazo MJ, Regueiro-Cueva A, Posada E, Poyatos S, et al. Chagas cardiomyopathy: the potential of diastolic dysfunction and brain natriuretic peptide in the early identification of cardiac damage. *PLoS Negl Trop Dis.* 4:e826. doi: 10.1371/journal.pntd.0000826
14. Barbosa MM, Nunes MD, Ribeiro AL, Barral MM, Rocha MO. N-terminal proBNP levels in patients with Chagas disease: a marker of systolic and diastolic dysfunction of the left ventricle. *Eur J Echocardiogr.* (2007) 8:204–12. doi: 10.1016/j.euje.2006.03.011
15. Nascimento CA, Gomes VA, Silva SK, Santos CR, Chambela MC, Madeira FS, et al. Left atrial and left ventricular diastolic function in chronic Chagas disease. *J Am Soc Echocardiogr.* (2013) 26:1424–33. doi: 10.1016/j.echo.2013.08.018
16. Barros MV, Machado FS, Ribeiro AL, da Costa Rocha MO. Diastolic function in Chagas' disease: an echo and tissue Doppler imaging study. *Eur J Echocardiogr.* (2004) 5:182–8. doi: 10.1016/S1525-2167(03)00078-7
17. Silbiger JJ. Pathophysiology and echocardiographic diagnosis of left ventricular diastolic dysfunction. *J Am Soc Echocardiogr.* (2019) 32:216–32.e2. doi: 10.1016/j.echo.2018.11.011
18. Nagueh SF, Smiseth OA, Appleton CP, Byrd BF, Dokainish H, Edvardsen T, et al. Recommendations for the evaluation of left ventricular diastolic function by echocardiography: an update from the american society of echocardiography and the european association of cardiovascular imaging. *J Am Soc Echocardiogr.* (2016) 29:277–314. doi: 10.1016/j.echo.2016.01.011
19. Nagueh SF, Abraham TP, Aurigemma GP, Bax JJ, Beladan C, Browning A, et al. Interobserver variability in applying american society of echocardiography/European association of cardiovascular imaging 2016 guidelines for estimation of left ventricular filling pressure. *Circ Cardiovasc Imaging.* (2019) 12:e008122. doi: 10.1161/CIRCIMAGING.118.008122
20. Nadar SK, Shaikh MM. Biomarkers in routine heart failure clinical care. *Card Fail Rev.* (2019) 5:50–6. doi: 10.15420/cfr.2018.27.2
21. Berliner D, Angermann CE, Ertl G, Störk S. Biomarkers in heart failure–better than history or echocardiography? *Herz.* (2009) 34:581–8. doi: 10.1007/s00059-009-3314-6
22. Nosaka K, Nakamura K, Kusano K, Toh N, Tada T, Miyoshi T, et al. Serum cystatin C as a biomarker of cardiac diastolic dysfunction in patients with cardiac disease and preserved ejection fraction. *Congest Heart Fail Greenwich Conn.* (2013) 19:E35–39. doi: 10.1111/chf.12039
23. Farcaş AD, Anton FP, Goidescu CM, Gavrilă IL, Vida-Simiti LA, Stoia MA. Serum Soluble ST2 and diastolic dysfunction in hypertensive patients. *Dis Markers.* (2017) 2017:2714095. doi: 10.1155/2017/2714095
24. Wei T, Zeng C, Chen L, Chen Q, Zhao R, Lu G, et al. Systolic and diastolic heart failure are associated with different plasma levels of B-type natriuretic peptide. *Int J Clin Pract.* (2005) 59:891–4. doi: 10.1111/j.1368-5031.2005.00584.x
25. Kim IY, Kim JH, Kim MJ, Lee DW, Hwang CG, Han M, et al. Plasma neutrophil gelatinase-associated lipocalin is independently associated with left ventricular hypertrophy and diastolic dysfunction in patients with chronic kidney disease. *PLoS ONE.* (2018) 13:e0205848. doi: 10.1371/journal.pone.0205848
26. Mady C, Fernandes F, Arteaga E, Ramires FJ, Buck PD, Salemi VM, et al. Serum NT pro-BNP: relation to systolic and diastolic function in cardiomyopathies and pericardiopathies. *Arq Bras Cardiol.* (2008) 91:46–54. doi: 10.1590/S0066-782X2008001300008
27. Nunes MP, Colosimo EA, Reis RC, Barbosa MM, da Silva JL, Barbosa F, et al. Different prognostic impact of the tissue Doppler-derived E/e' ratio on mortality in Chagas cardiomyopathy patients with heart failure. *J Heart Lung Transplant.* (2012) 31:634–41. doi: 10.1016/j.healun.2012.01.865
28. Fernandes F, Barbosa-Ferreira JM, Mady C. New diagnostic serum biomarkers for Chagas disease. *Expert Opin Med Diagn.* (2011) 5:203–11. doi: 10.1517/17530059.2011.566859
29. Nunes MC, Carmo AA, Rocha MO, Ribeiro AL. Mortality prediction in Chagas heart disease. *Expert Rev Cardiovasc Ther.* (2012) 10:1173–84. doi: 10.1586/erc.12.111
30. Echeverría LE, Rojas LZ, Calvo LS, Roa ZM, Rueda-Ochoa OL, Morillo CA, et al. Profiles of cardiovascular biomarkers according to severity stages of Chagas cardiomyopathy. *Int J Cardiol.* (2017) 227:577–82. doi: 10.1016/j.ijcard.2016.10.098
31. Sherbuk JE, Okamoto EE, Marks MA, Fortuny E, Clark EH, Galdos-Cardenas G, et al. Biomarkers and mortality in severe Chagas cardiomyopathy. *Glob Heart.* (2015) 10:173–80. doi: 10.1016/j.gheart.2015.07.003
32. Okamoto EE, Sherbuk JE, Clark EH, Marks MA, Gandarilla O, Galdos-Cardenas G, et al. Biomarkers in Trypanosoma cruzi-infected and uninfected individuals with varying severity of cardiomyopathy in Santa Cruz, Bolivia. *PLoS Negl Trop Dis.* (2014) 8:e3227. doi: 10.1371/journal.pntd.0003227
33. Lima-Costa MF, Cesar CC, Peixoto SV, Ribeiro AL. Plasma B-type natriuretic peptide as a predictor of mortality in community-dwelling older adults with Chagas disease: 10-year follow-up of the bambui cohort study of aging. *Am J Epidemiol.* (2010) 172:190–6. doi: 10.1093/aje/kwq106
34. Oliveira BM, Botoni FA, Ribeiro AL, Pinto AS, Reis AM, Nunes MD, et al. Correlation between BNP levels and Doppler echocardiographic parameters of left ventricle filling pressure in patients with Chagasic cardiomyopathy. *Echocardiogr Mt Kisco N.* (2009) 26:521–7. doi: 10.1111/j.1540-8175.2008.00842.x
35. Ansari U, Behnes M, Hoffmann J, Natale M, Fastner C, El-Battrawy I, et al. Galectin-3 Reflects the Echocardiographic Grades of Left Ventricular Diastolic Dysfunction. *Ann Lab Med.* (2018) 38:306–15. doi: 10.3343/alm.2018.38.4.306

Conflict of Interest: The authors declare that the research was conducted in the absence of any commercial or financial relationships that could be construed as a potential conflict of interest.

frontiers in Cardiovascular Medicine

SYSTEMATIC REVIEW
published: 31 January 2022
doi: 10.3389/fcvm.2021.787214

Association Between *Trypanosoma cruzi* DNA in Peripheral Blood and Chronic Chagasic Cardiomyopathy: A Systematic Review

Pau Bosch-Nicolau[1,2], *Juan Espinosa-Pereiro*[1,2], *Fernando Salvador*[1,2], *Adrián Sánchez-Montalvá*[1,2] *and Israel Molina*[1,2]*

[1] *Tropical Medicine & International Health Unit Vall d'Hebrón - Drassanes, Infectious Diseases Department, PROSICS Barcelona, University Hospital Vall d'Hebron, Barcelona, Spain,* [2] *Medicine Department, Universitat Autònoma de Barcelona, Barcelona, Spain*

Chronic chagasic cardiomyopathy (CCC) is the most important complication of patients with Chagas disease (CD). The role of persistent detection of DNA in peripheral blood and its association to CCC is unknown. We performed a systematic review up to July 2021, including studies that reported ratios of CCC and PCR positivity among non-treated adult patients. We identified 749 records and selected 12 for inclusion corresponding to 1,686 patients. Eight studies were performed in endemic countries and 4 in non-endemic countries. Only two studies showed an association between CCC and *Trypanosoma cruzi* parasitemia by means of PCR detection. Six studies reported greater positive PCR ratios among patients with CCC than in the patients with indeterminate chagas disease (ICD) with no statistical significance. A significant risk of bias has been detected among most of the studies. Therefore, while we performed a meta-analysis, wide inter-study heterogeneity impeded its interpretation.

Conclusions: With the available information, we could not establish a correlation between PCR-detectable parasitemia and CCC.

Systematic Review Registration:
https://www.crd.york.ac.uk/prospero/display_record.php?ID=CRD42020216072, identifier: CRD42020216072.

Keywords: Chagas disease, Chagas cardiomyopathy, *T. cruzi*, polymerase chain reaction, PCR

OPEN ACCESS

Edited by:
Livia Passos,
Brigham and Women's Hospital and Harvard Medical School, United States

Reviewed by:
Erik Josef Behringer,
Loma Linda University, United States
Marcelo Santos Da Silva,
São Paulo State University, Brazil

***Correspondence:**
Israel Molina
imolina@vhebron.net

Specialty section:
This article was submitted to General Cardiovascular Medicine, a section of the journal Frontiers in Cardiovascular Medicine

Received: *30 September 2021*
Accepted: *28 December 2021*
Published: *31 January 2022*

Citation:
Bosch-Nicolau P, Espinosa-Pereiro J, Salvador F, Sánchez-Montalvá A and Molina I (2022) Association Between Trypanosoma cruzi DNA in Peripheral Blood and Chronic Chagasic Cardiomyopathy: A Systematic Review. Front. Cardiovasc. Med. 8:787214. doi: 10.3389/fcvm.2021.787214

INTRODUCTION

Chagas disease (CD) is a protozoal disease caused by *Trypanosoma cruzi*, a zoonotic infection mainly found in endemic areas of the American continent. It affects about 8 million people worldwide and because of globalization and international migrations during the last decades, it has become a cause of concern in non-endemic countries (1).

Chagas disease has an acute phase that generally runs its course asymptomatic or with rather unspecific symptomatology. Once patients overcome this phase, they enter a chronic phase, defined by the absence of trypomastigotes in the blood smear. Most people with *T. cruzi* infection are diagnosed at this stage. Approximately 30–40% of chronically infected patients will develop visceral involvement comprising the chronic chagasic cardiomyopathy (CCC), the digestive form, or both during the following 10–30 years after infection (2).

CCC is considered the cause of at least 7,000 deaths every year and is the most common reason for performing heart transplants in Latin America. The principal underlying causes are sudden death from malignant arrhythmias and heart failure as a consequence of dilated cardiomyopathy (3).

Both host immune response and the persistence of infection are crucial on CCC progression (4). Host factors, such as genetic polymorphisms involved in the immune response have been proposed as prognosis markers (5). Regarding the role of *T. cruzi* persistence, several studies have evidenced that visceral involvement is directly linked to the parasite presence on such organs in both human and animal models (6). Besides, an association between certain discrete typing units (DTU), which are used to group *T. cruzi* genetic diversity, and its virulence and tissue tropism has been described (7).

Blood parasites can be detected by PCR. However, parasite dynamics is still a matter of debate. While in the acute phase, the presence of *T. cruzi* in the blood is constant, in the chronic phase low level parasitemia is observed in a subset of patients (8). Different PCR assays have been developed to detect the parasite DNA with initial difficulties in standardizing techniques to obtain reliable and comparable results (9). However, in recent years, notable advances have been made with new methodologies showing reliable results that have been used to monitor the parasite load in patients with CCC and follow-up the effectiveness of etiologic treatments (10). Besides, the relationship between parasitemia or the presence of parasitic DNA on peripheral blood, and disease progression is controversial (11, 12).

Therefore, this systematic review has the objective of assessing the association between the presence of parasitic DNA of *T. cruzi* on peripheral blood through PCR and CCC.

MATERIALS AND METHODS

Study Design

We conducted a systematic review following the standardized guidance (13), and we adhered to the Preferred Reporting Items for Systematic Reviews and Meta-Analyses (PRISMA) statement using a flow diagram and following its checklist to ensure that all recommended information is captured and findings are properly reported (14). The review protocol was registered in the PROSPERO database (registration ID number: CRD42020216072).

Eligibility Criteria and Patient Population

We included clinical trials, controlled observational and cross-sectional studies in adult patients (>16 years old) with chronic CD reporting data on the results of the peripheral blood *T. cruzi* PCR and CCC.

Eligible studies had to establish the chronic CD diagnosis through two different positive serological tests. Indeterminate Chagas disease (ICD) concerns patients diagnosed with a chronic CD that presented with normal ECG and/or echocardiogram, regardless of the presence or absence of gastrointestinal disease. CCC was defined as electrocardiographic or echocardiographic alterations not attributed to other conditions. We included studies considering any PCR protocol whenever the same procedure was maintained throughout the study.

Studies assessing the impact of treatment with benznidazole, nifurtimox, or azole-derivative drugs were excluded. In addition, we excluded studies focusing on acute infections, pregnant women, children, or immunocompromised patients.

Literature Search, Data Collection, and Reporting of Results

We searched Medline, EMBASE, and LILACS databases. Additionally, we tracked citations to relevant studies in Scopus and the ISI Web of Knowledge for review purposes, and manually screened references lists of these studies. We adapted the search strategy to the requirements of each database (**Supplementary Material Appendix 1**). There were no language or publication period restrictions. We conducted the last search during July 2021.

One reviewer (PBN) screened the titles and abstracts resulting from the search against inclusion criteria. We obtained a full-text copy of eligible references to finally decide on their inclusion. A second reviewer (JEP) independently checked the eligibility decisions for accuracy. We discussed disagreements until a decision was reached; and planned to involve a third investigator if discrepancies remained.

Two researchers (PBN and JEP) extracted data from included studies using the standardized extraction forms. No pilot study was conducted due to the low number of articles included. Whenever possible, article authors were contacted for unreported or additional data to minimize the missing data. For each study, we collected (when available): study design, baseline characteristics, cardiac involvement, PCR method, PCR status of the included patients at the inclusion, and association measures as reported by authors of each study. We independently assessed the risk of bias for each study using a modified Quality In Prognosis Studies (QUIPS). Tool checklist (**Supplementary Material Appendix 2**), appropriate for prognostic factor review questions (15).

Statistical Analysis

We described the population of each study and the frequencies of positive PCR among ICD and CCC participants. The association of PCR status and visceral involvement was extracted as the amount of positive PCR among ICD participants and CCC participants, using as association measure the odds ratios (ORs) and 95% *CI*. Pooled *OR* was calculated using the Mantel–Haenszel approach with a random effects model due to the heterogeneity of each study population. Inter-study heterogeneity was assessed with a restricted maximum likelihood model and reported as the I^2 and tau statistics. We adhered to the methods recommended in the Cochrane Handbook for Systematic Reviews of interventions whenever possible (16).

RESULTS

Our search retrieved 749 records. After removing duplicates and reading titles and abstracts, we discarded 719 records as they were *in vitro* experiments, were performed in animals,

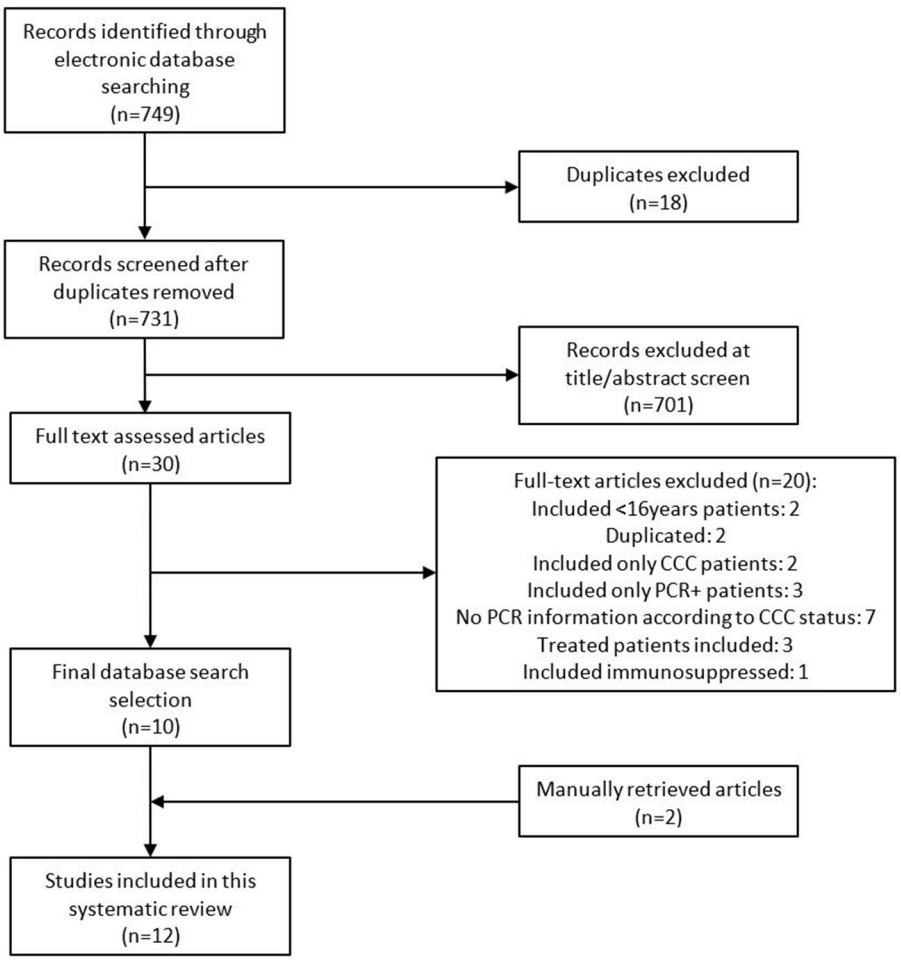

FIGURE 1 | The Preferred Reporting Items for Systematic Reviews and Meta-Analyses (PRISMA) flow diagram of included articles. CCC, chronic chagasic cardiomyopathy; PCR, polymerase chain reaction.

corresponded to *Trypanosoma* species other than *T. cruzi*, included acute infection patients or treated patients, or did not report visceral involvement. Of the remaining 30 reports, we proceeded to a full-text review and finally included 10 articles. The characteristics of excluded studies are reported in **Supplementary Material Appendix 3** (8, 11, 17–34). After checking the reference lists of these studies, we identified two additional eligible studies. The complete eligibility process is depicted in a PRISMA flowchart (**Figure 1**).

Finally, we included 12 studies comprising 1,686 patients (12, 35–45), which are described in **Table 1**. Eight studies were cross-sectional studies, 3 were designed as prospective cohorts, and 1 was a case-control study. Countries where studies were performed in endemic areas were as follows: 3/8 (37.5%) in Brazil, 3/8 (37.5%) in Chile, 1 (12.5%) in Argentina, and 1 (12.5%) in Bolivia. Among them, 1 was performed in a rural site, 2 in urban facilities, and 5 combined patients living in both urban and rural contexts. Four studies included patients from non-endemic countries: 3 from Spain where more than 90% of patients came from Bolivia and 1 from Japan. Patients' ages ranged from 16 to 81 years old, and most of them were women (58.8%; 885/1,505).

Chronic chagasic cardiomyopathy assessment was performed using ECG in all studies. In 4 (33.3%) studies, ECG was combined with echocardiography, in 1 (8%) was combined with chest radiography, and in 4 (33.3%), the 3 ancillary tests were performed. CCC classification was very heterogeneous and included either predefined criteria by the authors (35–37, 40, 43) or standardized classifications as Minnesota criteria (12, 38), Kuschnir criteria (39, 44, 45), Rocha criteria (42), and New York Heart Association (NYHA) classification (41). Among the included patients, 998 (59.2%) were classified as ICD and 688 (40.8%) as CCC. CCC proportion among different studies varied from 12.1% (40) in a study including young childbearing-aged women to 80% (43) in a study including patients under the suspicion of organ involvement in Latin-American people living in Japan. However, the last study included only 5 patients. Cardiologic characteristics of patients with CCC are summarized in **Supplementary Material Appendix 4**.

TABLE 1 | Summary of the characteristics of the included studies.

References and country	Study design	Study site	Included (excluded)	Age	Sex	Excluded comorbidities	CCC assessment	Clinical form	PCR technique*	PCR results	Association measure
Salomone et al. (35) Argentina	Cross-sectional	Endemic (urban)	68 (23)	55 y (SD ± 12) ICD: 52 y (SD ± 9) CCC: 59 y (SD ± 12)	64% F ICD: 70% F CCC: 59% F	Yes	EKG + EchoC	ICD: 27 (39.7%) CCC: 41 (60.3%)	Qualitative c-PCR 1 sample Kinetoplast DNA	Global + PCR: 14/68 (21%) ICD: 2/27 (7.4%) CCC: 12/41 (29.2%)	OR 5.17 (95%CI 1.06–25.36)
Carrasco et al. (36) Chile	Cross-sectional	Endemic (rural)	38 (225)	ICD: 40,57 y (SD ± 10.59) CCC: –HF 68.4 y (SD ± 12.9) –PM: 54.1 y (SD ± 8.4) –Altered EKG: 53.4 y (SD ± 19.1)	ICD: 62% M CCC: 62% M	No	EKG + EchoC + Thoracic X-Ray	ICD: 26 (68.4%) CCC: 12 (31.6%)	Qualitative c-PCR 1 sample Kinetoplast DNA	Global + PCR: 18/38 (54.7%) ICD: 10/26 (36%) CCC: 8/12 (66%)	OR 3.20 (95%CI 0.76–13.46)
Zulantay et al. (37) Chile	Prospective cohort	Endemic (urban and rural)	30 (0)	33.2 y (R 18–50)	53.3% M	Yes	EKG	ICD: 18 (60%) CCC: 12 (40%)	Qualitative c-PCR 1 sample Kinetoplast DNA	Global + PCR: 17/30 (56.6%) ICD: 10/18 (55.5%) CCC: 7/12 (58.3%)	OR 1.12 (95%CI 0.26–4.91)
Borges-Pereira et al. (38) Brazil	Cross-sectional	Endemic (rural)	12 (9)	48.6 y (R 16–82) ICD: 43.5 y CCC: 64.4 y	58,8% F ICD: 70% F CCC: 42.9% F	No	EKG	ICD: 6 (50%) CCC: 6 (50%)	Qualitative c-PCR 1 sample Kinetoplast DNA	Global + PCR: 9/12 (75%) ICD: 5/6 (83.3%) CCC: 4/6 (66.6%)	OR 0.40 (95%CI 0.03–6.18)
Murcia et al. (39) Spain	Prospective cohort	Non endemic	181 (0)	33 y (SD ± 11)	No reported	No reported	EKG + EchoC + Thoracic X-Ray	ICD: 116 (64%) CCC: 65 (36%)	Qualitative c-PCR 1 sample Kinetoplast DNA	Global + PCRs: 123/181 (68%) ICD: 81/116 (69,8%) CCC: 42/65 (64.6%)	OR 0.79 (95%CI 0.41–1.50)
Sabino et al. (12) Brazil	Cross-sectional	Endemic (urban and rural)	485 (115)	IND (PCR–): 48.4 y (SD ± 10.1) IND (PCR+): 49.1 y (SD ± 10.6) CCC (PCR–): 49.2 y (SD ± 6.3) CCC (PCR+): 47.8 y (SD ± 7.1)	53,6% M IND: 52,3% M CCC: 59,4% M	Yes	EKG + EchoC	ICD: 279 (57.5%) CCC: 206 (42.5%)	Quantitative rt-PCR 1 sample Kinetoplast DNA	Global + PCR: 304/485 (62.7%) ICD: 143/279 (51.3%) CCC: 161/206 (78.1%)	OR 3.48 (95%CI 2.31–5.23)

(Continued)

TABLE 1 | Continued

References and country	Study design	Study site	Included (excluded)	Age	Sex	Excluded comorbidities	CCC assessment	Clinical form	PCR technique*	PCR results	Association measure
Kaplinski et al. (40) Bolivia	Cross-sectional	Endemic (urban and rural)	83 (337)	ICD: 27 y (R 22–34) CCC: 32 y (R 24–39)	100% F	No reported	EKG	IND: 73 (87.9%) CCC: 10 (12.1%)	Quantitative rt-PCR 1 sample Kinetoplast DNA	Global + PCR: 36/83 (43.4%) ICD: 33/73 (45.2%) CCC: 3/10 (33.3%)	OR 0.52 (95%CI 0.12–2.17)
Apt et al. (41) Chile	Case-control	Endemic (urban and rural)	200 (0)	ICD: 50.5 y (R 20–77) CCC: 56.4 y (R 25–81)	ICD: 79% F CCC: 68% F	Yes	EKG + EchoC	ICD: 100 (50%) CCC: 100 (50%)	Qualitative c-PCR 1 sample Kinetoplast DNA	Global +PCR: 145/200 (72.5%) ICD: 72/100 (72%) CCC: 73/100 (73%)	OR 1.05 (95%CI 0.57–1.96)
Sánchez-Montalvá et al. (45) Spain	Cross-sectional	Non endemic	455 (316)	39 y (R 31–46.5) ICD: 37 y (R 31–44) CCC: 42 y (R 36–49)	68.2% F	Yes	EKG + EchoC + Thoracic X-Ray	ICD: 302 (66.4%) CCC: 153 (43.6%)	Qualitative rt-PCR 1 sample Satellite DNA	Global +PCR: 118/455 (25.9%) ICD: 76/302 (25.2%) CCC: 42/153 (27.4%)	OR 1.13 (95%CI 0.72–1.75)
D'Ávila et al. (42) Brazil	Cross-sectional	Endemic (urban and rural)	91 (0)	ICD: 44 y (SD ± 10.3) CCC: 54 y (SD ± 10.3)	ICD: 65.2% F CCC: 33.8% F	No reported	EKG + EchoC + Thoracic X-Ray	ICD: 23 (33.8%) CCC: 68 (66.2%)	Quantitative rt-PCR 1 sample Satellite DNA	Global + PCR: 65/91 (71.4%) ICD: 16/23 (69.6%) CCC: 49/68 (72%)	OR 1.13 (95%CI 0.40–3.17)
Salvador et al. (44) Spain	Prospective cohort	Non endemic	38 (16)	36 y (R 22–55)	75.6% F	No reported	EKG + Thoracic X-Ray	ICD: 27 (71%) CCC: 11 (29%)	Qualitative rt-PCR 1 sample Satellite DNA	Global + PCR: 16/38 (42.1%) ICD: 11/27 (40.7%) CCC: 5/11 (45.4%)	OR 1.21 (95%CI 0.29–4.98)
Imai et al. (43) Japan	Cross-sectional	Non endemic	5 (12)	57.6 y (R 49–68)	60% F	No	EKG + EchoC	ICD: 1 (20%) CCC: 4 (80%)	Qualitative rt-PCR 1 sample Satellite DNA	Global +PCR: 3/5 (60%) ICD: 1/1 (100%) CCC: 2/4 (50%)	OR 0.33 (95%CI 0.01–12.82)

CCC, chronic chagasic cardiomyopathy; c-PCR, conventional polymerase chain reaction; EchoC, echocardiography; ECG, electrocardiogram; ICD, indeterminate chagas disease; R, range; RR, risk ratio; rt-PCR, real time polymerase chain reaction; SD, standard deviation; y, years; PM, pacemaker; HF, heart failure.

**PCR methodology: specifying PCR technique (conventional PCR or real time PCR) and target of the used primer (kinetoplast DNA or nuclear satellite DNA).*

All the included studies used a PCR for DNA parasite detection in peripheral blood. However, many different protocols were used for its determination. All studies used a single venous blood sample for PCR determination. Six studies (50%) used a conventional PCR method (35–39, 41) while the other half used real-time PCR method (12, 40, 42–45). Only four studies used a quantitative method to report PCR results (12, 40–42) while the rest of the studies used a qualitative method. There is a wide variation regarding primers used. Most studies (8/12; 66.3% used a real time PCR method based on the amplification of a genomic DNA sequence of the Kinetoplast. In the other 4 studies, satellite DNA amplification was used (42–45). Parasite detection in patients with ICD ranged from 7.4 (35) to 100% (43). When considering patients with CCC, parasite detection varied from 27.4 (45) to 78.1% (12).

The results of the risk of bias assessment using the QUIPS scale are shown in **Supplementary Material Appendixes 5, 6**. Most studies included a representative population with CD. However, 2 studies were considered at an overall high risk as one included only childbearing-aged women (40), and the other included patients under suspicion of organ involvement (43). As per study attrition, most of the studies were classified as low risk of bias since basal characteristics including PCR and organ assessment were performed at the inclusion and, in consequence, data were available for all participants included in the studies. Regarding outcome measurement (PCR), all the studies specified their protocol and almost all included control samples and maintained the same procedure in all samples. As per CCC assessment, six studies were rated at low risk of bias since they included blind ECG assessment and/or double assessment by different investigators (12, 37, 38, 40, 41, 45). Conversely, two studies that neither used a standardized classification nor reported their ECG or echocardiographic findings were considered at high risk of bias (35, 43). Considering study confounders, all the studies but one was rated as having a moderate to high risk of bias. Most of the studies did not consider cardiovascular risk factors and other possible heart diseases or performed a stratified data analysis. Finally, result presentation and statistical analysis were classified at a moderate to high risk of bias in a wide group of studies. Most of them were designed for another purpose and we retrieved the specific information from their results.

An association between CCC and *T. cruzi* parasitemia by means of PCR detection was found in 2 studies (12, 35). They all were performed in endemic regions and found a greater PCR positivity between patients with CCC and ICD with *OR*s of 5.17 (*CI* 1.06–25.36) and 3.48 (*CI* 2.31–5.23). In one study, although a risk ratio (RR) of 4.45 was reported, it included both cardiac and digestive forms on the analysis, and when *OR* was calculated with only CCC patients, we could not achieve statistical significance (36). None of the non-endemic studies identified an association between parasite DNA detection in peripheral blood and CCC. Six studies reported greater positive PCR ratios among patients with CCC than in patients with ICD although differences did not achieve statistical significance (36, 37, 41, 42, 44, 45). The remaining 4 studies reported a positive PCR rate that favored patients with ICD (38–40, 43).

When we meta-analyzed the *OR*, pooled results showed that the estimated *OR* for positive *T. cruzi* PCR of patients with CCC compared to patients with ICD was 1.36 (95% *CI*: 0.87–2.12) *(***Figure 2***)*. However, we found significant heterogeneity among studied variables in the meta-regression analysis. To diminish variability, we grouped studies by patient's countries of origin and by PCR technique with the same results. Thus, no conclusions can be achieved from the meta-analysis.

DISCUSSION

In this review, despite 8 out of 12 studies reporting higher ratios of positive PCR among patients with CCC, we could not find a correlation between parasitemia by means of PCR and CCC. When we analyzed the characteristics of the included studies, in only 2 studies, the proportion of PCR positivity was significantly greater within CCC (12, 35). These studies were performed in an endemic region and their specific objective was to determine the correlation between parasitemia and CCC. It has been suggested that patients in endemic regions are prone to parasite re-exposure, contributing to higher rates of CCC and parasitemia among patients with CD (45). In the same line, in a study performed in a non-endemic country, the positive PCR ratio decreased in patients with longer periods since the first arrival (8). Also, geographic distribution should play a role in CCC development and parasitemia burden. *T. cruzi* genetic diversity is unequally distributed among different countries, and some authors have reported a cardiac tropism of some discrete typing units (DTUs) (7). In this review, included patients came mostly from 4 different countries and only one of them reported DTUs determination (42).

Age was higher among patients with CCC in studies performed in endemic countries recruiting the general population (range 49.2–68 years) than in non-endemic countries (range 33–42 years). Regardless of the age *per se* having been described as a risk factor for CCC and its mortality, results from different reports are inconsistent (46). On one hand, study participants in their second to the fourth decade of life may have not yet developed target organ damage, or it is too incipient, as it takes on average 20–30 years after the acute infection. On the other hand, older people often associate other cardiovascular risk factors and this could lead to a misinterpretation of the CCC assessment (47). In fact, only three studies were excluded from their analysis due to other cardiovascular risk factors (12, 41, 45). Male sex has been related to CCC development and higher mortality rates (48). Although, this predisposition was described as an independent risk factor from parasitemia (20). Among the included studies, the male proportion ranged from 31.8 to 66.2%. As none of the included studies conducted stratified analysis by sex or age, results should be interpreted with caution.

Classically, CCC assessment has involved ECF, chest X-ray, and clinical status, as they are easy to collect and widely available. Echography, a non-invasive examination, has been progressively studied in CD and its performance has been introduced in

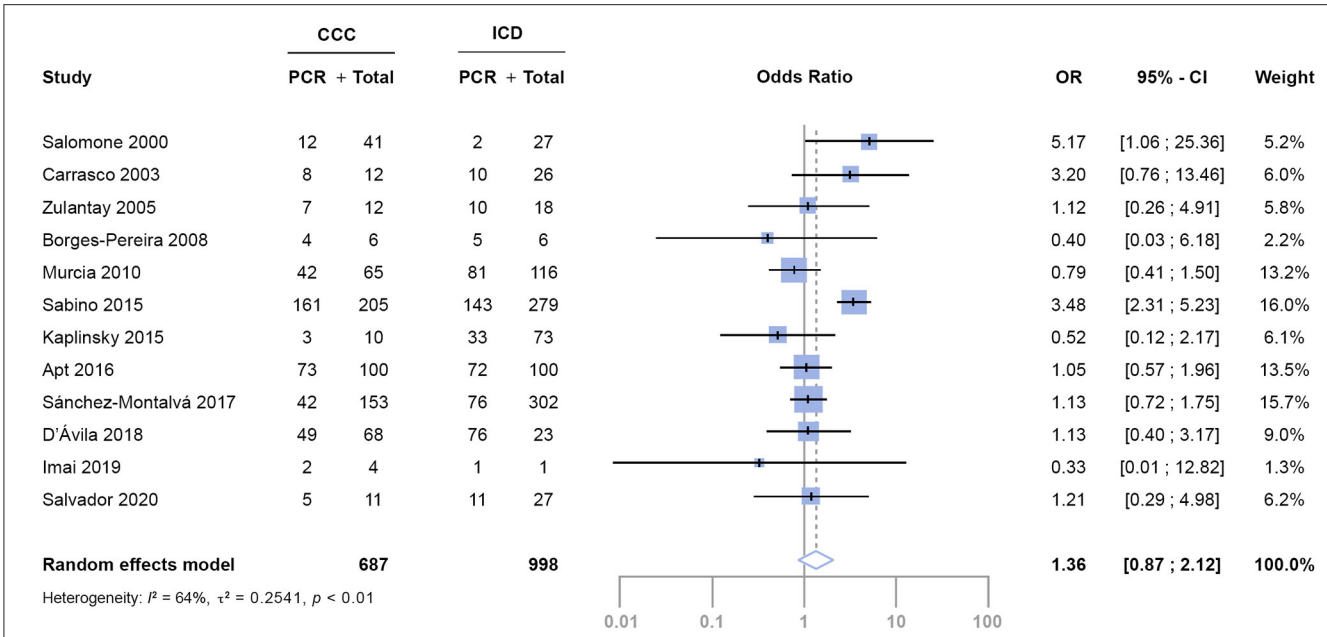

FIGURE 2 | Evaluation of the association between PCR detection between patients with CCC and ICD. CI, confidence interval; OR, odds ratio.

different CCC classifications (49). ECG abnormalities are usually seen before the patient develops a malignant arrhythmia or heart failure (50). However, echocardiographic alterations as diastolic dysfunction can appear before electrical abnormalities develop and may be used as an early marker of CCC (45). In this review, the CCC assessment was very heterogeneous. While 3 studies performed only an ECG and 1 study included a chest X-ray, 8 of 12 studies used echocardiography to complete the cardiac evaluation. CCC classifications were disparate, while 5 authors used a non-standardized classification (35–37, 40, 43), 7 used different standardized criteria (12, 38, 39, 41, 42, 44, 45). Conduction system alterations as right-bundle block and left anterior hemiblock prevailed over other arrhythmias or contraction abnormalities in most of the studies (**Supplementary Material Appendix 3**). Two studies (39, 42) did not provide cardiological findings of their participants, and only 4 studies (41, 42, 44, 45) provided the distribution of disease severity. As a result, between-study comparisons of CCC severity are not feasible.

Current PCR-based methods for *T. cruzi* detection have shown high sensitivity and specificity compared with classical methods, such as blood culture or xenodiagnosis (8). However, sample collection, conservation, sample volume, DNA extraction method, and primers used may influence its performance (9). As a result, in recent years, many initiatives have pursued the standardization of these techniques (33). In the present review, earlier studies used conventional PCR methods preferably using as molecular targets of the kinetoplast DNA sequences. On the other hand, later studies preferred real-time PCR (rt-PCR) techniques toward satellite or minicircle DNA sequences which showed better sensitivity and specificity results and allowed quantification (9). Only four studies used a quantitative method (12, 40–42) but parasitemia levels were not related to any clinical outcome. Parasitemia levels are usually low in chronic patients with CD compared with parasitemia levels in patients with acute CD. Different studies have analyzed the correlation between quantitative results of *T. cruzi* in peripheral blood and organ damage with inconsistent results (41, 50). Parasite detection ratios ranged widely within the included studies. In patients with ICD, the detection ranged from 7.4 (35) to 100% (43) while in patients with CCC varied from 27.4 (45) to 78.1% (12). Besides the previously described factors, parasite dynamics in blood have not been thoroughly characterized. Intermittent parasitemia is constant in the chronic phase of CD but its periodicity, triggers, determinants, or reservoirs are still unknown (8). Thus, although the internal variability is probably acceptable among all studies as they used the same method throughout, lack of sensitivity could result in low positive ratios precluding differences detection.

This systematic review has several limitations. As a neglected tropical disease, scarce investment over time has limited the generation of high-quality evidence (51). A significant risk of bias has been detected among most of the studies resulting from small sample sizes, differences among study designs, differences not reporting on basal characteristics, different CCC assessments, and PCR methods along with the fact that most of the studies were not even designed for this purpose. To improve studies comparability, we have grouped them by the main confounding factors: country of origin and quality of PCR technique but variability remained. Therefore, while we have performed a meta-analysis, wide inter-study heterogeneity (I^2 64%, $p < 0.01$) impedes a robust interpretation of its results. A patient-level meta-analysis could improve the consistency and robustness of the results and provide evidence to better inform physicians treating people living with CD.

In conclusion, with the current information, we could not establish a correlation between PCR-detectable parasitemia and CCC. Better prospective studies with a defined follow-up, representative population, homogeneous criteria, and standardized methods for PCR detection are needed to answer this question.

DATA AVAILABILITY STATEMENT

The original contributions presented in the study are included in the article/**Supplementary Material**, further inquiries can be directed to the corresponding author/s.

AUTHOR CONTRIBUTIONS

PB-N has majorly contributed to this study through study designing, abstract and articles revision, data analysis, and manuscript writing. JE-P has contributed to this study through abstract and article revision and final article review. FS, AS-M, and IM contributed through study design and article reviewing. All authors contributed to the article and approved the submitted version.

FUNDING

AS-M was supported by a postdoctoral grant Juan Rodés (JE18/00022) from the Instituto de Salud Carlos III through the Spanish Ministry of Economy and Competitiveness.

SUPPLEMENTARY MATERIAL

The Supplementary Material for this article can be found online at: https://www.frontiersin.org/articles/10.3389/fcvm.2021.787214/full#supplementary-material

REFERENCES

1. Basile L, Jansá JM, Carlier Y, Salamanca DD, Angheben A, Bartoloni A, et al. Chagas disease in European countries: the challenge of a surveillance system. *Eurosurveillance.* (2011) 16:19968. doi: 10.2807/ese.16.37.19968-en
2. Pérez-Molina J, Molina I. Chagas disease. *Lancet.* (2018) 391:82–94. doi: 10.1016/S0140-6736(17)31612-4
3. Bocchi E, Arias A, Verdejo H, Diez M, Gómez E, Castro DP. The reality of heart failure in Latin America. *J Am Coll Cardiol.* (2013) 62:949–58. doi: 10.1016/j.jacc.2013.06.013
4. Machado F, Dutra W, Esper L, Gollob K, Teixeira M, Factor S, et al. Current understanding of immunity to Trypanosoma cruzi infection and pathogenesis of Chagas disease. *Semin Immunopathol.* (2012) 34:753–70. doi: 10.1007/s00281-012-0351-7
5. Casares-Marfil D, Strauss M, Bosch-Nicolau P, Lo Presti M, Molina I, Chevillard C, et al. A genome-wide association study identifies novel susceptibility loci in chronic Chagas cardiomyopathy. *Clin Infect Dis.* (2021) 73:672–9. doi: 10.1093/cid/ciab090
6. Tarleton R. Parasite persistence in the aetiology of Chagas disease. *Int J Parasitol.* (2001) 31:550–4. doi: 10.1016/S0020-7519(01)00158-8
7. Burgos J, Diez M, Vigliano C, Bisio M, Risso M, Duffy T, et al. Molecular identification of Trypanosoma cruzi discrete typing units in end-stage chronic Chagas heart disease and reactivation after heart transplantation. *Clin Infect Dis.* (2010) 51:485–95. doi: 10.1086/655680
8. Sulleiro E, Salvador F, Martínez de Salazar P, Silgado A, Serre-Delcor N, Oliveira I, et al. Contributions of molecular techniques in the chronic phase of Chagas disease in the absence of treatment. *Enfermedades Infeccy Microbiol Clin.* (2020) 38:356–60. doi: 10.1016/j.eimce.2020.06.002
9. Schijman A, Bisio M, Orellana L, Sued M, Duffy T, Mejia Jaramillo A, et al. International study to evaluate PCR methods for detection of *Trypanosoma cruzi* DNA in blood samples from Chagas disease patients. *PLoS Negl Trop Dis.* (2011) 5:e931. doi: 10.1371/journal.pntd.0000931
10. Moreira OC, Ramírez JD, Velázquez E, Melo MFAD, Lima-Ferreira C, Guhl F, et al. Towards the establishment of a consensus real-time qPCR to monitor *Trypanosoma cruzi* parasitemia in patients with chronic Chagas disease cardiomyopathy: a substudy from the BENEFIT trial. *Acta Trop.* (2013) 125:23–31. doi: 10.1016/j.actatropica.2012.08.020
11. Norman FF, Pérez-Ayala A, Pérez-Molina JA, Flores-Chavez M, Cañavate C, López-Vélez R. Lack of association between blood-based detection of Trypanosoma cruzi DNA and cardiac involvement in a non-endemic area. *Ann Trop Med Parasitol.* (2011) 105:425. doi: 10.1179/1364859411Y.0000000033
12. Sabino E, Ribeiro A, Lee T, Oliveira C, Carneiro-Proietti A, Antunes A, et al. Detection of Trypanosoma cruzi DNA in blood by PCR is associated with Chagas cardiomyopathy and disease severity. *Eur J Heart Fail.* (2015) 17:416–23. doi: 10.1002/ejhf.220
13. Riley R, Moons K, Snell K, Ensor J, Hooft L, Altman D, et al. A guide to systematic review and meta-analysis of prognostic factor studies. *BMJ.* (2019) 364. doi: 10.1136/bmj.k4597
14. Page MJ, McKenzie JE, Bossuyt PM, Boutron I, Hoffmann TC, Mulrow CD, et al. The PRISMA 2020 statement: an updated guideline for reporting systematic reviews. *BMJ.* (2021) 372:n71. doi: 10.1136/bmj.n71
15. Hayden J, van der Windt D, Cartwright J, Côté P, Bombardier C. Assessing bias in studies of prognostic factors. *Ann Intern Med.* (2013) 158:280–6. doi: 10.7326/0003-4819-158-4-201302190-00009
16. *Cochrane Handbook for Systematic Reviews of Interventions | Cochrane Training*. Available online at: https://training.cochrane.org/handbook (accessed September 15, 2021).
17. Marcon GG, Andrade P, de Albuquerque D, Wanderley JS, de Almeida E, Guariento M, et al. Use of a nested polymerase chain reaction (N-PCR) to detect Trypanosoma cruzi in blood samples from chronic chagasic patients and patients with doubtful serologies. *Diagn Microbiol Infect Dis.* (2002) 43:39–43. doi: 10.1016/S0732-8893(02)00366-8
18. Borges-Pereira J, Castro J, Campos J, Nogueira S, Zauza P, Marques P, et al. [Study of the infection and morbidity of Chagas' disease in municipality of João Costa: National Park Serra da Capivara, Piauí, Brazil]. *Rev Soc Bras Med Trop.* (2002) 35:315–22. doi: 10.1590/S0037-86822002000400007
19. Brenière S, Bosseno M, Noireau F, Yacsik N, Liegeard P, Aznar C, et al. Integrate study of a Bolivian population infected by Trypanosoma cruzi, the agent of Chagas disease. *Mem Inst Oswaldo Cruz.* (2002) 97:289–95. doi: 10.1590/S0074-02762002000300002
20. Basquiera A, Sembaj A, Aguerri A, Omelianiuk M, Guzmán S, Moreno Barral J, et al. Risk progression to chronic Chagas cardiomyopathy: influence of male sex and of parasitaemia detected by polymerase chain reaction. *Heart.* (2003) 89:1186–90. doi: 10.1136/heart.89.10.1186
21. Pompilio M, Dorval M, Cunha R, Britto C, Borges-Pereira J. [Epidemiological, clinical and parasitological aspects of Chagas' disease in Mato Grosso do Sul State]. *Rev Soc Bras Med Trop.* (2005) 38:473–8. doi: 10.1590/S0037-86822005000600005
22. Hidron A, Gilman R, Justiniano J, Blackstock A, Lafuente C, Selum W, et al. Chagas cardiomyopathy in the context of the chronic disease transition. *PLoS Negl Trop Dis.* (2010) 4:e688. doi: 10.1371/journal.pntd.0000688
23. Llaguno MM, Pertili L, da Silva M, Bunazar P, Reges A, Faleiros A, et al. The relationship between heart rate variability and serum cytokines in chronic chagasic patients with persistent parasitemia. *Pacing Clin Electrophysiol.* (2011) 34:724–35. doi: 10.1111/j.1540-8159.2010.03025.x

24. Ballinas-Verdugo M, Reyes P, Mejia-Dominguez A, López R, Matta V, Monteón V. Enzyme-linked immunosorbent assay and polymerase chain reaction performance using Mexican and Guatemalan discrete typing unit I strains of Trypanosoma cruzi. *Vector Borne Zoonotic Dis.* (2011) 11:1569–75. doi: 10.1089/vbz.2010.0205
25. de Freitas V, da Silva S, Sartori A, Bezerra R, Westphalen E, Molina T, et al. Real-time PCR in HIV/*Trypanosoma cruzi* coinfection with and without Chagas disease reactivation: association with HIV viral load and CD4 level. *PLoS Negl Trop Dis.* (2011) 5. doi: 10.1371/journal.pntd.0001277
26. Ramos J, Torrús D, Amador C, Jover F, Pérez-Chacón F, Ponce Y, et al. Multicenter epidemiological and clinical study on imported Chagas diseases in Alicante, Spain. *Pathog Glob Health.* (2012) 106:340–5. doi: 10.1179/2047773212Y.0000000039
27. Saavedra M, Zulantay I, Apt W, Martínez G, Rojas A, Rodríguez J. Chronic Chagas disease: PCR-xenodiagnosis without previous microscopic observation is a useful tool to detect viable *Trypanosoma cruzi*. *Biol Res.* (2013) 46:295–8. doi: 10.4067/S0716-97602013000300011
28. Gilber S, Alban S, Gobor L, Bescrovaine J, Myiazaki M, Thomaz-Soccol V. Comparison of conventional serology and PCR methods for the routine diagnosis of *Trypanosoma cruzi* infection. *Rev Soc Bras Med Trop.* (2013) 46:310–5. doi: 10.1590/0037-8682-0046-2013
29. Melo M, Moreira O, Tenório P, Lorena V, Lorena-Rezende I, Júnior W, et al. Usefulness of real time PCR to quantify parasite load in serum samples from chronic Chagas disease patients. *Parasit Vectors.* (2015) 8:154. doi: 10.1186/s13071-015-0770-0
30. Antunes A, Ribeiro A, Sabino E, Silveira M, Oliveira C, Botelho A. Benznidazole therapy for Chagas disease in asymptomatic Trypanosoma cruzi -seropositive former blood donors: evaluation of the efficacy of different treatment regimens. *Rev Soc Bras Med Trop.* (2016) 49:713–20. doi: 10.1590/0037-8682-0165-2016
31. Pereira M, Batista A, Aguiar C, Marcon G, Martins L, Guariento M, et al. The detection of Trypanosoma cruzi by nested-PCR in elderly patients: relationship to the clinical and epidemiological profile. *Pathog Glob Health.* (2016) 110:228–32. doi: 10.1080/20477724.2016.1232850
32. Volpato F, Sousa G, D'Ávila D, Galvão L, Chiari E. Combined parasitological and molecular-based diagnostic tools improve the detection of *Trypanosoma cruzi* in single peripheral blood samples from patients with Chagas disease. *Rev Soc Bras Med Trop.* (2017) 50:506–15. doi: 10.1590/0037-8682-0046-2017
33. Sulleiro E, Muñoz-Calderon A, Schijman A. Role of nucleic acid amplification assays in monitoring treatment response in chagas disease: Usefulness in clinical trials. *Acta Trop.* (2019) 199:105120. doi: 10.1016/j.actatropica.2019.105120
34. Buss L, Campos de Oliveira-da Silva L, Moreira C, Manuli E, Sales F, Morales I, et al. Declining antibody levels to Trypanosoma cruzi correlate with polymerase chain reaction positivity and electrocardiographic changes in a retrospective cohort of untreated Brazilian blood donors. *PLoS Negl Trop Dis.*(2020) 14:1–14. doi: 10.1371/journal.pntd.0008787
35. Salomone O, Juri D, Omelianiuk M, Sembaj A, Aguerri A, Carriazo C, et al. Prevalence of circulating Trypanosoma cruzi detected by polymerase chain reaction in patients with Chagas' cardiomyopathy. *Am J Cardiol.* (2000) 85:1274–6. doi: 10.1016/S0002-9149(00)00747-5
36. Carrasco V, Andrade W, Jercic MI, Fernández GJ, Miranda C, Rivera J. [Clinical study of measure of parasitemia in patients infected with Trypanosoma cruzi in Atacama, Chile]. *Rev Med Chil.* (2003) 131:881–6. doi: 10.4067/S0034-98872003000800007
37. Zulantay I, Arribada A, Honores P, Sánchez G, Solari A, Ortiz S, et al. [No association between persistence of the parasite and electrocardiographic evolution in treated patients with Chagas disease]. *Rev Med Chil.* (2005) 133:1153–60. doi: 10.4067/S0034-98872005001000004
38. Borges-Pereira J, Sarquis O, Zauza P, Britto C, Lima M. [Epidemiology of Chagas disease in four rural localities in Jaguaruana, State of Ceará: seroprevalence of infection, parasitemia and clinical characteristics]. *Rev Soc Bras Med Trop.* (2008) 41:345–51. doi: 10.1590/S0037-86822008000400005
39. Murcia L, Carrilero B, Muñoz M, Iborra M, Segovia M. Usefulness of PCR for monitoring benznidazole response in patients with chronic Chagas' disease: a prospective study in a non-disease-endemic country. *J Antimicrob Chemother.* (2010) 65:1759–64. doi: 10.1093/jac/dkq201
40. Kaplinski M, Jois M, Galdos-Cardenas G, Rendell V, Shah V, Do R, et al. Sustained domestic vector exposure is associated with increased chagas cardiomyopathy risk but decreased parasitemia and congenital transmission risk among young women in Bolivia. *Clin Infect Dis.* (2015) 61:918–26. doi: 10.1093/cid/civ446
41. Apt W, Arribada A, Zulantay I, Saavedra M, Muñoz C, Toro B, et al. Chronic Chagas cardiopathy in Chile. Importance of *Trypanosoma cruzi* burden and clinical evaluation. *Acta Trop.* (2016) 162:155–66. doi: 10.1016/j.actatropica.2016.06.025
42. D'Ávila D, Galvão L, Sousa G, Britto C, Moreira O, Chiari E. Monitoring the parasite load in chronic Chagas disease patients: comparison between blood culture and quantitative real time PCR. *PLoS ONE.* (2018) 13. doi: 10.1371/journal.pone.0208133
43. Imai K, Misawa K, Osa M, Tarumoto N, Sakai J, Mikita K, et al. Chagas disease: a report of 17 suspected cases in Japan, 2012-2017. *Trop Med Health.* (2019) 47:38. doi: 10.1186/s41182-019-0168-3
44. Salvador F, Sánchez-Montalva A, Martínez-Gallo M, Sulleiro E, Franco-Jarava, C, et al. et al. Serum IL-10 levels and its relationship with parasitemia in chronic Chagas disease patients. *Am J Trop Med Hyg.* (2020) 102:159–63. doi: 10.4269/ajtmh.19-0550
45. Sánchez-Montalvá A, Salvador F, Rodríguez-Palomares J, Sulleiro E, Sao-Avilés A, Roure S, et al. Chagas cardiomyopathy: usefulness of EKG and echocardiogram in a non-endemic country. *PLoS ONE* (2016) 11:e0157597. doi: 10.1371/journal.pone.0157597
46. Rassi A, Rassi A, Rassi S. Predictors of mortality in chronic Chagas disease: a systematic review of observational studies. *Circulation.* (2007) 115:1101–8. doi: 10.1161/CIRCULATIONAHA.106.627265
47. Triposkiadis F, Xanthopoulos A, Butler J. Cardiovascular aging and heart failure: JACC review topic of the week. *J Am Coll Cardiol.* (2019) 74:804–13. doi: 10.1016/j.jacc.2019.06.053
48. Rassi A, Rassi A Jr. , Little W, Xavier S, Rassi S, Rassi AG, et al. Development and validation of a risk score for predicting death in Chagas' heart disease. *N Engl J Med.* (2006) 355:799–808. doi: 10.1056/NEJMoa053241
49. Rocha M, Ribeiro A, Teixeira M. Clinical management of chronic Chagas cardiomyopathy. *Front Biosci.* (2003) 8:480–6. doi: 10.2741/926
50. Echeverría L, Rojas L, Rueda-Ochoa O, Gómez-Ochoa S, González Rugeles C, Díaz M, et al. Circulating Trypanosoma cruzi load and major cardiovascular outcomes in patients with chronic Chagas cardiomyopathy: a prospective cohort study. *Trop Med Int Health.* (2020) 25:1534–41. doi: 10.1111/tmi.13487
51. Sangenito LS, Branquinha MH, Santos ALS. Funding for Chagas disease: a 10-year (2009-2018) survey. *Trop Med Infect Dis.* (2020) 5. doi: 10.3390/tropicalmed5020088

Conflict of Interest: The authors declare that the research was conducted in the absence of any commercial or financial relationships that could be construed as a potential conflict of interest.

Publisher's Note: All claims expressed in this article are solely those of the authors and do not necessarily represent those of their affiliated organizations, or those of the publisher, the editors and the reviewers. Any product that may be evaluated in this article, or claim that may be made by its manufacturer, is not guaranteed or endorsed by the publisher.

frontiers in Cardiovascular Medicine

ORIGINAL RESEARCH
published: 02 February 2022
doi: 10.3389/fcvm.2022.787423

T-Cell Subpopulations Exhibit Distinct Recruitment Potential, Immunoregulatory Profile and Functional Characteristics in Chagas versus Idiopathic Dilated Cardiomyopathies

*Eula G. A. Neves[1], Carolina C. Koh[1], Thaiany G. Souza-Silva[1], Lívia Silva Araújo Passos[1,2], Ana Carolina C. Silva[1], Teresiama Velikkakam[1], Fernanda Villani[1,3], Janete Soares Coelho[1,4], Claudia Ida Brodskyn[5], Andrea Teixeira[6], Kenneth J. Gollob[7,8], Maria do Carmo P. Nunes[9] and Walderez O. Dutra[1,8,9]**

[1] Department of Morphology, Cell-Cell Interactions Laboratory, Institute of Biological Sciences, Federal University of Minas Gerais, Belo Horizonte, Brazil, [2] Brigham and Womens Hospital, Harvard University, Boston, MA, United States, [3] Minas Gerais State University, Divinópolis, Brazil, [4] Ezequiel Dias Foundation, Belo Horizonte, Brazil, [5] Gonçalo Moniz Research Center, Fundação Oswaldo Cruz (FIOCRUZ), Salvador, Brazil, [6] Rene Rachou Institute, Fundação Oswaldo Cruz (FIOCRUZ), Belo Horizonte, Brazil, [7] Hospital Israelita Albert Einstein, São Paulo, Brazil, [8] Instituto Nacional de Ciência e Tecnologia em Doenças Tropicais, INCT-DT, Salvador, Brazil, [9] Graduate Program in Infectology and Tropical Medicine, School of Medicine, Federal University of Minas Gerais, Belo Horizonte, Brazil

Chronic Chagas cardiomyopathy (CCC) is one of the deadliest cardiomyopathies known and the most severe manifestation of Chagas disease, which is caused by infection with the parasite *Trypanosoma cruzi*. Idiopathic dilated cardiomyopathies (IDC) are a diverse group of inflammatory heart diseases that affect the myocardium and are clinically similar to CCC, often causing heart failure and death. While T-cells are critical for mediating cardiac pathology in CCC and IDC, the mechanisms underlying T-cell function in these cardiomyopathies are not well-defined. In this study, we sought to investigate the phenotypic and functional characteristics of T-cell subpopulations in CCC and IDC, aiming to clarify whether the inflammatory response is similar or distinct in these cardiomyopathies. We evaluated the expression of systemic cytokines, determined the sources of the different cytokines, the expression of their receptors, of cytotoxic molecules, and of molecules associated with recruitment to the heart by circulating $CD4^+$, $CD8^+$, and CD4-CD8- T-cells from CCC and IDC patients, using multiparameter flow cytometry combined with conventional and unsupervised machine-learning strategies. We also used an *in silico* approach to identify the expression of genes that code for key molecules related to T-cell function in hearts of patient with CCC and IDC. Our data demonstrated that CCC patients displayed a more robust systemic inflammatory cytokine production as compared to IDC. While $CD8^+$ T-cells were highly activated in CCC as compared to IDC, $CD4^+$ T-cells were more activated in IDC. In addition to differential expression of functional molecules, these cells also displayed distinct expression of molecules

OPEN ACCESS

Edited by:
Leonardo Roever, Federal University of Uberlandia, Brazil

Reviewed by:
Paulo M. Dourado, University of São Paulo, Brazil
Ronald J. Vagnozzi, University of Colorado Anschutz Medical Campus, United States
Celio Geraldo Freire-de-Lima, Federal University of Rio de Janeiro, Brazil
Joao Santana Silva, Oswaldo Cruz Foundation (Fiocruz), Brazil

***Correspondence:**
Walderez O. Dutra
waldutra@gmail.com

Specialty section:
This article was submitted to General Cardiovascular Medicine, a section of the journal Frontiers in Cardiovascular Medicine

Received: *30 September 2021*
Accepted: *10 January 2022*
Published: *02 February 2022*

Citation:
Neves EGA, Koh CC, Souza-Silva TG, Passos LSA, Silva ACC, Velikkakam T, Villani F, Coelho JS, Brodskyn CI, Teixeira A, Gollob KJ, Nunes MCP and Dutra WO (2022) T-Cell Subpopulations Exhibit Distinct Recruitment Potential, Immunoregulatory Profile and Functional Characteristics in Chagas versus Idiopathic Dilated Cardiomyopathies. Front. Cardiovasc. Med. 9:787423. doi: 10.3389/fcvm.2022.787423

associated with recruitment to the heart. *In silico* analysis of gene transcripts in the cardiac tissue demonstrated a significant correlation between CD8 and inflammatory, cytotoxic and cardiotropic molecules in CCC transcripts, while no correlation with CD4 was observed. A positive correlation was observed between CD4 and perforin transcripts in hearts from IDC but not CCC, as compared to normal tissue. These data show a clearly distinct systemic and local cellular response in CCC and IDC, despite their similar cardiac impairment, which may contribute to identifying specific immunotherapeutic targets in these diseases.

Keywords: T-cells, cytokines, chemokines, inflammation, Chagas cardiomyopathy, idiopathic cardiomyopathy

INTRODUCTION

Heart diseases are the leading cause of death worldwide (1). Chronic Chagas cardiomyopathy (CCC) is the most severe manifestation of Chagas disease, resulting from an intense inflammatory reaction triggered by the infection by the intracellular protozoan *Trypanosoma cruzi*, and affecting about 30% of the infected population (2). CCC is characterized by arrhythmias, thromboembolism, heart dilation and failure, and sudden death (3–5). It is considered the leading cause of non-ischemic cardiomyopathy in Latin America, and poses an economic burden of over $7 billion/year in already impoverished populations (6–8). Idiopathic dilated cardiomyopathy (IDC) comprises a heterogeneous group of clinical diseases characterized by an enlarged left ventricle with poor contractility, sharing clinical features with CCC (9–11). IDC is also the result of an inflammatory response, with evolution to congestive heart failure and death (9, 12, 13). It is one of the main causes of heart transplants in Brazil (14, 15). IDC etiology can be related to genetic and non-genetic causes, such as metabolic issues, autoimmunity or associated with previous viral infection (16, 17). Previous clinical studies have shown that CCC displays a worse prognosis when compared with cardiomyopathies of different etiologies, including IDC (18–20). This is probably related to progressive remodeling of the myocardium and consequent hypertrophy (21), in response to the intense chronic inflammation observed in CCC (22–25).

The inflammatory infiltrate present in the myocardium of CCC patients contains macrophages and B cells, but it is mainly composed of T-cells, primarily cytotoxic $CD8^+$ T-cells followed by $CD4^+$ T-cells (22). Although the recruitment mechanisms of these cells to the cardiac tissue of Chagas patients have not been clarified, the expression of chemotactic receptors that preferentially recruit inflammatory Th1 cells has been associated with severity of CCC (26–28). Exacerbated expression of inflammatory cytokines by circulating $CD4^+$, $CD8^+$ and CD4-CD8- (double negative, DN) T-cells has also been associated with CCC, as well as with worse ventricular function in these patients (29–33).

In addition to the indistinguishable clinical profile, some histopathological features observed in IDC are also shared by CCC, such as the occurrence of fibrosis and necrosis of cardiomyocytes (13). The inflammatory infiltrate associated with IDC is also mainly mononuclear, containing T and B cells, as well as macrophages (34). While CCR2 is critical for cellular recruitment in experimental models of IDC (35), it is not clear what chemokines and receptors mediate cell recruitment to human heart in IDC.

In this study, we sought to investigate phenotypic and functional features of T-cell subpopulations in CCC and IDC, aiming to clarify whether the characteristics of T-cells in the inflammation-mediated pathology is similar or distinct in these diseases. Our results showed several immunological differences related to cytokine expression, cytotoxic molecule expression and potential of recruitment to the heart in CCC vs. IDC. These systemic differences were mirrored by *in silico* analysis of transcripts found in the hearts from CCC and IDC patients, suggesting that despite the similar degree of left ventricular dysfunction and clinical resemblance, the underlying immunological mechanisms are quite distinct in CCC and IDC. Our results, in addition to providing original information regarding distinct T-cell characteristics related to disease pathology in these clinically similar diseases, point to potential targets for adjuvant immunotherapeutic approaches, potentially contributing to future clinical management of dilated cardiomyopathies.

PATIENTS, MATERIALS, AND METHODS

Patients

This was an observational study, with a cross-sectional analysis, including patients who were referred to a tertiary cardiology outpatient service (Hospital das Clínicas, UFMG) for management of heart failure. The patients were classified into 2 groups according to the underlying cause of cardiomyopathy. Chronic Chagas cardiomyopathy (CCC) was defined by left ventricular enlargement with systolic dysfunction in the presence of positive serologic tests for antibodies against *T. cruzi.* Idiopathic dilated cardiomyopathy (IDC) was also characterized by dilated left ventricle with systolic dysfunction, but negative serological tests for Chagas disease in the absence of abnormal loading conditions or coronary artery disease sufficient to cause global systolic impairment (36).

To analyze the *ex vivo* cellular immune profile in T lymphocyte subpopulations, peripheral blood samples of 24 individuals with CCC and 13 with IDC were collected. The demographic and clinical features of patients included in the study of T-cell responses are represented in **Table 1**. This table

TABLE 1 | Demographic and clinical features of patients evaluated in the study for *ex vivo* T-cell analysis.

Characteristics	CCC group (*N* = 24)	IDC group (*N* = 17)	*P*-value
Age (years)	61.5 (51.5 ± 69.8)	60.0 (50.0 ± 69.0)	0.429
LVEF (%)	38.4 ± 11.6	35.3 ± 9.2	0.209
LVDD (mm)	46.3 ± 13.6	62.9 ± 9.0	**0.001**
LVSD (mm)	40.5 ± 10.0	51.0 ± 8.2	**0.004**
Left Atrial diameter (mm)	39.0 ± 10.0	44.4 ± 6.6	0.08
SPAP (mmHg)	34.1 ± 4.5	33.8 ± 13.0	0.471
Heart rate (bpm)	60.0 (54.8 ± 61.5)	68.0 (57.0 ± 80.0)	0.148
A (cm/s)	63.0 (36.2 ± 78.8)	34 (30.0 ± 89.5)	0.347
E (cm/s)	66.0 ± 13.5	56.8 ± 4.6	0.11
DT (ms)	199.5 ± 65.1	205.0 ± 67.4	0.443

Data are presented as mean ± SD or median and interquartile range. Sex Variable were presented by percentage (%). LVEF, left ventricular ejection fraction; LVDD, left ventricular end-diastolic diameter; LVSD, left ventricular end-systolic diameter; SPAP, systolic pulmonary artery pressure; A, late diastolic trans mitral flow velocity; E, early diastolic trans mitral flow velocity; DT, deceleration time. The p-values in bold indicates statistically significant differences between CCC and IDC.

shows the similarity between the degree of cardiac involvement and clinical parameters measured in CCC and IDC patients. Except for left ventricular systolic and diastolic diameter, all other parameters were similar between groups. Plasma samples from 38 patients of the CCC group and 5 of IDC group were employed to measure circulating soluble factors. Detailed assessment, including physical examinations, electrocardiogram, chest X-rays, and echocardiogram, were performed to characterize the clinical status, as previously defined by us (3).

All individuals went through cardiological clinical follow-up at the Hospital das Clínicas of Universidade Federal de Minas Gerais (UFMG) and accepted to participate voluntarily in the research. All were informed about the objectives of our study and signed the Informed Consent Form. This study was approved by the Comitê de Ética em Pesquisa of Universidade Federal de Minas Gerais (COEP-UFMG – ETIC006/05) and Comissão Nacional de Ética em Pesquisa (CONEP no. 2.809.859) and conformed to the ethical guidelines of the 1975 Declaration of Helsinki.

Blood Sampling and Collection of Peripheral Blood Mononuclear Cells (PBMC) and Plasma

Peripheral blood samples were collected by venipuncture in tubes containing sodium heparin (Vacutainer, Becton Dickinson, San Jose, CA, USA). PBMC were isolated by differential centrifugation at 600 g for 40 min, using Ficoll-Paque PLUS (GE Healthcare, Sweeden), as previously done by us (37). Plasma was retrieved and PBMC were washed with phosphate buffered saline three times, and resuspended in RPMI 1640 medium (Thermo Fisher Scientific, Waltham, US), supplemented with 5% inactivated human serum (Thermo Fisher Scientific, Waltham, US), 1% antibiotic (penicillin, 200 U/mL; and streptomycin, 0.1 mg/mL, -Thermo Fisher Scientific, Waltham, US) and 1 mM of L-glutamine (Sigma-Aldrich, St. Louis, US) at a concentration of 1×10^7 cells/ml. The cells were kept in a CO_2 incubator at 37°C for 18 h, and 1 μg/mL of Brefeldin A (Biolegend, San Diego, CA) was added in the last 4 h to prevent cytokine secretion.

To assess the frequency of TNF in $CD8^+$ T lymphocytes and for the correlation analysis with the frequency of IFN-gamma in $CD4^+$ and $CD8^+$ T lymphocytes, PBMC from 7 CCC patients and 8 IDC patients were stimulated with PMA (1 ng/mL, Sigma-Aldrich, St. Louis, US) and Ionomycin (500 ng/mL, Sigma-Aldrich, St. Louis, US), under the same conditions mentioned above.

Measurement of Soluble Cytokines and Chemokines

Plasma obtained from peripheral blood as mentioned above was used to measure the following molecules: cytokines (IL1-Ra, IL-2, IL-6, IL-7, IL-10, IL-15, IL-17) and chemokines (CCL3, CCL4, CCL5) using the Bio-Plex ProTM Human Cytokine Standard 27-plex Kit (Bio-Rad—Hercules, CA, USA). Experiments were performed according to the manufacturer's instructions. The data were acquired by the Bio-Plex 200 instrument equipped with the Manager software, and the results were expressed as the mean fluorescence intensity (MFI) after background subtraction.

Flow Cytometric Analysis

PBMC (2×10^5/tube) were stained for 30 min at 4°C with a combination of anti-cell surface molecules monoclonal antibodies conjugated to fluorochromes. Anti-CD4 PercpCy5 (clone A161A1), CD8 APCcy7 (clone SK1), TCR alpha-beta FITC (Clone IP-26) and TCR gamma-delta BV421 (clone B1) were used for phenotypic identification of T-cell subpopulations; anti-TNFR1 APC (Clone W15099A) and anti-IL10R PE (clone 3F9), for evaluation of immunoregulatory cytokines receptors; anti-CCR5 BV510 (clone J418F1), anti-CXCR3 pecy7 (clone G025H7), and anti-CCR4 BV510 (clone L291H4), for analysis of chemokine receptor expression.

After the incubation period, cells were washed twice by centrifugation (10 min, 4°C, 600 g) with PBS containing 1% BSA and fixed with 2% paraformaldehyde solution for 20 min. After total removal of the fixing solution by centrifugation and washing with PBS, the cells were permeabilized for 15 min with 0.5% saponin and then submitted to intracellular staining with anti-IFN-gamma BV510 (clone 4S.B3), anti-TNF BV510 (clone MAb11), anti-IL-10 APC, (clone JES3-19F1), anti-IL-17 BV510 (clone (BL168), anti-granzyme A PE (CB9), anti-perforin PE (clone B-D48), anti-Eomes APC (clone # 644730) and anti-cMET APC (clone # 95106). All combinations employed antibodies labeled with different fluorochromes. Anti-Eomes and anti-cMET antibodies were from R&D Systems (Minneapolis), and all others were from Biolegend (San Diego, CA, USA).

Subsequently, the cells were washed twice with a 0.5% saponin solution and resuspended in PBS for acquisition in a FACSCanto II flow cytometer (Becton & Dickinson, San Jose, CA, USA). A minimum of 100,000 gated events was acquired and analyzed using the software Flowjo (Ashland, Oregon-US), employing supervised analysis and unsupervised machine-learning strategies. We analyzed forward scatter area (FSC-A) vs. forward scatter height (FSC-H) to remove doublets.

Lymphocytes were selected based on FSC-A vs. side scatter area (SSC-A). The analysis strategy for evaluating the different T-cell subpopulations is represented in **Figure 2A**.

In silico Analysis of mRNA Expression Profile

Data containing the gene expression profile by microarray analysis were obtained from the Gene Expression Omnibus (GEO) database (http://www.ncbi.nlm.nih.gov/geo/). A total of 17 samples of the human left ventricular free wall heart tissue were available for comparison between CCC ($n = 10$) and healthy donors ($n = 7$), under the Gene Expression Omnibus accession number GSE84796; files were selected to compare the gene expression profile of CD4, CD8, IFN-gamma, IL-10, Il-17, granzyme A, perforin, CCR5, CCL3, CCL4, CCL5, Eomes, and HGF; data Evaluated by SurePrint G3 Human GeneExpression v1 8x60K Arrays (Agilent Technologies, Les Ulis, França) (38). Additionally, through accession number GPL2041, files corresponding to gene transcripts of CD4, CD8, Granzyme A, Perforin, CCR5, CCL5, and Eomes were selected from the analysis of 7 samples of the left ventricular anterior free wall from patients with IDC and 8 of healthy donors (GeneChip® Human Gene 1.0 array-Affymetrix) (39). Gene expression profile data from both studies were represented using mRNA fluorescence intensity.

Protein-Protein Interaction Network and Enriched Pathways Analysis

The network was constructed using NetworkAnalyst.ca. through direct relationships between proteins and altered soluble factors in CCC and IDC. Pairwise correlation prediction was determined based on IMEx database. Resulting high-scoring genes were used to identify hub genes. Enriched pathway analysis emerging as a result of interconnections in the network were generated using Kyoto Encyclopedia of Genes and Genomes (KEGG).

Statistical Analysis

To assess the systemic profile of soluble factors, the phenotypic and functional cellular profile of T-cell subpopulations among cardiomyopathies, and comparative analysis of the *in silico* study, the data were analyzed using the GraphPad Prism 8 software (GraphPad Software, La Jolla—CA, USA). After evaluating the Gaussian distribution using the Shapiro-Wilk test, the parametric data were analyzed using the unpaired *t*-test end non-parametric data were submitted to the Mann-Whitney test. The data were represented in the graphs using minimum and maximum values. Correlation analysis of the plasma profile of the chemokine CCL4 with its ligand CCR5 in $CD4^+$, $CD8^+$ and gamma-$delta^+$ DN T cells, as well as the evaluation of association the % expression of IFN-gamma with $cMET^+$ $CCR5^+$ and $CXCR3^+$ $CCR4^+$ cells in different cardiomyopathies, was performed using Pearson's test for parametric data and Spearman's test for non-parametric data.

To assess a possible pattern of differentiation between groups, using data from soluble cytokines, we built a representative heat map analysis using the Clustvis software, which uses the R-version 0.7.7 package, where it is possible to identify the cluster between the samples and define the homogeneity or heterogeneity in the distribution of data between the groups. Rows and columns are grouped using the correlation distance and the mean link. Additionally, principal component analysis (PCA) was performed, in which the X- and Y-axes show the % of the total variance. Prediction ellipses indicate a probability of 0.95 that a new observation will fall inside the ellipse (40).

For the qualitative representation of the cellular immune profile, analysis of the t-distributed stochastic neighbor-embedding (t-SNE) algorithm was performed, a tool that allows the visualization of multidimensional data in 2 dimensions (t-SNE1 and t-SNE2) (41). Then, the t-SNE analysis was generated using the Barnes-Hut algorithm with 1,000 interactions and a perplexity parameter of 30. The molecules selected for this analysis were CD4, CD8, TCR gamma-delta, CXCR3, CCR4, and cMET.

RESULTS

The Levels of Inflammatory, Proliferative, and Regulatory Cytokines Are Elevated in Plasma of CCC, as Compared to IDC Patients

First, we assessed the systemic soluble cytokine profile in plasma samples of patients with different cardiomyopathies. Our data showed an increase in cytokines with an inflammatory profile (IL-6), proliferative (IL-2, IL-7, IL-15), and regulatory (IL-10 and IL-17) in the CCC group compared to IDC (**Figure 1A**). On the other hand, the level of the IL-1 receptor antagonist (IL-1RA) were higher in IDC than CCC (**Figure 1A**). Heatmap analysis showed clear segregation between groups, with a strong correlation between IL-15 and IL-2 and IL-10 and IL-7 (**Figure 1B**). PCA analysis reinforced the distinct soluble cytokine profile between cardiomyopathies, shown by the prediction ellipses, with a total variation of 70.7%, with 52.3% on the X-axis and 18.4% on the Y-axis (**Figure 1C**). Network analysis using the molecules that were altered in CCC (**Figure 1A**) as compared to IDC shows the inflammatory cytokine IL-6, the proliferative cytokines IL-15 and IL-2 and the modulatory cytokine IL-10 as central nodes, with high centrality (**Figure 1D**). Enriched pathway analysis emerging as a result of interconnections in the network generated by KEGG, showed a predominance of inflammatory networks in CCC. Of note, T-cell signaling and TNF signaling pathways emerge within the first 20 pathways with lowest false discovery rate (FDR, adjusted *p*-value) in CCC (**Figure 1D**, yellow mark).

Inflammatory $CD8^+$ T-Cells Are More Frequent in CCC Patients, While Inflammatory $CD4^+$ T-Cells Are Associated With IDC

To evaluate cellular responses, we first determined the overall frequency of circulating T-cell subpopulations, evaluating the frequencies of $CD4^+$, $CD8^+$, TCRgamma-$delta^+$ and TCRalpha-$beta^+$ DN T-cells in the different cardiomyopathies. **Figure 2A** shows the analysis strategy employed. Our data showed that the frequencies of $CD4^+$, $CD8^+$ and alpha-$beta^+$ DN T-cells were

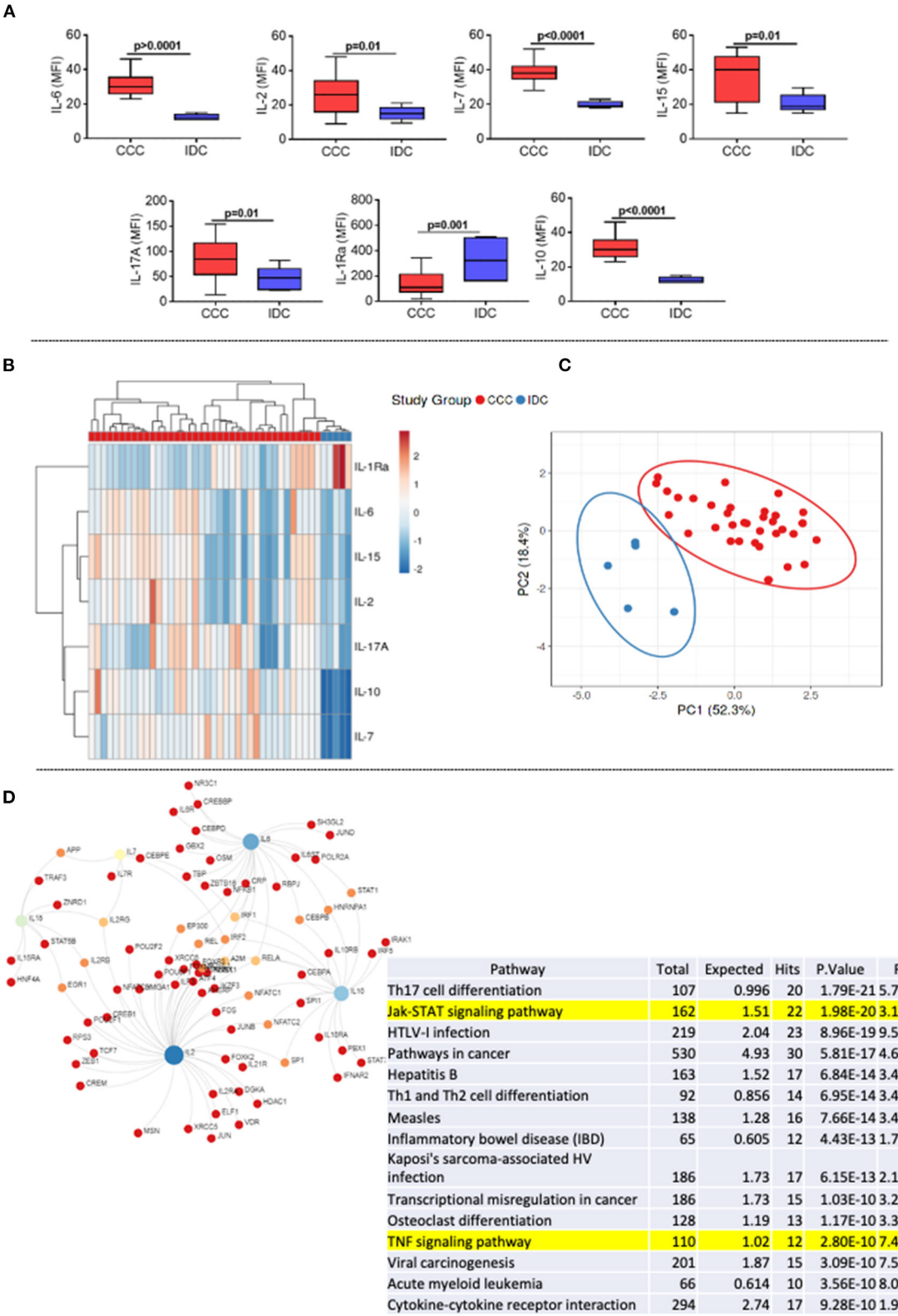

Pathway	Total	Expected	Hits	P.Value	FDR
Th17 cell differentiation	107	0.996	20	1.79E-21	5.71E-19
Jak-STAT signaling pathway	162	1.51	22	1.98E-20	3.15E-18
HTLV-I infection	219	2.04	23	8.96E-19	9.50E-17
Pathways in cancer	530	4.93	30	5.81E-17	4.62E-15
Hepatitis B	163	1.52	17	6.84E-14	3.48E-12
Th1 and Th2 cell differentiation	92	0.856	14	6.95E-14	3.48E-12
Measles	138	1.28	16	7.66E-14	3.48E-12
Inflammatory bowel disease (IBD)	65	0.605	12	4.43E-13	1.76E-11
Kaposi's sarcoma-associated HV infection	186	1.73	17	6.15E-13	2.17E-11
Transcriptional misregulation in cancer	186	1.73	15	1.03E-10	3.26E-09
Osteoclast differentiation	128	1.19	13	1.17E-10	3.37E-09
TNF signaling pathway	110	1.02	12	2.80E-10	7.41E-09
Viral carcinogenesis	201	1.87	15	3.09E-10	7.55E-09
Acute myeloid leukemia	66	0.614	10	3.56E-10	8.09E-09
Cytokine-cytokine receptor interaction	294	2.74	17	9.28E-10	1.97E-08

FIGURE 1 | Comparative analysis of plasma cytokines levels between the study groups. **(A)** Comparative analysis of plasma cytokine levels between patients with Chronic Chagas cardiomyopathy (CCC, $n = 38$) and Idiopathic cardiomyopathy (IDC, $n = 5$). Plasma soluble cytokine levels were measured using the Bio-Plex ProTM Human Cytokine Standard 27-plex Kit, and results are expressed in MFI, as described in Materials and Methods. Graphs are expressed as boxplots, with the

(Continued)

FIGURE 1 | minimum and maximum values indicated. *p*-values < 0.05 were considered statically significant and are shown in the Figure. **(B)** Representative heat map analysis of cytokine plasma levels. Both rows and columns are grouped using correlation distance and mean link. In the color gradient bar, blue indicates lower plasma levels, while red indicates higher levels. Vertical lines represent each sample evaluated, and horizontal lines represent each molecule in the study. **(C)** Principal component analyses (PCA) between measured cytokines and evaluated study groups; the X and Y axes show % of the total variance. Prediction ellipses indicate with a probability of 0.95 that a new observation will fall within the ellipse. **(D)** Network and enriched pathway analysis in CCC. Protein-protein network interactions were performed considering the molecules altered in CCC as compared to IDC. Blue and light green represent rub nodes. Different colors distinguish nodes with different numbers of interactions. Bottom table shows a pathway enrichment analysis derived from protein-protein interactions based on Kyoto Encyclopedia of Genes and Genomes (KEGG) algorithm, showing the top 20 hits for CCC with lowest false discovery rates (FDR). T-cell signaling and TNF signaling pathways are highlighted.

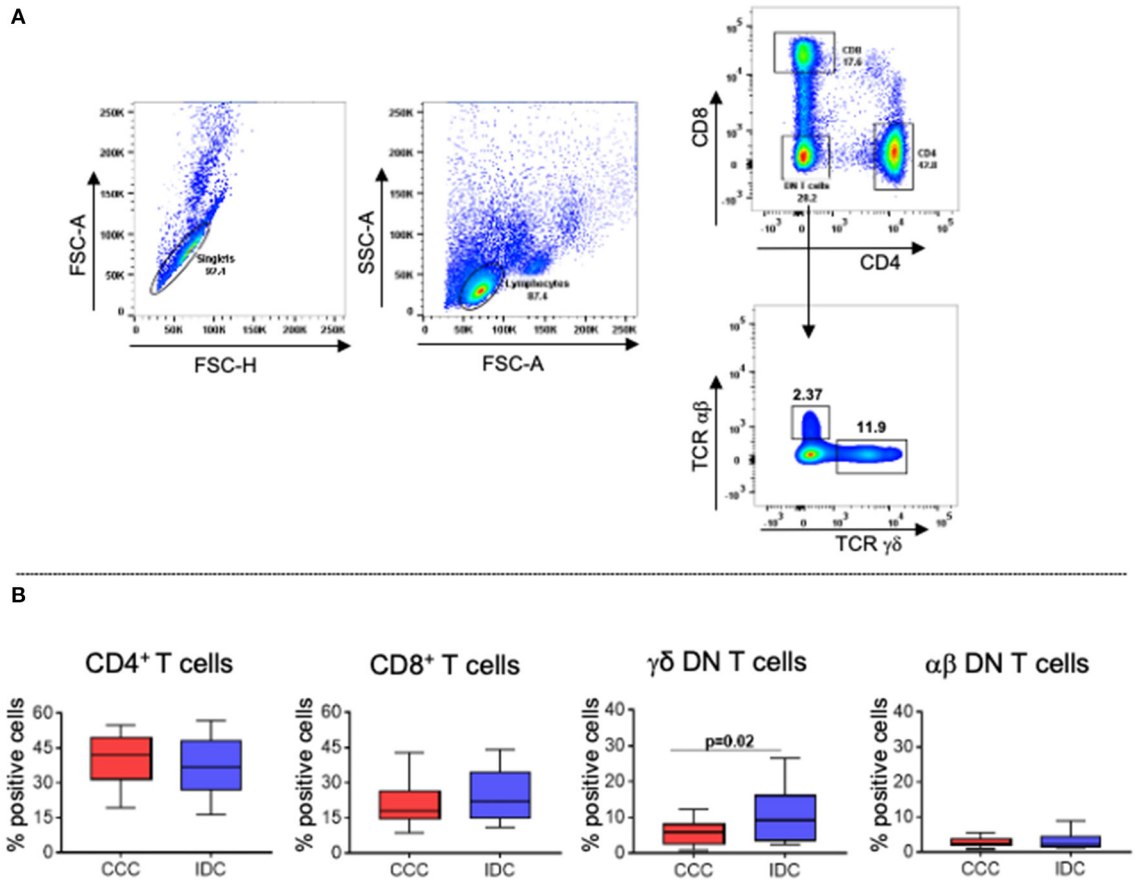

FIGURE 2 | Frequency of different T lymphocyte subpopulations in peripheral blood of patients with chronic Chagas cardiomyopathy and idiopathic cardiomyopathy. **(A)** Representative dot plots of the analysis strategy used in the study: To remove doublets, the parameters FSC-A × FSC-H were used; lymphocytes were selected according to size (FSC-A) and granularity (SSC-A) parameters. For phenotypic separation of cell subpopulations, CD8 and CD4 surface markers were selected, followed by selection of CD4−CD8− cells to identify gamma−delta$^+$ and alpha−beta$^+$ DN T cells. **(B)** Frequency of CD4$^+$ T cells, CD8$^+$ T cells, gamma−delta$^+$ DN T cells (CCC, n = 17; IDC, n = 13), and alpha−beta$^+$ DN T cells (CCC, n = 10; IDC, n = 10). Graphs are expressed as boxplots, with the minimum and maximum values indicated.

similar between the groups (**Figure 2B**). However, we observed higher frequency in DN T-cells expressing the TCR gamma-delta in IDC compared to CCC patients (**Figure 2B**).

To assess the functional profile of the different T-cell subpopulations, we evaluated the expression of the inflammatory cytokines IFN-gamma and TNF, as well as of the regulatory cytokine IL-10, and of IL-17. We observed an increase in the frequency of IFN-gamma (**Figure 3A**) in CD4$^+$ T-cells in the CCC group compared to IDC, while TNF was increased in CD4$^+$ T-cells from IDC as compared to CCC (**Figure 3B**). The frequency of CD8$^+$IL-10$^+$ T-cells was increased in CCC as compared to IDC (**Figure 3C**). IL-17 expression was increased in CD8$^+$ and alpha-beta$^+$ DN T-cells from CCC as compared to IDC (**Figure 3D**).

Analysis of TNF receptor 1 (TNFR1) and IL-10 receptor (IL-10R) expression showed that, while there was no difference in the expression of IL-10R by the different T-cell subpopulations (**Figure 3E**), TNFR1 was upregulated in CD4$^+$ T-cells and TCRgamma-delta$^+$ DN T-cells from IDC than CCC, and higher in CD8$^+$ cells from CCC compared to IDC (**Figure 3F**).

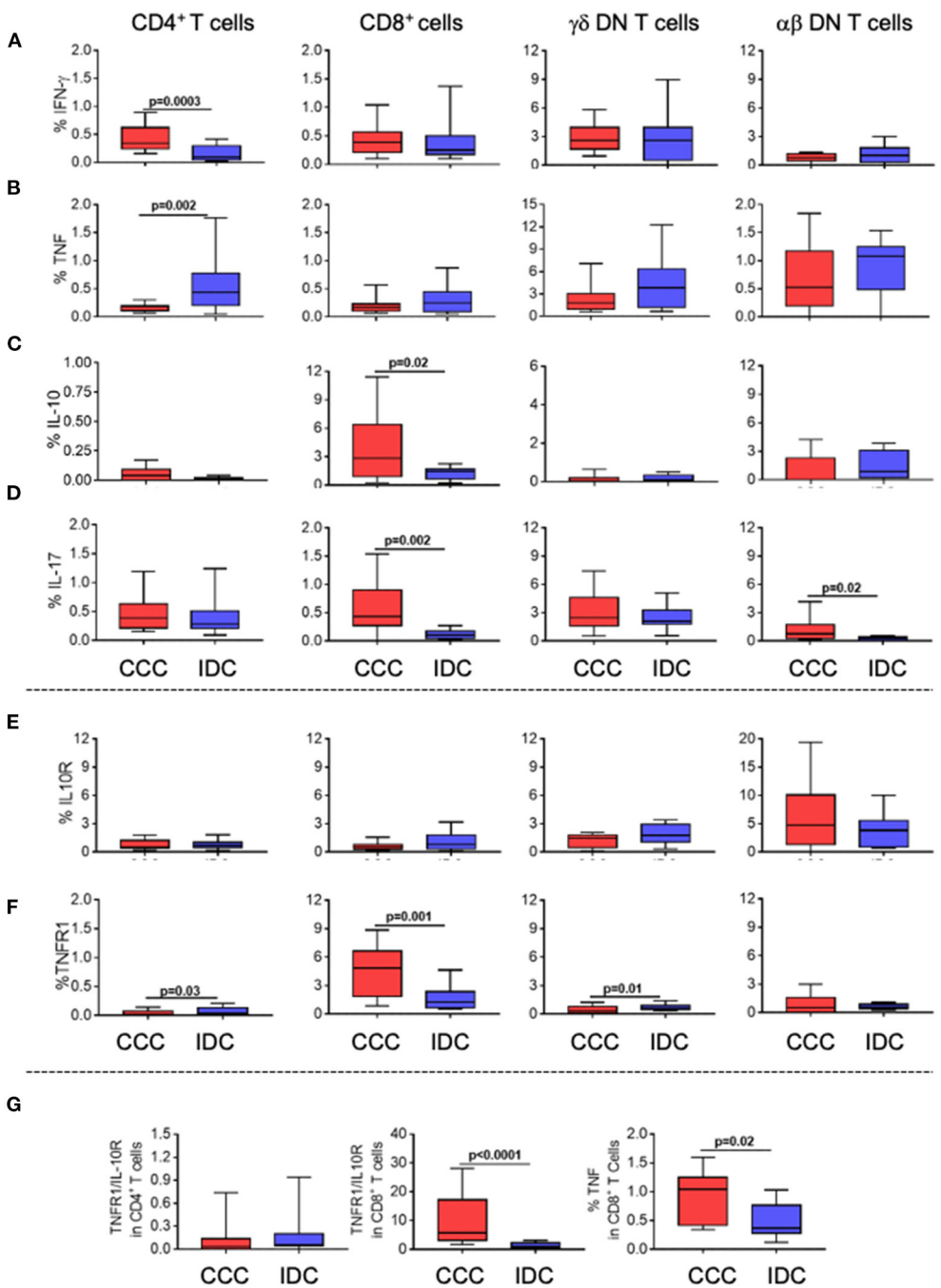

FIGURE 3 | Cellular immune profile of cytokines and immunoregulatory receptors in T-cell subpopulations in different cardiomyopathies. Frequency of expression of cytokines and immunoregulatory receptors **(A)** IFN-gamma, **(B)** TNF, **(C)** IL-10 **(D)** IL-17 **(E)** IL-10R, **(F)** TNF-R1. The analysis was performed as described in the materials and methods for comparison between the different groups in $CD4^+$, $CD8^+$, gamma-delta$^+$ (CCC, $n = 17$, IDC, $n = 13$) and alpha-beta$^+$ DN T cells (CCC, $n = 10$, IDC, $n = 10$). **(G)** analysis of the ratio of TNFR1+/IL10R+ cells in $CD4^+$ and $CD8^+$ T cells; TNF expression in $CD8^+$ T cells stimulated with PMA/Ionomycin (CCC, $n = 7$; IDC, $n = 8$). Values of $p < 0.05$ were considered statistically significant. Graphs are expressed as boxplots, with the minimum and maximum values indicated.

We observed a higher TNFR1/IL-10R ratio in $CD8^+$ T-cells from CCC as compared to IDC, and a tendency of increased TNFR1/IL-10R ratio in $CD4^+$ cells in IDC (**Figure 3G**). In addition, we observed a higher frequency of $CD8^+TNF^+$ T-cells in CCC as compared to IDC after *in vitro* stimulation (**Figure 3G**). Together, these data suggest that $CD8^+$ T-cells and $CD4^+$ T-cells from CCC and IDC, respectively, display a predominantly inflammatory profile.

To determine the cytotoxic potential of the different T-cell subpopulations, we evaluated the frequency of expression of

Eomes, perforin, and granzyme A. We observed a significant higher frequency of Eomes only in $CD8^+$ T-cells in the CCC group compared to IDC (**Figure 4A**). No differences were observed in perforin expression comparing CCC and IDC (**Figure 4B**). Expression of granzyme A was increase in $CD4^+$ T-cells in CCC patients compared to IDC (**Figure 4C**).

We also verified the percentage contribution of the different T-cell subpopulations to the expression of the different cytotoxic molecules. It is quite clear that $CD8^+$ cells are the main expressors of cytotoxic molecules, as compared to the other T-cell subpopulations analyzed in both CCC and IDC (**Figure 4D**). In addition to $CD8^+$ T cells, DN TCR alpha beta T cells showed a statistically significant increase in the contribution to perforin expression in IDC compared to CCC, emerging as an important source of perforin expression in IDC (**Figure 4D**).

Analysis of Chemokine and Chemokine Receptor Expression Reveals Distinct Recruitment Potential of T-Cell Subpopulations in the Different Cardiomyopathies

The expression of the chemotactic receptor CCR5, which has been associated with CCC, was significantly higher in $CD4^+$, $CD8^+$, and TCRgamma-delta$^+$ DN T-cells in the CCC group as compared to IDC (**Figure 5A**). We also measured the systemic expression of the chemokines CCL3, CCL4, and CCL5, which are ligands for CCR5 and associated with cellular recruitment to inflammatory sites. Our data showed increased plasma levels in these chemokines in the CCC group as compared to IDC (**Figure 5B**).

To determine the association between the $CD4^+$, $CD8^+$, and TCRgamma-delta$^+$ DN T-cells expressing CCR5 with plasma levels of the chemokine ligands, we performed a correlation analysis between these molecules in the CCC group. While no correlation was observed between the cells expressing CCR5 and CCL3 or CCL5, we observed a positive and statistically significant correlation between expression of CCL4 and the frequency of $CD8^+CCR5^+$, but not with $CD4^+$ nor gamma-delta$^+$ DN T-cells (**Figure 5C**). These data indicate an association between CCL4 expression and $CD8^+CCR5^+$ T-cells in CCC.

We also evaluated the frequency of expression of the chemokine receptors CXCR3, CCR4, and the cardiotropic molecule cMET in $CD4^+$, $CD8^+$, and TCRgamma-delta$^+$ DN T-cells, using multiparameter flow cytometry, combined with conventional and unsupervised machine-learning strategies. Through clustering by similarity using unsupervised analysis, we found different population clusters, which revealed differences in the expression density of the mentioned molecules. We identified clusters 1 (**Figure 6A**), distributed within the CCC group (red color, **Figure 6B**), and clusters 2 and 3 (**Figure 6A**), predominantly located in the IDC group (blue color, **Figure 6B**). Cluster 1 shows the colocalization between cMET and CD8 expression, while clusters 2 and 3 demonstrate co-localization of CXCR3 and CCR4 in $CD4^+$ T-cells and gamma-delta DN T-cells, respectively. Conventional quantitative analysis confirmed the data observed by tSNE, showing a significant higher expression of $CD8^+cMET^+$ T-cells, as well as $CD8^+cMET^+CCR5^+$ T-cells in the CCC group compared to IDC (**Figure 6C**). A positive correlative analysis between the frequency of $CD8^+CCR5^+cMET^+$ T-cells and the inflammatory cytokine IFN-gamma or Eomes was observed in CCC but not IDC (**Figures 6D,E**).

As observed in the unsupervised qualitative analysis, the frequency of CCR4 and the co-expression of CXCR3 and CCR4 were higher in $CD4^+$ T-cells in IDC when compared to the CCC (**Figure 6F**). A positive correlation between the frequency of $CXCR3^+CCR4^+$ $CD4^+$ T-cells and the inflammatory cytokine IFN-gamma was observed in IDC but not CCC (**Figure 6G**). In addition, the expression of CXCR3 and CCR4 were higher in TCRgamma-delta$^+$ DN T-cells in IDC than CCC (**Figure 6H**). These data support the hypothesis of a distinct cell recruitment potential of activated T-cells populations in the different cardiomyopathies.

We performed a combined analysis of the parameters that were statistically significant comparing between groups, including cytokine, cytotoxic molecule, and chemotactic receptor expression by $CD4^+$ and $CD8^+$ T-cells in IDC and CCC, respectively. The Clustvis algorithm showed a distribution that generated a cellular immune signature profile that segregated the CCC and IDC groups, emphasizing the cellular immunological differences between the cardiomyopathies (**Supplementary Figure 1**).

In silico Analysis Reveals Inflammatory and Cytotoxic Potential by $CD8^+$ T-Cells in the Heart of Patients With CCC

We employed an *in silico* approach to evaluate the expression of mRNA that code for molecules related to CD4 and CD8 function in heart tissue obtained from CCC and IDC patients, using mRNA profiles available in different publicly available gene banks. Our data demonstrated up-regulation of gene transcripts for CD8, IFN-gamma, granzyme A, perforin, Eomes, CCR5, and their ligands, CCL3, CCL4, and CCL5, in cardiac tissue samples from CCC patients, compared to healthy donors (**Figure 7A**). Additionally, to assess the association of $CD8^+$ cells with the mRNA expression intensity of the different up-regulated molecules, we used a correlation matrix, which showed an association between CD8 and HGF (cMET receptor ligand), CCR5, CCL4, CCL5, perforin, granzyme A, IL-10 and IFN-gamma in the CCC group (**Figure 7B**). A significant correlation was observed only between CD8 and Eomes in the control group, and no correlation of inflammatory nor cytotoxic molecules were observed with CD4 transcripts in CCC (**Figure 7B**).

Gene transcription profile data showed that the mRNA fluorescence intensity for the molecules CD4, CD8, Granzyme A, perforin, CCR5, CCL5, and Eomes was similar between IDC and control group (**Figure 7C**). Despite similar expression, the correlation analysis showed an association between CD4 and perforin in IDC but not in control (**Figure 7D**). Interestingly, there was also a statistically significant correlation between CD8 with CCR5 and perforin in IDC, but this was also observed in healthy individuals (**Figure 7D**).

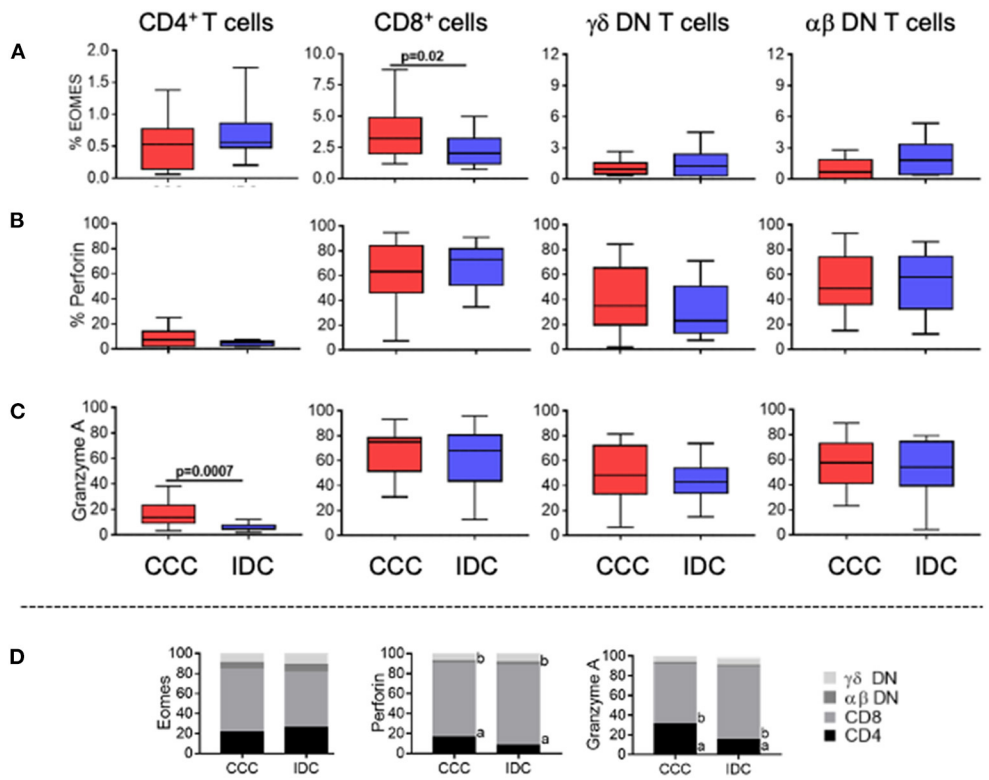

FIGURE 4 | Expression of cytotoxic molecules by the different T-cell subpopulations. Frequency of expression of molecules associated with cytotoxic function **(A)** Eomes, **(B)** perforin and **(C)** granzyme A are shown. Graphs are expressed as boxplots, with the minimum and maximum values indicated. **(D)** Contribution of different cell subpopulations to the expression of different cytotoxic molecules. The analysis was performed as described in the materials and methods for comparison between the different groups in CD4$^+$, CD8$^+$, gamma-delta$^+$ DN T cells (CCC, $n = 17$, IDC, $n = 13$) and alpha-beta$^+$ DN T cells (CCC, $n = 10$, IDC, $n = 10$). Values of $p < 0.05$ were considered statistically significant.

DISCUSSION

Although both CCC and IDC are cardiomyopathies associated with high morbidity and mortality, CCC has been associated with a worse prognosis (3, 18, 42–44). While these cardiomyopathies are clinically indistinguishable, the worse prognosis observed in CCC suggests that distinct pathogenic mechanisms may be involved in the progression of these diseases. In this work, we evaluated immunological characteristics of patients with CCC or IDC and observed that CCC displays a more inflammatory systemic profile as compared to IDC. In addition, the T-cell responses, which are critical given the chronic nature of these diseases, are also quite distinct in CCC and IDC, as seen by the differential expression of immunoregulatory cytokines, cytotoxic molecules and molecules that address T-cells to the heart. Importantly, *in silico* analysis of mRNA transcripts from CCC and IDC heart tissue confirmed these differences, strengthening the hypothesis that distinct underlying immunopathology mechanisms are involved in CCC and IDC. These results point to distinct targets potentially employable as adjuvant immunotherapeutic approaches to treat these diseases.

The establishment of a predominantly systemic inflammatory immune response in individuals infected with *T. cruzi* seems to be crucial for the development of cardiac pathology (22, 29, 45–49). Here, we described elevated plasma levels of IL-6, IL-2, IL-7, IL-15, IL-17A, and IL-10 in the CCC group, as compared to IDC. In addition, dendrogram analysis showed that comparative expression of these molecules led to complete segregation between the groups. This data also reinforce the robust immune activation observed in CCC patients (50–53). Network analysis showed that IL-6, IL-2, IL-15 and IL-10 emerged as node molecules with high centrality, suggesting a broad involvement of these immune molecules in CCC. KEGG enrichment analyses identified inflammatory pathways as the main ones amongst the first 20 pathways with lowest FDR, of particular interest, the T-cell signaling and the TNF signaling pathways. These data corroborate previous studies that highlight the role of inflammatory molecules in the immunopathology of Chagas disease (54–56). Exploiting the molecules that compose these pathways may provide potential targets to treat CCC.

Given that T-cells are central in the adaptive immune response observed in chronic diseases, including CCC and IDC (30, 32, 33, 57–61), we proposed to evaluate the functional characteristics of different T-cell subpopulations present in the peripheral blood of CCC and IDC patients. Our results suggest that while CD8$^+$

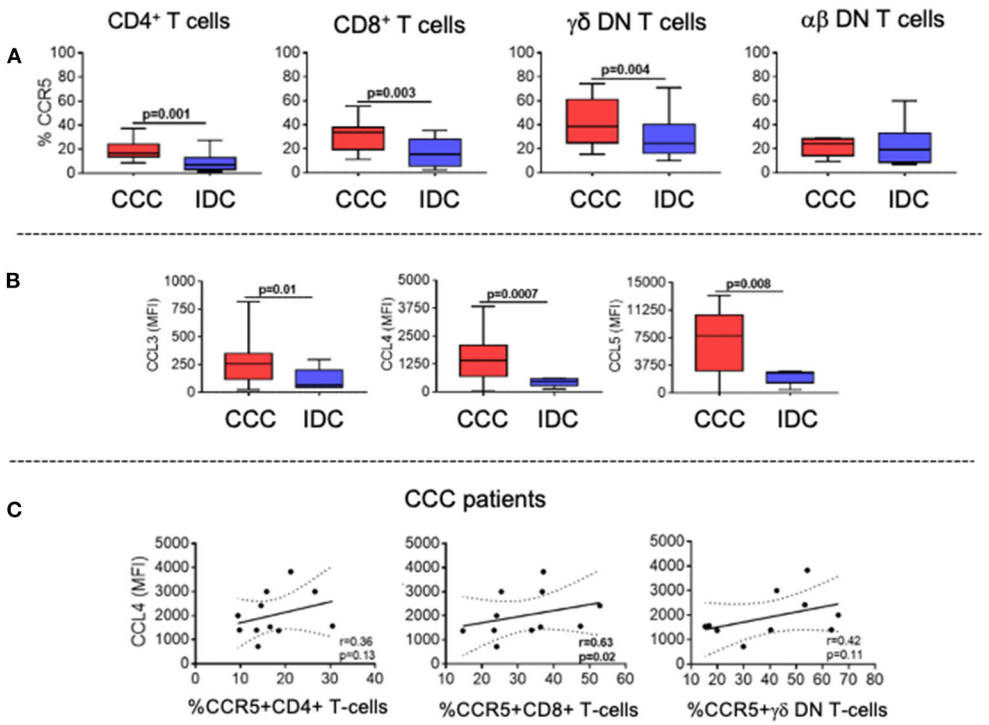

FIGURE 5 | Expression of CCR5 by the different T-cell subpopulations and of its soluble chemokine ligands CCL3, CCL4, CCL5. **(A)** Evaluation of the frequency of expression of CCR5 by $CD4^+$, $CD8^+$, gamma-delta$^+$ DN T cells (CCC, $n = 17$, IDC, $n = 13$) and alpha-beta+ DN T cells (CCC, $n = 10$, IDC, $n = 10$). The analysis was performed as described in the materials and methods for comparison between the different groups. **(B)** Plasma levels of soluble chemokines (CCL3, CCL4, CCL5) in samples from patients with Chronic Chagas cardiomyopathy (CCC, $n = 38$) and idiopathic cardiomyopathy (IDC, $n = 5$). Graphs are expressed as boxplots, with the minimum and maximum values indicated. **(C)** Correlation analysis between plasma levels of CCL4 and the frequency of expression of CCR5 in $CD4^+$, $CD8^+$ and gamma-delta$^+$ DN T cells in CCC group. Parametric data were analyzed using Pearson's correlation test and non-parametric data using Spearman's test. Values of $p < 0.05$ were considered statistically significant.

T-cells are the main ones associated with the immunoregulatory potential in CCC, $CD4^+$ T-cells are associated with IDC. $CD8^+$ cells display increased frequency of expression of TNFR1, TNF, IL-10, and IL-17 when compared to IDC, and $CD4^+$ T-cells display increased expression of TNF and TNFR1 in IDC as compared to CCC. Increase expression of cytokines with different functional profiles observed in CCC is possibly related to a control mechanism for the intense inflammation observed in those patients (53, 62–66). Analysis of the ratio TNFR1/IL-10R revealed a predominantly inflammatory profile in $CD8^+$ T-cells from CCC compared to IDC. A similar tendency was observed in the $CD4^+$ T-cells from IDC, although not statistically significant. Previous studies have shown that $CD8^+$ T cells expressing TNF are indeed the predominant cell type in the hearts of CCC patients (45), and that $CD4^+$ T cells expressing activation molecules are present in the heart of IDC patients, although not increased in relation to other leukocytes (67). Of note, the TNF signaling pathway appeared as one of the key pathways associated with the altered cytokine profile in CCC, strengthening the role of this molecule in CCC and suggesting this pathway as a potential intervention target.

T-cell cytotoxic function is essential for resistance to *T. cruzi* infection through the lysis of infected cells (68–70), and may also be important in IDC where viral infection may have played a role (17, 71, 72). However, uncontrolled T-cell mediated cytotoxicity may contribute to cardiac injury and dysfunction (45, 73, 74). To determine the cytotoxic potential of the different cell populations, we evaluated the expression of Eomes, a critical transcription factor for the differentiation of activated $CD8^+$ T-cells and for controlling expression of inflammatory cytokines, and the cytotoxic molecules granzyme A and perforin (75). It is noteworthy to mention that expression of most cytotoxic molecules was similar between groups in all T-cell populations. Thus, these cells may potentially be related to pathology in both diseases. However, we observed a high expression of Eomes by $CD8^+$ T-cells in CCC, reinforcing the previously suggested role for these cells in CCC pathology (45).

While our data also evidenced the effector capacity of T *helper* lymphocytes in CCC, shown by the increased frequency of expression of granzyme A in $CD4^+$ T-cells, as compared to IDC, the presence of cytotoxic $CD4^+$ T-cells in the hearts of CCC has not been investigated. These cells recognize antigenic peptides via MHC class II and are capable of secreting cytolytic granules that can induce apoptosis of target cells (76, 77). Thus, it is valid to speculate that $CD4^+$ T-cells may also contribute to the immunopathology in CCC. Favoring this hypothesis,

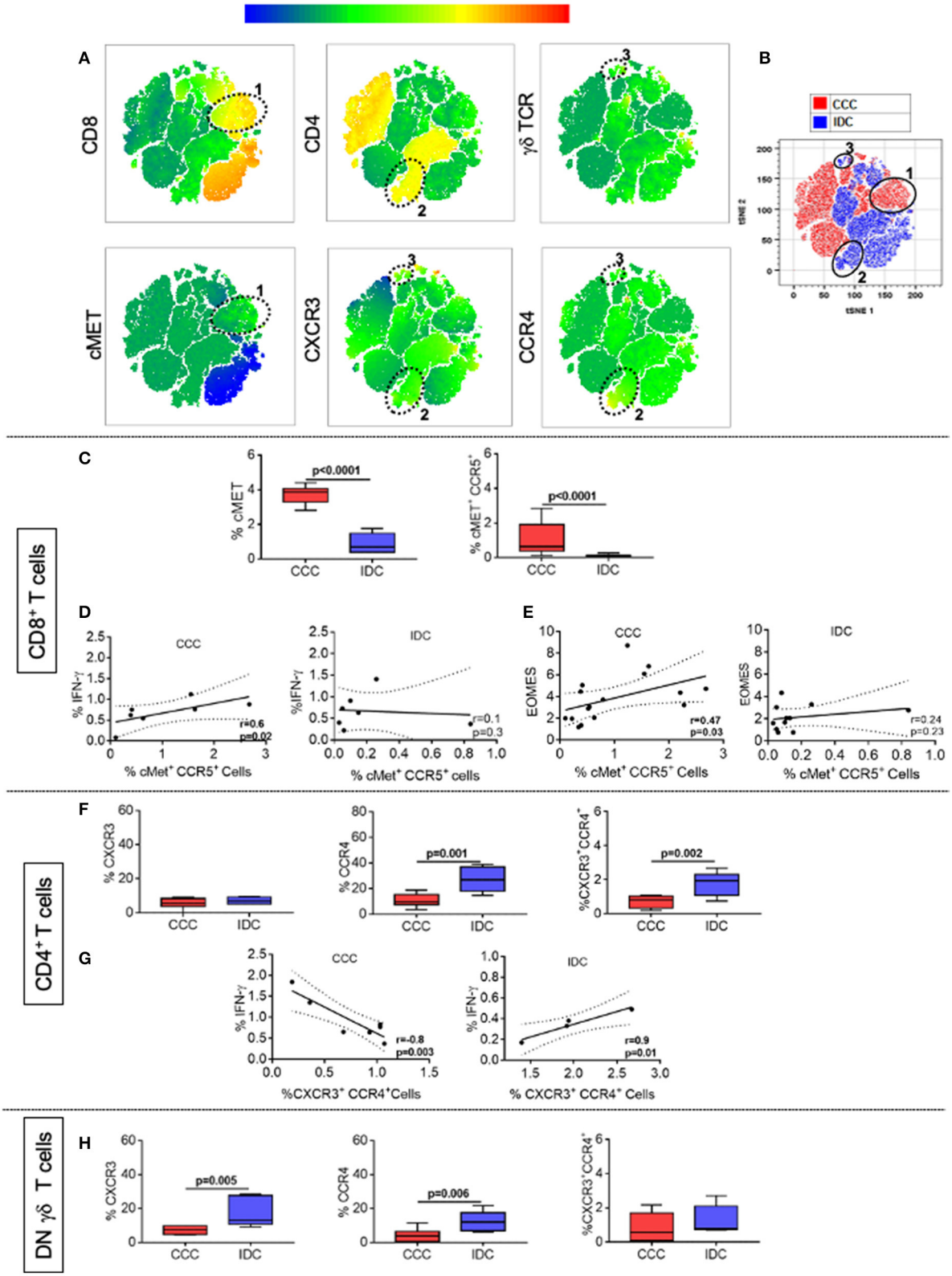

FIGURE 6 | CCR4 and CXCR3 expression reveals distinct recruitment potential between cardiomyopathies. **(A)** Representation of t-distributed stochastic neighbor embedding (t-SNE) using the expression density of CD4, CD8, cMET, TCR gamma-delta, CXCR3, and CCR4, with emphasis on clusters 1, 2, and 3 shown by the ellipses. Cluster 1 shows the colocalization between cMET and CD8 expression, while clusters 2 and 3 demonstrate the expression of CXCR3 and CCR4 by $CD4^+$

(Continued)

FIGURE 6 | and gamma-delta$^+$ DN T cells, respectively. **(B)** tSNE generated showing the stratification between the CCC (red) and IDC (blue) groups after overlaping the islands formed by the algorithm. **(C)** Frequency (%) of cMET$^+$ and co-expression of cMET$^+$CCR5$^+$ in CD8$^+$ T cells (CCC, $n = 17$, IDC, $n = 13$). **(D)** Correlation analysis between the frequency of CD8$^+$ IFN-gamma$^+$ cells stimulated with PMA/Ionomycin (CCC, $n = 7$; IDC, $n = 8$) and CD8$^+$cMET$^+$ CCR5$^+$ cells. **(E)** Correlation analysis between the frequency of CD8$^+$Eomes$^+$ cells and CD8$^+$cMET$^+$CCR5$^+$ cells. **(F)** Frequency (%) of CXCR3, CCR4 and co-expression of CXCR3$^+$ CCR4$^+$ in CD4$^+$ T cells (CCC, $n = 8$; IDC, $n = 5$). **(G)** Correlation analysis between the frequency of CD4$^+$ IFN-gamma$^+$ cells stimulated with PMA/Ionomycin (CCC, $n = 7$, IDC, $n = 5$) and CD4$^+$ CXCR3$^+$ CCR4$^+$ cells. **(H)** Frequency of CXCR3, CCR4 and co-expression of CXCR3$^+$ CCR4$^+$ in gamma-delta$^+$ DN T cells (CCC, $n = 8$; IDC, $n = 5$). The analysis was performed as described in the materials and methods for comparison between the different groups. Graphs are expressed as boxplots, with the minimum and maximum values indicated. Values of $p < 0.05$ were considered statistically significant.

pro-inflammatory and potentially effector CD4$^+$ T-cells have been associated with pathology in experimental models of *T. cruzi* infection, particularly in the absence of regulatory B-cells (78).

To determine the underlying mechanism related to the recruitment of these different T-cell populations to the heart tissue of CCC or IDC patients, we first evaluated the expression of the chemotactic receptors CCR5 and cMET, which display cardio tropic activity (79). In addition, cytolytic CD8$^+$ T-cells expressing cMET have been associated with increased intracellular levels of inflammatory cytokines such as IFN-gamma and TNF (80). The upregulation of CCR5 in CD8$^+$ T-cells from *T. cruzi*-infected mice has been associated with tissue damage (81, 82). Genetic variants of CCR5 have been associated with human Chagas disease (83), and high CCR5 expression by leukocytes has also been associated with severe CCC (27, 84). The analysis of CCR5 expression frequency showed a high frequency of CD4$^+$, CD8$^+$ and TCRgamma-delta+ DN T-cells expressing this molecule in CCC compared to IDC. Moreover, a positive correlation between the frequency of CD8$^+$ CCR5$^+$ and CCL4, a ligand for CCR5, was observed in CCC but not IDC. The high frequency of cMET$^+$ cells in the CCC group compared to IDC, as well as the association between CD8$^+$cMET$^+$CCR5$^+$ T-cells with the frequency of CD8$^+$IFN-gamma$^+$ and CD8$^+$EOMES$^+$ T-cells only in the CCC patient group, strongly suggest that these molecules mediate the recruitment of inflammatory and cytotoxic CD8$^+$ T-cells to cardiac tissue in CCC. Our data from the *in silico* analysis support this hypothesis, since it revealed an increase in the intensity of CD8 transcripts in the cardiac tissue of CCC patients compared to healthy donors. Furthermore, there was a correlation between the intensity of expression of CD8 mRNA and molecules with inflammatory potential (IFN-gamma), cytotoxic (Eomes, granzyme A, perforin), regulatory (IL-10), and cardiotropic (CCR5, CCL4, and CCL5 and HGF) in CCC but not IDC. Importantly, previous studies in experimental models of *T. cruzi* infection have shown that treatment with Met-RANTES, a CCR5 antagonist, ameliorated the cardiac tissue damage observed in treated animals (85). Thus, controlling the recruitment of potentially cytotoxic CCR5$^+$CD8$^+$ T-cells may emerge as a possible immunotherapeutic strategy in CCC.

The increased expression of CCR4, which has been related to T-cell infiltration in heart inflammatory conditions in a murine model (79, 86), and CXCR3$^+$ CCR4$^+$ cells by CD4$^+$ T-cells in IDC implicates these molecules in the recruitment of this cell subpopulation to the heart, revealing distinct cell recruitment mechanisms in CCC and IDC. In addition, gamma-delta+ DN T-cells also express higher CXCR3 receptors in IDC as compared to CCC, suggesting a potential role for these cells in IDC (87–90). *In silico* analysis showed an association of CD4 with perforin in IDC, which was not observed in healthy hearts, adding to the hypothesis that these cells are involved in tissue pathology in IDC. The identification of TCRgamma-delta+ DN T-cells was not possible in this analysis since this can only be determined using multiparameter immunostaining *in situ*, or single cell analysis, due to the need to exclude CD4 and CD8 expression in the gamma-delta+ T-cells. The use of a small molecule CXCR3 receptor antagonist has been shown to improve cardiac remodeling (91) in experimental models, opening perspectives for studying its use in human cardiomyopathies, where this molecule may play a role, such as in IDC.

CXCR3 and CCR4 expression have been shown to be induced by cMET, which has cardiotropic effects (79). Although the expression of this molecule is low in IDC, it is possible that the observed levels are sufficient to induce these chemokine receptors. We also observed an association of CD8$^+$ T-cells and cMET in CCC. Thus, it is tempting to hypothesize that, despite the involvement of distinct T-cell populations in IDC and CCC, control of cMET expression (or its ligand, HGF), may emerge as a strategy to control T-cell recruitment in IDC and CCC. Specific inhibition of cMET has shown promising effects to treat several types of cancer (92). However, given that the HGF/cMET axis is important in heart function (93), more in-depth studies need to be performed to evaluate this possibility.

LIMITATIONS OF THE STUDY

Despite dealing with clinically similar cardiomyopathies, it is important to bear in mind that these diseases develop under a distinct time scale, which may impact the differential immune responses observed. It is, however, difficult to determine exactly when disease started, posing a limitation as to the role of time to disease development and intensity of the observed immune response. In addition, while the pathology associated with both diseases may develop over years, CCC results from an acquired infection, not the same in IDC. This difference in etiology may also influence the inflammatory response, potentially explaining the exuberant response observed in CCC. The results shown in this study significantly add to the current literature as they represent, to the best of our knowledge, the first comparison of cellular and systemic immune response between CCC and IDC, two deadly cardiomyopathies. In addition to bringing insights to the mechanisms of pathology underlying these diseases, our studies point to potential targets that may be applied to control the immune response and,

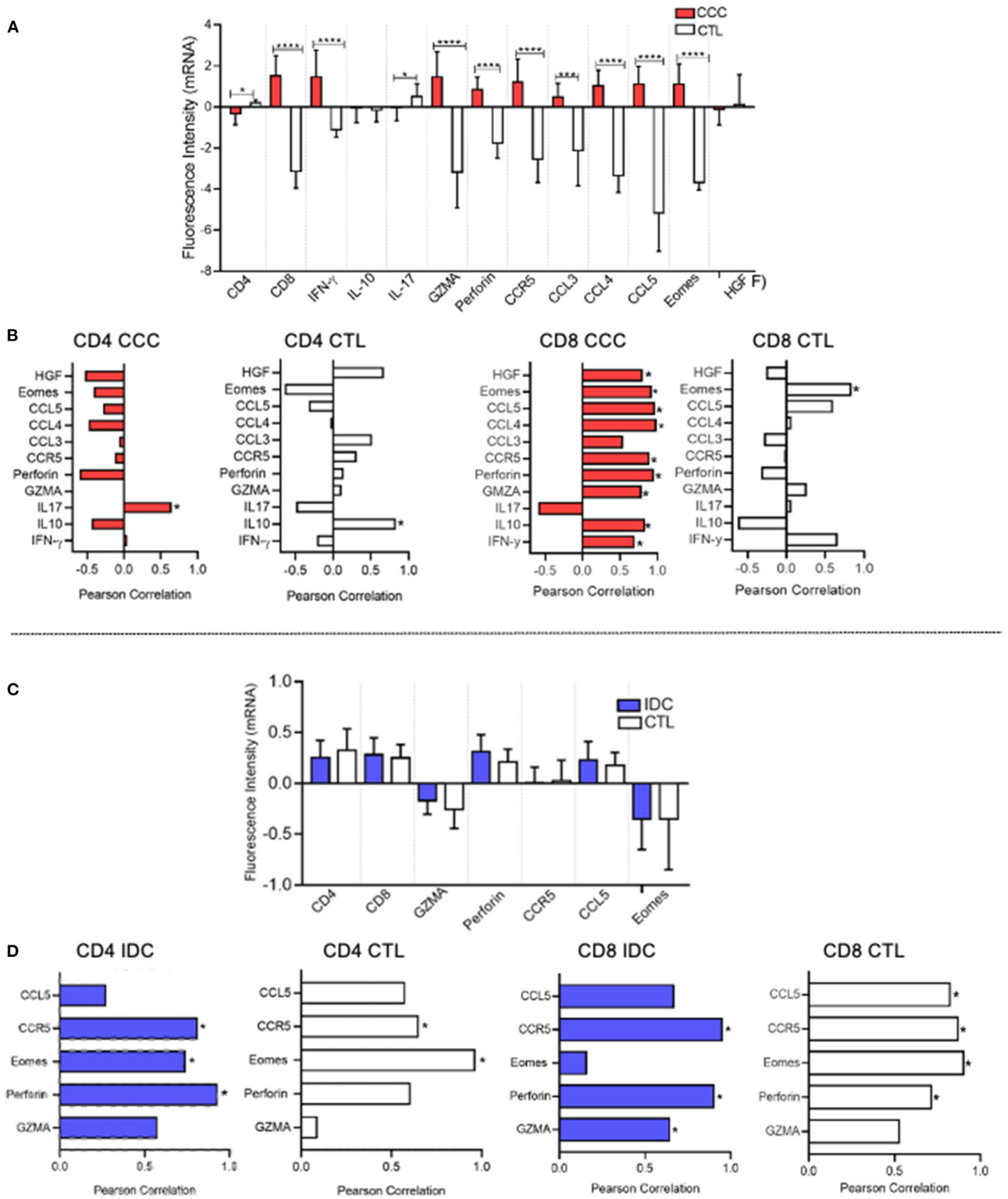

FIGURE 7 | *In silico* analysis shows association between CD8 and CD4 mRNA with cytotoxic molecules in CCC and IDC hearts, respectively. **(A)** *In silico* comparative analysis between the expression of gene transcripts of molecules related to the function of $CD4^+$ and $CD8^+$ cells in cardiac tissue samples from patients with chronic Chagas cardiomyopathy (CCC, $n = 10$) and healthy donors (CTL, $n = 7$) **(B)** Correlation analysis between the intensity of CD8 and CD4 mRNA expression and functional molecules associated with inflammatory, regulatory, cytotoxic, and cardiotropic function in the CCC and CTL group. **(C)** Comparative analysis between the expression of gene transcripts of molecules related to the function of $CD4^+$ and $CD8^+$ cells in cardiac tissue samples from patients with

(Continued)

FIGURE 7 | idiopathic cardiomyopathy (IDC, $n = 7$) and Healthy donors (CTL, $n = 8$) **(D)** Correlation analysis between the intensity of CD4 and CD8 mRNA expression and functional molecules associated with inflammatory, regulatory, cytotoxic and cardiotropic function in the IDC and CTL group. Microarray data were available in Expression Omnibus databases for download [GEO- (http://www.ncbi.nlm.nih.gov/geo/)] were downloaded and subjected to statistical analysis by Graphpad Prism 8; Parametric data were analyzed by the test Student's t and non-parametric by Mann–Whitney test. Values of $p < 0.05$ were considered statistically significant. Pearson's test performed correlation analysis. *$p < 0.05$, *** and ****$p < 0.0001$.

thus, pathology in these diseases. However, further studies need to be developed to validate these potential strategies and instruct clinical practice, which were not within the scope of present study.

CONCLUSION AND FUTURE DIRECTIONS

In conclusion, the data from the comparative analysis between the different cardiomyopathies that manifest clinically as heart failure showed that CCC is associated with a strong immune activation, with a soluble cytokine signature that distinguishes it from IDC. The *ex vivo* analysis of peripheral T-cell responses, involving cytokine and cytotoxic molecule expression, and the *in silico* analysis of cardiac tissue suggest that inflammatory and cytotoxic $CD8^+$ T-cells are strongly associated with CCC, while $CD4^+$ T-cells are associated with IDC. Furthermore, differential expression of chemotactic receptors by $CD4^+$ and $CD8^+$ T-cells, suggest distinct mechanisms of recruitment to the heart in IDC and CCC. Our data demonstrated clear immunological differences in otherwise clinically similar cardiomyopathies, clarifying mechanisms of immunopathology and pointing to potential targets for immune-mediated intervention in these diseases. Our data demonstrate clear immunological differences in clinically similar cardiomyopathies, elucidating the involvement of molecules potentially involved in the immunopathology of these diseases and pointing to potential targets for immunity-mediated intervention. Future studies, using modulators of chemokine receptor function and TNF-mediated inflammatory responses, are underway in our laboratory to validate whether the modulation of cellular recruitment and inflammatory responses will have a direct translational application in CCC and IDC.

DATA AVAILABILITY STATEMENT

The original contributions presented in the study are included in the article/**Supplementary Material**, further inquiries can be directed to the corresponding author/s.

ETHICS STATEMENT

The studies involving human participants were reviewed and approved by COEP-UFMG/CONEP. The patients/participants provided their written informed consent to participate in this study.

AUTHOR CONTRIBUTIONS

EN and CK performed all cell processing and cultures, as well as FACS analysis. AS, TV, FV, and JC aided in sample collection and blood processing. TS-S performed *in silico* analyses. LP performed the network and KEEG analyses. MN was responsible for clinical care, characterization, and for overlooking material collection from all patients. CB aided in experimental design and provided the Eomes antibody used in initial experiments. AT was responsible for the Bioplex assays. KG contributed to experimental design and data analysis. WD designed the studies and overlooked all experiments and data analysis. All authors contributed to writing and reviewing the manuscript.

FUNDING

This work was supported by FAPEMIG (#Universal 2014), CNPq (#Universal 2015), INCT-DT, and NIAID-NIH (1R01AI138230-01). CK, MN, TS-S, CB, KG, and WD are CNPq fellows and EGAN is a CAPES fellow.

ACKNOWLEDGMENTS

The authors would like to thank all professionals involved in patient care at the Federal University of Minas Gerais.

SUPPLEMENTARY MATERIAL

The Supplementary Material for this article can be found online at: https://www.frontiersin.org/articles/10.3389/fcvm.2022.787423/full#supplementary-material

REFERENCES

1. Roth GA, Mensah GA, Johnson CO, Addolorato G, Ammirati E, Baddour LM, et al. Global burden of cardiovascular diseases and risk factors, 1990-2019: update from the GBD 2019 study. *J Am Coll Cardiol.* (2020) 76:2982–3021. doi: 10.1016/j.jacc.2020.11.010
2. Bocchi EA, Bestetti RB, Scanavacca MI, Cunha Neto E, Issa VS. Chronic chagas heart disease management: from etiology to cardiomyopathy treatment. *J Am Coll Cardiol.* (2017) 70:1510–24. doi: 10.1016/j.jacc.2017.08.004
3. Nunes MCP, Beaton A, Acquatella H, Bern C, Bolger AF, Echeverría LE, et al. Chagas cardiomyopathy: an update of current clinical knowledge and management: a scientific statement from the American Heart Association. *Circulation.* (2018) 138:e169–209. doi: 10.1161/CIR.0000000000000599
4. Rojas LZ, Glisic M, Pletsch-Borba L, Echeverría LE, Bramer WM, Bano A, et al. Electrocardiographic abnormalities in Chagas disease in the general population: a systematic review and meta-analysis. *PLoS Negl Trop Dis.* (2018) 12:e0006567. doi: 10.1371/journal.pntd.0006567
5. Torres RM, Correia D, Pereira C, Dutra WO, Talvani A, Sousa AS, et al. Prognosis of chronic Chagas heart disease and other pending clinical challenges. *Mem Inst Oswaldo Cruz.* (2021) 116:1–17.doi: 10.1590/0074-02760210172

6. Benziger CP, do Carmo GAL, Ribeiro ALP. Chagas cardiomyopathy: clinical presentation and management in the Americas. *Cardiol Clin.* (2017) 35:31–47. doi: 10.1016/j.ccl.2016.08.013
7. Bartsch SM, Avelis CM, Asti L, Hertenstein DL, Ndeffo-Mbah M, Galvani A, et al. The economic value of identifying and treating Chagas disease patients earlier and the impact on *Trypanosoma cruzi* transmission. *PLoS Negl Trop Dis.* (2018) 12:e0006809. doi: 10.1371/journal.pntd.0006809
8. Olivera MJ, Buitrago G. Economic costs of Chagas disease in Colombia in 2017: a social perspective. *Int J Infect Dis.* (2020) 91:196–201. doi: 10.1016/j.ijid.2019.11.022
9. Schultheiss HP, Fairweather DL, Caforio ALP, Escher F, Hershberger RE, Lipshultz SE, et al. Dilated cardiomyopathy. *Nat Rev Dis Prim.* (2019) 5:32. doi: 10.1038/s41572-019-0084-1
10. Barbosa MM, Rocha MOC, Botoni FA, Ribeiro ALP, Nunes MCP. Is atrial function in Chagas dilated cardiomyopathy more impaired than in idiopathic dilated cardiomyopathy? *Eur J Echocardiogr.* (2011) 12:643–7. doi: 10.1093/ejechocard/jer096
11. Santos OR, da Costa Rocha MO, de Almeida FR, da Cunha PFS, Souza SCS, Saad GP, et al. Speckle tracking echocardiographic deformation indices in Chagas and idiopathic dilated cardiomyopathy: incremental prognostic value of longitudinal strain. *PLoS ONE.* (2019) 14:e0221028. doi: 10.1371/journal.pone.0221028
12. Maron BJ, Towbin JA, Thiene G, Antzelevitch C, Corrado D, Arnett D, et al. Contemporary definitions and classification of the cardiomyopathies. *Circulation.* (2006) 113:1807–16. doi: 10.1161/CIRCULATIONAHA.106.174287
13. De Leeuw N, Ruiter DJ, Balk AHMM, De Jonge N, Melchers WJG, Galama JMD. Histopathologic findings in explanted heart tissue from patients with end-stage idiopathic dilated cardiomyopathy. *Transpl Int.* (2001) 14:299–306. doi: 10.1007/s001470100339
14. Bocchi EA, Fiorelli A. The paradox of survival results after heart transplantation for cardiomyopathy caused by *Trypanosoma cruzi*. *Ann Thorac Surg.* (2001) 71:1833–8. doi: 10.1016/S0003-4975(01)02587-5
15. Moreira LFP. II Diretriz Brasileira de Transplante Cardíaco. *Arq Bras Cardiol.* (2010) 95:1–2. doi: 10.1590/S0066-782X2010001100001
16. Hazebroek M, Dennert R, Heymans S. Idiopathic dilated cardiomyopathy: possible triggers and treatment strategies. *Netherlands Hear J.* (2012) 20:332–5. doi: 10.1007/s12471-012-0285-7
17. Kühl U, Pauschinger M, Noutsias M, Seeberg B, Bock T, Lassner D, et al. High prevalence of viral genomes and multiple viral infections in the myocardium of adults with "idiopathic" left ventricular dysfunction. *Circulation.* (2005) 111:887–93. doi: 10.1161/01.CIR.0000155616.07901.35
18. Pereira Nunes Mdo C, Barbosa MM, Ribeiro ALP, Fenelon LMA, Rocha MOC. Predictors of mortality in patients with dilated cardiomyopathy: relevance of Chagas disease as an etiological factor. *Rev Española Cardiol.* (2010) 63:788–97. doi: 10.1016/S1885-5857(10)70163-8
19. Barbosa AP, Cardinalli Neto A, Otaviano AP, Rocha BF, Bestetti RB. Comparison of outcome between Chagas cardiomyopathy and idiopathic dilated cardiomyopathy. *Arq Bras Cardiol.* (2011) 97:517–25. doi: 10.1590/S0066-782X2011005000112
20. Freitas HFG, Chizzola PR, Paes ÂT, Lima ACP, Mansur AJ. Risk stratification in a Brazilian hospital-based cohort of 1220 outpatients with heart failure: role of Chagas' heart disease. *Int J Cardiol.* (2005) 102:239–47. doi: 10.1016/j.ijcard.2004.05.025
21. Roever L, Chagas ACP. Editorial: cardiac remodeling: new insights in physiological and pathological. *Front Physiol.* (2017) 8:751. doi: 10.3389/fphys.2017.00751
22. Higuchi Mde L, Gutierrez PS, Aiello VD, Palomino S, Bocchi E, Kalil J, et al. Immunohistochemical characterization of infiltrating cells in human chronic chagasic myocarditis: comparison with myocardial rejection process. *Virchows Arch A Pathol Anat Histopathol.* (1993) 423:157–60. doi: 10.1007/BF01614765
23. Benvenuti LA, Higuchi ML, Reis MM. Upregulation of adhesion molecules and class I HLA in the myocardium of chronic chagasic cardiomyopathy and heart allograft rejection, but not in dilated cardiomyopathy. *Cardiovasc Pathol.* (2000) 9:111–7. doi: 10.1016/S1054-8807(00)00027-2
24. De Lourdes Higuchi M, Fukasawa S, De Brito T, Parzianello LC, Bellotti G, Ramires JAF. Different microcirculatory and interstitial matrix patterns in idiopathic dilated cardiomyopathy and Chagas' disease: a three dimensional confocal microscopy study. *Heart.* (1999) 82:279–85. doi: 10.1136/hrt.82.3.279
25. Mocelin AO, Issa VS, Bacal F, Guimarães GV, Cunha E, Bocchi EA. The influence of aetiology on inflammatory and neurohumoral activation in patients with severe heart failure: a prospective study comparing Chagas' heart disease and idiopathic dilated cardiomyopathy. *Eur J Heart Fail.* (2005) 7:869–73. doi: 10.1016/j.ejheart.2004.10.014
26. Cunha-Neto E, Nogueira LG, Teixeira PC, Ramasawmy R, Drigo SA, Goldberg AC, et al. Immunological and non-immunological effects of cytokines and chemokines in the pathogenesis of chronic Chagas disease cardiomyopathy. *Mem Inst Oswaldo Cruz.* (2009) 104:252–8. doi: 10.1590/S0074-02762009000900032
27. Gomes JAS, Bahia-Oliveira LMG, Rocha MOC, Busek SCU, Tekeira MM, Silva JS, et al. Type 1 chemokine receptor expression in Chagas' disease correlates with morbidity in cardiac patients. *Infect Immun.* (2005) 73:7960–6. doi: 10.1128/IAI.73.12.7960-7966.2005
28. de Miranda MB, de Melo AS, Almeida MS, Marinho SM, Oliveira Junior W, de Gomes YM. *Ex vivo* T-lymphocyte chemokine receptor phenotypes in patients with chronic Chagas disease. *Rev Soc Bras Med Trop.* (2017) 50:689–92. doi: 10.1590/0037-8682-0025-2017
29. Gomes JAS, Rocha MOC, Gazzinelli G, Fiocruz R. Evidence that development of severe cardiomyopathy in human Chagas' disease is due to a Th1-specific immune response. *Infect Immun.* (2003) 71:1185–93. doi: 10.1128/IAI.71.3.1185-1193.2003
30. Menezes CAS, Rocha MOC, Souza PEA, Chaves ACL, Gollob KJ, Dutra WO. Phenotypic and functional characteristics of CD28+ and CD28- cells from chagasic patients: distinct repertoire and cytokine expression. *Clin Exp Immunol.* (2004) 137:129–38. doi: 10.1111/j.1365-2249.2004.02479.x
31. Abel LCJ, Rizzo LV, Ianni B, Albuquerque F, Bacal F, Carrara D, et al. Chronic Chagas' disease cardiomyopathy patients display an increased IFN-γ response to *Trypanosoma cruzi* infection. *J Autoimmun.* (2001) 17:99–107. doi: 10.1006/jaut.2001.0523
32. Amaral Villani FN, Da Costa Rocha MO, Pereira Nunes MDC, Do Valle Antonelli LR, Dias Magalhães LM, Coelho Dos Santos JS, et al. *Trypanosoma cruzi*-induced activation of functionally distinct αβ and γδ CD4- CD8- T cells in individuals with polar forms of Chagas' disease. *Infect Immun.* (2010) 78:4421–30. doi: 10.1128/IAI.00179-10
33. Passos LSA, Magalhães LMD, Soares RP, Marques AF, Nunes MdCP, Gollob KJ, et al. Specific activation of CD4–CD8– double-negative T cells by Trypanosoma cruzi-derived glycolipids induces a proinflammatory profile associated with cardiomyopathy in Chagas patients. *Clin Exp Immunol.* (2017) 190:122–32. doi: 10.1111/cei.12992
34. Tschöpe C, Ammirati E, Bozkurt B, Caforio ALP, Cooper LT, Felix SB, et al. Myocarditis and inflammatory cardiomyopathy: current evidence and future directions. *Nat Rev Cardiol.* (2021) 18:169–93. doi: 10.1038/s41569-020-00435-x
35. Pappritz K, Savvatis K, Miteva K, Kerim B, Dong F, Fechner H, et al. Immunomodulation by adoptive regulatory T-cell transfer improves Coxsackievirus B3-induced myocarditis. *FASEB J.* (2018) 32:6066–78. doi: 10.1096/fj.201701408R
36. Elliott P, Andersson B, Arbustini E, Bilinska Z, Cecchi F, Charron P, et al. Classification of the cardiomyopathies: a position statement from the european society of cardiology working group on myocardial and pericardial diseases. *Eur Heart J.* (2008) 29:270–6. doi: 10.1093/eurheartj/ehm342
37. Bottrel RLA, Dutra WO, Martins FA, Gontijo B, Carvalho E, Barral-Netto M, et al. Flow cytometric determination of cellular sources and frequencies of key cytokine-producing lymphocytes directed against recombinant LACK and soluble leishmania antigen in human cutaneous leishmaniasis. *Infect Immun.* (2001) 69:3232–9. doi: 10.1128/IAI.69.5.3232-3239.2001
38. Laugier L, Frade AF, Ferreira FM, Baron MA, Teixeira PC, Cabantous S, et al. Whole-genome cardiac DNA methylation fingerprint and gene expression analysis provide new insights in the pathogenesis of chronic Chagas disease cardiomyopathy. *Clin Infect Dis.* (2017) 65:1103–11. doi: 10.1093/cid/cix506
39. Tsubakihara M, Allen PD, dos Remedios CG, Dzau V, Liew CC. *Data From: CardioChip Gene Expression Analysis of 50 Heart Failure Samples Including Eight Different Etiologies.* (2005). Available online at: https://www.ncbi.nlm.nih.gov/geo/query/acc.cgi?acc=GPL2041 (accessed August 10, 2021).

40. Metsalu T, Vilo J. ClustVis: a web tool for visualizing clustering of multivariate data using Principal Component Analysis and heatmap. *Nucleic Acids Res.* (2015) 43:W566–70. doi: 10.1093/nar/gkv468
41. Belkina AC, Ciccolella CO, Anno R, Halpert R, Snyder-cappione JE. stochastic neighbor embedding improve visualization and analysis of large datasets. *Nat Commun.* (2019) 10:1–12. doi: 10.1038/s41467-019-13055-y
42. Carlos Pinto Dias J, Novaes Ramos A, Dias Gontijo E, Luquetti A, Aparecida Shikanai-Yasuda M, Rodrigues Coura J, et al. II Consenso Brasileiro em Doença de Chagas, 2015. *Epidemiol Serviços Saúde.* (2016) 25:1–10. doi: 10.5123/S1679-49742016002100003
43. Bestetti RB, Muccillo G. Clinical course of chagas' heart disease: a comparison with dilated cardiomyopathy. *Int J Cardiol.* (1997) 60:187–93. doi: 10.1016/S0167-5273(97)00083-1
44. Chadalawada S, Rassi A, Samara O, Monzon A, Gudapati D, Vargas Barahona L, et al. Mortality risk in chronic Chagas cardiomyopathy: a systematic review and meta-analysis. *ESC Hear Fail.* (2021) 8:5466–81. doi: 10.1002/ehf2.13648
45. Reis DD, Jones EM, Tostes S, Lopes ER, Gazzinelli G, Colley DG, et al. Characterization of inflammatory infiltrates in chronic chagasic myocardial lesions: presence of tumor necrosis factor-α+ cells and dominance of granzyme A+, CD8+ lymphocytes. *Am J Trop Med Hyg.* (1993) 48:637–44. doi: 10.4269/ajtmh.1993.48.637
46. Bertulucci D, Rodrigues R, Antonia M, Romano A, Pereira DL, De Paula V, et al. *In situ* expression of regulatory cytokines by heart inflammatory cells in Chagas' disease patients with heart failure. *Clin Dev Immunol.* (2012) 2012:361730. doi: 10.1155/2012/361730
47. Dutra WO, Menezes CAS, Villani FNA, da Costa GC, da Silveira ABM, Reis DDÁ, et al. Cellular and genetic mechanisms involved in the generation of protective and pathogenic immune responses in human Chagas disease. *Mem Inst Oswaldo Cruz.* (2009) 104:208–18. doi: 10.1590/S0074-02762009000900027
48. Gómez-Olarte S, Bolaños NI, Echeverry M, Rodríguez AN, Cuéllar A, Puerta CJ, et al. Intermediate monocytes and cytokine production associated with severe forms of Chagas disease. *Front Immunol.* (2019) 10:1671. doi: 10.3389/fimmu.2019.01671
49. Rocha IH, Ferreira Marques AL, Moraes GV, Alves da Silva DA, da Silva MV, Rodrigues V, et al. Metabolic and immunological evaluation of patients with indeterminate and cardiac forms of Chagas disease. *Medicine.* (2020) 99:e23773. doi: 10.1097/MD.0000000000023773
50. Dutra WO, Gollob KJ, Gazzinelli G. Cytokine mRNA profile of peripheral blood mononuclear cells isolated from individuals with *Trypanosoma cruzi* chronic infection. Scand *J Immunol.* (1997) 45:74–80. doi: 10.1046/j.1365-3083.1997.d01-362.x
51. Sousa GR, Gomes JAS, Fares RCG, Damásio MPDS, Chaves AT, Ferreira KS, et al. Plasma cytokine expression is associated with cardiac morbidity in chagas disease. *PLoS ONE.* (2014) 9:e87082. doi: 10.1371/journal.pone.0087082
52. Salvador F, Sánchez-Montalvá A, Martínez-Gallo M, Sulleiro E, Franco-Jarava C, Avilés AS, et al. Serum IL-10 levels and its relationship with parasitemia in chronic Chagas disease patients. *Am J Trop Med Hyg.* (2020) 102:159–63. doi: 10.4269/ajtmh.19-0550
53. Neves EGA, Koh CC, Padilha da Silva JL, Passos LSA, Villani FNA, dos Santos JSC, et al. Systemic cytokines, chemokines and growth factors reveal specific and shared immunological characteristics in infectious cardiomyopathies. *Cytokine.* (2021) 148:155711. doi: 10.1016/j.cyto.2021.155711
54. Teixeira PC, Ducret A, Langen H, Nogoceke E, Santos RHB, Silva Nunes JP, et al. Impairment of multiple mitochondrial energy metabolism pathways in the heart of Chagas disease cardiomyopathy patients. *Front Immunol.* (2021) 12:755782. doi: 10.3389/fimmu.2021.755782
55. Wang Y, Wessel N, Kohse F, Khan A, Schultheiss H, Moreira MdCV, et al. Measurement of multiple cytokines for discrimination and risk stratification in patients with Chagas' disease and idiopathic dilated cardiomyopathy. *PLoS Negl Trop Dis.* (2021) 15:e0008906. doi: 10.1371/journal.pntd.0008906
56. Ouarhache M, Marquet S, Frade AF, Ferreira AM, Ianni B, Almeida RR, et al. Rare pathogenic variants in mitochondrial and inflammation-associated genes may lead to inflammatory cardiomyopathy in Chagas disease. *J Clin Immunol.* (2021) 41:1048–63. doi: 10.1007/s10875-021-01000-y
57. Dutra WO, Martins-Filho OA, Cancado JR, Pinto-Dias JC, Brener Z, Freeman GL, et al. Activated T and B lymphocytes in peripheral blood of patients with Chagas' disease. *Int Immunol.* (1994) 6:499–506. doi: 10.1093/intimm/6.4.499
58. Ueno A, Murasaki K, Hagiwara N, Kasanuki H. Increases in circulating T lymphocytes expressing HLA-DR and CD40 ligand in patients with dilated cardiomyophthy. *Heart Vessels.* (2007) 22:316–21. doi: 10.1007/s00380-007-0977-x
59. Efthimiadis I, Skendros P, Sarantopoulos A, Boura P. CD4+/DC25+T-lymphocytes and Th1/Th2 regulation in dilated cardiomyopahy. *Hippokratia.* (2011) 15:335–42.
60. Passos LSA, Koh CC, Magalhães LMD, Nunes MdCP, Gollob KJ, Dutra WO. Distinct CD4–CD8– (double-negative) memory T-cell subpopulations are associated with indeterminate and cardiac clinical forms of Chagas disease. *Front Immunol.* (2021) 12:761795. doi: 10.3389/fimmu.2021.761795
61. Llaguno M, Da Silva MV, Batista LR, Da Silva DAA, De Sousa RC, De Resende LAPR, et al. T-cell immunophenotyping and cytokine production analysis in patients with chagas disease 4 years after benznidazole treatment. *Infect Immun.* (2019) 87:1–11. doi: 10.1128/IAI.00103-19
62. Cunha-Neto E, Coelho V, Guilherme L, Fiorelli A, Stolf N, Kalil J. Autoimmunity in Chagas' disease: identification of cardiac myosin-B13 Trypanosoma cruzi protein crossreactive T cell clones in heart lesions of a chronic Chagas' cardiomyopathy patient. *J Clin Invest.* (1996) 98:1709–12. doi: 10.1172/JCI118969
63. De Bona E, Lidani KCF, Bavia L, Omidian Z, Gremski LH, Sandri TL, et al. Autoimmunity in chronic chagas disease: a road of multiple pathways to cardiomyopathy? *Front Immunol.* (2018) 9:1842. doi: 10.3389/fimmu.2018.01842
64. Bach-Elias M, Bahia D, Teixeira DC, Cicarelli RMB. Presence of autoantibodies against small nuclear ribonucleoprotein epitopes in Chagas' patients' sera. *Parasitol Res.* (1998) 84:796–9. doi: 10.1007/s004360050490
65. Benvenuti LA, Roggério A, Freitas HFG, Mansur AJ, Fiorelli A, Higuchi ML. Chronic American trypanosomiasis: parasite persistence in endomyocardial biopsies is associated with high-grade myocarditis. *Ann Trop Med Parasitol.* (2008) 102:481–7. doi: 10.1179/136485908X311740
66. Vago AR, Andrade LO, Leite AA, d'Ávila Reis D, Macedo AM, Adad SJ, et al. Genetic characterization of Trypanosoma cruzi directly from tissues of patients with chronic chagas disease: differential distribution of genetic types into diverse organs. *Am J Pathol.* (2000) 156:1805–9. doi: 10.1016/S0002-9440(10)65052-3
67. Holzinger C, Schöllhammer A, Imhof M, Reinwald C, Kramer G, Zuckermann A, et al. Phenotypic patterns of mononuclear cells in dilated cardiomyopathy. *Circulation.* (1995) 92:2876–85. doi: 10.1161/01.CIR.92.10.2876
68. Dotiwala F, Mulik S, Polidoro RB, Ansara JA, Burleigh BA, Walch M, et al. Killer lymphocytes use granulysin, perforin and granzymes to kill intracellular parasites. *Nat Med.* (2016) 22:210–6. doi: 10.1038/nm.4023
69. De Alencar BCG, Persechini PM, Haolla FA, De Oliveira G, Silverio JC, Lannes-Vieira J, et al. Perforin and gamma interferon expression are required for CD4+ and CD8+ T-cell-dependent protective immunity against a human parasite, Trypanosoma cruzi, elicited by heterologous plasmid DNA prime-recombinant adenovirus 5 boost vaccination. *Infect Immun.* (2009) 77:4383–95. doi: 10.1128/IAI.01459-08
70. Müller U, Sobek V, Balkow S, Hölscher C, Müllbacher A, Museteanu C, et al. Concerted action of perforin and granzymes is critical for the elimination of *Trypanosoma cruzi* from mouse tissues, but prevention of early host death is in addition dependent on the FasL/Fas pathway. *Eur J Immunol.* (2003) 33:70–8. doi: 10.1002/immu.200390009
71. Badorff C, Noutsias M, Kühl U, Schultheiss HP. Cell-mediated cytotoxicity in hearts with dilated cardiomyopathy: correlation with interstitial fibrosis and foci of activated T lymphocytes. *J Am Coll Cardiol.* (1997) 29:429–34. doi: 10.1016/S0735-1097(96)00475-5
72. Escher F, Kühl U, Lassner D, Stroux A, Gross U, Westermann D, et al. High perforin-positive cardiac cell infiltration and male sex predict adverse long-term mortality in patients with inflammatory cardiomyopathy. *J Am Heart Assoc.* (2017) 6:e005352. doi: 10.1161/JAHA.116.005352
73. Silverio JC, Pereira IR, Cipitelli MdC, Vinagre NF, Rodrigues MM, Gazzinelli RT, et al. CD8+ T-cells expressing interferon gamma or perforin play antagonistic roles in heart injury in experimental trypanosoma cruzi-elicited cardiomyopathy. *PLoS Pathog.* (2012) 8:e1002645. doi: 10.1371/journal.ppat.1002645

74. Santos-Zas I, Lemarié J, Zlatanova I, Cachanado M, Seghezzi JC, Benamer H, et al. Cytotoxic CD8+ T cells promote granzyme B-dependent adverse post-ischemic cardiac remodeling. *Nat Commun.* (2021) 12:1–13. doi: 10.1038/s41467-021-21737-9
75. Pearce EL. Control of effector CD8+ T cell function by the transcription factor eomesodermin. *Science.* (2003) 302:1041–3. doi: 10.1126/science.1090148
76. Takeuchi A, Saito T. CD4 CTL, a cytotoxic subset of CD4+T cells, their differentiation and function. *Front Immunol.* (2017) 8:194. doi: 10.3389/fimmu.2017.00194
77. Keesen TSL, Gomes JAS, Fares RCG, de Araújo FF, Ferreira KS, Chaves AT, et al. Characterization of CD4 + cytotoxic lymphocytes and apoptosis markers induced by *Trypanossoma cruzi* infection. *Scand J Immunol.* (2012) 76:311–9. doi: 10.1111/j.1365-3083.2012.02730.x
78. Serrán MG, Boari JT, Vernengo FF, Beccaría CG, Ramello MC, Bermejo DA, et al. Unconventional pro-inflammatory CD4+ T cell response in B cell-deficient mice infected with *Trypanosoma cruzi*. *Front Immunol.* (2017) 8:1548. doi: 10.3389/fimmu.2017.01548
79. Komarowska I, Coe D, Wang G, Haas R, Mauro C, Kishore M, et al. Hepatocyte growth factor receptor C-met instructs T cell cardiotropism and promotes T cell migration to the heart via autocrine chemokine release. *Immunity.* (2015) 42:1087–99. doi: 10.1016/j.immuni.2015.05.014
80. Benkhoucha M, Molnarfi N, Kaya G, Belnoue E, Bjarnadóttir K, Dietrich P, et al. Identification of a novel population of highly cytotoxic c-Met-expressing CD 8 $^{+}$ T lymphocytes. *EMBO Rep.* (2017) 18:1545–58. doi: 10.15252/embr.201744075
81. Machado FS, Koyama NS, Carregaro V, Ferreira BR, Milanezi CM, Teixeira MM, et al. CCR5 plays a critical role in the development of myocarditis and host protection in mice infected with *Trypanosoma cruzi*. *J Infect Dis.* (2005) 191:627–36. doi: 10.1086/427515
82. Kroll-palhares K, Silvério JC, Alice A, Michailowsky V, Marino AP, Silva NM, et al. TNF / TNFR1 signaling up-regulates CCR5 expression by CD8 + T lymphocytes and promotes heart tissue damage during *Trypanosoma cruzi* infection : beneficial effects of TNF-a blockade. *Mem Inst Oswaldo Cruz.* (2008) 103:375–85. doi: 10.1590/S0074-02762008000400011
83. Juiz NA, Estupiñán E, Hernández D, Garcilazo A, Chadi R, Morales Sanfurgo G, et al. Association study between CCR2-CCR5 genes polymorphisms and chronic Chagas heart disease in Wichi and in admixed populations from Argentina. *PLoS Negl Trop Dis.* (2019) 13:e0007033. doi: 10.1371/journal.pntd.0007033
84. Roffe E, Dos Santos LI, Santos MO, Henriques PM, Teixeira-Carvalho A, Martins-Filho OA, et al. Increased frequencies of circulating CCR5+ memory T cells are correlated to chronic chagasic cardiomyopathy progression. *J Leukoc Biol.* (2019) 106:641–52. doi: 10.1002/JLB.MA1118-472R
85. Medeiros GA, Silvério JC, Marino APMP, Roffê E, Vieira V, Kroll-Palhares K, et al. Treatment of chronically Trypanosoma cruzi-infected mice with a CCR1/CCR5 antagonist (Met-RANTES) results in amelioration of cardiac tissue damage. *Microbes Infect.* (2009) 11:264–73. doi: 10.1016/j.micinf.2008.11.012
86. Hüser N, Tertilt C, Gerauer K, Maier S, Traeger T, Aßfalg V, et al. CCR4-deficient mice show prolonged graft survival in a chronic cardiac transplant rejection model. *Eur J Immunol.* (2005) 35:128–38. doi: 10.1002/eji.200324745
87. Altara R, Mallat Z, Booz GW, Zouein FA. The CXCL10/CXCR3 axis and cardiac inflammation: implications for immunotherapy to treat infectious and noninfectious diseases of the heart. *J Immunol Res.* (2016) 2016:4396368. doi: 10.1155/2016/4396368
88. Altara R, Manca M, Brandão RD, Zeidan A, Booz GW, Zouein FA. Emerging importance of chemokine receptor CXCR3 and its ligands in cardiovascular diseases. *Clin Sci.* (2016) 130:463–78. doi: 10.1042/CS20150666
89. Fernandes JL, Mamoni RL, Orford JL, Garcia C, Selwyn AP, Coelho OR, et al. Increased Th1 activity in patients with coronary artery disease. *Cytokine.* (2004) 26:131–7. doi: 10.1016/j.cyto.2004.01.007
90. Mo WX, Yin SS, Chen H, Zhou C, Zhou JX, Zhao LD, et al. Chemotaxis of Vδ 2 T cells to the joints contributes to the pathogenesis of rheumatoid arthritis. *Ann Rheum Dis.* (2017) 76:2075–84. doi: 10.1136/annrheumdis-2016-211069
91. Koren L, Barash U, Zohar Y, Karin N, Aronheim A. The cardiac maladaptive ATF3-dependent cross-talk between cardiomyocytes and macrophages is mediated by the IFNγ-CXCL10-CXCR3 axis. *Int J Cardiol.* (2017) 228:394–400. doi: 10.1016/j.ijcard.2016.11.159
92. Zhang Y, Xia M, Jin K, Wang S, Wei H, Fan C, et al. Function of the c-Met receptor tyrosine kinase in carcinogenesis and associated therapeutic opportunities. *Mol Cancer.* (2018) 17:1–14. doi: 10.1186/s12943-017-0753-1
93. Gallo S, Sala V, Gatti S, Crepaldi T. HGF/Met axis in heart function and cardioprotection. *Biomedicines.* (2014) 2:247–62. doi: 10.3390/biomedicines2040247

Conflict of Interest: The authors declare that the research was conducted in the absence of any commercial or financial relationships that could be construed as a potential conflict of interest.

The reviewer JS declared a shared affiliation with one of the authors AT, to the handling editor at time of review.

Publisher's Note: All claims expressed in this article are solely those of the authors and do not necessarily represent those of their affiliated organizations, or those of the publisher, the editors and the reviewers. Any product that may be evaluated in this article, or claim that may be made by its manufacturer, is not guaranteed or endorsed by the publisher.

frontiers in Cardiovascular Medicine

ORIGINAL RESEARCH
published: 11 March 2022
doi: 10.3389/fcvm.2022.783974

Sex Differences in Cardiac Pathology of SARS-CoV2 Infected and *Trypanosoma cruzi* Co-infected Mice

*Dhanya Dhanyalayam†, Hariprasad Thangavel†, Kezia Lizardo†, Neelam Oswal, Enriko Dolgov, David S. Perlin and Jyothi F. Nagajyothi**

Center for Discovery and Innovation, Hackensack Meridian Health, Nutley, NJ, United States

Coronavirus disease-2019 (COVID-19) caused by Severe Acute Respiratory Syndrome Coronavirus 2 (SARS-CoV-2; CoV2) is a deadly contagious infectious disease. For those who survive COVID-19, post-COVID cardiac damage greatly increases the risk of cardiomyopathy and heart failure. Currently, the number of COVID-related cases are increasing in Latin America, where a major COVID comorbidity is Chagas' heart disease, which is caused by the parasite *Trypanosoma cruzi*. However, the interplay between indeterminate Chagas disease and COVID-19 is unknown. We investigated the effect of CoV2 infection on heart pathology in *T. cruzi* infected mice (coinfected with CoV2 during the indeterminate stage of *T. cruzi* infection). We used transgenic human angiotensin-converting enzyme 2 (huACE2/hACE2) mice infected with CoV2, *T. cruzi*, or coinfected with both in this study. We found that the viral load in the hearts of coinfected mice is lower compared to the hearts of mice infected with CoV2 alone. We demonstrated that CoV2 infection significantly alters cardiac immune and energy signaling via adiponectin (C-ApN) and AMP-activated protein kinase (AMPK) signaling. Our studies also showed that increased β-adrenergic receptor (b-AR) and peroxisome proliferator-activated receptors (PPARs) play a major role in shifting the energy balance in the hearts of coinfected female mice from glycolysis to mitochondrial β-oxidation. Our findings suggest that cardiac metabolic signaling may differently regulate the pathogenesis of Chagas cardiomyopathy (CCM) in coinfected mice. We conclude that the C-ApN/AMPK and b-AR/PPAR downstream signaling may play major roles in determining the progression, severity, and phenotype of CCM and heart failure in the context of COVID.

Keywords: Chagas' heart disease, CoV2 infection, inflammation, cardiomyopathy, adiponectin, mitochondrial oxidation, energy metabolism, glycolysis

OPEN ACCESS

Edited by:
Maria Nunes, Federal University of Minas Gerais, Brazil

Reviewed by:
Ana Carolina Leão, Baylor College of Medicine, United States
Zhengyuan Xia, The University of Hong Kong, Hong Kong SAR, China

***Correspondence:**
Jyothi F. Nagajyothi
Jyothi.Nagajyothi@HMH-CDI.org

†These authors have contributed equally to this work

Specialty section:
This article was submitted to General Cardiovascular Medicine, a section of the journal Frontiers in Cardiovascular Medicine

Received: *27 September 2021*
Accepted: *11 February 2022*
Published: *11 March 2022*

Citation:
Dhanyalayam D, Thangavel H, Lizardo K, Oswal N, Dolgov E, Perlin DS and Nagajyothi JF (2022) Sex Differences in Cardiac Pathology of SARS-CoV2 Infected and Trypanosoma cruzi Co-infected Mice. Front. Cardiovasc. Med. 9:783974. doi: 10.3389/fcvm.2022.783974

INTRODUCTION

COVID-19 illness, caused by severe acute respiratory syndrome coronavirus 2 (SARS-CoV-2; CoV2), results in debilitating disease manifestations in many infected people and increases mortality in people with comorbidities, including heart disease (1–6). The causes of death in COVID-19 patients include cardiomyopathy, stroke, cardiac arrest, sepsis, and organ failure (7–10). Furthermore, post-COVID patients exhibit various degrees of cardiac damage, which may cause debilitating long-term effects on heart function (11–13). Thus, the post-COVID effect may pose

a major threat for the development of cardiomyopathy and heart failure, especially in individuals with pre-existing heart conditions.

Although currently deaths due to COVID-19 are subsiding in many countries due to vaccination (14), COVID-19 is still a major threat in Latin America, where a major COVID-19 comorbidity is Chagas Disease (CD). CD is caused by the parasite *Trypanosoma cruzi*, which infects an estimated eight million people in Latin America and is also increasingly found in non-endemic countries, including 300,000 infected individuals in the United States (15). Of these chronically infected individuals, 30% will develop chronic Chagas cardiomyopathy (CCM) and congestive heart failure, which are significant causes of morbidity and mortality (16). Thus, vulnerable COVID-19 patients with CD constitute a major health burden in the Americas. In addition, the post-COVID effect on CCM in CD patients could create a health crisis in Latin America during the post-COVID era since hundreds of thousands of asymptomatic (indeterminate) CD patients likely already have or will contract COVID-19. A recent clinical registry data study from Brazil suggests that Chagas disease and SARS-CoV-2 coinfection do not lead to worse in-hospital outcomes (17). In another case study, the authors reported that COVID-19 infected CD patients ($n = 2$) presented with a rapid disease progression, and despite all efforts of the medical team, both patients died (18). These authors also suggested that COVID-19 may lead to lymphopenia, which could curb the anti–*T. cruzi* immune response and increase the risk of death in coinfected patients (18). However, there is limited clinical data or information from animal models on the interplay between indeterminate/asymptomatic CD and COVID susceptibility, severity, risk of mortality, and long-term effects on heart pathology in post-COVID CD patients.

Recent clinical meta-analysis data for COVID-19 suggest that male sex is independently associated with hospitalization, ICU admissions, need for vasopressors or endotracheal intubation and mortality (19). Many clinical studies have also reported that males have a higher mortality rate due to Chagas' heart disease (20, 21). Male CD patients are also at higher risk for myocardial fibrosis and more severe ventricular remodeling (21). However, the role of sex differences in the interactions between COVID and CD is unknown.

In the present pilot study, we investigated the effect of CoV2 infection on heart metabolism and pathogenesis in mice with indeterminate stage *T. cruzi* infection. We used huACE2 mice (male and female) infected with CoV2, *T. cruzi*, or coinfected with both. Our results show that the pulmonary pathology in coinfected male mice was significantly reduced compared to CoV2 infected male mice and the viral load in the lungs of coinfected mice was reduced compared to CoV2 infected mice. We also show the presence of CoV2 in the hearts of infected mice and that the viral load was significantly reduced in the lungs of coinfected mice compared to mice infected with CoV2 alone. Our data show no difference in heart viral loads between the male and female coinfected mice. However, our data demonstrate a significant difference in the effect of CoV2 infection on cardiac adipogenic metabolism, inflammation, energy metabolism, and mitochondrial functions between male and female coinfected mice compared to their respective control groups. Our data suggest that adiponectin-AMP-activated protein kinase (C-ApN-AMPK) signaling and peroxisome proliferator-activated receptor (PPARγ and PPARα) signaling dominates in the hearts of coinfected mice. At the same time, high level β-adrenergic receptor (b-AR) activity in the hearts of female coinfected mice shifts the energy metabolic pathways toward lipid β-oxidation pathway and is likely responsible for sex differences in the pathogenesis of post-COVID dilated cardiomyopathy, cardiac atrophy and heart failure.

MATERIALS AND METHODS

Biosafety

All aspects of this study were approved by the Institutional Animal Care and Use and Institutional Biosafety Committee of Center for Discovery and Innovation of Hackensack University Medical Center (IACUC 282) and adhere to the National Research Council guidelines.

Animal Model and Experimental Design

The transgenic mice expressing the human angiotensin-converting enzyme 2 (huACE2) (Jackson Laboratories, Bar Harbor, ME) were bred at Hackensack Meridian Health - Center for Discovery and Innovation (CDI). The Brazil strain of *T. cruzi* was maintained by passage in C3H/HeJ mice (Jackson Laboratories, Bar Harbor, ME). Both male and female mice ($N = 16$) were intraperitoneally (i.p.) infected with 10^3 trypomastigotes at 6 weeks of age. Mice were maintained on a 12-h light/dark cycles and housed in groups of 3–5 per cage with unlimited access to water and chow. Once they reached indeterminate stage (22) (65 DPI; no circulating parasitemia and pro-inflammatory markers), one set of mice was coinfected intra-nasally with 1 x 10^4 pfu SARS-CoV2 (NR-52281, Isolate USA-WA1/2020 COV-2 virus, NIH-BEI resources). After 10 DPI CoV2 (i.e., 75 DPI *T. cruzi* infection), we collected samples (heart, lungs, white adipose tissue (WAT) and blood; $n = 4$/sex/subset). Age and sex matched huACE2 mice infected with SARS-CoV2 alone, as well as uninfected huACE2 mice, served as controls (**Supplementary Figure 1**). The heart samples were used in the present study.

Immunoblot Analysis

Tissue lysates were prepared as previously described (22). Each sample containing 30 μg of protein were resolved on SDS-PAGE and separately on native gel electrophoresis and the proteins were transferred to nitrocellulose membrane for immunoblot analysis. Adiponectin-specific mouse monoclonal antibody (#ab22554, Abcam), AdipoR1-specific rabbit polyclonal antibody (#ab70362, Abcam), AdipoR2-specific rabbit polyclonal antibody (#ABT12, Sigma-Aldrich), PPARα-specific rabbit polyclonal antibody (#PA1-822A, Thermo Fisher Scientific), PPARγ-specific rabbit polyclonal antibody (#2492, Cell Signaling Technology), pAMPK-specific rabbit monoclonal antibody (#2535S, Cell Signaling Technology), Cytochrome C-specific rabbit monoclonal antibody (#4280S, Cell Signaling Technology), Superoxide

dismutase 1-specific mouse monoclonal antibody (#4266S, Cell Signaling Technology), Hexokinase 2-specific rabbit monoclonal antibody (#2867S, Cell Signaling Technology), β1 adrenergic receptor-specific rabbit polyclonal antibody (#12271S, Cell Signaling Technology), F4/80-specific rat monoclonal antibody (#NB 600-404, Novus Biologicals), TNFα-specific rabbit polyclonal antibody (#ab6671, Abcam), pHSL (Ser563)-specific rabbit monoclonal antibody(#4139, Cell Signaling Technology), ATGL-specific rabbit monoclonal antibody(#30A4, Cell Signaling Technology, Perilipin-specific rabbit monoclonal antibody (#D1D8, Cell Signaling Technology), IFNγ-specific rabbit monoclonal antibody (#EPR1108, Abcam), CD4-specific rabbit polyclonal antibody (#NBP1-19371, Novus biologicals), CD8-specific rabbit polyclonal antibody(#NBP2-29475, Novus biologicals), T-cadherin-specific rabbit polyclonal antibody (#ABT121, Millipore), FABP4-specific rabbit monoclonal antibody (#3544, Cell Signaling Technology), IL6-specific mouse monoclonal antibody (#66146-1-lg, Proteintech), IL10-specific rabbit polyclonal antibody (#20850-1-AP, Proteintech), BNIP3-specific rabbit monoclonal antibody (#44060, Cell Signaling Technology), Caspase 3-specific rabbit polyclonal antibody (#9662, Cell Signaling Technology) were used as primary antibodies. Horseradish peroxidase (HRP)-conjugated anti-mouse immunoglobulin (#7076, Cell Signaling Technology) or HRP-conjugated anti-rabbit immunoglobulin (#7074, Cell Signaling Technology) antibody was used to detect specific protein bands (as shown in the figure legends) using a chemiluminescence system. β-actin-specific rabbit monoclonal antibody (#4970S, Cell Signaling Technology) or Guanosine nucleotide dissociation inhibitor (GDI) (#71-0300, Invitrogen) were used as protein loading controls.

Determination of Parasite (*T. cruzi*) Load in the Tissue

A quantitative real time polymerase chain reaction (q-RT-PCR) was used to quantify the parasite load by using PCR SYBR Green Master Mix (Roche, Applied Science, CT) containing $MgCl_2$ by employing QuantStudio 3 Real Time PCR system (Thermo Fisher). DNA isolation, preparation of standard curve and qPCR analysis was performed as previously published (23).

Determination of SARS-CoV-2 Load in the Tissue

Total RNA was isolated from the hearts using Trizol reagent. The number of SARS-COV-2 copies were quantified using 2019-nCoV_N2 primer/probe mix and One-Step PrimeScript RT-PCR kit from Takara Bio Inc. All assays were performed on Agilent AriaMx Real-time PCR System according to the following cycling conditions: 15 min at 42 °C (1 cycle, reverse transcription), followed by 10 sec at 95 °C (1 cycle, hot start) and continuing with 5 s at 95 °C, and 30 s at 55°C (40 cycles, PCR amplification).

Histological and Morphometric Analysis of the Heart

The hearts were harvested immediately after sacrificing the mice. The hearts were cut 5 mm above the apex in cross section through the ventricles, fixed in formaldehyde, analyzed by histological staining as described earlier (24). Hematoxylin and eosin (H&E) and Masson's trichrome staining were performed, and the images were captured and analyzed as previously described (25). Four to six sections of each heart were scored blindly. For each myocardial sample, histologic evidence of myocarditis and inflammation was classified in terms of degree of infiltration of immune cells, fibrosis and accumulation of lipid droplets in capillaries was graded on a five-point scale ranging from 0 to 4+. A zero-score indicated lowest or negligible changes and 4 the most damaged state. The cardiomyocyte cell size in the heart sections was analyzed by counting the number of cardiomyocyte nucleus/5 images/heart section (40 x images of H&E stained heart sections). We performed morphometric analysis as described earlier (24). Briefly, the H&E sections of the hearts were used to analyze the thickness of the left ventricular wall (LVW), right ventricular wall (RVW) and the intra-septal wall (24). The thickness of the LVW, RVW and septal wall was measured at five different locations at a magnification of 10x (24). The average value of the 5 measurements was calculated for each mouse.

Right Ventricle Hypertrophy

Myocyte profiles in cross section were selected for the analysis of myocyte size adjacent to the inner wall of the right ventricles from the microscopic images of Masson-Trichrome sections (**Supplementary Figure 3**). The cardiomyocytes have a prolate spheroid shape. Cardiomyocyte length (Dmaj) and diameter (Dmin) were measured on digitized images of tissue slices stained with trichrome stain as reported earlier (**Supplementary Figure 3C**) (26, 27). Each cell was recognized based on the intercellular collagen network. A total of 40 cells/sex/group were measured and the mean of the cell volume was calculated using the web-based tool [https://www.easycalculation.com/shapes/surface-area-of-prolate-spheroid.php].

Histological Analysis of the Lungs

Freshly isolated lung tissues were fixed with 10% neutral-buffered formalin for a minimum of 48 h and then embedded in paraffin wax (n = 4/sex). Hematoxylin and eosin (H&E) staining was performed, and the images were captured as previously published (25). Four to six sections of each lung were scored blindly. For each lung sections, the histological evidence of pulmonary pathology was classified in terms of the presence of infiltration of immune cells, granulomas, accumulation of lipid droplets and fibrosis as published earlier (23, 25).

Immunohistochemical Analysis of Perilipin and Phospho-Perilipin

Freshly isolated heart tissues were fixed with 10% neutral-buffered formalin for a minimum of 48 h and then embedded in paraffin wax (n = 4/sex) and sectioned for immunohistochemical analysis (IHC). IHC was performed using perilipin and phospho-perilipin specific antibody with a dilution of 1:100 followed by corresponding HRP-conjugated goat anti-rabbit or anti-mouse immunoglobulin as previously described (23, 25). The positive

staining intensities of the images were quantified using NIH-Image J software for a minimum of 5 images of each heart (23).

Statistical Analysis

Statistical analysis was performed using GraphPad Prism (GraphPad Software, Inc., La Jolla, CA, USA). We performed statistical analysis by comparing the data between the infected groups (CoV2/*T. cruzi*/coinfection) and uninfected control groups. For the coinfection group, since the baseline is mice infected with *T. cruzi*, we also performed statistical data analysis and fold change analysis by comparing the data between the coinfected groups and *T. cruzi* infected groups. Comparisons between groups were made using Two-Way ANOVA (GraphPad) and unpaired Student's *t*-test (Microsoft Excel) as appropriate. Values of $p < 0.05$ were considered statistically significant. Data represent means ± S.E.M.

RESULTS

We developed indeterminate CD model by infecting one set of hACE2 mice with a low dose (1000 parasite) of *Trypanosoma cruzi* (22). At 65 DPI, *T. cruzi* infected mice showed no parasitemia or significant changes in inflammatory markers in blood (data not shown). We analyzed the parasite load in the hearts of *T. cruzi* infected and coinfected mice by qPCR and detected 1.5–3 pg of *T. cruzi* DNA/ng of host DNA (23). We found no significant difference in the parasite load in the hearts between male and female, and *T. cruzi* infected and coinfected mice. To investigate the pathological effects of CoV2 infection on the hearts in *T. cruzi* compromised mice, we performed histological and biochemical analyses of heart and lung samples obtained from the following three different murine models of infections: the *T. cruzi* model (infected with *T. cruzi*), the CoV2 model (infected with SARS-CoV2), and the coinfection model [infected with *T. cruzi* followed by SARS-CoV2 infection at the indeterminate stage (65DPI)]. Uninfected mice served as controls. We used $n = 8$ mice/group for both sexes. We observed no mortality during CoV2 infection in mice with or without *T. cruzi* infection. During the histological analysis of the lung and heart samples, we observed a significant difference in their pathology between the sexes. Therefore, we analyzed all the data separately for males and females in each group as presented below.

Asymptomatic *T. cruzi* Infection Modulates Pulmonary Pathology During CoV2 Infection in huACE2 Mice

We and others have shown that *T. cruzi* infection alters immune and metabolic signaling in mice during acute and chronic stages (28, 29). Here, we analyzed whether asymptomatic (indeterminate stage) *T. cruzi* infection-induced immune and metabolic changes regulate pulmonary pathology in intranasally CoV2 infected huACE2 mice 10 days post-CoV2 infection. Histological analysis of H&E stained lung sections of uninfected (control), CoV2 infected (positive control), *T. cruzi* infected, and coinfected mice were analyzed for infiltrated immune cells, accumulated lipid droplets, fibrosis, and granulomas (**Figure 1A**). Histological analysis showed significantly increased infiltrated immune cells and lipid droplets in the lungs of *T. cruzi* infected mice compared to uninfected mice (**Figures 1A,B**). The alveolar space was more constrained and interstitial tissue thickened in male *T. cruzi* infected mice compared to female T. *cruzi* mice. CoV2 infection also significantly increased infiltration of immune cells and lipid droplets in the lungs compared to uninfected mice (sex and age matched). However, the number of granulomas and their size were greater in male CoV2 mice compared to female CoV2 mice. Interestingly, both the number and size of granulomas were greater in the lungs of female coinfected mice than in male coinfected mice. For both sexes, we observed vascular leakage (hemosiderin) and neutrophilic alveolitis in the lungs in CoV2/coinfected mice. These analyses demonstrated that: (i) the pulmonary pathology in coinfection is reduced compared to CoV2 infection alone; and (ii) although males are more susceptible to severe pulmonary CoV2 infection in general, in the context of *T. cruzi* coinfection females are more susceptible to severe pulmonary CoV2 infection compared to males.

Asymptomatic *T. cruzi* Infection Reduces Viral Burden in the Lungs of huACE2 Mice Coinfected With SARS-CoV2

ACE2 is a known receptor for the cell entry of SARS-CoV2 (30, 31). It has been shown that ACE2 expression levels were positively associated with immune signatures and no significant difference in their levels between males and females or between younger and older persons in any tissue (32). Since *T. cruzi* infection can alter the immune signature, we analyzed the effect of *T. cruzi* infection on the expression levels of ACE2 in the lungs and hearts by Western blotting (**Figure 2A**). As expected, CoV2 infection significantly increased ACE2 levels in the lungs in huACE2 mice in both males ($p \leq 0.0001$) and females ($p \leq 0.01$) compared to uninfected sex-matched mice (**Figure 2A**). The levels of ACE2 were significantly higher ($p \leq 0.001$) in the lungs of both male and female *T.cruzi* infected mice compared to sex matched control mice (**Figure 2A**). CoV2 infection further significantly increased ($p \leq 0.01$) the levels of ACE2 in the lungs of both males and females in coinfected mice (**Figure 2A**). Our data showed a significant increase in ACE2 levels in the lungs of coinfected mice compared to only CoV2 infected mice (**Figure 2A**). We observed no difference in the levels of ACE2 in the lungs between the sexes in coinfected mice. In the hearts, in uninfected female mice, the levels of ACE2 were significantly lower ($p \leq 0.01$) compared to uninfected male mice (**Figure 2A**). CoV2 infection significantly increased ACE2 levels in the hearts of male ($p \leq 0.05$) mice. *T. cruzi* infection did not significantly alter the levels of ACE2 in the hearts of male and female mice compared to sex matched uninfected control mice. ACE2 levels in the hearts significantly increased in coinfected male ($p \leq 0.01$) and coinfected female ($p \leq 0.0001$) mice compared to sex matched *T. cruzi* infected mice, and significantly increased only in coinfected female mice ($p \leq 0.0001$) compared to sex matched uninfected mice. These data suggest that ACE2 is highly

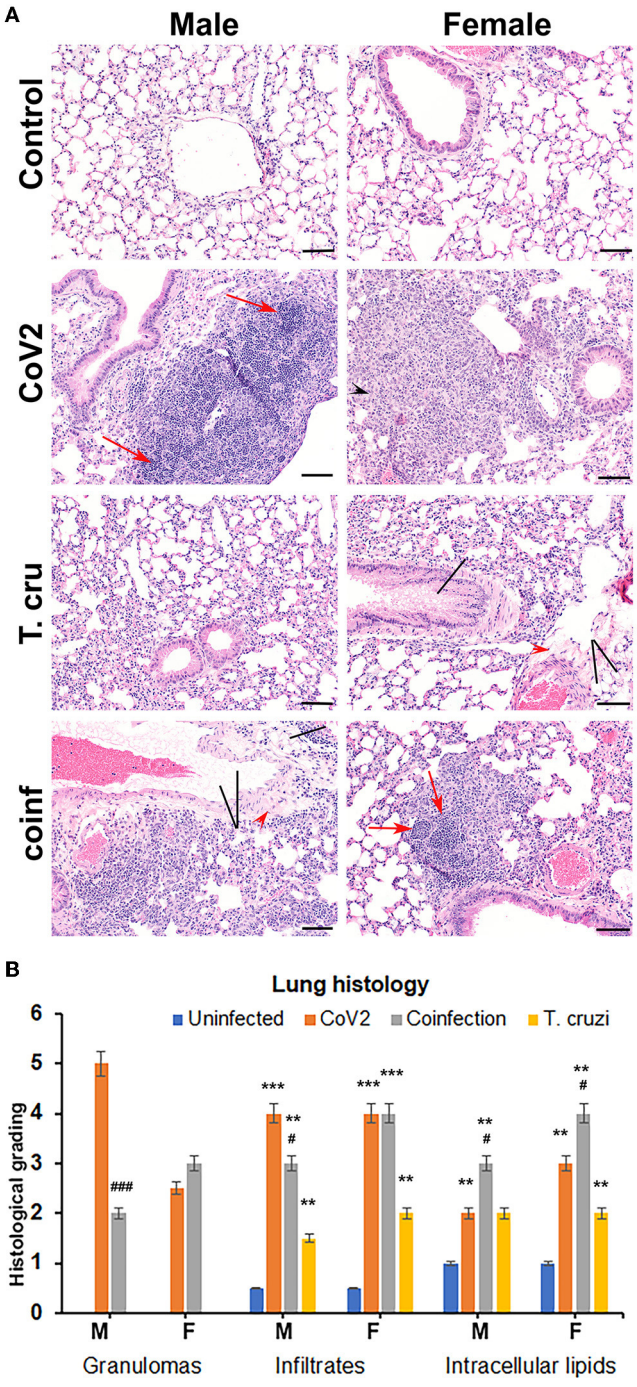

FIGURE 1 | *T. cruzi* infection modulates pulmonary pathology in CoV2 infected huACE2 mice. **(A)** H&E stained lung sections ($n = 4$/sex, a minimum of five images/section were analyzed) of both male and female uninfected, CoV2 infected, *T. cruzi* infected, and coinfected huACE2 mice showing infiltrated immune cells (black arrowhead), accumulated lipid droplets (black line), fibrosis (red arrowhead), and granulomas (red arrow) (20x magnification, bar-200μm). **(B)** Histological grading of lung pathology was carried out according to experimental groups and classified in terms of granulomas (numbers), infiltrated immune cells, and accumulated lipid droplets. Each class was

(Continued)

FIGURE 1 | graded on a 6-point scale ranging from 0 to 5 as discussed in Materials and Methods. Values plotted are mean ± standard error (SE) from $n = 5$. The error bars represent the standard error of the mean. $^{**}P < 0.01$ and $^{***}P < 0.001$, between the indicated groups and uninfected mice. $^{\#}p \leq 0.05$ and $^{\#\#\#}p \leq 0.001$ for comparisons between CoV2 infected and co-infected mice.

expressed in the lungs of coinfected male and female mice and in the hearts of coinfected female mice compared to CoV2 infected (male/female) mice.

Lung viral loads quantitated by qPCR analysis were significantly greater ($p \leq 0.01$) in male CoV2 infected mice compared to female CoV2 infected mice (**Figure 2B**). Interestingly, although ACE2 levels were significantly higher in the lungs of male coinfected mice compared to male CoV2 infected mice (**Figure 2A**), the viral load in the lungs of male coinfected mice was significantly lower ($p \leq 0.001$) compared to male CoV2 mice (**Figure 2B**). Between coinfected males and females, the viral load in the lungs of female mice was significantly higher ($p \leq 0.01$) compared to male mice (**Figure 2B**). However, the viral load in the lungs of coinfected female mice was not significantly altered compared to CoV2 infected female mice. These data suggest that males are likely more susceptible to pulmonary CoV2 infection in general, but that females may be more susceptible to pulmonary CoV2 infection in the context of CD. ACE2 levels were either similar (in males) or significantly greater (in females) in coinfected mice compared to CoV2 infected male or female mice (**Figure 2A**). However, the viral load was significantly lower in the hearts of coinfected male and female mice (4.7-fold and 3.6-fold, respectively, $p \leq 0.001$) compared to CoV2 infected male and female mice (**Figure 2B**). These data suggest that: (i) CoV2 infects myocardium in huACE2 mice infected intranasally with SARS-CoV2 and (ii) indeterminate stage *T. cruzi* infection reduces the viral load in the heart during CoV2 infection.

Sex Dependent Morphological Changes in the Hearts of Mice Infected With CoV2, *T. cruzi*, and Coinfection

We have shown that CoV2 infects and persists in the hearts of intra-nasally infected mice (**Figure 2B**). Histological analysis of the hearts was performed using H&E (**Figure 3A**) and Masson-trichrome (**Figure 3B**) stained sections as described in Materials and Methods. Microscopic analysis of the heart sections of CoV2 infected mice demonstrated the presence of infiltrated immune cells, increased accumulation of lipid droplets in the capillaries, enlarged cardiomyocyte nuclei, and increased fibrosis compared to control mice (**Figures 3A,B** and **Supplementary Figure 2**). The H&E sections showed significantly reduced cytoplasmic coloration in LV of female coinfected mice compared to their sex matched counterparts (**Figure 3A**), which is an indication of reduced intracellular protein levels. H&E sections of the hearts showed the presence of myocytes with significantly increased cell size in LV in coinfected male mice compared to coinfected female mice and

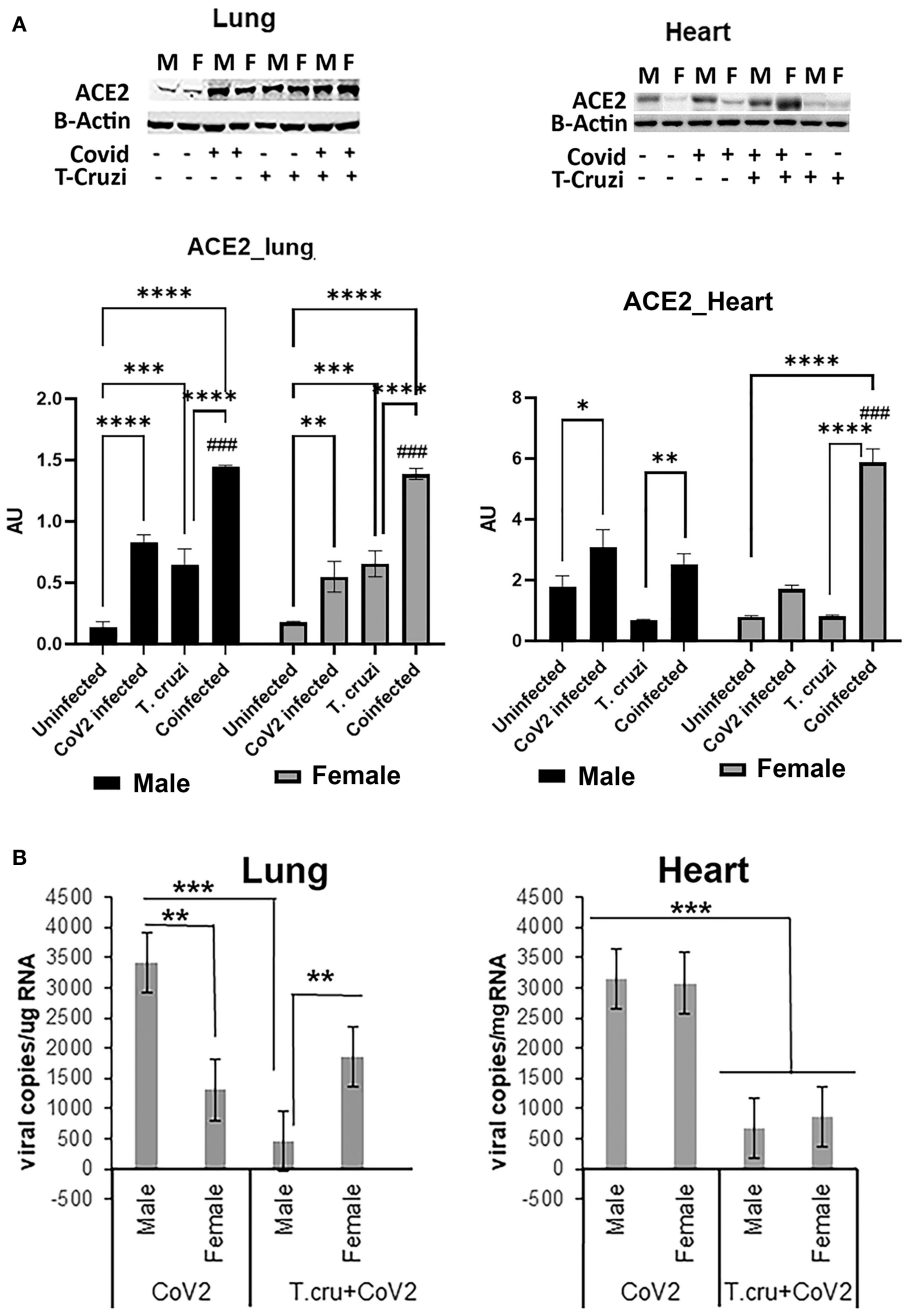

FIGURE 2 | Changes in ACE2 levels and viral load in the lungs and hearts of CoV2 infected, *T. cruzi* infected, and coinfected hACE2 mice. **(A)** Immunoblot analysis (upper panel) of ACE2 in the lungs (left) and hearts (right). GDI was used as loading control. Fold changes in the protein levels of ACE2 were normalized to GDI expression and are shown as a bar graph (A dot plot displaying individual data point is shown in **Supplementary Figure 4**). The error bars represent standard error of the mean. $^{*}p < 0.05$, $^{**}p < 0.01$, $^{***}p < 0.001$ and $^{****}p < 0.0001$ compared to uninfected sex matched mice ($n = 4$/sex/group) ($^{\#\#\#}p < 0.001$ for comparisons between CoV2 infected and coinfected mice). **(B)** Number of viral copies/μg of RNA in the lungs (left) and hearts (right) quantitated by qPCR in male and female CoV2 and coinfected mice. The error bars represent standard error of the mean ($^{**}p \leq 0.01$ and $^{***}p \leq 0.001$) (M, male; F, female).

also compared to uninfected mice (**Supplementary Figure 3** and **Supplementary Table 1A**). In RV, we measured the major (D_{maj}) and minor (D_{min}) cardiomyocyte dimensions and calculated cardiomyocyte volume, assuming a cell shape in the form of prolate ellipsoid (**Supplementary Figures 3B,C**) as discussed in Methods (26, 27). The histological measurements showed that the cardiomyocytes volume was significantly higher in RV ($p \leq 0.001$ males: and $p \leq 0.01$ females) of coinfected mice compared to uninfected mice (**Supplementary Tables 1A,B**). We also measured interstitial fibrosis and extracellular space expansion in RV using the microscopic images of Trichrome sections (data not shown) (**Supplementary Figure 3**). The collagen layer in

the extracellular space was significantly expanded ($p \leq 0.05$) in coinfected males compared to coinfected females. These data suggest that cardiomyocytes size significantly increased in male coinfected mice compared to female coinfected mice, however, the extracellular membrane space significantly disintegrated in between the cardiomyocytes in coinfected female mice compared to coinfected male mice. These data further indicate that coinfected male mice display a hypertrophied cardiomyocyte phenotype and the female coinfected mice display an atrophied cardiomyocyte phenotype. The male coinfected mice showed significantly elevated fibrosis compared to female coinfected mice (**Figure 3B**). The levels of accumulated lipid droplets in the capillaries, infiltrated immune cells and fibrosis in RV in male coinfected mice were significantly greater compared to female coinfected mice (**Figure 3C** and **Supplementary Figure 2**).

The changes in cardiomyocyte size affect the size of the hearts (**Supplementary Figure 3**). Therefore, we performed the morphometric analysis of the hearts as described in Materials and Methods. The thickness of the left ventricular wall (LVW), right ventricular wall (RVW) and septal wall (SW) differed between males and females and infected and coinfected mice compared to sex matched control mice (**Supplementary Table 1B**). LVW thickness significantly decreased in female mice singly infected with CoV2 or *T. cruzi* compared to female control mice; however, no significant difference was observed in female coinfected mice. LVW thickness in male CoV2/*T. cruzi* singly infected and coinfected mice showed no significant differences compared to male control mice. RVW thickness significantly decreased in female control mice compared to male control mice, and it was further decreased in female coinfected mice. Interestingly, the thickness of RVW was significantly reduced in male coinfected mice compared to male *T. cruzi* infected mice, which was not observed for female coinfected and *T. cruzi* infected mice. SW thickness increased in female CoV2 mice and was inversely proportional to the decreased LVW thickness compared to female control mice.

CoV2 Infection Alters Cardiac Lipid Metabolism Differently in Male and Female huACE2 Mice With and Without Indeterminate *T. cruzi* Infection

Earlier we demonstrated that *T. cruzi* infection causes increased cardiac lipid accumulation, which elevates cardiac mitochondrial and endoplasmic dysfunction (33, 34). We performed immunohistochemistry (IHC) staining of perilipin (lipid droplet associated protein) and phospho-perilipin (marker of break-down of lipid droplets) to analyze the levels of micro-lipid droplets in the myocardium (**Figure 4**). The IHC analysis showed significantly increased ($p \leq 0.001$) levels of perilipin and significantly decreased ($p \leq 0.001$) levels of phospho-perilipin in the myocardium of *T. cruzi* infected mice compared to uninfected mice. However, in the myocardium of coinfected mice, the levels of perilipin significantly decreased ($p \leq 0.001$) compared to *T. cruzi* infected mice, suggesting that accumulated lipid droplets in the cardiomyocytes were used up during the CoV2 infection (**Figure 4**). The levels of perilipin also increased in the myocardium of CoV2 infected mice compared to uninfected mice (**Figure 4**). Interestingly, male CoV2 mice showed significantly greater ($p \leq 0.01$) levels of phospho-perilipin compared to female CoV2 mice, which is similar to the myocardium of coinfected mice (**Figure 4**). These data suggest that the myocardium uses accumulated lipids rapidly during CoV2 infection; however, the rate of lipid catabolism may differ between males and females.

CoV2 Infection Alters Cardiac Adiponectin (C-ApN) Levels and Adiponectin (ApN) Signaling in the Hearts in Coinfected Mice

We detected no change in parasite load in the heart between *T. cruzi* and coinfected mice (data not shown); however, we observed significant heart morphological changes, including accumulation of lipid droplets (**Figures 3**, **4**). Because adiponectin and it's signaling are associated with adipogenesis and lipid oxidation, we examined and quantified the levels of adipogenic markers such as adiponectin (ApN) and its receptors in the hearts by Western blotting in coinfected and CoV2 infected mice and compared with *T. cruzi* infected and uninfected mice (**Figure 5**). We measured the levels of cardiac high-molecular weight ApN (C-HMW ApN), a.k.a. its anti-inflammatory/anti-fibrotic/metabolically active form (35, 36) by native gel (**Figure 5A**). Previously we showed a strong correlation between C-ApN levels and progression of cardiomyopathy during CD, wherein elevated levels of C-ApN were associated with mortality due to cardiac dilation (22). As expected, the levels of C-HMW ApN significantly ($p \leq 0.0001$) increased in the hearts of *T. cruzi* infected mice both in males and females compared to sex matched uninfected mice. However, although the levels of C-HMW ApN significantly increased ($p \leq 0.0001$) in coinfected male mice compared to uninfected male mice, no significant difference was observed compared to *T. cruzi* infected male mice (**Figure 5A**). In female coinfected mice, the levels of C-HMW ApN significantly decreased ($p \leq 0.05$) compared to *T. cruzi* infected female mice; however, these levels were still significantly increased ($p \leq 0.01$) compared to uninfected female mice (**Figure 5A**). CoV2 infection did not alter C-HMW-ApN levels in either male or female mice. These data indicate that the levels of anti-inflammatory C-HMW-ApN are high in the hearts of *T. cruzi* infected and coinfected mice and significantly elevated in male mice compared to female mice. The regulatory actions of ApN are mainly mediated by its receptors Adiponectin-R1 and -R2 (Adipo R1 and R2) and T-cadherin (37–39). We found that the levels of AdipoR1, AdipoR2 and T-cadherin were significantly altered in the hearts between the sexes and infections (**Figure 5B**). In particular, the levels of R1 significantly increased in CoV2 ($p \leq 0.01$) and coinfected ($p \leq 0.0001$) male mice compared to their sex matched controls (**Figure 5B**). In females, AdipoR1 significantly increased ($p \leq 0.0001$) only in the hearts of CoV2 infected (not in coinfected female mice) compared to uninfected female mice (**Figure 5B**). Between males and females AdipoR1 significantly ($p \leq 0.05$) increased in female uninfected and CoV2 infected

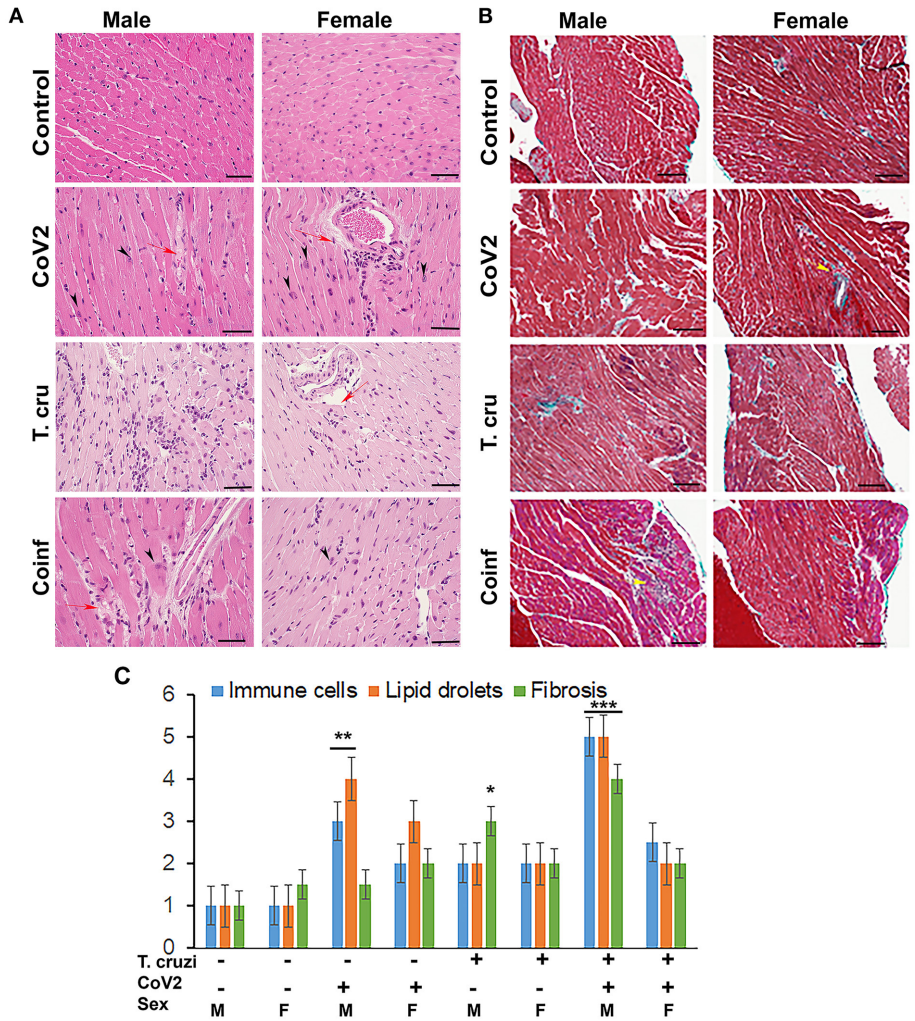

FIGURE 3 | Histology of the myocardium of uninfected, CoV2 infected, *T. cruzi* infected, and coinfected huACE2 mice ($n = 4$/sex, a minimum of five images/section were analyzed). **(A)** H&E stained sections of left ventricles showing the accumulation of lipid droplets in the capillaries (red arrow) and presence of enlarged cardiomyocyte nuclei (black arrowhead) in infected mice (20x magnification). **(B)** Masson-trichrome stained sections of right ventricles showing fibrosis (blue and purple) and the presence of immune cells (yellow arrows) in the right ventricles (RV) of infected/coinfected mice (20x magnification; bar – 100 μm) (Additional images are shown in **Supplementary Figures 2, 3**). **(C)** Histological grading of heart sections showing the levels of immune infiltrates, lipid droplet accumulation, and fibrosis among CoV2 infected, *T. cruzi* infected, and coinfected mice compared to uninfected mice in both sexes. The error bars represent standard error of the mean. $^{*}p < 0.05$, $^{**}p < 0.01$ and $^{***}p < 0.001$ compared with uninfected sex matched mice (M, male; F, female).

female mice compared to their male counterparts; however, it was significantly reduced ($p \leq 0.05$) in coinfected female mice compared to coinfected male mice. The levels of AdipoR2 significantly decreased ($p \leq 0.01$) in CoV2 infected male and female mice compared to their sex matched uninfected mice (**Figure 5B**). The levels of AdipoR2 also significantly decreased ($p \leq 0.05$) in female coinfected mice compared to female uninfected mice. Interestingly, the levels of AdopoR2 were significantly reduced in female mice (uninfected and infected (*T. cruzi*/CoV2/coinfected) compared to their respective male mice (**Figure 5B**). Another ApN receptor, T-cadherin, significantly increased ($p \leq 0.001$) only in female CoV2 infected mice compared to uninfected mice. Taken together, these data suggest that C-HMW ApN may regulate anti-inflammatory and metabolic signaling in the hearts of coinfected male mice via AdipoR1.

Cardiac Immune Signaling Differs Between Male and Female Coinfected and CoV2 Infected Mice

Because we observed significant changes in the levels of HMW adiponectin in the hearts during infection, which may affect immune signaling, we analyzed the levels of infiltrated macrophages and the levels of proinflammatory TNFα in the hearts by immunoblot analysis (**Figure 6A**). The cardiac levels of F4/80 significantly increased in CoV2 infected ($p \leq 0.01$) and coinfected ($p \leq 0.0001$) male mice compared to sex

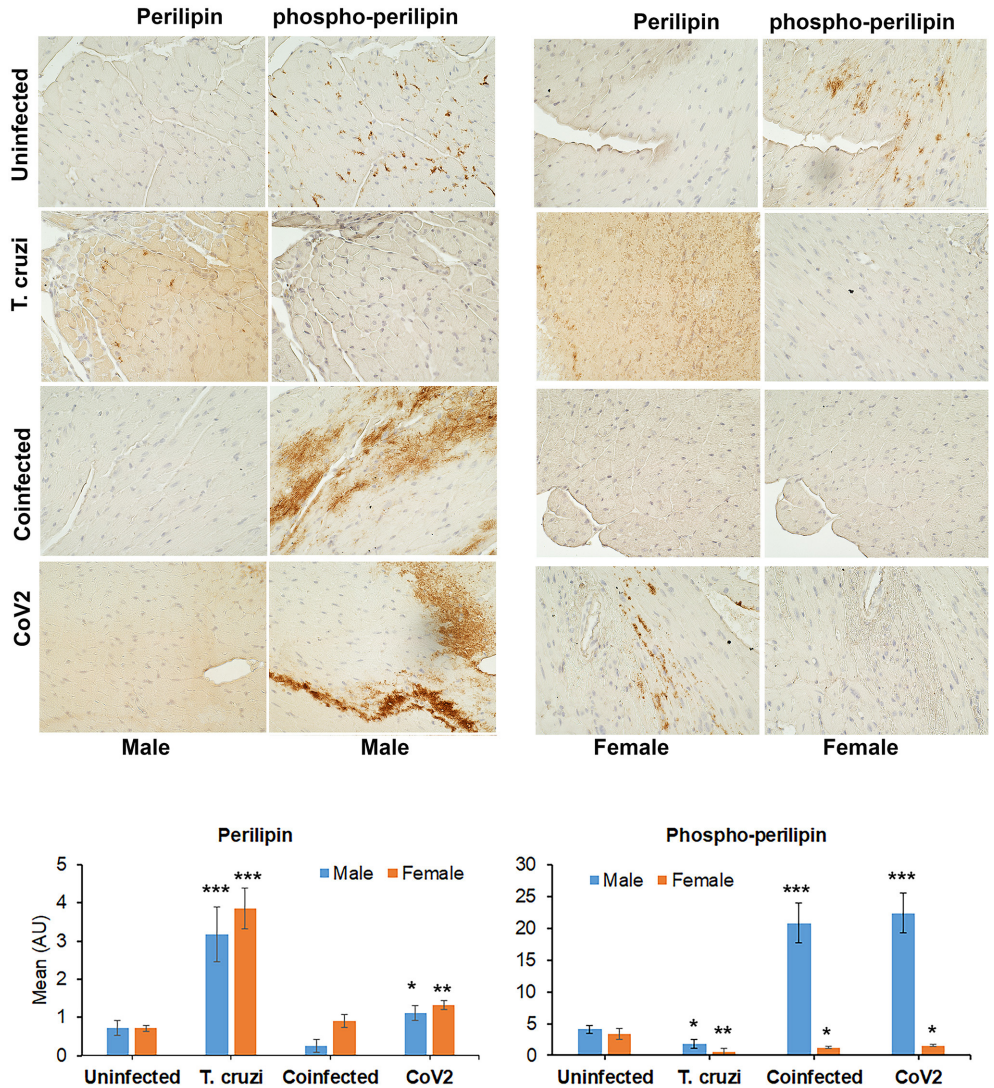

FIGURE 4 | Immunohistochemistry staining (top panel) of huACE2 mouse myocardium using anti-perilipin (left) and anti-phospho-perilipin (right) antibody. The stained sections show altered levels of perilipin and phospho-perilipin during indeterminate *T. cruzi* infection and coinfection in both male and female mice compared to uninfected and CoV2 infected mice. IHC staining intensity (bottom panel) was analyzed using ImageJ software. Positive staining intensities of perilipin and phospho-perilipin were calculated and plotted separately ($n = 4$ mice, a minimum of five images/section were analyzed). The error bars represent standard error of the mean. *$p < 0.05$, **$p < 0.01$ and ***$p < 0.001$ compared with uninfected sex matched mice (M, male; F, female).

matched uninfected mice. The levels of F4/80 significantly increased ($p \leq 0.01$) in the hearts of coinfected male mice compared to CoV2 singly infected male mice (**Figures 6A,B**), suggesting significant infiltration of macrophages in the hearts of coinfected male mice (but not in coinfected female mice). The levels of F4/80 significantly increased ($p \leq 0.05$) in singly CoV2-infected and coinfected males compared to singly CoV2-infected and coinfected females (**Figures 6A,B**). Interestingly, the cardiac levels of TNFα significantly increased ($p \leq 0.0001$) in CoV2 infected male mice but not in CoV2 infected female mice compared to their respective sex matched uninfected mice (**Figures 6A,C**). The cardiac levels of TNFα significantly decreased ($p \leq 0.001$) in coinfected male mice compared to CoV2 infected male mice (**Figures 6A,C**). These data suggested that although the levels of infiltrated immune cells are increased in the hearts of male coinfected mice during CoV2 infection, the levels of pro-inflammatory TNF are decreased, which may be due to the increased levels of cardiac HMW adiponectin that can regulate macrophage activation (36, 40).

CoV2 Infection Differently Alters Cardiac Lipid and Glucose Metabolism in the Hearts of Coinfected Male and Female Mice

ApN regulates glucose (AMPK/glycolysis) and lipid (PPARs) metabolism (41–44). Therefore, we analyzed heart levels of pAMPK and hexokinase II (HK) as markers of glucose

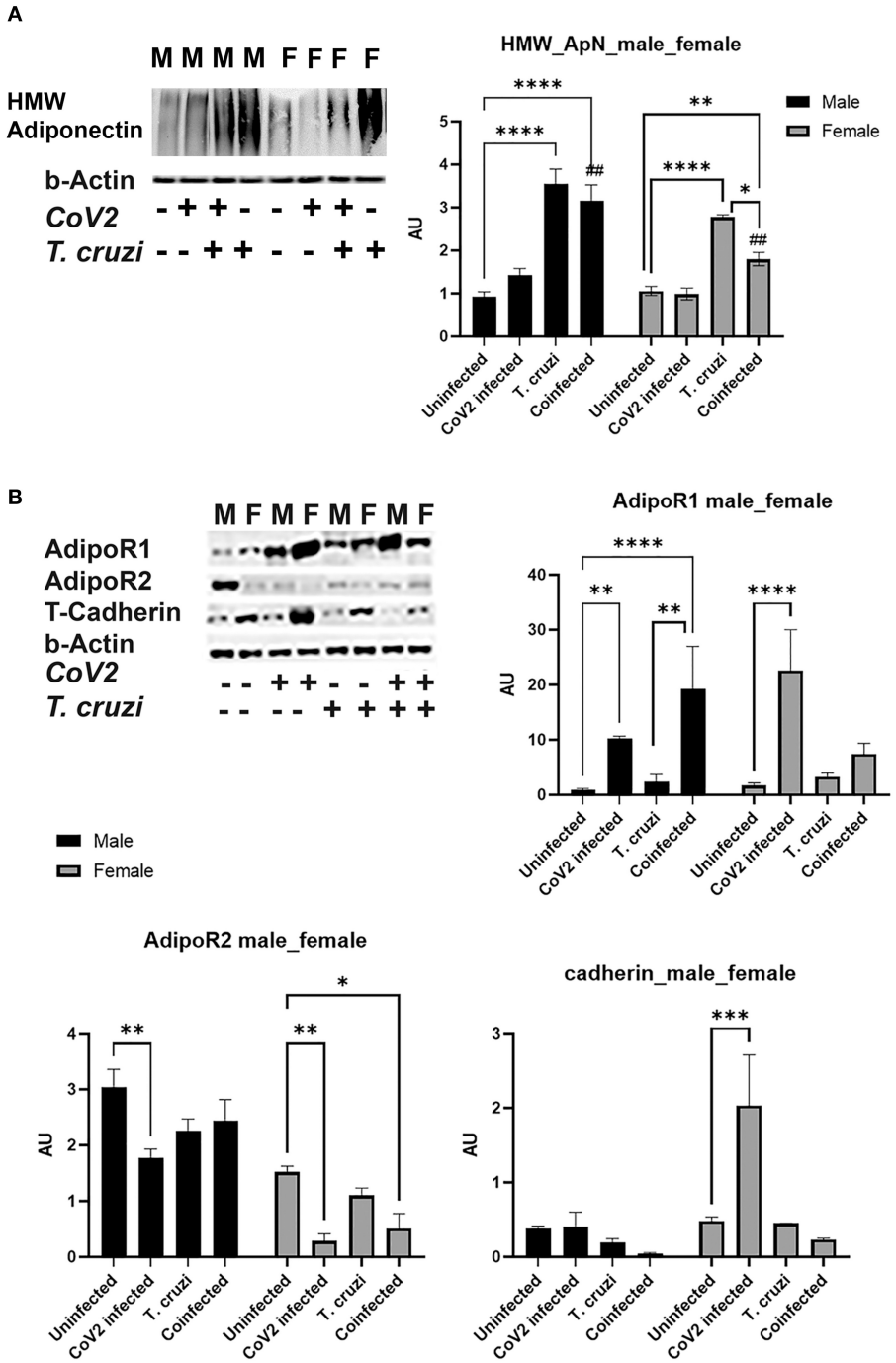

FIGURE 5 | Immunoblot analysis of adipogenic markers in the hearts of Cov2 infected, *T. cruzi* infected, and coinfected huACE2 mice. Western blot images of **(A)** cardiac high-molecular weight adiponectin (HMW ApN) and **(B)** ApN receptors (Adipo R1, R2 and T-cadherin). β-Actin was used as loading control. Fold-changes in the protein levels of adipogenic markers normalized to β-Actin are shown as bar graphs. (A dot plot displaying individual data point is shown in **Supplementary Figure 4**). The error bars represent standard error of the mean. $^{*}p < 0.05$, $^{**}p < 0.01$, $^{***}p < 0.001$ and $^{****}p < 0.0001$ compared to uninfected sex matched mice ($n = 4$/sex/group) ($^{\#\#}p \leq 0.01$ for comparisons between CoV2 infected and coinfected mice) (M, male; F, female).

metabolism and PPARα and PPARγ as markers of lipid oxidation and lipogenesis, respectively (**Figure 7**). Western blotting analysis demonstrated significantly increased pAMPK ($p \leq 0.0001$) in the hearts of coinfected male and female mice compared to their respective sex matched uninfected controls (**Figure 7A**). Another marker of glycolysis, hexokinase-2

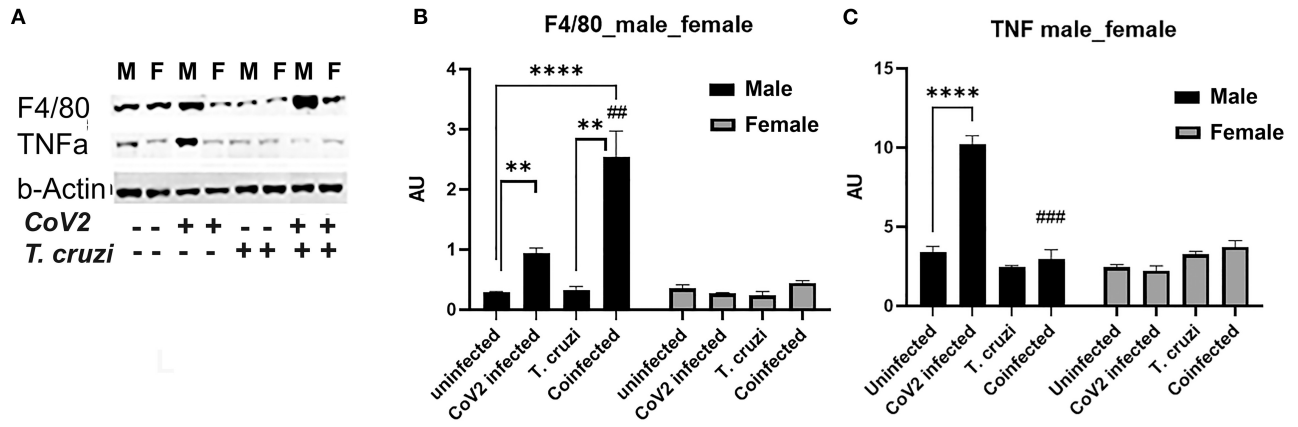

FIGURE 6 | Immunoblot analysis of inflammatory markers in the hearts of CoV2 infected, *T. cruzi* infected, and coinfected huACE2 mice. Western blot images **(A)** of macrophage marker (F4/80) and proinflammatory cytokine TNFα. β-Actin was used as loading control. Fold changes in the protein levels of F4/80 **(B)** and TNFα **(C)** were normalized to β-Actin expression and are shown as bar graphs (A dot plot displaying individual data point presented in **Supplementary Figure 4**). The error bars represent standard error of the mean. $^{**}p < 0.01$ and $^{****}p < 0.0001$ compared to uninfected sex matched mice ($n = 4$/sex/group). ($^{\#\#}p \leq 0.01$, and $^{\#\#\#}p \leq 0.001$ for comparisons between CoV2 infected and coinfected mice) (M, male; F, female).

(HK2), significantly increased in coinfected male mice ($p \leq 0.001$) and significantly decreased in coinfected female mice compared to sex matched uninfected mice (**Figure 7A**). These data suggest that glycolysis is significantly increased in coinfected male mice and significantly decreased in coinfected female mice. Infection with CoV2 alone significantly increased pAMPK ($p \leq 0.0001$) only in male mice (compared to uninfected male mice), and its levels were significantly reduced ($p \leq 0.0001$) in CoV2 infected female mice compared to CoV2 infected male mice (**Figure 7A**). The levels of HK also significantly decreased ($p \leq 0.0001$) in CoV2 infected female mice compared to CoV2 infected male mice. These data suggest that, in general during CoV2 infections, the myocardium of male mice shifts their energy resources toward glycolysis, whereas the myocardium of female mice shuts down the glycolysis pathway.

ApN/AMPK signaling also regulates lipid metabolism. Western blotting analysis demonstrated significantly increased PPARα in the hearts of both coinfected male ($p \leq 0.0001$) and coinfected female ($p \leq 0.0001$) mice compared to sex matched uninfected mice. However, the levels of PPARα in the hearts of coinfected female mice was significantly higher ($p \leq 0.0001$) compared to coinfected male mice. CoV2 infection alone also significantly increased ($p \leq 0.05$) cardiac PPARα levels in male mice compared to uninfected male mice (**Figure 7B**). The cardiac levels of PPARγ significantly increased ($p \leq 0.0001$) only in coinfected female mice compared to uninfected female mice and other groups (**Figure 7B**). These data suggest that both lipogenesis and lipid oxidation dominate in the hearts of coinfected female mice, and that these hearts mainly depend on lipid oxidation and utilization as their energy resource during CoV2 infection, whereas coinfected male mice hearts may utilize both glucose and lipids as sources of energy.

Beta-Adrenergic Receptors Play a Major Role in the Hearts of Coinfected Female Mice

Beta-adrenergic receptors (b-AR) are implicated in various heart diseases (45, 46), and several studies have demonstrated that chronic *T. cruzi* infection causes dysfunctional b-AR signaling in the hearts in Chagas' mouse models (47–49). Increased b-AR activity causes lipolysis resulting in the release of free fatty acids and their derivatives, which are the ligands for PPARα and PPARγ (50–52). PPARα is involved in fatty acid oxidation, whereas PPARγ is implicated in lipogenesis (53–56). Our data also indicated that increased PPARα and PPARγ expression in the hearts of female coinfected mice may be induced via a different mechanism and not via the HMW-ApN-AMPK axis (**Figure 7**). Because b-AR are highly sensitive to estrogen (57–59), we investigated whether b-AR play an important role in inducing PPAR levels in female mice by Western blotting analysis (**Figure 8**). We observed significantly increased ($p \leq 0.05$) b-AR in female uninfected mice compared to male uninfected mice, indicating that females may be more sensitive to b-AR stimulation. The levels of b-AR significantly increased in the hearts of coinfected mice both in males ($p \leq 0.0001$) and females ($p \leq 0.001$) compared to their sex matched uninfected mice (**Figure 8A**). However, the levels of b-AR significantly increased ($p \leq 0.0001$) in the hearts of coinfected female mice compared to coinfected male mice, suggesting that in female coinfected mice b-AR activation may significantly increase cardiac lipolysis and lipid metabolism (**Figures 7**, **8A**).

The cardiac levels of PPARγ and PPARα significantly increased ($p \leq 0.0001$) in coinfected female mice compared to coinfected male mice and other groups (**Figure 7**). Because increased PPARs may elevate lipid mitochondrial β-oxidation, we analyzed the levels of Cytochrome C (Cyto) and superoxide

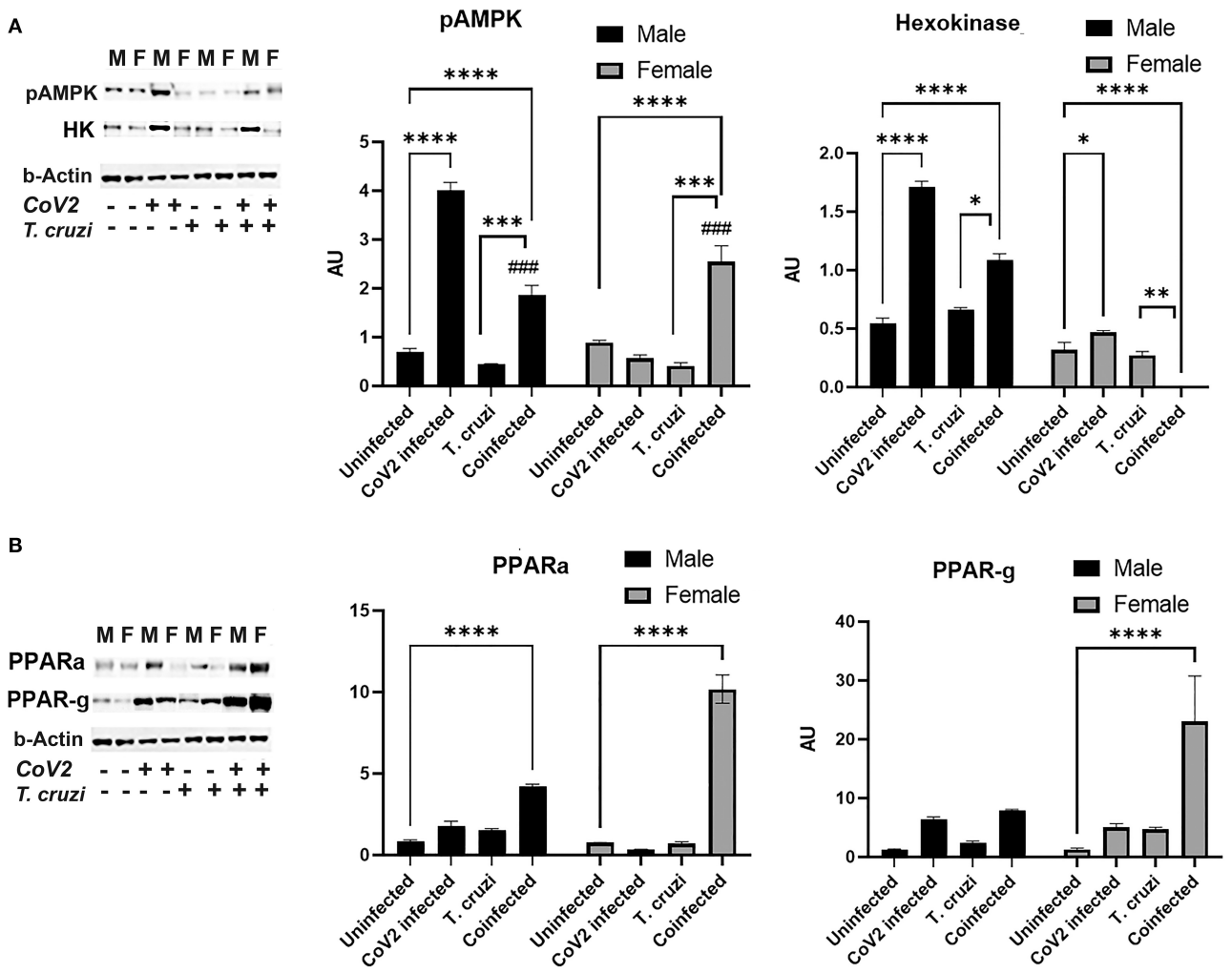

FIGURE 7 | Immunoblot analysis of markers of glucose and lipid metabolism in the hearts of CoV2 infected, *T. cruzi* infected, and coinfected huACE2 mice. Immunoblot images of **(A)** markers of glucose metabolism (pAMPK and hexokinase II) and **(B)** markers of lipid metabolism (PPARα and PPARγ). β-Actin was used as loading control. Fold changes in the protein levels normalized to β-Actin are shown as bar graphs (A dot plot displaying individual data points is presented in **Supplementary Figure 4**). The error bars represent standard error of the mean. $^{*}p < 0.05$, $^{**}p < 0.01$, $^{***}p < 0.001$ and $^{****}p < 0.0001$ compared to uninfected sex matched mice ($n = 4$/sex/group) ($^{\#\#\#}p \leq 0.001$ for comparisons between CoV2 infected and coinfected mice) (M, male; F, female).

dismutase (SOD) (**Figure 8A**). Western blotting analysis showed a significant increase in Cyto ($p \leq 0.05$) and SOD ($p \leq 0.0001$) in the hearts of coinfected male mice and a significant increase in Cyto ($p \leq 0.0001$) but a significant decrease in SOD ($p \leq 0.05$) in the hearts of coinfected female mice compared to their respective sex matched uninfected mice (**Figures 8B,C**). In fact, the levels of Cyto significantly increased ($p \leq 0.0001$) in the hearts of coinfected female mice compared to coinfected male mice, suggesting greater levels of mitochondrial oxidative phosphorylation in the hearts of coinfected female mice. *T. cruzi* infected mice (both males and females) showed significantly increased SOD ($p \leq 0.0001$) in the hearts during the indeterminate stage compared to uninfected mice. Together, these data suggested that lipid catabolism and oxidation are higher in female hearts compared to male hearts in coinfected mice, which may prevent the progression of cardiac dilation due to intracellular lipotoxicity (60), but may also cause increased oxidative stress. The reduced levels of SOD in the hearts in coinfected female mice also suggest increased oxidative stress and mitochondrial dysfunction in these mice. Increased mitochondrial dysfunction is associated with cachexia and atrophy (61, 62). On the other hand, in coinfected males, the cardiac accumulation of HMW-ApN and AMPK activation may increase glycolysis and also adipogenesis, which may cause lipotoxicity leading to cardiac steatosis, hypertrophy and early dilated cardiomyopathy in post-COVID mice.

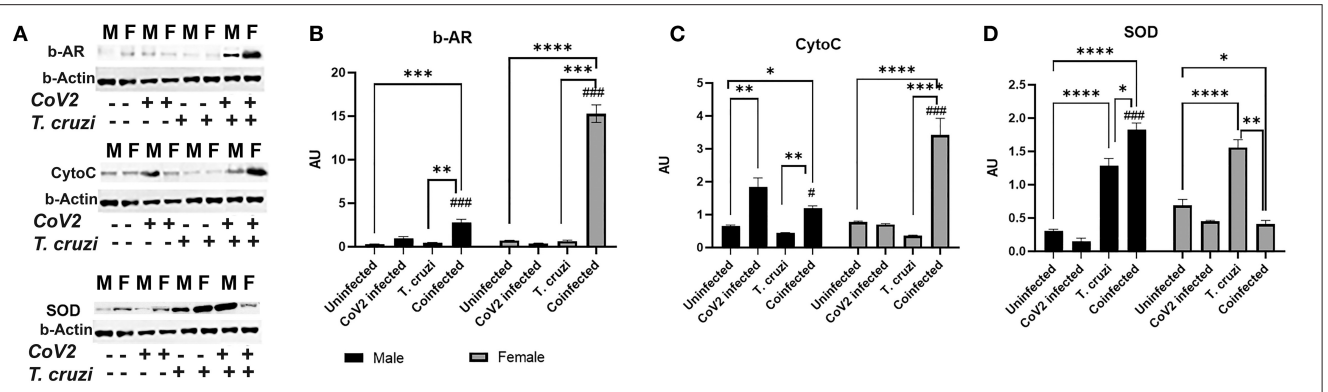

FIGURE 8 | Immunoblot analysis of β-Adrenergic Receptor and markers of mitochondrial β-oxidation in the hearts of CoV2 infected, *T. cruzi* infected, and coinfected huACE2 mice. Western blot images **(A)** of β-Adrenergic Receptor (β-AR), cytochrome C (Cyto C), and superoxide dismutase (SOD). β-Actin was used as loading control. Fold changes in the protein levels of β-AR **(B)**, Cyto C **(C)** and SOD **(D)** were normalized to β-Actin expression and are shown as bar graphs (A dot plot displaying individual data points is presented in **Supplementary Figure 4**). The error bars represent standard error of the mean. $^{*}p < 0.05$, $^{**}p < 0.01$, $^{***}p < 0.001$ and $^{****}p < 0.0001$ compared to uninfected sex matched mice ($n = 4$/sex/group) ($^{\#}p \leq 0.05$ and $^{\#\#\#}p \leq 0.001$ for comparisons between CoV2 infected and coinfected mice) (M, male; F, female).

DISCUSSION

Many clinical and *in vivo* studies have examined the effect of comorbidities, such as diabetes, asthma, hypertension, and cardiac diseases, on the pulmonary pathogenesis and susceptibility to CoV2 infection. However, the effects of metabolic and immunologic changes associated with chronic infectious disease on the risk of developing severe COVID have not been extensively investigated and neither have been the post-COVID effects on the manifestation/activation of other infectious diseases. The present study examines: (i) the effect of *T. cruzi* infection-induced immune and metabolic responses on the susceptibility to CoV2 infection and (ii) the early effect of CoV2 infection on the pathogenesis and risk of developing cardiomyopathy in *T. cruzi* infected mice coinfected with CoV2 during the indeterminate CD stage. We also examined the effects of CoV2 infection on the morphology and metabolic signaling in the hearts of non-CD mice and compared the results with our coinfection model to evaluate the role of *T. cruzi* infection-induced immune and metabolic changes in regulating cardiac viral load and inflammation during CoV2 infection using hACE2 murine models. Moreover, this study assessed whether the relationship between *T. cruzi* and CoV2 infections differs between male and female mice. Specifically, to understand the interplay between *T. cruzi* and CoV2 infections, we used transgenic hACE2 mice (males and females) nasally infected with SARS-CoV2 in mice pre-infected with *T. cruzi*. Our study revealed that: (a) *T. cruzi*-CoV2 coinfection increased ACE2 levels in the lungs and hearts, but the viral load significantly decreased compared to CoV2 infection alone, and (b) there was no observed difference between viral loads in the hearts of male and female coinfected/CoV2 mice. However, CoV2 infection differently altered immune and metabolic status in the hearts of male and female mice (both in CoV2 and coinfection models). More importantly, our study showed that the impact of CoV2 infection on cardiac metabolism and progression of dilated CCM in coinfected mice is sex-dependent: male coinfected mice were more susceptible to developing hypertrophied dilated CCM, whereas female coinfected mice were more susceptible to developing cardiac cachexia.

The viral load in the lungs in female CoV2 infected mice were significantly lower compared to male CoV2 infected mice, which is reminiscent to the observations made in COVID patients (19). Some clinical studies also suggested that the mortality rate of women in young COVD-19 patients is lower than that of men, while there is no difference between the mortality rate of women and men in elderly patients (63, 64). However, not many clinical studies suggesting sex difference in cardiac pathology during COVID are reported. Our study shows for the first time that the viral load in the hearts of coinfected mice is lower compared to CoV2 singly infected mice, although the cardiac levels of ACE2 were similar (in males) or greater (in females) in coinfected mice compared to CoV2 singly infected mice. The significantly reduced viral load in the hearts of coinfected mice may be due to the altered immune and metabolic changes caused by *T. cruzi* infection during acute and indeterminate stages. Similar to the hearts, we also observed significantly reduced viral loads in the lungs of coinfected male mice compared to CoV2 singly infected mice, even though the levels of ACE2 were significantly greater in coinfected male mice. These data suggest that the rates of viral entry, infection, severity, and pathology are not regulated just by the levels of ACE2 receptor, and that the immune and metabolic status of the organ may play a major role in regulating COVID pathology.

T. cruzi infection causes increased accumulation of lipid droplets in the capillaries and micro-lipid droplets in the cardiomyocytes in the myocardium, which in turn alters cardiac metabolic status (**Figures 2**, **4**) (22, 33). The increase in lipid accumulation in the myocardium in *T. cruzi* infected mice may be due to the increased cardiac HMW-ApN levels, which regulates adipogenesis, lipid oxidation, and anti-inflammatory signaling (as shown by increased SOD and reduced TNFα levels) during

the indeterminate stage (22, 34). The levels of HMW-ApN in the hearts of coinfected mice were significantly greater compared to CoV2 alone infected mice, which might have contributed to the reduced TNFα levels (although there was increased infiltration of macrophages) in the hearts of coinfected mice (**Figures 3**, **5**, **6**). Interestingly, although we observed a similar pattern of altered HMW-ApN and reduced TNFα in the hearts of coinfected males and females, histological and morphological analyses showed significant differences between cardiomyocyte cell size, cell number and presence, localization, and size of lipid droplets between the sexes. The hearts of coinfected male mice showed a hypertrophied and dilated myocardium phenotype, whereas coinfected female mice displayed an atrophied and cachexic myocardium phenotype (**Supplementary Figure 3** and **Supplementary Table 1A**). We also observed a shrunken heart phenotype in coinfected female mice (**Supplementary Table 1B**). This was reminiscent of cardiac atrophy observed in cancer patients (65).

CD has been tightly linked to alterations in metabolic substrate utilization and impairments of mitochondrial oxidative capacity and endoplasmic reticulum functions in the hearts (22, 33, 66–68). It is known that patients with heart disease exhibit a shift from fatty acid oxidation toward greater dependance on glucose as a source for cellular energy adenosine triphosphate (ATP) (69). Thus, mitochondria have become a key target in combating this metabolic reprogramming in heart disease including CD (66). Exhaustion of mitochondria or increased mitochondrial oxidative stress results in mutations in mitochondrial DNA, mitochondrial dysfunction and oxidative stress causing cachexia, cardiac atrophy and heart failure (70). During viral and parasitic infections, the myocardium tends to shift its energy utilization from fatty acid oxidation to glycolysis. Increased activation of AMPK in the hearts of infected mice is an indicator of depletion of ATP (23, 71–73). Although the levels of adiponectin and activated AMPK significantly increased in the hearts of both male and female coinfected mice, the downstream mechanism(s) of HMW-ApN/AMPK pathway significantly differed between male and female coinfected mice (**Figure 9**), in that in male coinfected mice AMPK/PPARα and AMPK/glycolysis increased, whereas in female coinfected mice AMPK/PPARα/PPARγ increased. This may be due to the significant increase in b-AR in coinfected female mice. Thus, in coinfected female mice even in the presence of AMPK activation, glycolysis was completely turned off due to a strong increase in b-AR induced lipolysis (PPARs) and the myocardium may have used only fatty acids as their energy source. In female mice, increased estrogen levels could stimulate b-AR (74), which can activate lipolysis and release free fatty acids, positively regulating PPARs (75, 76). The increased activation of PPARγ and PPARα (in the myocardium in female coinfected mice) may form a vicious cycle in inducing lipogenesis and lipid β-oxidation, respectively, overburdening mitochondrial oxidative phosphorylation and causing dysfunctional mitochondria, cachexia and atrophy. The reduced levels of cardiac SOD (even with increased levels of Cyto), reduced coloration of eosin staining in the heart sections, and decreased cardiomyocyte size (heart size) in the hearts of coinfected female mice suggest oxidative stress, cachexia and atrophy, respectively. Overall, these data suggest that CoV2 infection and coinfection with *T. cruzi* differently affect cardiac metabolic and immune status in male and female mice via host C-ApN/AMPK and b-AR/PPAR-signaling, respectively. Thus, the C-ApN/AMPK and b-AR/PPAR downstream signaling may play major roles in determining the progression, severity, and phenotype of CCM and heart failure in the context of COVID.

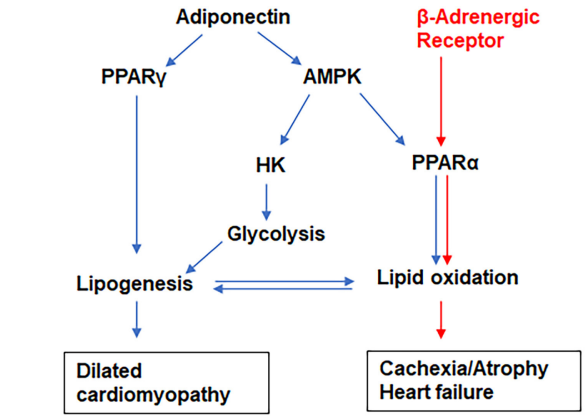

FIGURE 9 | The proposed models of signaling pathways that differentiate the pathogenesis of dilated cardiomyopathy (indicated by blue arrows) and cachexia (indicated by red arrows) in male and female coinfected mice, respectively. The adiponectin/AMPK/glycolysis pathway dominates in the hearts of male coinfected mice, whereas β-adrenergic receptor signaling activates lipid metabolic pathways in female coinfected mice.

The present study investigated the immediate effect of CoV2 infection on heart pathology in CoV2/*T. cruzi* single infections and CoV2 coinfection in the *T. cruzi* indeterminate model, whereas any potential long-term effects remain to be explored. Further studies including a greater number of male and female mice at different time stamps are warranted to evaluate the long-term post-COVID effects on the development and progression of Chagas cardiomyopathy. Our data from this pilot study indicate that the risk of developing dilated cardiomyopathy in *T. cruzi* infected males may be greater than in females and that the risk of developing cachexia-associated heart failure in *T. cruzi*-CoV2 coinfected females may be greater than in coinfected males.

DATA AVAILABILITY STATEMENT

The original contributions presented in the study are included in the article/**Supplementary Materials**, further inquiries can be directed to the corresponding author.

ETHICS STATEMENT

The animal study was reviewed and approved by Hackensack University IACUC committee.

AUTHOR CONTRIBUTIONS

JN contributed to conception, study design, funding acquisition, supervision, validation, and writing/reviewing the manuscript. DP contributed to the validation and reviewing the manuscript. DD and KL performed the investigation and data analysis. NO performed formal data analysis. HT performed the investigation, data analysis and writing the manuscript. ED provided technical help. All authors contributed to the article and approved the submitted version.

FUNDING

This study was supported by grants from the National Institute of Allergy and Infectious Diseases (National Institutes of Health AI150765-01) to JN.

ACKNOWLEDGMENTS

We thank Erika Shor at the Center for Discovery and Innovation, Hackensack University for a critical reading of the manuscript. We also thank Steven Park at the CDI for the managerial support to executing the BSL3 work.

SUPPLEMENTARY MATERIAL

The Supplementary Material for this article can be found online at: https://www.frontiersin.org/articles/10.3389/fcvm.2022.783974/full#supplementary-material

Supplementary Figure 1 | Flow chart of the experimental design.

Supplementary Figure 2 | H&E sections (top panel) and Masson trichrome images (bottom panel) of right ventricles (RV) of coinfected male and female mice showing fibrosis (blue and purple), infiltration of immune cells (yellow arrow), accumulation of lipid droplets (red arrow), and enlarged nuclei (green arrowhead) (40X magnified; bar-50μm).

Supplementary Figure 3 | Alterations in cardiomyocyte size during CoV2/T. cruzi infection and coinfection in male and female mice: **(A)** H&E sections showing the average cell size in left ventricles (cardiomyocytes - green arrowhead; endothelial cells - yellow arrowhead; macro-lipid droplets - black arrowhead; and immune cells - red arrowhead) (40X magnified; bar-50μm). **(B)** Masson trichrome images (gray scale) of right ventricles showing changes in extracellular collagen layer (white) and thickness of intercellular collagen network during infection and coinfection (40X magnified; bar-50μm). **(C)** Illustration of cardiomyocyte hypertrophy determination by measuring cardiomyocyte length (Dmaj) and diameter (Dmin) and intercellular collagen thickness using histological sections (Masson trichrome) of the hearts. The data are presented as **Supplementary Table 1A**.

Supplementary Figure 4 | Changes in the levels of ACE2 and metabolic signaling markers (Western blot analysis) in the heart/lungs are compared between male and female mice during CoV2/T. cruzi infections and coinfection. Fold changes in the protein levels were normalized to GDI and are represented as a dot plot. The error bars represent standard error of the mean. $^{*}P < 0.05$, $^{**}P < 0.01$, $^{***}P < 0.001$ and $^{****}P < 0.0001$compared between males and females in each group.

Supplementary Table 1A | Cardiomyocyte volume by histology. Cardiomyocyte length and width were measured ($n = 40$ cells/sex/group) on microscopic images of the cardiac histology sections (right ventricles) and the volume was calculated as described in Methods. The significance p-value for differences in volume was calculated by t-test comparing each group to sex matched uninfected mice and is denoted by "*" ($^{*}p \leq 0.05$, $^{**}p \leq 0.01$ and $^{***}p \leq 0.001$).

Supplementary Table 1B | Morphometric analysis of the hearts of CoV2/T. cruzi infected and coinfected male and female mice. The thickness of the right ventricle wall (RVW), left ventricle wall (LVW) and intra-septal wall (Septal -W) was measured as mentioned in materials and methods and is presented in mm. The significance p-value for differences in wall thickness was calculated by t-test comparing each group to sex matched uninfected mice and is denoted by "*" ($^{*}p \leq 0.05$, $^{**}p \leq 0.01$ and $^{***}p \leq 0.001$). The significance p-value for differences in wall thickness between coinfected and sex matched T. cruzi infected mice is denoted by "#" (# $p \leq 0.05$).

REFERENCES

1. WHO. Available online at: https://www.who.int/emergencies/diseases/novel-coronavirus-2019 (accessed August 16, 2021).
2. Guo W, Li M, Dong Y, Zhou H, Zhang Z, Tian C, et al. Diabetes is a risk factor for the progression and prognosis of COVID-19. *Diabetes Metab Res Rev*. (2020) 36:e3319. doi: 10.1002/dmrr.3319
3. Dietz W, Santos-Burgoa C. Obesity and its implications for COVID-19 mortality. *Obesity*. (2020) 28:1005. doi: 10.1002/oby.22818
4. Li B, Yang J, Zhao F, Zhi L, Wang X, Liu L, et al. Prevalence and impact of cardiovascular metabolic diseases on COVID-19 in China. *Clin Res Cardiol*. (2020) 109:531–8. doi: 10.1007/s00392-020-01626-9
5. Driggin E, Madhavan MV, Bikdeli B, Chuich T, Laracy J, Biondi-Zoccai G, et al. Cardiovascular considerations for patients, health care workers, and health systems during the COVID-19 pandemic. *J Am Coll Cardiol*. (2020) 75:2352–71. doi: 10.1016/j.jacc.2020.03.031
6. Basu-Ray I, Almaddah NK, Adeboye A, Soos MP. *Cardiac Manifestations of Coronavirus (COVID-19)*. Treasure Island (FL): StatPearls Publishing (2021). Available online at: https://www.ncbi.nlm.nih.gov/books/NBK556152/ (accessed August 16, 2021).
7. Guo T, Fan Y, Chen M, Wu X, Zhang L, He T, et al. Cardiovascular implications of fatal outcomes of patients with coronavirus disease 2019 (COVID-19). *JAMA Cardiol*. (2020) 5:811–8. doi: 10.1001/jamacardio.2020.1017
8. Argulian E, Sud K, Vogel B, Bohra C, Garg VP, Talebi S, et al. Right ventricular dilation in hospitalized patients with COVID-19 infection. *JACC Cardiovasc Imaging*. (2020) 13:2459–61. doi: 10.1016/j.jcmg.2020.05.010
9. Zhou F, Yu T, Du R, Fan G, Liu Y, Liu Z, et al. Clinical course and risk factors for mortality of adult inpatients with COVID-19 in Wuhan, China: a retrospective cohort study. *Lancet*. (2020) 395:1054–62. doi: 10.1016/S0140-6736(20)30566-3
10. Ranard LS, Fried JA, Abdalla M, Anstey DE, Givens RC, Kumaraiah D, et al. Approach to acute cardiovascular complications in COVID-19 infection. *Circ Heart Fail*. (2020) 13:e007220. doi: 10.1161/CIRCHEARTFAILURE.120.007220
11. Puntmann VO, Carerj ML, Wieters I, Fahim M, Arendt C, Hoffmann J, et al. Outcomes of cardiovascular magnetic resonance imaging in patients recently recovered from coronavirus disease 2019 (COVID-19). *JAMA Cardiol*. (2020) 5:1265–73. doi: 10.1001/jamacardio.2020.3557
12. Becker RC. Anticipating the long-term cardiovascular effects of COVID-19. *J Thromb Thrombolysis*. (2020) 50:512–24. doi: 10.1007/s11239-020-02266-6
13. Mitrani RD, Dabas N, Goldberger JJ. COVID-19 cardiac injury: implications for long-term surveillance and outcomes in survivors. *Heart Rhythm*. (2020) 17:1984–90. doi: 10.1016/j.hrthm.2020.06.026
14. The Lancet. COVID-19 in Latin America: a humanitarian crisis. *Lancet*. (2020) 396:1463. doi: 10.1016/S0140-6736(20)32328-X
15. Montgomery SP, Starr MC, Cantey PT, Edwards MS, Meymandi SK. Neglected parasitic infections in the United States: chagas disease. *Am J Trop Med Hyg*. (2014) 90:814–8. doi: 10.4269/ajtmh.13-0726

16. Zheng C, Quintero O, Revere EK, Oey MB, Espinoza F, Puius YA, et al. Chagas disease in the New York city metropolitan area. *Open Forum Infect Dis*. (2020) 7:ofaa156. doi: 10.1093/ofid/ofaa156
17. Molina I, Marcolino MS, Pires MC, Ramos LEF, Silva RT, Guimaraes-Junior MH, et al. Chagas disease and SARS-CoV-2 coinfection does not lead to worse in-hospital outcomes. *Sci Rep*. (2021) 11:20289. doi: 10.1038/s41598-021-96825-3
18. Alberca RW, Yendo TM, Leuzzi Ramos YA, Fernandes IG, Oliveira LM, Teixeira FME, et al. Case report: COVID-19 and chagas disease in two coinfected patients. *Am J Trop Med Hyg*. (2020) 103:2353–6. doi: 10.4269/ajtmh.20-1185
19. Gomez JMD, Du-Fay-de-Lavallaz JM, Fugar S, Sarau A, Simmons JA, Clark B, et al. Sex differences in COVID-19 hospitalization and mortality. *J Womens Health*. (2021) 30:646–53. doi: 10.1161/circ.142.suppl_3.17393
20. Basquiera AL, Sembaj A, Aguerri AM, Omelianiuk M, Guzman S, Moreno Barral J, et al. Risk progression to chronic chagas cardiomyopathy: influence of male sex and of parasitaemia detected by polymerase chain reaction. *Heart*. (2003) 89:1186–90. doi: 10.1136/heart.89.10.1186
21. Assuncao AN Jr, Jerosch-Herold M, Melo RL, Mauricio AV, Rocha L, Torreao JA, et al. Chagas' heart disease: gender differences in myocardial damage assessed by cardiovascular magnetic resonance. *J Cardiovasc Magn Reson*. (2016) 18:88. doi: 10.1186/s12968-016-0307-5
22. Lizardo K, Ayyappan JP, Oswal N, Weiss LM, Scherer PE, Nagajyothi JF. Fat tissue regulates the pathogenesis and severity of cardiomyopathy in murine chagas disease. *PLoS Negl Trop Dis*. (2021) 15:e0008964. doi: 10.1371/journal.pntd.0008964
23. Nagajyothi F, Weiss LM, Zhao D, Koba W, Jelicks LA, Cui MH, et al. High fat diet modulates trypanosoma cruzi infection associated myocarditis. *PLoS Negl Trop Dis*. (2014) 8:e3118. doi: 10.1371/journal.pntd.0003118
24. Harash G, Richardson KC, Alshamy Z, Hunigen H, Hafez HM, Plendl J, et al. Heart ventricular histology and microvasculature together with aortic histology and elastic lamellar structure: a comparison of a novel dual-purpose to a broiler chicken line. *PLoS ONE*. (2019) 14:e0214158. doi: 10.1371/journal.pone.0214158
25. Ayyappan JP, Ganapathi U, Lizardo K, Vinnard C, Subbian S, Perlin DS, et al. Adipose tissue regulates pulmonary pathology during TB infection. *mBio*. (2019) 10:e02771–18. doi: 10.1128/mBio.02771-18
26. Coelho-Filho OR, Shah RV, Mitchell R, Neilan TG, Moreno H Jr, Simonson B, et al. Quantification of cardiomyocyte hypertrophy by cardiac magnetic resonance: implications for early cardiac remodeling. *Circulation*. (2013) 128:1225–33. doi: 10.1161/CIRCULATIONAHA.112.000438
27. Tracy RE. Cardiac myocyte sizes in right compared with left ventricle during overweight and hypertension. *J Am Soc Hypertens*. (2014) 8:457–63. doi: 10.1016/j.jash.2014.05.004
28. Lizardo K, Ayyappan JP, Ganapathi U, Dutra WO, Qiu Y, Weiss LM, et al. Diet alters serum metabolomic profiling in the mouse model of chronic chagas cardiomyopathy. *Dis Markers*. (2019) 2019:4956016. doi: 10.1155/2019/4956016
29. Gonzalez FB, Villar SR, Toneatto J, Pacini MF, Marquez J, D'Attilio L, et al. Immune response triggered by Trypanosoma cruzi infection strikes adipose tissue homeostasis altering lipid storage, enzyme profile and adipokine expression. *Med Microbiol Immunol*. (2019) 208:651–66. doi: 10.1007/s00430-018-0572-z
30. Scialo F, Daniele A, Amato F, Pastore L, Matera MG, Cazzola M, et al. ACE2: the major cell entry receptor for SARS-CoV-2. *Lung*. (2020) 198:867–77. doi: 10.1007/s00408-020-00408-4
31. Zamorano Cuervo N, Grandvaux N. ACE2: evidence of role as entry receptor for SARS-CoV-2 and implications in comorbidities. *Elife*. (2020) 9:e61390. doi: 10.7554/eLife.61390
32. Li MY, Li L, Zhang Y, Wang XS. Expression of the SARS-CoV-2 cell receptor gene ACE2 in a wide variety of human tissues. *Infect Dis Poverty*. (2020) 9:45. doi: 10.1186/s40249-020-00662-x
33. Ayyappan JP, Lizardo K, Wang S, Yurkow E, Nagajyothi JF. Inhibition of ER stress by 2-aminopurine treatment modulates cardiomyopathy in a murine chronic chagas disease model. *Biomol Ther*. (2019) 27:386–94. doi: 10.4062/biomolther.2018.193
34. Ayyappan JP, Lizardo K, Wang S, Yurkow E, Nagajyothi JF. Inhibition of SREBP improves cardiac lipidopathy, improves endoplasmic reticulum stress, and modulates chronic chagas cardiomyopathy. *J Am Heart Assoc*. (2020) 9:e014255. doi: 10.1161/JAHA.119.014255
35. Pandey GK, Vadivel S, Raghavan S, Mohan V, Balasubramanyam M, Gokulakrishnan K. High molecular weight adiponectin reduces glucolipotoxicity-induced inflammation and improves lipid metabolism and insulin sensitivity via APPL1-AMPK-GLUT4 regulation in 3T3-L1 adipocytes. *Atherosclerosis*. (2019) 288:67–75. doi: 10.1016/j.atherosclerosis.2019.07.011
36. Choi HM, Doss HM, Kim KS. Multifaceted physiological roles of adiponectin in inflammation and diseases. *Int J Mol Sci*. (2020) 21:1219. doi: 10.3390/ijms21041219
37. Yamauchi T, Kamon J, Ito Y, Tsuchida A, Yokomizo T, Kita S, et al. Cloning of adiponectin receptors that mediate antidiabetic metabolic effects. *Nature*. (2003) 423:762–9. doi: 10.1038/nature01705
38. Hug C, Wang J, Ahmad NS, Bogan JS, Tsao TS, Lodish HF. T-cadherin is a receptor for hexameric and high-molecular-weight forms of Acrp30/adiponectin. *Proc Natl Acad Sci U S A*. (2004) 101:10308–13. doi: 10.1073/pnas.0403382101
39. Nguyen TMD. Adiponectin: role in physiology and pathophysiology. *Int J Prev Med*. (2020) 11:136. doi: 10.4103/ijpvm.IJPVM_193_20
40. Lovren F, Pan Y, Quan A, Szmitko PE, Singh KK, Shukla PC, et al. Adiponectin primes human monocytes into alternative anti-inflammatory M2 macrophages. *Am J Physiol Heart Circ Physiol*. (2010) 299:H656–63. doi: 10.1152/ajpheart.00115.2010
41. Astapova O, Leff T. Adiponectin and PPARgamma: cooperative and interdependent actions of two key regulators of metabolism. *Vitam Horm*. (2012) 90:143–62. doi: 10.1016/B978-0-12-398313-8.00006-3
42. Song J, Choi SM, Kim BC. Adiponectin regulates the polarization and function of microglia via PPAR-gamma signaling under amyloid beta toxicity. *Front Cell Neurosci*. (2017) 11:64. doi: 10.3389/fncel.2017.00064
43. Tardelli M, Claudel T, Bruschi FV, Moreno-Viedma V, Trauner M. Adiponectin regulates AQP3 via PPARalpha in human hepatic stellate cells. *Biochem Biophys Res Commun*. (2017) 490:51–4. doi: 10.1016/j.bbrc.2017.06.009
44. Dupont J, Chabrolle C, Rame C, Tosca L, Coyral-Castel S. Role of the peroxisome proliferator-activated receptors, adenosine monophosphate-activated kinase, and adiponectin in the ovary. *PPAR Res*. (2008) 2008:176275. doi: 10.1155/2008/176275
45. Madamanchi A. Beta-adrenergic receptor signaling in cardiac function and heart failure. *Mcgill J Med*. (2007) 10:99–104. doi: 10.26443/mjm.v10i2.458
46. Bernstein D, Fajardo G, Zhao M. The role of beta-adrenergic receptors in heart failure: differential regulation of cardiotoxicity and cardioprotection. *Prog Pediatr Cardiol*. (2011) 31:35–8. doi: 10.1016/j.ppedcard.2010.11.007
47. Sterin-Borda L, Gorelik G, Postan M, Gonzalez Cappa S, Borda E. Alterations in cardiac beta-adrenergic receptors in chagasic mice and their association with circulating beta-adrenoceptor-related autoantibodies. *Cardiovasc Res*. (1999) 41:116–25. doi: 10.1016/S0008-6363(98)00225-9
48. Fretes RE, Paglini P, Fernandez AR, Enders J, de Fabro SP. Trypanosoma cruzi: increased 5'-nucleotidase activity associated with dysfunction of adrenergic receptors in acutely infected albino Swiss mice. *J Parasitol*. (1999) 85:970–2. doi: 10.2307/3285840
49. Bustamante JM, Rivarola HW, Fernandez AR, Enders JE, Ricardo F, d'Oro Gloria DL, et al. Trypanosoma cruzi reinfections provoke synergistic effect and cardiac beta-adrenergic receptors' dysfunction in the acute phase of experimental Chagas' disease. *Exp Parasitol*. (2003) 103:136–42. doi: 10.1016/S0014-4894(03)00096-1
50. Collins S. Beta-adrenoceptor signaling networks in adipocytes for recruiting stored fat and energy expenditure. *Front Endocrinol*. (2011) 2:102. doi: 10.3389/fendo.2011.00102
51. Jaworski K, Sarkadi-Nagy E, Duncan RE, Ahmadian M, Sul HS. Regulation of triglyceride metabolism. IV. Hormonal regulation of lipolysis in adipose tissue. *Am J Physiol Gastrointest Liver Physiol*. (2007) 293:G1–4. doi: 10.1152/ajpgi.00554.2006
52. Schmidt SL, Bessesen DH, Stotz S, Peelor FF 3rd, Miller BF, Horton TJ. Adrenergic control of lipolysis in women compared with men. *J Appl Physiol (1985)*. (2014) 117:1008–19. doi: 10.1152/japplphysiol.00003.2014
53. Pawlak M, Lefebvre P, Staels B. Molecular mechanism of PPARalpha action and its impact on lipid metabolism, inflammation and fibrosis

in non-alcoholic fatty liver disease. *J Hepatol.* (2015) 62:720–33. doi: 10.1016/j.jhep.2014.10.039
54. Tahri-Joutey M, Andreoletti P, Surapureddi S, Nasser B, Cherkaoui-Malki M, Latruffe N. Mechanisms mediating the regulation of peroxisomal fatty acid beta-oxidation by PPARalpha. *Int J Mol Sci.* (2021) 22:8969. doi: 10.3390/ijms22168969
55. Medina-Gomez G, Gray S, Vidal-Puig A. Adipogenesis and lipotoxicity: role of peroxisome proliferator-activated receptor gamma (PPARgamma) and PPARgammacoactivator-1 (PGC1). *Public Health Nutr.* (2007) 10:1132–7. doi: 10.1017/S1368980007000614
56. Souza-Mello V. Peroxisome proliferator-activated receptors as targets to treat non-alcoholic fatty liver disease. *World J Hepatol.* (2015) 7:1012–9. doi: 10.4254/wjh.v7.i8.1012
57. Machuki JO, Zhang HY, Harding SE, Sun H. Molecular pathways of oestrogen receptors and beta-adrenergic receptors in cardiac cells: recognition of their similarities, interactions and therapeutic value. *Acta Physiol.* (2018) 222:e12978. doi: 10.1111/apha.12978
58. Chu SH, Goldspink P, Kowalski J, Beck J, Schwertz DW. Effect of estrogen on calcium-handling proteins, beta-adrenergic receptors, and function in rat heart. *Life Sci.* (2006) 79:1257–67. doi: 10.1016/j.lfs.2006.03.037
59. Hart EC, Charkoudian N, Miller VM. Sex, hormones and neuroeffector mechanisms. *Acta Physiol.* (2011) 203:155–65. doi: 10.1111/j.1748-1716.2010.02192.x
60. Schulze PC. Myocardial lipid accumulation and lipotoxicity in heart failure. *J Lipid Res.* (2009) 50:2137–8. doi: 10.1194/jlr.R001115
61. Antunes D, Padrao AI, Maciel E, Santinha D, Oliveira P, Vitorino R, et al. Molecular insights into mitochondrial dysfunction in cancer-related muscle wasting. *Biochim Biophys Acta.* (2014) 1841:896–905. doi: 10.1016/j.bbalip.2014.03.004
62. Beltra M, Pin F, Ballaro R, Costelli P, Penna F. Mitochondrial dysfunction in cancer cachexia: impact on muscle health and regeneration. *Cells.* (2021) 10:3150. doi: 10.3390/cells10113150
63. Gao S, Jiang F, Jin W, Shi Y, Yang L, Xia Y, et al. Risk factors influencing the prognosis of elderly patients infected with COVID-19: a clinical retrospective study in Wuhan, China. *Aging.* (2020) 12:12504–16. doi: 10.18632/aging.103631
64. Su W, Qiu Z, Zhou L, Hou J, Wang Y, Huang F, et al. Sex differences in clinical characteristics and risk factors for mortality among severe patients with COVID-19: a retrospective study. *Aging.* (2020) 12:18833–43. doi: 10.18632/aging.103793
65. Sweeney M, Yiu A, Lyon AR. Cardiac atrophy and heart failure in cancer. *Card Fail Rev.* (2017) 3:62–5. doi: 10.15420/cfr.2017:3:2
66. Teixeira PC, Ducret A, Langen H, Nogoceke E, Santos RHB, Silva Nunes JP, et al. Impairment of multiple mitochondrial energy metabolism pathways in the heart of chagas disease cardiomyopathy patients. *Front Immunol.* (2021) 12:755782. doi: 10.3389/fimmu.2021.755782
67. Nagajyothi JF, Weiss LM. Advances in understanding the role of adipose tissue and mitochondrial oxidative stress in Trypanosoma cruzi infection. *F1000Res.* (2019) 8:F1000 Faculty Rev-1152. doi: 10.12688/f1000research.19190.1
68. Gupta S, Wen JJ, Garg NJ. Oxidative stress in chagas disease. *Interdiscip Perspect Infect Dis.* (2009) 2009:190354. doi: 10.1155/2009/190354
69. Lai L, Leone TC, Keller MP, Martin OJ, Broman AT, Nigro J, et al. Energy metabolic reprogramming in the hypertrophied and early stage failing heart: a multisystems approach. *Circ Heart Fail.* (2014) 7:1022–31. doi: 10.1161/CIRCHEARTFAILURE.114.001469
70. Lee DE, Brown JL, Rosa-Caldwell ME, Perry RA, Brown LA, Haynie WS, et al. Cancer-induced cardiac atrophy adversely affects myocardial redox state and mitochondrial oxidative characteristics. *JCSM Rapid Commun.* (2021) 4:3–15. doi: 10.1002/rco2.18
71. Ma Y, Li J. Metabolic shifts during aging and pathology. *Compr Physiol.* (2015) 5:667–86. doi: 10.1002/cphy.c140041
72. Khairallah M, Khairallah R, Young ME, Dyck JR, Petrof BJ, Des Rosiers C. Metabolic and signaling alterations in dystrophin-deficient hearts precede overt cardiomyopathy. *J Mol Cell Cardiol.* (2007) 43:119–29. doi: 10.1016/j.yjmcc.2007.05.015
73. Karwi QG, Uddin GM, Ho KL, Lopaschuk GD. Loss of metabolic flexibility in the failing heart. *Front Cardiovasc Med.* (2018) 5:68. doi: 10.3389/fcvm.2018.00068
74. Riedel K, Deussen AJ, Tolkmitt J, Weber S, Schlinkert P, Zatschler B, et al. Estrogen determines sex differences in adrenergic vessel tone by regulation of endothelial beta-adrenoceptor expression. *Am J Physiol Heart Circ Physiol.* (2019) 317:H243–54. doi: 10.1152/ajpheart.00456.2018
75. Mottillo EP, Granneman JG. Intracellular fatty acids suppress beta-adrenergic induction of PKA-targeted gene expression in white adipocytes. *Am J Physiol Endocrinol Metab.* (2011) 301:E122–31. doi: 10.1152/ajpendo.00039.2011
76. Mottillo EP, Bloch AE, Leff T, Granneman JG. Lipolytic products activate peroxisome proliferator-activated receptor (PPAR) alpha and delta in brown adipocytes to match fatty acid oxidation with supply. *J Biol Chem.* (2012) 287:25038–48. doi: 10.1074/jbc.M112.374041

Conflict of Interest: The authors declare that the research was conducted in the absence of any commercial or financial relationships that could be construed as a potential conflict of interest.

Publisher's Note: All claims expressed in this article are solely those of the authors and do not necessarily represent those of their affiliated organizations, or those of the publisher, the editors and the reviewers. Any product that may be evaluated in this article, or claim that may be made by its manufacturer, is not guaranteed or endorsed by the publisher.

frontiers | Frontiers in Cardiovascular Medicine

ORIGINAL RESEARCH
published: 19 May 2022
doi: 10.3389/fcvm.2022.750876

Modulation of Regulatory T Cells Activity by Distinct CD80 and CD86 Interactions With CD28/CTLA-4 in Chagas Cardiomyopathy

*Bruna F. Pinto[1], Nayara I. Medeiros[1,2], Andrea Teixeira-Carvalho[2], Jacqueline A. Fiuza[2], Silvana M. Eloi-Santos[2], Maria C. P. Nunes[3], Silvana A. Silva[3], Tereza C. M. Fontes-Cal[1], Mayara Belchior-Bezerra[1], Walderez O. Dutra[1,4], Rodrigo Correa-Oliveira[2,4] and Juliana A. S. Gomes[1]**

[1] Departamento de Morfologia, Laboratório de Biologia das Interações Celulares, Instituto de Ciências Biológicas, Universidade Federal de Minas Gerais, Belo Horizonte, Brazil, [2] Instituto René Rachou, Fundação Oswaldo Cruz–FIOCRUZ, Belo Horizonte, Brazil, [3] Departamento de Clínica Médica, Faculdade de Medicina, Universidade Federal de Minas Gerais, Belo Horizonte, Brazil, [4] Instituto Nacional de Ciência e Tecnologia Doenças Tropicais, Belo Horizonte, Brazil

OPEN ACCESS

Edited by:
Dragos Cretoiu, Carol Davila University of Medicine and Pharmacy, Romania

Reviewed by:
Paulo M. Dourado, University of São Paulo, Brazil
Valdo Jose Dias Da Silva, Universidade Federal do Triângulo Mineiro, Brazil

***Correspondence:**
Juliana A. S. Gomes
juliana@icb.ufmg.br

Specialty section:
This article was submitted to General Cardiovascular Medicine, a section of the journal Frontiers in Cardiovascular Medicine

Received: *31 July 2021*
Accepted: *08 April 2022*
Published: *19 May 2022*

Citation:
Pinto BF, Medeiros NI, Teixeira-Carvalho A, Fiuza JA, Eloi-Santos SM, Nunes MCP, Silva SA, Fontes-Cal TCM, Belchior-Bezerra M, Dutra WO, Correa-Oliveira R and Gomes JAS (2022) Modulation of Regulatory T Cells Activity by Distinct CD80 and CD86 Interactions With CD28/CTLA-4 in Chagas Cardiomyopathy. Front. Cardiovasc. Med. 9:750876. doi: 10.3389/fcvm.2022.750876

Chagas cardiomyopathy is the symptomatic cardiac clinical form (CARD) of the chronic phase of Chagas disease caused by *Trypanosoma cruzi* infection. It was described as the most fibrosing cardiomyopathies, affecting approximately 30% of patients during the chronic phase. Other less frequent symptomatic clinical forms have also been described. However, most patients who progress to the chronic form develop the indeterminate clinical form (IND), may remain asymptomatic for life, or develop some cardiac damage. Some mechanisms involved in the etiology of the clinical forms of Chagas disease have been investigated. To characterize the contribution of CD80 and CD86 co-stimulatory molecules in the activation of different $CD4^+$ (Th1, Th2, Th17, and Treg) and $CD8^+$ T lymphocyte subsets, we used blocking antibodies for CD80 and CD86 receptors of peripheral blood mononuclear cells (PBMC) in cultures with *T. cruzi* antigens from non-infected (NI), IND, and CARD individuals. We demonstrated a higher frequency of $CD8^+$ $CD25^+$ T lymphocytes and $CD8^+$ Treg cells after anti-CD80 antibody blockade only in the CARD group. In contrast, a lower frequency of $CD4^+$ Treg lymphocytes after anti-CD86 antibody blockade was found only in IND patients. A higher frequency of $CD4^+$ Treg $CD28^+$ lymphocytes, as well as an association between $CD4^+$ Treg lymphocytes and $CD28^+$ expression on $CD4^+$ Treg cells in the CARD group, but not in IND patients, and once again only after anti-CD80 antibody blockade, was observed. We proposed that Treg cells from IND patients could be activated *via* CD86-CTLA-4 interaction, leading to modulation of the immune response only in asymptomatic patients with Chagas disease, while CD80 may be involved in the proliferation control of T $CD8^+$ lymphocytes, as also in the modulation of regulatory cell activation *via* CD28 receptor. For the first time, our data highlight the role of CD80 in modulation of Treg lymphocytes activation in patients with CARD, highlighting a key molecule in the development of Chagas cardiomyopathy.

Keywords: Chagas disease, CD80 co-stimulatory molecule, Treg cells, immune response, Chagas cardiomyopathy

INTRODUCTION

Chagas disease, also known as American trypanosomiasis, is a neglected tropical parasitic disease caused by the protozoan *Trypanosoma cruzi* (1), affecting approximately 8 million people worldwide (2). The increase in morbidity in non-endemic regions, as well as the resurgence of transmission in endemic countries, is currently becoming a major focus of attention (3).

During the chronic phase, approximately 60% of patients do not develop specific clinical symptoms of the disease, classified as indeterminate clinical form (IND) (4–7). They can remain asymptomatic throughout their lives (8). However, in the 10–20 years of range, IND patients are likely to develop some cardiac damage (8, 9). Another 30% of infected individuals develop severe cardiomyopathy with progressive myocardium damage due to inflammation and fibrosis (4, 7). Heart failure caused by chronic Chagas disease has the worst prognosis among other cardiomyopathies (4, 7, 10, 11).

Some mechanisms involved in the etiology of the clinical forms of Chagas disease have been investigated, but even 112 years after the first description of this morbidity, science still does not understand why different clinical manifestations are developing in the chronic phase of the infection. The study of the immune response is crucial to determine the development of the disease by mobilizing multiple humoral and cellular mechanisms of the innate and acquired immune response (12, 13).

During an acute *T. cruzi* infection, antigen-presenting cells, such as monocytes, activate $CD4^+$ T lymphocytes and initiate IL-12 secretion, which is the primary driver of IFN-γ-producing T helper 1 (Th1) cell differentiation. Th1 is essential for controlling the replication of the parasite but not for completely eliminating them, which contributes to the establishment of low-grade chronic persistent infection (7, 10, 14). While IND patients develop mechanisms to regulate the immune response, such as IL-10 production and Treg cell activation, CARD patients have a strong Th1-lymphocyte. This Th1 mechanism contributes to high levels of IFN-γ and TNF-α pro-inflammatory cytokines that lead to an exacerbated and uncontrolled inflammatory response (15–19).

Trypanosoma cruzi infection also leads to CD8 T^+ lymphocytes activation, which shows cytotoxic activity by destroying infected cells with *T. cruzi* amastigotes, as well as through the production of IFN-γ for infection control (20–22). Studies with cardiac tissue biopsy fragments from patients with CARD have shown a high frequency of T cells in the inflammatory infiltrate, mainly $CD8^+$ T lymphocytes, which contributes to cardiac fibers destruction, fibrosis development, and tissue damage (23–25).

Two signals are required for T $CD4^+$ and T $CD8^+$ lymphocyte activation. The first is mediated by the MHC and TCR receptors and the second by the CD80 and CD86 co-stimulating molecules that interact with the CD28 or CTLA-4 receptors present in the lymphocyte cell surface (26, 27). The interaction of the TCR receptor with the MHC-bound peptide is not sufficient for lymphocyte activation and a second activation signal is required (26, 28, 29). The interaction of CD80 or CD86 with CD28 leads to lymphocyte proliferation, and the interaction with CTLA-4 leads to inhibition of lymphocyte activity and thus downregulates the immune response (27, 30–32). CD28 receptor is constitutively expressed on T cells, has low avidity for CD80 and CD86 molecules and when activated, it triggers strongly up-regulates T cell cytokine production (26, 27, 33, 34). On the contrary, CTLA-4 has high avidity for CD80 and CD86 molecules, and its expression is rapidly increased only after T cell activation (33, 35). CTLA-4-deficient mice showed elevated leukocyte infiltrate in various organs, pointing to the role of CTLA-4 as a negative regulator of T cell activation (36). In Chagas disease, it was observed that there was a higher frequency of $CD80^+$ monocytes in IND and CARD patients and a lower frequency of $CD86^+$ monocytes only in the CARD form (30, 37, 38). The IND group also showed a higher CTLA-4 expression on T lymphocytes after exposure of monocytes to the Y strain of *T. cruzi* (30).

Although the expression of these co-stimulating molecules is essential for the activation or inhibition of lymphocytes (39–41), few studies to date have demonstrated the capacity of these receptors to activate $CD4^+$ and $CD8^+$ T lymphocytes in Chagas disease (38, 42). We previously demonstrated that CD86 may be involved in immunoregulation by CTLA-4 association, suggesting a strategy to control inflammation and tissue damage in IND patients (38).

This study characterizes the contribution of CD80 and CD86 co-stimulatory molecules in the activation of $CD4^+$ subpopulations (Th1, Th2, Th17, and Treg) and $CD8^+$ T lymphocyte subsets by blocking antibodies to inhibit CD80 and CD86 receptors of peripheral blood mononuclear cells (PBMC) in cultures with *T. cruzi* antigens. We demonstrated that CD80 and CD86 receptors have different functions in lymphocytes activation from patients with Chagas disease, and CD80 may be responsible for the modulation of Treg lymphocytes activation in patients with CARD, pointing out a key molecule in the development of cardiomyopathy.

MATERIALS AND METHODS

Study Population

The patients who agreed to participate in this study were selected at the outpatient clinic of the Ambulatório de Doenças infecto-parasitárias Alda Falcão in Instituto René Rachou and Ambulatório Bias Fortes of the Hospital das Clinicas of Universidade Federal de Minas Gerais, Belo Horizonte, Minas Gerais, Brazil.

Serology for Chagas disease was defined by the following tests: indirect immunofluorescence, ELISA, or indirect hemagglutination, and patients were considered infected when they tested positive for at least two different serological tests. In total, 20 patients with Chagas disease were grouped as indeterminate (IND) and cardiac (CARD) clinical forms. The IND group (n = 9) included asymptomatic individuals who tested positive for Chagas disease but did not have significant alterations in electrocardiography, echocardiogram, esophagogram, chest X-ray, and barium enema. The CARD group (n = 11) was represented by patients with alterations

in electrocardiography who were already monitored by the responsible physicians at Ambulatório de Doenças infecto-parasitárias Alda Falcão in Instituto René Rachou and Ambulatório Bias Fortes of the Hospital das Clinicas of Universidade Federal de Minas Gerais. Left ventricular end-diastolic diameter/body surface area ≥31 mm (64.8 ± 5.9 mm) and left ventricular ejection fraction <55% (34 ± 10%) were used as echocardiographic parameters of Chagas dilated cardiomyopathy. The non-infected group (NI, $n = 9$) included normal, healthy individuals from non-endemic areas for Chagas disease who tested negative for *T. cruzi* infection. The age of the patients included in this study was between 30 and 75 years.

Trypanosoma cruzi Soluble Antigen Preparations

Tissue culture-derived trypomastigotes of the CL-Brener strain of *T. cruzi* were isolated from LLC cells maintained in RPMI 1640 medium (Gibco, Thermo Fisher Scientific, United States) supplemented with 10% fetal bovine serum, as previously described (43). Later, trypomastigotes were collected from the supernatant and were lysed and homogenized by a glass homogenizer and Teflon pestle in cold phosphate-buffered saline (PBS, Sigma, United States). Next, the suspensions were centrifuged at 23,000 × *g* for 60 min at 4°C, and the supernatant was collected, dialyzed for 24 h at 4°C against PBS, and sterilized by filtration on 0.2 μm pore size membranes. The protein concentration was measured by Nanodrop (Thermo Scientific, United States), and the material was separated into aliquots and stored at −70°C. Parasites obtained were used to infect PBMC from patients and healthy individuals at a final concentration of 20 μg/ml.

Obtaining Peripheral Blood Mononuclear Cells

The peripheral blood of the individuals was collected in a sterile Vacutainer tube containing heparin and was slowly added over Ficoll-Hypaque (Sigma) in a proportion of 1:1 in a 14-ml polypropylene tube (Falcon, United States). It was centrifuged at 400 × *g* for 40 min at room temperature, and, at the end of the centrifugation, peripheral blood mononuclear cells (PBMC) ring was obtained between the Ficoll-Hypaque mixture and the plasma. The plasma was carefully removed, subsequently stored in 2 ml aliquots, and duly identified at −20°C. The PBMC was removed with the aid of a micropipette and transferred to a 50-ml Falcon tube. The cells were washed three times by centrifugation at 400 × *g* for 10 min at 4°C in sterile PBS and resuspended in RPMI 1640 medium to 10^7 cells/ml. All manipulations were performed under sterile conditions in a laminar flow hood.

Anti-CD80 and Anti-CD86 Blocking Assay

To perform co-stimulation blockade by anti-CD80 and anti-CD86 antibodies, CMBLAST medium was used, containing 1.6% L-glutamine (Sigma), 3% penicillin and streptomycin, and 5% inactivated AB-type human serum (Sigma) diluted in RPMI 1640 medium. PBMC culture was carried out in polypropylene tubes of 5 ml at a concentration of 10^7 cells/ml with CMBLAST medium. TRYPO (20 μg/ml), anti-CD80 monoclonal antibody blockade (2D10.4, 5 μg/ml), or anti-CD86 monoclonal antibody blockade (IT2.2, 5 μg/ml) (Thermo Fisher Scientific, Waltham, MA, United States) were added to the tubes, obtaining a final volume of 1.5 ml. As a control, the same conditions described above were used in tubes in the absence of TRYPO stimulation, as well as in the absence of anti-CD80 or anti-CD86 monoclonal antibody blockade. The tubes were incubated for 18 h at 37°C under 5% CO_2 (Forma Scientific, United States).

Flow Cytometry

After *in vitro* assay, Brefeldin-A (1 mg/ml [Sigma, United States]) was added to the cells, incubated for 4 h, and then washed in sterile PBS. Brefeldin-A is a blocker of protein trafficking to the Golgi complex, leading to the accumulation of intracellular proteins and being a potent inhibitor of cell secretion (44). The cells were transferred to 5-ml polystyrene tubes containing the corresponding surface antibodies and were incubated for 30 min in the dark at room temperature. Next, cells were washed with PBS-W (PBS pH 7.4, containing 0.5% BSA and 0.1% sodium azide) and were fixed with 2% formaldehyde, followed by incubation for 20 min in the dark at room temperature. A total of 2.5 ml of PBS-P (PBS, pH 7.4 containing 0.5% BSA, 0.1% sodium azide, and 0.5% saponin) were added, and tubes were incubated for 15 min in the dark at room temperature. To evaluate intracellular markers, 2 μl of anti-cytokine antibody was added to each tube and incubated for 1 h at room temperature. Then, cells were washed with 1 ml of PBS-P, 150 μl of PBS was added to the tubes, and the samples containing the cell suspension were used to acquire data on a flow cytometer (FACS LSR Fortessa, BD, United States). A total of 50,000 events were analyzed using size (FSC) and granularity (SSC) parameters. Monoclonal antibodies were conjugated to FITC, PERCP (or PE-Cy5 or PERCP-Cy5.5), APC, APCCy7, PE-Cy7, and BV421. The analyzed molecules (clones) were CD4 (RPA-T4), CD28 (CD28.2), CTLA-4 (BNI3), CD25 (M-A251), HLA-DR (G46-6), CD80 (2D10), CD86 (2331), Tbet (4B10), GATA-3 (L50-823), RORγT (Q21-559), FOXP3 (PCH101), IFN-γ (25723.11), IL-4 (8D4-8), IL-10 (JES3-19F1), and IL-17 (eBio64DEC17).

Statistical Analysis

For each co-stimulatory molecule blockade antibody (anti-CD80 and anti-CD86), four treatments were prepared: (A) only medium (control); (B) medium with TRYPO; (C) medium with blockade antibody; and (D) medium with TRYPO and blockade antibody.

The data in each NI, IND, and CARD group were normalized using ratio calculation of the four treatments. First, the values obtained in (C) treatment were divided by (A) treatment values. This ratio (C/A) demonstrates the effect of co-stimulatory molecules blockade in cells. Second, the values obtained in

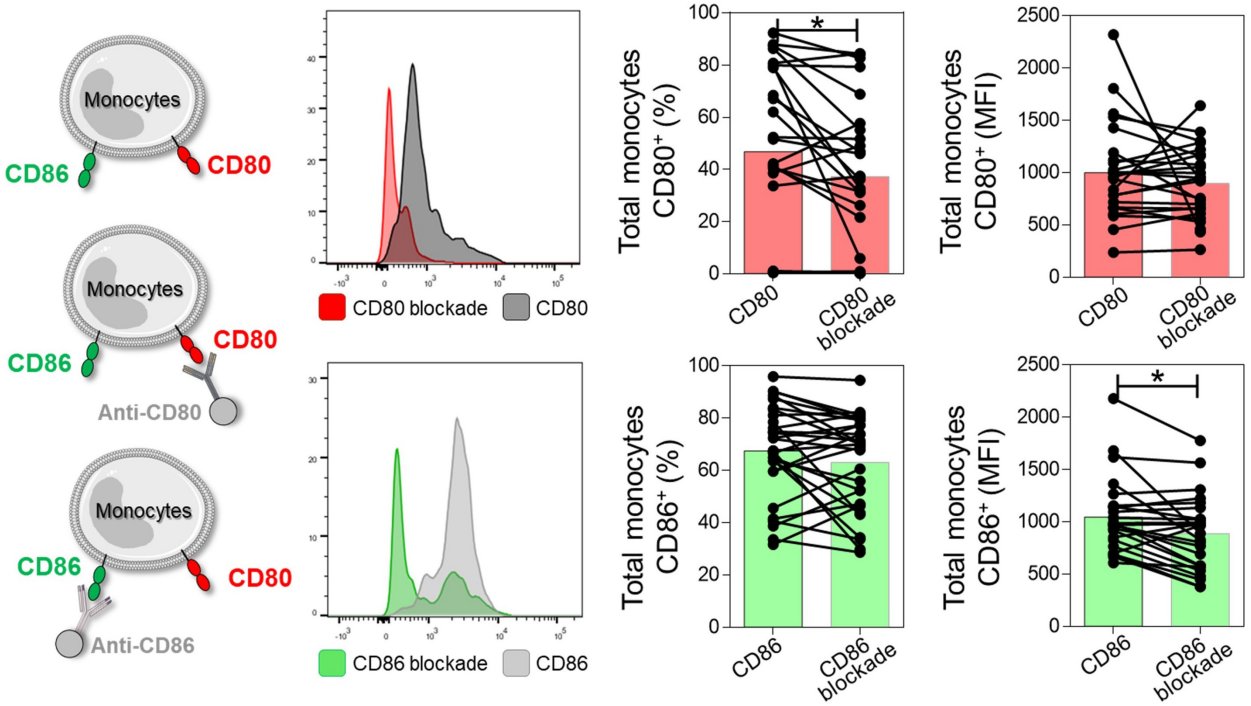

FIGURE 1 | Representation of the reduction of CD80 and CD86 molecules after antibody blockade. Histogram representation, frequency of $CD80^+$ or $CD86^+$ monocytes, and mean fluorescence intensity (MFI) after and before anti-CD80 and anti-CD86 antibody blockade of PBMC cultures from total group (NI, IND, and CARD, $n = 29$). For this analysis, monocytes were delimited through granularity (SSC) vs. HLA-DR parameters and subsequent evaluation of the CD80 and CD86 co-stimulatory molecules. Statistical differences ($p < 0.05$) were obtained by Wilcoxon signed-rank test. Bars represent the median values.

the (D) treatment were divided by (B) treatment values. This ratio (D/B) demonstrates the effect of co-stimulatory molecules blockade in cells and the effects of stimulation with TRYPO. Finally, from a new division [(D/B)/(C/A)], we obtained a normalized quotient, corresponding to the effect of co-stimulatory molecules blockade and the TRYPO stimulation, nullifying the medium variations.

To analyze the pattern of cytokines expressed by $CD4^+$ T lymphocytes (IFN-γ, IL-4, IL-17, and IL-10), we calculated a relative expression index through the ratio between the effect of anti-CD86 blockade and the effect of anti-CD80 blockade in TRYPO stimulation. For the analysis of cytokines and the proportion of co-stimulatory molecules expressed by lymphocyte subsets, raw data obtained from treatments only after TRYPO stimulation (treatments B and D) were used.

Afterward, the statistical analysis was performed comparing the quotient of each NI, IND, and CARD group. All data assumed a non-Gaussian distribution. Differences between groups were analyzed by non-parametric Kruskal–Wallis test followed by Dunn's multiple comparisons test, using the GraphPad Prism version 5.0 software (San Diego, United States). Paired analysis through Wilcoxon signed-rank test was used to verify differences between the total groups (NI, IND, and CARD, $n = 29$) before and after anti-CD86 blockade on anti-CD80 antibody blockade.

The association between Treg lymphocytes and CD28 and CTLA-4 receptors was determined from the linear regression, considering the coefficient of determination (R^2) for the quality of fit and the F test to measure the variance between pairs ($p < 0.05$). For all analyses, the confidence interval was 95%, and significant statistical differences were considered when $p < 0.05$.

RESULTS

The Use of Blocking Monoclonal Antibodies Reduces the Frequency and Mean Fluorescence Intensity of CD80 and CD86 Receptors, Respectively

Although the role of CD80 and CD86 co-stimulatory molecules is already known to activate adaptive immunity, the involvement of these molecules in Chagas disease is poorly studied. Thus, using monoclonal blocking antibody for CD80 and CD86 receptors, we assessed the functional phenotypic profile of $CD4^+$ T and $CD8^+$ T lymphocytes and their subsets from cultures of PBMC after TRYPO stimulation from healthy and Chagas disease patients.

First, to validate the anti-CD80 and anti-CD86 blocking assay, we evaluated the expression of CD80 and CD86 co-stimulatory molecules before and after anti-CD80 and anti-CD86 antibody blockade in PBMC culture from NI, IND, and CARD groups. Reduction in the frequency of total monocytes $CD80^+$ and mean fluorescence intensity (MFI) of CD86 were observed after anti-CD80 and anti-CD86 antibody blockade, respectively (**Figure 1**).

CD86 Contributes to Control the Inflammatory Response While CD80 Has a Protective Profile Only in Asymptomatic Patients With Chagas Disease

To assess the effect of CD80 and CD86 co-stimulatory molecules on the activation or inhibition of total $CD4^+$ T lymphocytes, we analyzed the relationship between these molecules and their CD28 and CTLA-4 ligands. However, no difference was observed in these molecules. In addition, we evaluated the main cytokines produced by total $CD4^+$ T cells after anti-CD80 or anti-CD86 antibody blockade from PBMC cultures of Chagas disease patients and healthy individuals. We observed a significant reduction in the frequency of $CD4^+$ IL-17^+ T lymphocytes in IND patients when compared to the NI group only in the presence of anti-CD80 antibody blockade (**Figure 2A**). Other significant differences were not observed.

Next, to analyze the pattern of cytokines expressed by $CD4^+$ T lymphocytes (IFN-γ, IL-4, IL-17, and IL-10), we calculated a relative expression index through the ratio between anti-CD86/anti-CD80 blockade from PBMC cultures of NI, IND, and CARD groups. Our data demonstrated a higher frequency of $CD4^+$ IFN-γ^+ T lymphocytes after anti-CD86 antibody blockade compared to anti-CD80 antibody blockade in IND compared to patients with CARD (**Figure 2B**). Other significant differences were not observed.

$CD8^+$ T Lymphocytes Activation Could Be Modulated by CD80 Co-stimulatory Molecule

$CD8^+$ T lymphocytes play a crucial role during the acute and chronic phases of Chagas disease, and, considering that their activation may be dependent of CD80 and CD86 molecules performance (20, 45, 46), our next step was to evaluate the expression of the CD25, CD28, and CTLA-4 activation molecules in total $CD8^+$ T lymphocytes after anti-CD80 or anti-CD86 antibody blockade of NI, IND, and CARD groups. The results showed a higher frequency of $CD8^+$ $CD25^+$ T lymphocytes in the CARD group when compared to the IND group only after anti-CD80 antibody blockade (**Figure 3**). Other significant differences were not observed.

CD80 and CD86 Modulate Regulatory T Cells Activity in Cardiac and Indeterminate Patients, Respectively

After anti-CD80 and anti-CD86 blocking assays on $CD4^+$ and $CD8^+$ T total lymphocytes, we wondered what role these co-stimulatory molecules play in activating the $CD4^+$ and $CD8^+$ T subsets. The data show a lower frequency of $CD4^+$ Treg cells in IND when compared to the NI group only with anti-CD86 antibody blockade (**Figure 4A**). In contrast, the CARD group showed a higher frequency of $CD8^+$ Treg lymphocytes in comparison with IND individuals only in PBMC cultures after anti-CD80 antibody blockade (**Figure 4B**). Other significant differences were not observed.

Subsequently, we evaluated the expression of IFN-γ, IL-4, IL-17, and IL-10 cytokines by Th1, Th2, Th17, and $CD4^+$ Treg lymphocytes, respectively, in PBMC cultures with TRYPO, with anti-CD80 antibody blockade, and with anti-CD86 antibody blockade from NI, IND, and CARD groups. A lower frequency of Treg IL-10^+ lymphocytes when compared to Th1 IFN-γ^+ cells in the three PBMC cultures and from all groups evaluated was observed, except in the case of the IND group after CD80 blockade. Our results also showed a reduction in the frequency of Treg IL-10^+ cells in comparison with Th2 IL-4^+ lymphocytes in PBMC cultures with TRYPO and with anti-CD86 antibody blockade from NI and CARD groups, as well as in PBMC culture with anti-CD80 antibody blockade from the CARD group. In addition, only in PBMC culture with anti-CD80 antibody blockade from the CARD group was observed lower frequency of Treg IL-10^+ lymphocytes when compared to Th17 IL-17^+ cells (**Figure 4C**). Other significant differences were not observed.

CD80 Appears to Modulate Treg Activation Only in Cardiac Patients *via* CD28 Receptor

We evaluated the proportion of CD28 and CTLA-4 ligands in each lymphocyte subsets in PBMC cultures with TRYPO, with anti-CD80 antibody blockade, and with anti-CD86 antibody blockade from NI, IND, and CARD individuals. In patients with Chagas disease, regardless of the clinical form, the same proportion of CD28 on Th1, Th2, Th17, and $CD4^+$ Treg was observed in the three cultures of PBMC evaluated. In contrast, we found a higher proportion of $CD8^+$ Treg $CD28^+$ cells in PBMC culture with anti-CD80 antibody blockade from CARD patients compared to PBMC culture with anti-CD86 antibody blockade and to IND group. When we analyzed the frequency of CTLA-4, we observed a similar proportion of this ligand on the Th1, Th2, Th17, and $CD8^+$ Treg lymphocyte subsets of Chagas disease patients. On the contrary, lower proportion of $CD4^+$ Treg CTLA-4^+ lymphocytes was observed only in PBMC culture with anti-CD86 antibody blockade from IND group in comparison with PBMC culture with anti-CD80 antibody blockade and the CARD group (**Figure 5**).

Our next step was to assess significantly the expression of CTLA-4 and CD28 ligands on $CD4^+$ and $CD8^+$ Treg lymphocytes after anti-CD80 or anti-CD86 antibody blockade in PBMC cultures of NI, IND, and CARD individuals. Our results showed a higher frequency of $CD4^+$ Treg $CD28^+$ lymphocytes in CARD in comparison with NI group only after anti-CD80 antibody blockade (**Figure 6**). Other significant differences were not observed.

Finally, to understand the possible relationship between CD80 and CD86 co-stimulatory molecules and CD28 and CTLA-4 expressed in $CD4^+$ and $CD8^+$ Treg lymphocytes, we investigated the interaction between these molecules after anti-CD80 or anti-CD86 antibody blockade of NI, IND, and CARD groups through

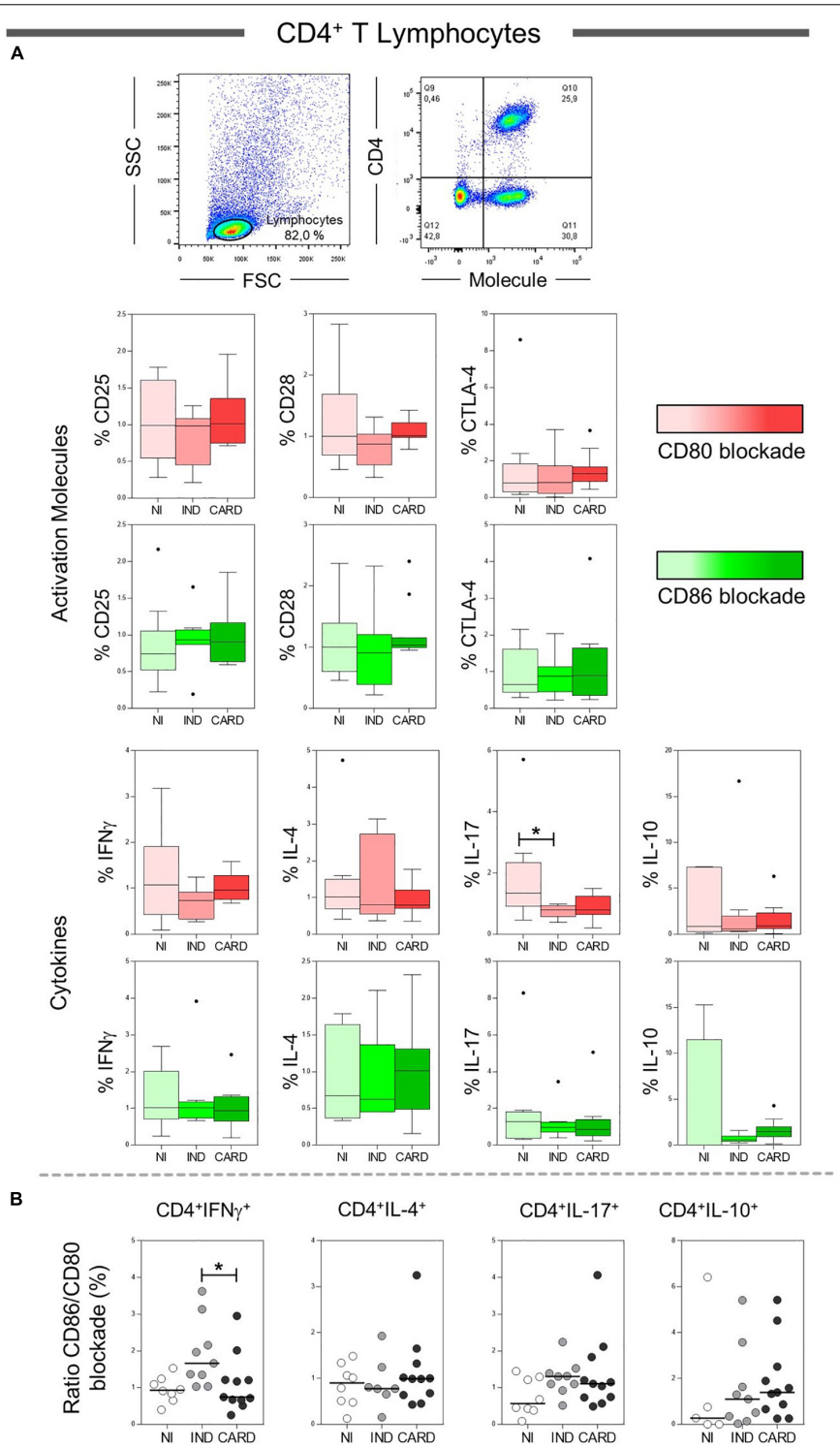

FIGURE 2 | Analysis of the phenotypic-functional profile of CD4$^+$ T lymphocytes after anti-CD80 and anti-CD86 antibody blockade. Flow cytometry gate strategy of non-infected (NI) individuals is represented. Frequency of T CD4$^+$ lymphocytes expressing CD25, CD28, and CTLA-4 activations molecules and IFN-γ, IL-4, IL-17, and IL-10 cytokines **(A)** in PBMC culture from NI individuals (n = 9), indeterminate (IND, n = 9), and cardiac (CARD, n = 11) clinical forms of Chagas disease, after TRYPO *in vitro* stimulation and anti-CD80 and anti-CD86 antibody blockade. Relative expression index of IFN-γ, IL-4, IL-17, and IL-10 cytokines through CD86/CD80 blockade ratio by CD4$^+$ T lymphocytes **(B)**. Statistical differences ($p < 0.05$) between groups were obtained by Kruskal–Wallis test, followed by Dunn's post-test, and represented by asterisk (*) and lines. Boxes demonstrate the median and interquartile ranges, whiskers evidence the highest and lowest observation, and dots represent the outliers.

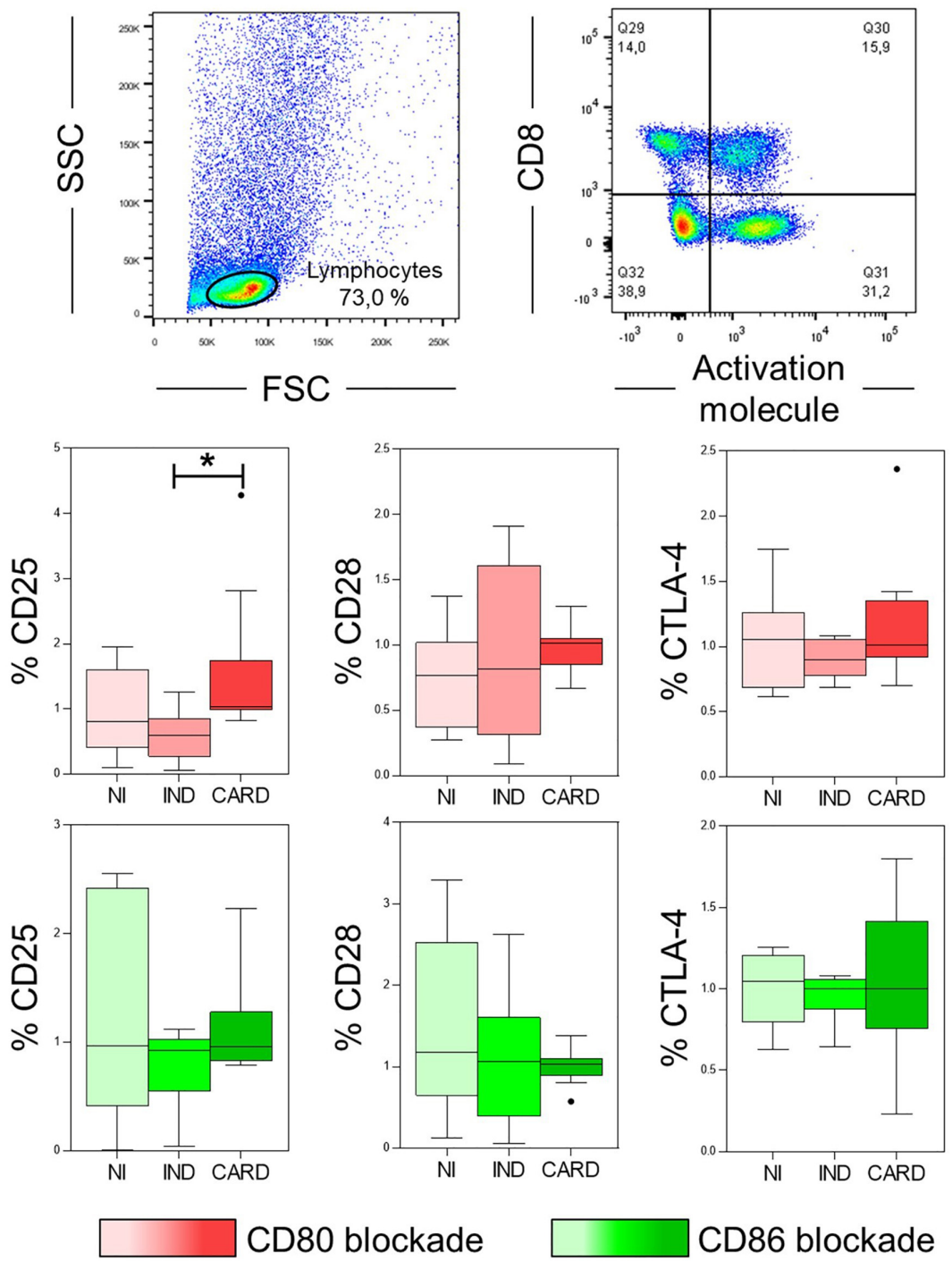

FIGURE 3 | Analysis of the phenotypic-functional profile of $CD8^+$ T lymphocytes after anti-CD80 and anti-CD86 antibody blockade. Flow cytometry gate strategy of non-infected (NI) individuals is represented. Frequency of T $CD8^+$ lymphocytes expressing CD25, CD28, and CTLA-4 activations molecules in PBMC culture from NI individuals (n = 9), indeterminate (IND, n = 9), and cardiac (CARD, n = 11) clinical forms of Chagas disease, after *in vitro* stimulation with *T. cruzi* antigens and anti-CD80 and anti-CD86 antibody blockade. Statistical differences ($p < 0.05$) between groups were obtained by Kruskal-Wallis test, followed by Dunn's post-test, and represented by asterisk (*) and lines. Boxes demonstrate the median and interquartile ranges, whiskers evidence the highest and lowest observation, and dots represent the outliers.

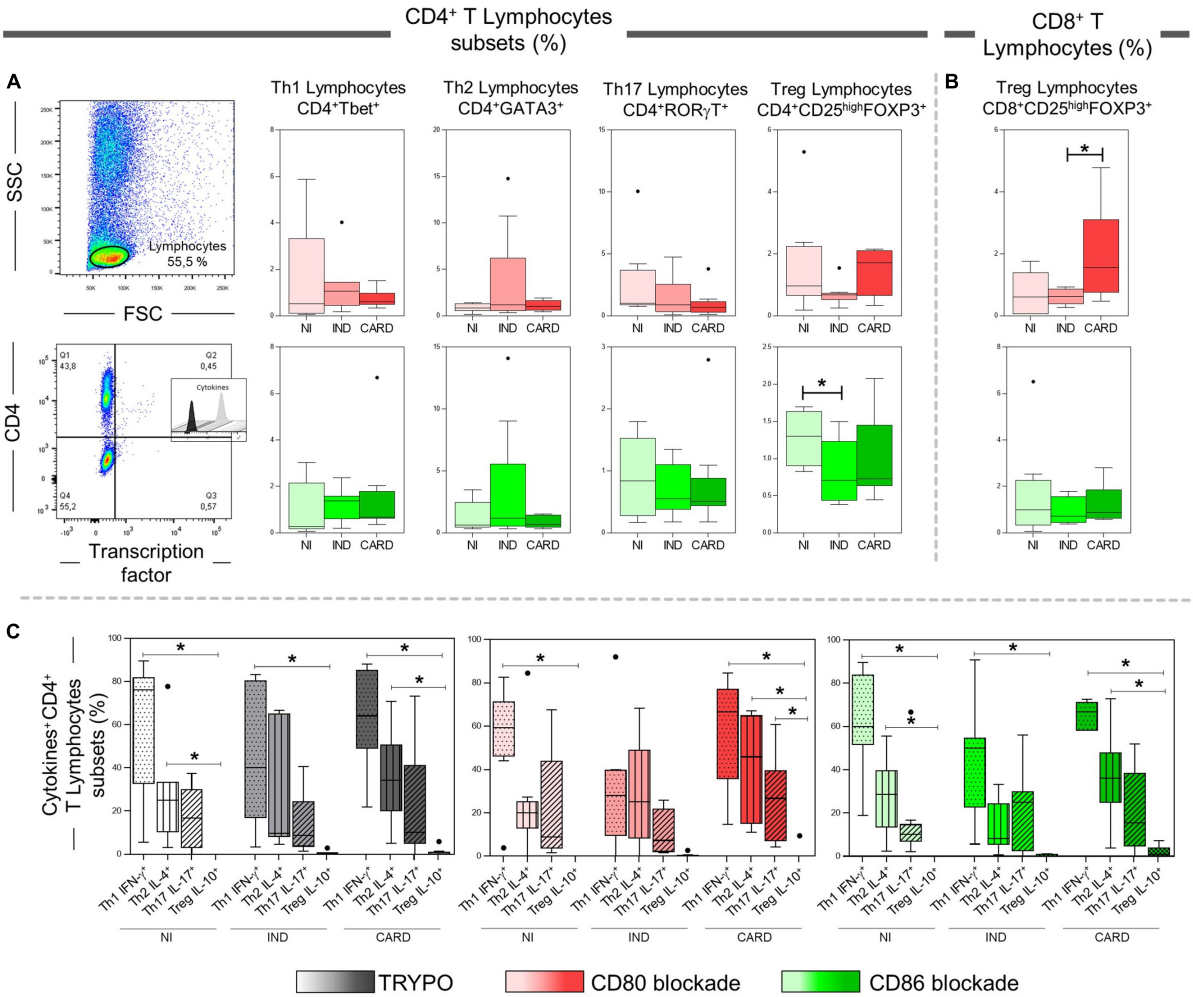

FIGURE 4 | Analysis of CD4$^+$ and CD8$^+$ T lymphocytes subsets after anti-CD80 and anti-CD86 antibody blockade and pattern of expressed cytokines in PBMC cultures with TRYPO, CD80, or CD86 antibody blockade. Flow cytometry gate strategy of non-infected (NI) individuals is represented. Frequency of Th1, Th2, Th17, and CD4$^+$ Treg lymphocytes **(A)** and CD8$^+$ Treg lymphocytes **(B)** after *in vitro* stimulation with *T. cruzi* antigens and anti-CD80 and anti-CD86 antibody blockade. Th1 IFN-γ$^+$, Th2 IL-4$^+$, Th17 IL-17$^+$, and CD4$^+$ Treg IL-10$^+$ PBMC cultures with TRYPO, with anti-CD80 antibody blockade, and with anti-CD86 antibody blockade **(C)** from NI individuals (n = 9), indeterminate (IND, n = 9), and cardiac (CARD, n = 11) clinical forms of Chagas disease. Statistical differences ($p < 0.05$) between groups were obtained by Kruskal–Wallis test, followed by Dunn's post-test, and represented by asterisk (*) and lines. Boxes demonstrate the median and interquartile ranges, whiskers evidence the highest and lowest observation, and dots represent the outliers.

linear regression analysis. We found a significant association between CD4$^+$ Treg lymphocytes and CD4$^+$ Treg CD28$^+$ cells in NI (R^2 = 0.62/p = 0.02) and CARD (R^2 = 0.38/p = 0.04) groups, but not in IND patients, and only in PBMC cultures after anti-CD80 blockade (**Figure 7**). Other significant differences were not observed.

DISCUSSION

Inflammatory stimuli modulate the expression of CD80 and CD86 co-stimulatory ligands, resulting in the activation or attenuation of signals that determine the nature and development of the subsequent immune response (32). It has been demonstrated that the absence of the second signal mediated by CD80 and CD86 to T cell activation drives lymphocyte anergy (26), and the simultaneous blockade of these both molecules results in exacerbated *T. cruzi* infection in a murine model (47). Therefore, CD80 and CD86 co-stimulatory molecules play a critical role in the control of the immune responses. However, little is known about the role of these molecules in activating adaptive immunity mediated by CD4$^+$ and CD8$^+$ T lymphocytes and their subsets during the chronic phase of Chagas disease. We previously described that IND and CARD patients differentially expressed CD80 and CD86 co-stimulatory molecules, and we proposed that CD86 may be involved in the immunomodulation in asymptomatic patients (38). Here, we confirmed the regulatory performance of CD86 and highlighted the role of the CD80 molecule in the regulation of Treg activation in patients with CARD.

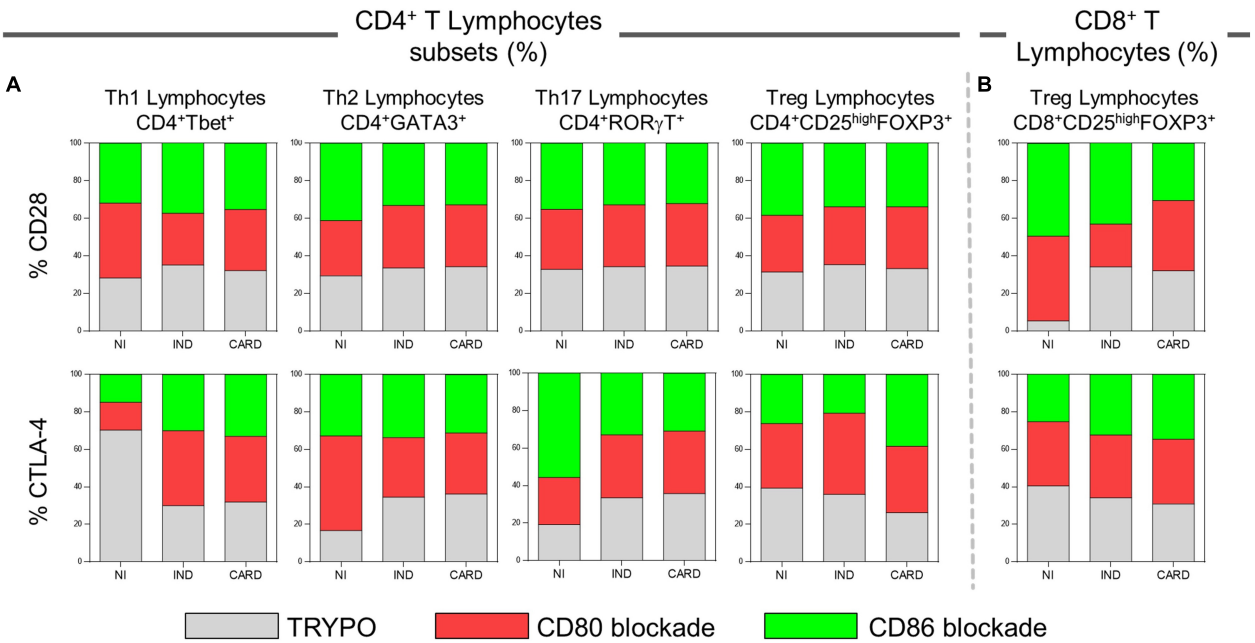

FIGURE 5 | Proportion of CD28 and CTLA-4 expression by lymphocyte subsets. Proportion of CD28 and CTLA-4 ligands on Th1, Th2, Th17, $CD4^+$ Treg **(A)**, and $CD8^+$ Treg lymphocytes **(B)** in PBMC cultures with TRYPO, with anti-CD80 antibody blockade, and with anti-CD86 antibody blockade from NI individuals (n = 9), indeterminate (IND, n = 9), and cardiac (CARD, n = 11) clinical forms of Chagas disease.

We evaluated the role of CD80 and CD86 molecules in targeting $CD4^+$ T lymphocytes, and we found that blocking the CD80 receptor led to a reduction in the frequency of $CD4^+$IL-17^+ T lymphocytes in IND patients. It has been proposed that IL-17 is associated with better cardiac function in patients with Chagas disease (48, 49) and this cytokine may regulate the immune response and the development of cardiac lesions during *T. cruzi* infection (50). On the contrary, our results showed that only after anti-CD86 antibody blockade, higher frequency of $CD4^+$ IFN-γ^+ T lymphocyte was observed also in the IND group. IFN-γ production is required to control replication of the parasite during the acute phase of *T. cruzi* infection, even as contributing to the increase of the inflammatory process during the chronic phase (12, 15, 51). Thereby, we proposed that CD86 can control IFN-γ^+ expression by $CD4^+$ T cells in asymptomatic patients, regulating the development of exacerbated inflammation, and CD80 displays a protective role through the regulation of IL-17, participating in myocardium tissue homeostasis only in IND patients.

We demonstrated a higher frequency of $CD8^+$ $CD25^+$ T lymphocytes and $CD8^+$ Treg cells in the CARD group after anti-CD80 antibody blockade in contrast with lower frequency of $CD4^+$ Treg lymphocytes after anti-CD86 antibody blockade found only in IND patients. It has been proposed that even IND patients has the highest frequency of Treg cells in peripheral blood and these cells was associated with a better clinical prognosis in patients with the asymptomatic clinical form of Chagas disease (19, 38, 52), CARD patients also have higher frequency of Treg lymphocytes in comparison with NI individuals (38). Thus, even though patients with CARD present an imbalance in the production of effector and immunoregulatory mechanisms that contribute to the worsening of myocardial damage, these individuals are able to produce regulatory T lymphocytes to try to control inflammation. On the contrary, the production of Treg lymphocytes in IND patients indeed appears to be a key factor in regulating the inflammatory process, preventing tissue damage. Here, we proposed that these regulatory cells can be activated in both IND and CARD clinical forms of chronic Chagas disease by opposite co-stimulation molecules. We have previously demonstrated an association between CD86 receptor expressed in non-classical monocytes with Treg lymphocytes, while a negative correlation with CD80 by total monocytes and these regulatory cells was found in patients without cardiomyopathy (NI and IND), but not in CARD group (38). Moreover, as observed in this study, only anti-CD86 antibody blockade, but not CD80, led to a reduction of $CD4^+$ Treg IL-10^+ cells in IND patients. These findings suggest that while CD86, but not CD80, may contribute to the activation of Treg lymphocytes as well as the production of IL-10 by these cells only in IND individuals, leading to modulation of the immune response, in the CARD group, CD80 may be responsible for controlling $CD8^+$ $CD25^+$ T lymphocyte activation and could be involved in the modulation of Treg cell induction.

Activation or inhibition of T lymphocytes requires the interaction between CD80 and CD86 co-stimulatory molecules with their ligands CD28 and CTLA-4 that can direct the plasticity in T lymphocyte subset activation (32). Through comparing the proportion of CD28 and CTLA-4 ligands in each lymphocyte subsets between patients with Chagas disease, we observed a higher proportion of CD28 on $CD8^+$ Treg cells only after

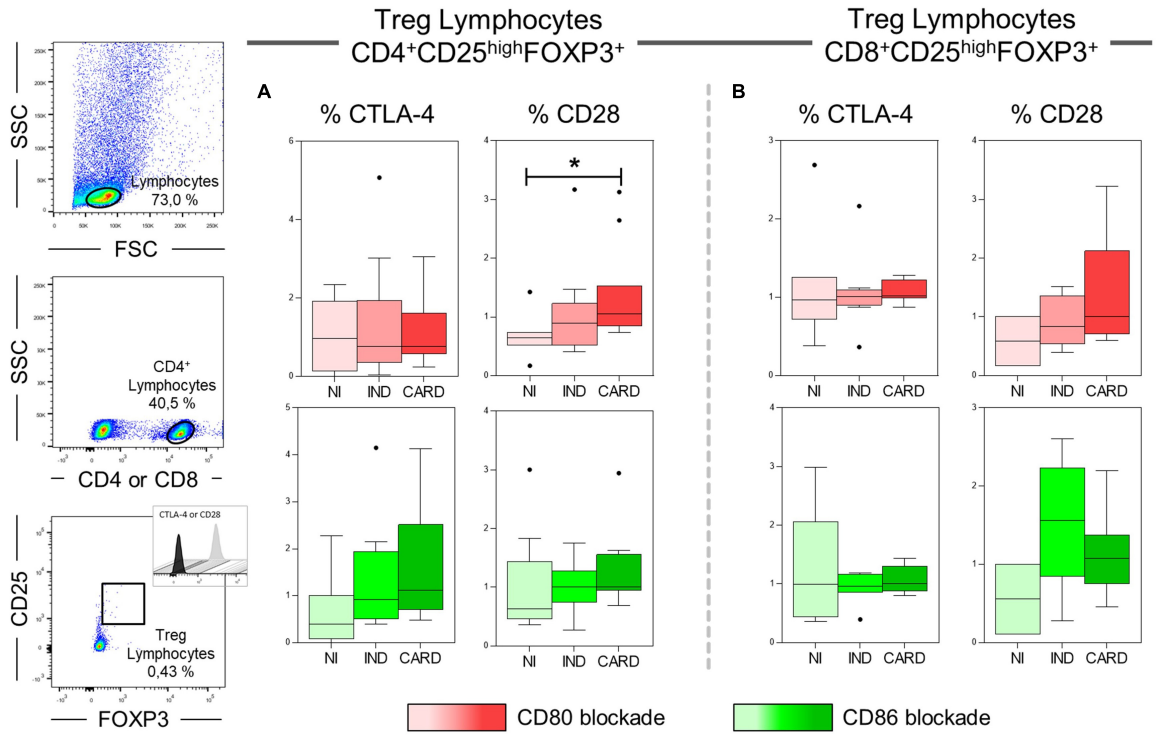

FIGURE 6 | Analysis of the frequency of CD28 and CTLA-4 ligands on Treg lymphocytes after anti-CD80 and anti-CD86 antibody blockade. Flow cytometry gate strategy of non-infected (NI) individuals is represented. Frequency of T $CD4^+$ Treg lymphocytes **(A)** and $CD8^+$ Treg lymphocytes **(B)** expressing CD28 and CTLA-4 in PBMC culture from NI individuals (n = 9), indeterminate (IND, n = 9), and cardiac (CARD, n = 11) clinical forms of Chagas disease, after *in vitro* stimulation with *T. cruzi* antigens and anti-CD80 and anti-CD86 antibody blockade. Statistical differences ($p < 0.05$) between groups were obtained by Kruskal–Wallis test, followed by Dunn's post-test, and represented by asterisk (*) and lines. Boxes demonstrate the median and interquartile ranges, whiskers evidence the highest and lowest observation, and dots represent the outliers.

anti-CD80 blockade from CARD in comparison with anti-CD86 blockade and to IND group. Moreover, lower proportion of CTLA-4 on $CD4^+$ Treg lymphocytes was observed only after anti-CD86 blockade from IND in comparison with anti-CD80 antibody blockade and to CARD group. Interestingly, when we evaluated the statistical results, we found a higher frequency of $CD4^+$ Treg $CD28^+$ lymphocytes in CARD group only after anti-CD80 antibody blockade. Furthermore, we verified an association between $CD4^+$ Treg lymphocytes and $CD28^+$ expression on $CD4^+$ Treg cells in CARD group, but not in IND patients, and once again only in after anti-CD80 antibody blockade. Previously, it has been demonstrated by our research group that there is an association between CD80 and CD28, and between CD86 and CTLA-4 receptors on total $CD4^+$ T lymphocytes, as also, increased frequency of $CD4^+$CTLA-4^+ T lymphocytes in IND group (38). CTLA-4 is constitutively expressed in murine and human Tregs being a key molecule involved in Treg-mediated suppression (53–55). CTLA-4 interacts with CD80 and CD86 on professional antigen-presenting cell (APCs), such as monocytes, and captures these ligands in a process called trans-endocytosis (56). Thus, CD80 and CD86 become unavailable to interact with CD28, leading to indirect inhibition of total T lymphocytes. Furthermore, it has been demonstrated that $CD25^+CD4^+$ Treg cells from deficient CD28 mice exhibited suppressive activity, indicating that this molecule is dispensable for the Treg-mediated suppression (54). Thus, we suggested that this CTLA-4-mediated suppression mechanism could be used by Treg cells only in IND, but not by CARD patients, since Chagas cardiomyopathy patients demonstrated a higher frequency of Treg $CD28^+$ lymphocytes and not CTLA-4, as shown by IND patients in our previous studies (38).

Therefore, we proposed that Treg cells from IND patients could be activated *via* CD86-CTLA-4 interaction, leading to modulation of the immune response only in asymptomatic patients with Chagas disease, while CD80 may be an important molecule capable of modulating the expression of CD28 in Treg lymphocytes only from patients with CARD. Nolan et al., evaluated the role of CD80 and CD86 in mice and human with sepsis and observed that upregulation of CD80 on circulating monocytes was associated with severity of illness, while CD86 appears to have a protective performance, suggesting a relatively anti-inflammatory role of this co-stimulatory molecule *in vivo* (57). In addition, positive regulation of CD80 directs the polarization of Th1 lymphocytes (58). Therefore, we suggested that CD80 may be involved in the proliferation control of T $CD8^+$ lymphocytes, as well as in the modulation of regulatory cells activation *via* CD28 receptor.

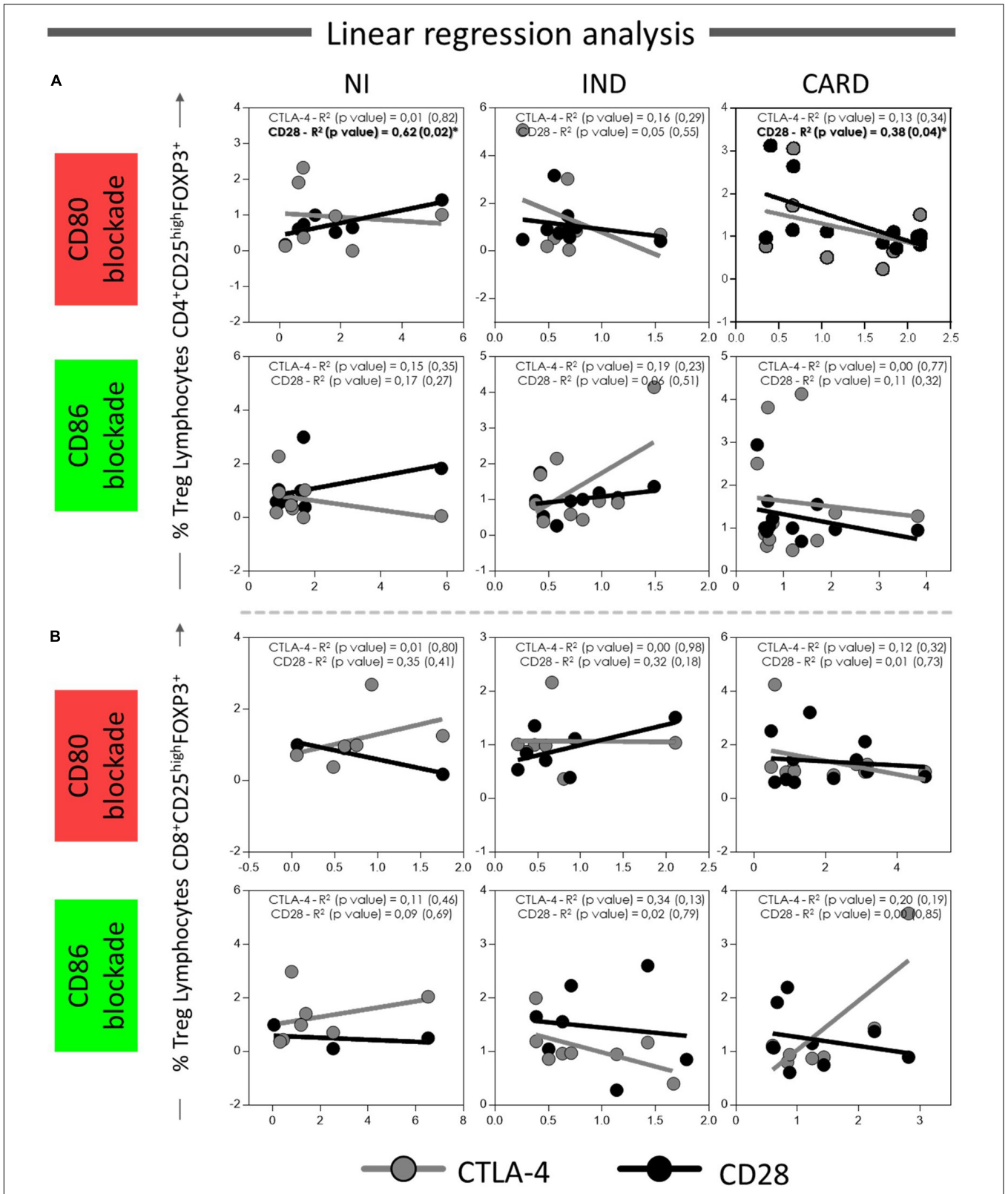

FIGURE 7 | Linear regression analysis between $CD4^+$ and $CD8^+$ Treg lymphocytes and CD28 and CTLA4 ligands on Treg lymphocytes. Association between $CD4^+$ Treg lymphocytes **(A)** and $CD8^+$ Treg lymphocytes **(B)** with CD28 and CTLA-4 expressed in $CD4^+$ and $CD8^+$ Treg cells from PBMC culture of NI individuals ($n = 9$), indeterminate (IND, $n = 9$), and cardiac (CARD, $n = 11$) clinical forms of Chagas disease, after *in vitro* stimulation with *T. cruzi* antigens and anti-CD80 and anti-CD86 antibody blockade. Data are presented by R-squared (R^2), and significant statistical differences were considered when $p < 0.05$.

Here, we highlighted for the first time the role of CD80 in modulation of Treg lymphocyte activation in CARD patients, maybe by performance with CD28 receptor, pointing out a key molecule in the development of Chagas cardiomyopathy. It is important to mention that even though the CD80 and CD86 blockade used here reduced statistically both the frequency and the expression of these receptors in human monocytes, the *in vitro* experiments performed are limited by not completely blocking these receptors. Thus, the use of other methodological approaches, such as molecular tools to repress the expression of these receptors or to block their actions can provide more information about the role of CD80 and CD86 in chagasic pathology. Therefore, further studies are still needed to understand the immunological mechanisms involved in establishing the different clinical forms of Chagas disease.

DATA AVAILABILITY STATEMENT

The raw data supporting the conclusions of this article will be made available by the authors, without undue reservation.

ETHICS STATEMENT

The studies (0021.0438.438-10) involving human participants were reviewed and approved by the Ethics Committee of the René Rachou Institute, FIOCRUZ, Minas Gerais (CEPSH-IRR #15/2011). The patients/participants provided their written informed consent to participate in this study.

AUTHOR CONTRIBUTIONS

BP did the statistical analysis, figures, and wrote the study. NM and JG delineated the experiments and discussed the results. AT-C, WD, and RC-O contributed to the design of the study and discussions of the results. SE-S, MN, and SS select and lead clinical management of patients. BP, NM, JF, TF-C, and MB-B performed the experiments. JG contributed to the conception and coordinated the study. All authors contributed to manuscript revision, read, and approved the submitted version.

FUNDING

JG received sources of support provided by Conselho Nacional do Desenvolvimento Científico e Tecnológico (CNPq: #474796/2012, #306447/2015-0, and #302681/2018-3), Fundação de Amparo à Pesquisa do Estado de Minas Gerais (FAPEMIG, #02419-15 and FAPEMIG-PPM #00233-17), Pró-Reitoria de Pesquisa da Universidade Federal de Minas Gerais-PRPq, and Coordenação de Aperfeiçoamento de Pessoal de Nível Superior (PROEX-CAPES). BP, NM, AT-C, WD, RC-O, and JG received financial support from CNPq fellowship program. TF-C and MB-B received financial support from CAPES.

ACKNOWLEDGMENTS

We would like to thank the Plataforma de Citometria, FIOCRUZ, for the technical assistance.

REFERENCES

1. Chagas C. Nova espécie mórbida do homem produzida por um Trypanosoma (*Trypanosoma cruzi*). *Brazil Med.* (1909) 23:161.
2. WHO. *Chagas Disease (American Trypanosomiasis)*. Geneva: WHO (2020).
3. Andrade DV, Gollob KJ, Dutra WO. Acute Chagas disease: new global challenges for an old neglected disease. *PLoS Neglect Trop Dis.* (2014) 8:e3010. doi: 10.1371/journal.pntd.0003010
4. Ayo CM, Dalalio MMD, Visentainer JEL, Reis PG, Sippert EA, Jarduli LR, et al. Genetic susceptibility to chagas disease: an overview about the infection and about the association between disease and the immune response genes. *Biomed Res Int.* (2013) 2013:13. doi: 10.1155/2013/284729
5. Ribeiro ALP. Forma indeterminada da doença de Chagas: considerações acerca do diagnóstico e do prognóstico. *Rev Soc Brasil Med Trop.* (1998) 1998:301–14. doi: 10.1590/s0037-86821998000300008
6. Moncayo A. Chagas disease: current epidemiological trends after the interruption of vectorial and transfusional transmission in the southern cone countries. *Mem Instit Oswaldo Cruz.* (2003) 98:577–91. doi: 10.1590/s0074-02762003000500001
7. Nogueira LG. *Myocardial Gene Expression of T-bet, GATA-3, Ror*. London: Hindawi Publishing CorporationMediators of Inflammation (2014).
8. Prata A. *Classificação da Infecção Chagásica no Homem. 109-113*. Uberaba: Revista da Sociedade Brasileira de Medicina Tropical (1990).
9. Malik LH, Singh GD, Amsterdam EA. The epidemiology, clinical manifestations, and management of chagas heart disease. *Clin Cardiol.* (2015) 38:565–9. doi: 10.1002/clc.22421
10. Frade AF, Pissetti CW, Ianni BM, Saba B, Lin-Wang HT, Nogueira LG, et al. Genetic susceptibility to Chagas disease cardiomyopathy: involvement of several genes of the innate immunity and chemokine-dependent migration pathways. *BMC Infect Dis.* (2013) 13:17. doi: 10.1186/1471-2334-13-587
11. Bogliolo. Anatomie causes of cardiac insufficiency in chronic chagasic cardiopathy (myocarditis) studied in comparison to anatomic causes of cardiac insufficiency in other cardiopathies. *Arq Bras Cardiol.* (1976) 29:419–24.
12. Chaves AT, Estanislau J, Fiuza JA, Carvalho AT, Ferreira KS, Fares RCG, et al. Immunoregulatory mechanisms in Chagas disease: modulation of apoptosis in T-cell mediated immune responses. *BMC Infect Dis.* (2016) 16:11. doi: 10.1186/s12879-016-1523-1
13. Savino W, Villa-Verde DMS, Mendes-da-Cruz DA, Silva-Monteiro E, Perez AR, Aoki MD, et al. Cytokines and cell adhesion receptors in the regulation of immunity to *Trypanosoma cruzi*. *Cytokine Growth Factor Rev.* (2007) 18:107–24. doi: 10.1016/j.cytogfr.2007.01.010
14. Rodrigues DBR, dos Reis MA, Romano A, Pereira SAD, Teixeira VDA, Tostes S, et al. In Situ expression of regulatory cytokines by heart inflammatory cells in Chagas' Disease patients with heart failure. *Clin Dev Immunol.* (2012) 2012:361730. doi: 10.1155/2012/361730
15. Gomes JA, Bahia-Oliveira LM, Rocha MO, Martins-Filho OA, Gazzinelli G, Correa-Oliveira R. Evidence that development of severe cardiomyopathy in human Chagas' disease is due to a Th1-specific immune response. *Infect Immun.* (2003) 71:1185–93. doi: 10.1128/IAI.71.3.1185-1193.2003
16. Dutra WO, Menezes CAS, Magalhaes LMD, Gollob KJ. Immunoregulatory networks in human Chagas disease. *Parasite Immunol.* (2014) 36:377–87. doi: 10.1111/pim.12107
17. Cunha-Neto E, Kalil J. Heart-infiltrating and peripheral T cells in the pathogenesis of human Chagas' disease cardiomyopathy. *Autoimmunity.* (2001) 34:187–92. doi: 10.3109/08916930109007383

18. Cunha-Neto E, Dzao VJ, Allen PD, Stamatiou D, Benvenutti L, Higuchi ML, et al. Cardiac gene expression profiling provides evidence for cytokinopathy as a molecular mechanism in Chagas' disease cardiomyopathy. *Am J Pathol.* (2005) 167:305–13. doi: 10.1016/S0002-9440(10)62976-8
19. de Araújo FF, Corrêa-Oliveira R, Rocha MOC, Chaves AT, Fiuza JA, Fares RCG, et al. Foxp3^{+}CD25^{high}CD4^{+} regulatory T cells from indeterminate patients with Chagas disease can suppress the effector cells and cytokines and reveal altered correlations with disease severity. *Immunobiology.* (2012) 217:768–77. doi: 10.1016/j.imbio.2012.04.008
20. Brener Z, Gazzinelli RT. Immunological control of *Trypanosoma cruzi* infection and pathogenesis of Chagas' disease. *Int Arch Allergy Immunol.* (1997) 114:103–10. doi: 10.1159/000237653
21. Martin D, Tarleton R. Generation, specificity, and function of CD8(+) T cells in *Trypanosoma cruzi* infection. *Immunol Rev.* (2004) 201:304–17. doi: 10.1111/j.0105-2896.2004.00183.x
22. Junqueira C, Caetano B, Bartholomeu DC, Melo MB, Ropert C, Rodrigues MM, et al. The endless race between *Trypanosoma cruzi* and host immunity: lessons for and beyond Chagas disease. *Expert Rev Mol Med.* (2010) 12:23. doi: 10.1017/S1462399410001560
23. Higuchi MD, Gutierrez PS, Aiello VD, Palomino S, Bocchi E, Kalil J, et al. Immunohistochemical characterization of infiltrating cells in human chronic chagasic myocarditis – comparison with myocardial rejection process. *Virchows Arch Pathol Anat Histopathol.* (1993) 423:157–60. doi: 10.1007/BF01614765
24. Reis DD, Jones EM, Tostes S, Lopes ER, Gazzinelli G, Colley DG, et al. Characterization of inflammatory infiltrates in chronic chagasic myocardial lesions–presence of tumor necrosis factor-alpha+ cells and dominance of granzyme A+, CD8+ lymphocytes. *Am J Trop Med Hygiene.* (1993) 48:637–44. doi: 10.4269/ajtmh.1993.48.637
25. Higuchi MD, Reis MM, Aiello VD, Benvenuti LA, Gutierrez PS, Bellotti G, et al. Association of an increase in CD8+ T cells with the presence of *Trypanosoma cruzi* antigens in chronic, human, chagasic myocarditis. *Am J Trop Med Hygiene.* (1997) 56:485–9. doi: 10.4269/ajtmh.1997.56.485
26. Sharpe AH, Freeman GJ. The B7-CD28 superfamily. *Nat Rev Immunol.* (2002) 2:116–26. doi: 10.1038/nri727
27. Linsley PS, Ledbetter JA. The role of the CD28 receptor during t-cell responses to antigen. *Annu Rev Immunol.* (1993) 11:191–212. doi: 10.1146/annurev.iy.11.040193.001203
28. VanGool SW, Vandenberghe P, DeBoer M, Ceuppens JL. CD80, CD86, and CD40 provide accessory signals in a multiple-step T-cell activation model. *Immunol Rev.* (1996) 153:47–83. doi: 10.1111/j.1600-065x.1996.tb00920.x
29. Schwartz RH. A cell-culture model for lymphocyte-t clonal anergy. *Science.* (1990) 248:1349–56. doi: 10.1126/science.2113314
30. Souza PEA, Rocha MOC, Menezes CAS, Coelho JS, Chaves ACL, Gollob KJ, et al. *Trypanosoma cruzi* infection induces differential modulation of costimulatory molecules and cytokines by monocytes and T cells from patients with indeterminate and cardiac Chagas' disease. *Infect Immun.* (2007) 75:1886–94. doi: 10.1128/IAI.01931-06
31. Saito T, Yamasaki S. Negative feedback of T cell activation through inhibitory adapters and costimulatory receptors. *Immunol Rev.* (2003) 192:143–60. doi: 10.1034/j.1600-065x.2003.00022.x
32. Collins M, Ling V, Carreno BM. The B7 family of immune-regulatory ligands. *Genome Biol.* (2005) 6:7.
33. Linsley PS, Greene JL, Brady W, Bajorath J, Ledbetter JA, Peach R. Human B7-1 (CD80) AND B7-2 (CD86) bind with similar avidities but distinct kinetics to CD28 and CTLA-4 receptors. *Immunity.* (1994) 1:793–801. doi: 10.1016/s1074-7613(94)80021-9
34. Gross JA, Callas E, Allison JP. Identification and distribution of the costimulatory receptor CD28 IN the mouse. *J Immunol.* (1992) 149:380–8.
35. Brunet JF, Denizot F, Luciani MF, Rouxdosseto M, Suzan M, Mattei MG, et al. A new member of the immunoglobulin superfamily–CTLA-4. *Nature.* (1987) 328:267–70. doi: 10.1038/328267a0
36. Waterhouse P, Penninger JM, Timms E, Wakeham A, Shahinian A, Lee KP, et al. Lymphoproliferative disorders with early lethality in mice deficient in CTLA-4. *Science.* (1995) 270:985–8. doi: 10.1126/science.270.5238.985
37. Soares AKD, Neves PAF, Cavalcanti M, Marinho SM, de Oliveira W, de Souza JR, et al. Expression of co-stimulatory molecules CD80 and CD86 is altered in CD14(+)HLA-DR+ monocytes from patients with Chagas disease following induction by *Trypanosoma cruzi* recombinant antigens. *Rev Soc Brasil Med Trop.* (2016) 49:632–6. doi: 10.1590/0037-8682-0149-2016
38. Pinto BF, Medeiros NI, Teixeira-Carvalho A, Eloi-Santos SM, Fontes-Cal TCM, Rocha DA, et al. CD86 expression by monocytes influence an immunomodulatory profile in asymptomatic patients with chronic chagas disease. *Front Immunol.* (2018) 9:454. doi: 10.3389/fimmu.2018.00454
39. Florcken A, Johannsen M, Nguyen-Hoai T, Gerhardt A, Miller K, Dorken B, et al. Immunomodulatory molecules in renal cell cancer: CD80 and CD86 are expressed on tumor cells. *Int J Clin Exp Pathol.* (2017) 10:1443–54.
40. Gardner D, Jeffery LE, Sansom DM. Understanding the CD28/CTLA-4 (CD152) pathway and Its implications for costimulatory blockade. *Am J Transplant.* (2014) 14:1985–91. doi: 10.1111/ajt.12834
41. Liu WX, Yang ZC, Chen Y, Yang HY, Wan XX, Zhou XD, et al. The association between CTLA-4, CD80/86, and CD28 Gene polymorphisms and rheumatoid arthritis: an original study and meta-analysis. *Front Med.* (2021) 8:10. doi: 10.3389/fmed.2021.598076
42. Pinto BF, Medeiros NI, Fontes-Cal TCM I, Naziazeno M, Correa-Oliveira R, Dutra WO, et al. The role of co-stimulatory molecules in chagas disease. *Cells.* (2018) 7:20. doi: 10.3390/cells7110200
43. Souza PEA, Rocha MOC, Rocha-Vieira E, Menezes CAS, Chaves ACL, Gollob KJ, et al. Monocytes from patients with indeterminate and cardiac forms of Chagas' disease display distinct phenotypic and functional characteristics associated with morbidity. *Infect Immun.* (2004) 72:5283–91. doi: 10.1128/IAI.72.9.5283-5291.2004
44. Chardin P, McCormick F. Brefeldin a: the advantage of being uncompetitive. *Cell.* (1999) 97:153–5. doi: 10.1016/s0092-8674(00)80724-2
45. Higuchi MD, Benvenuti LA, Reis MM, Metzger M. Pathophysiology of the heart in Chagas' disease: current status and new developments. *Cardiovasc Res.* (2003) 60:96–107. doi: 10.1016/S0008-6363(03)00361-4
46. Junqueira C, Caetano B, Bartholomeu DC, Melo MB, Ropert C, Rodrigues MM, et al. The endless race between *Trypanosoma cruzi* and host immunity: lessons for and beyond Chagas disease. *Expert Rev Mol Med.* (2010) 12:23. doi: 10.1017/S1462399410001560
47. Miyahira Y, Katae M, Kobayashi S, Takeuchi T, Fukuchi Y, Abe R, et al. Critical contribution of CD28-CD80/CD86 costimulatory pathway to protection from *Trypanosoma cruzi* infection. *Infect Immun.* (2003) 71:3131–7. doi: 10.1128/IAI.71.6.3131-3137.2003
48. Magalhaes LMD, Villani FNA, Nunes MDP, Gollob KJ, Rocha MOC, Dutra WO. High Interleukin 17 expression is correlated with better cardiac function in human chagas disease. *J Infect Dis.* (2013) 207:661–5. doi: 10.1093/infdis/jis724
49. Sousa GR, Gomes JAS, Damasio MPS, Nunes MCP, Costa HS, Medeiros NI, et al. The role of interleukin 17-mediated immune response in Chagas disease: high level is correlated with better left ventricular function. *PLoS One.* (2017) 12:e0172833. doi: 10.1371/journal.pone.0172833
50. Guedes PMD, Gutierrez FRS, Maia FL, Milanezi CM, Silva GK, Pavanelli WR, et al. IL-17 produced during *Trypanosoma cruzi* infection plays a central role in regulating parasite-induced myocarditis. *PLoS Negl Trop Dis.* (2010) 4:11. doi: 10.1371/journal.pntd.0000604
51. Bonney KM, Taylor JM, Thorp EB, Epting CL, Engman DM. Depletion of regulatory T cells decreases cardiac parasitosis and inflammation in experimental Chagas disease. *Parasitol Res.* (2015) 114:1167–78. doi: 10.1007/s00436-014-4300-3
52. Vitelli-Avelar DM, Sathler-Avelar R, Dias JC, Pascoal VP, Teixeira-Carvalho A, Lage PS, et al. Chagasic patients with indeterminate clinical form of the disease have high frequencies of circulating CD3^{+}CD16^{-}CD56^{+} natural killer T cells and CD4^{+}CD25^{High} regulatory T lymphocytes. *Scand J Immunol.* (2005) 62:297–308. doi: 10.1111/j.1365-3083.2005.01668.x
53. Schmidt A, Oberle N, Krammer PH. Molecular mechanisms of Treg-mediated T cell suppression. *Front Immunol.* (2012) 3:20. doi: 10.3389/fimmu.2012.00051
54. Takahashi T, Tagami T, Yamazaki S, Uede T, Shimizu J, Sakaguchi N, et al. Immunologic self-tolerance maintained by CD25(+)CD4(+) regulatory T cells

constitutively expressing cytotoxic T lymphocyte-associated antigen 4. *J Exp Med.* (2000) 192:303–9. doi: 10.1084/jem.192.2.303
55. Dieckmann D, Plottner H, Berchtold S, Berger T, Schuler G. Ex vivo isolation and characterization of CD4(+)CD25(+) T cells with regulatory properties from human blood. *J Exp Med.* (2001) 193:1303–10. doi: 10.1084/jem.193.11.1303
56. Qureshi OS, Zheng Y, Nakamura K, Attridge K, Manzotti C, Schmidt EM, et al. Trans-endocytosis of CD80 and CD86: a molecular basis for the cell-extrinsic function of CTLA-4. *Science.* (2011) 332:600–3.
57. Nolan A, Kobayashi H, Naveed B, Kelly A, Hoshino Y, Hoshino S, et al. Differential role for CD80 and CD86 in the regulation of the innate immune response in murine polymicrobial sepsis. *PLoS One.* (2009) 4:e6600.
58. Balkhi MY, Latchumanan VK, Singh B, Sharma P, Natarajan K. Cross-regulation of CD86 by CD80 differentially regulates T helper responses from *Mycobacterium tuberculosis* secretory antigen-activated dendritic cell subsets. *J Leukocyte Biol.* (2004) 75:874–83. doi: 10.1189/jlb.1003476

Conflict of Interest: The authors declare that the research was conducted in the absence of any commercial or financial relationships that could be construed as a potential conflict of interest.

Publisher's Note: All claims expressed in this article are solely those of the authors and do not necessarily represent those of their affiliated organizations, or those of the publisher, the editors and the reviewers. Any product that may be evaluated in this article, or claim that may be made by its manufacturer, is not guaranteed or endorsed by the publisher.

Advantages of publishing in Frontiers

OPEN ACCESS
Articles are free to read for greatest visibility and readership

FAST PUBLICATION
Around 90 days from submission to decision

HIGH QUALITY PEER-REVIEW
Rigorous, collaborative, and constructive peer-review

TRANSPARENT PEER-REVIEW
Editors and reviewers acknowledged by name on published articles

Frontiers
Avenue du Tribunal-Fédéral 34
1005 Lausanne | Switzerland

Visit us: www.frontiersin.org
Contact us: frontiersin.org/about/contact

REPRODUCIBILITY OF RESEARCH
Support open data and methods to enhance research reproducibility

DIGITAL PUBLISHING
Articles designed for optimal readership across devices

FOLLOW US
@frontiersin

IMPACT METRICS
Advanced article metrics track visibility across digital media

EXTENSIVE PROMOTION
Marketing and promotion of impactful research

LOOP RESEARCH NETWORK
Our network increases your article's readership